

INTEGRATION OF SOLAR ENERGY AND INDUSTRIAL WASTE HEAT INTO
AN INDUSTRIAL ZONE WITH HEAT DISTRIBUTION NETWORK AND
OPTIMIZATION OF ENERGY SOURCES FOR UNITS

A THESIS SUBMITTED TO
THE GRADUATE SCHOOL OF NATURAL AND APPLIED SCIENCES
OF
MIDDLE EAST TECHNICAL UNIVERSITY

BY

SASAN KARIMI

IN PARTIAL FULFILLMENT OF THE REQUIREMENTS
FOR
THE DEGREE OF MASTER OF SCIENCE
IN
MECHANICAL ENGINEERING

MAY 2019

Approval of the thesis:

**INTEGRATION OF SOLAR ENERGY AND INDUSTRIAL WASTE HEAT
INTO AN INDUSTRIAL ZONE WITH HEAT DISTRIBUTION NETWORK
AND OPTIMIZATION OF ENERGY SOURCES FOR UNITS**

submitted by **SASAN KARIMI** in partial fulfillment of the requirements for the degree of **Master of Science in Mechanical Engineering Department, Middle East Technical University** by,

Prof. Dr. Halil Kalıpçılar
Dean, Graduate School of **Natural and Applied Sciences**

Prof. Dr. Mehmet Ali Sahir Arıkan
Head of Department, **Mechanical Engineering**

Prof. Dr. Almıla Güvenç Yazıcıoğlu
Supervisor, **Mechanical Engineering, METU**

Prof. Dr. Derek K. Baker
Co-Supervisor, **Mechanical Engineering, METU**

Examining Committee Members:

Prof. Dr. İlker Tarı
Mechanical Engineering, METU

Prof. Dr. Almıla Güvenç Yazıcıoğlu
Mechanical Engineering, METU

Assoc. Prof. Dr. Merve Erdal
Mechanical Engineering, METU

Assist. Prof. Dr. Özgür Ekici
Mechanical Engineering, Hacettepe University

Assoc. Prof. Dr. Merih Aydınalp Köksal
Environmental Engineering, Hacettepe University

Date: 13.05.2019

I hereby declare that all information in this document has been obtained and presented in accordance with academic rules and ethical conduct. I also declare that, as required by these rules and conduct, I have fully cited and referenced all material and results that are not original to this work.

Name, Surname: Sasan Karimi

Signature:

ABSTRACT

INTEGRATION OF SOLAR ENERGY AND INDUSTRIAL WASTE HEAT INTO AN INDUSTRIAL ZONE WITH HEAT DISTRIBUTION NETWORK AND OPTIMIZATION OF ENERGY SOURCES FOR UNITS

Karımı, Sasan
Master of Science, Mechanical Engineering
Supervisor: Prof. Dr. Almıla Güvenç Yazıcıoğlu
Co-Supervisor: Prof. Dr. Derek K. Baker

May 2019, 213 pages

In the context of European Union INSHIP (Integrating National Research Agendas on Solar Heat for Industrial Process) project, solar energy and industrial waste heat integration into two food industry Units are simulated and optimized in Izmir, Turkey. Two Units could be connected by a Heat Distribution Network (HDN) to share energy between them. Unit's thermal systems simulation and energy sources optimization is done by TRNSYS and MATLAB respectively, to use both software capabilities.

In each time interval, initially MATLAB models Configurations' total fuel cost by nonlinear objective functions. Then it minimizes obtained functions with nonlinear optimization method and finally, based on optimization results, MATLAB controls TRNSYS components to operate Units in optimal condition with minimum cost. In fact, Thermal systems simulation and optimization is done simultaneously in this study. Simulations and optimizations are done for February and June as selected simulation periods. Four different Configurations are defined and investigated in separated sections, to simulate Units with different solar energy or industrial waste heat integration options.

Simulating different Configurations, defining different energy integration options and optimizing systems simultaneously, provide a new perspective to solar energy integration into thermal systems in this study.

The results indicate that Configuration with high-temperature industrial waste heat integration is the cheapest one between studied systems. In February, because there is not much available solar energy, solar collectors increase Units' total cost. However, in June, solar collectors reduce more Configurations' cost in separated collector forms. In addition, the central solar field integration into Configurations, increases fuel consumption and total cost in both February and June while it uses more collector area in comparison with separated collectors. The main reason behind this is small used storage tanks' function which causes much solar energy to be wasted. In conclusion, separated solar collectors and storage tanks show better performance than central solar field among studied Configurations.

Keywords: Nonlinear Optimization, Heat Distribution Network, Solar Process Heat

ÖZ

ISI DAĞITIM AĞI İLE ENDÜSTRİYEL BİR BÖLGEYE AİT GÜNEŞ ENERJİSİ VE ENDÜSTRİYEL ATIKLARIN ENTEGRASYONU VE BİRİMLER İÇİN ENERJİ KAYNAKLARININ OPTİMİZASYONU

Karımı, Sasan
Yüksek Lisans, Makina Mühendisliği
Tez Danışmanı: Prof. Dr. Almıla Güvenç Yazıcıoğlu
Ortak Tez Danışmanı: Prof. Dr. Derek K. Baker

Mayıs 2019, 213 sayfa

Avrupa Birliği INSHIP (Endüstriyel Süreç için Güneş Enerjisi ile İlgili Ulusal Araştırma Gündemlerinin Entegre Edilmesi) projesi kapsamında, Türkiye'de iki gıda endüstrisi birimine güneş enerjisi ve endüstriyel atık ısı entegrasyonu simülasyon ve optimizasyonu yapılmıştır. İki ünite arasında enerji paylaşımını sağlayabilmek için bir Isı Dağıtım Ağı (HDN) ile birbirine bağlanabilir. Ünitenin termal sistemler simülasyonu ve enerji kaynakları optimizasyonu, her iki yazılım özelliğini de kullanmak için sırasıyla TRNSYS ve MATLAB ile yapılmıştır.

Her bir zaman aralığında, başlangıçta MATLAB, Konfigürasyonların toplam yakıt maliyetini doğrusal olmayan amaç fonksiyonlarına göre modeller. Ardından, doğrusal olmayan optimizasyon yöntemiyle elde edilen işlevleri en aza indirir ve son olarak, optimizasyon sonuçlarına dayanarak, MATLAB, TRNSYS bileşenlerini, Birimlerin minimum maliyetle en iyi şartta çalıştırmak için kontrol eder. Aslında, bu çalışmada Termal sistem simülasyonu ve optimizasyonu eş zamanlı olarak yapılmıştır. Simülasyonlar ve optimizasyonlar, seçilen simülasyon periyodu olarak Şubat ve Haziran ayları için yapılmıştır. Farklı güneş enerjisi veya endüstriyel atık ısı

entegrasyon seçeneklerine sahip Üniteleri simüle etmek için dört farklı Konfigürasyon ayrı bölümlerde tanımlanmış ve araştırılmıştır.

Bu çalışmada, farklı konfigürasyonları simüle etmek, farklı enerji entegrasyon seçeneklerini tanımlamak ve sistemleri eş zamanlı optimize etmek, termal sistemlere güneş enerjisi entegrasyonunda yeni bir bakış açısı kazandırmıştır.

Sonuçlar yüksek sıcaklıkta endüstriyel atık ısı entegrasyonuna sahip konfigürasyonun incelenen sistemler arasında en ucuz olanı olduğunu göstermektedir. Şubat ayında, güneş enerjisinin düşük olduğu için, güneş kolektörleri Birimlerin toplam maliyetini arttırmaktadır. Bununla birlikte, Haziran ayında güneş kolektörleri ayrı kolektör formlarında daha fazla Yapılandırma maliyetini düşürmektedir. Ek olarak, merkezi güneş alanı konfigürasyonlarına entegrasyon, hem Şubat hem de Haziran aylarında yakıt tüketimini ve toplam maliyetini arttırırken, ayrı kolektörlere kıyasla daha fazla kolektör alanı kullanmaktadır. Bunun arkasındaki asıl sebep, kullanılmış olan küçük depolama tanklarının güneş enerjisinin boşa harcanmasına neden olmasıdır. Sonuç olarak, ayrılmış güneş kolektörleri ve depolama tankları, incelenen Konfigürasyonlar arasında merkezi güneş alanından daha iyi performans göstermektedir.

Anahtar Kelimeler: Doğrusal Olmayan Optimizasyon, Isı Dağıtım Ağı, Güneş Enerjisi

To my parents

ACKNOWLEDGEMENTS

I would like to express my sincerest appreciation to my thesis co-supervisor, Prof. Dr. Derek K. Baker for his guidance and support. Dr. Baker was in USA during writing this thesis. Dr. Baker is a real academician who taught me correct research methodology and many things.

Words cannot express how grateful I am to my parents Masumeh Behjetkhah and Ali Karimi for their irreplaceable unfailing support and continuous encouragement throughout my years of study. This accomplishment would not have been possible without them.

TABLE OF CONTENTS

ABSTRACT	v
ÖZ	vii
ACKNOWLEDGEMENTS	x
TABLE OF CONTENTS	xi
LIST OF TABLES	xiv
LIST OF FIGURES	xvi
LIST OF ABBREVIATIONS	xxii
LIST OF SYMBOLS	xxiii
1. INTRODUCTION	1
2. SURVEY OF LITERATURE AND OBJECTIVES	5
2.1. Literature Review	5
2.2. Motivation and Objectives	17
2.3. Thesis Scope	19
3. TRNSYS COMPONENTS MATHEMATICAL MODELS	25
3.1. TRNSYS	25
3.2. TRNSYS Components Mathematical Models	28
3.2.1. Boiler (Type 700)	29
3.2.2. Heat Exchanger with Hot-Side Bypass (HX1)	31
3.2.3. Counterflow Heat Exchanger (HX2)	33
3.2.4. Solar Collector (Type 1b)	36
3.2.5. Heat Storage Tank (Type 4) [49]	37
3.2.6. MATLAB Link	39

3.2.7. Weather Data Processor	39
3.2.8. Forcing Function	40
3.2.9. Pump (Type 3d).....	42
3.2.10. Tee-Piece, Flow Mixer and Flow Diverter.....	43
4. IZMIR AND SOLAR ENERGY	47
4.1. Solar Collectors' Inclination and Azimuth Angles.....	47
4.2. Selection of time periods to simulate.....	49
5. COST OPTIMIZATION AND ECONOMIC PARAMETERS.....	53
5.1. Optimization Procedure	53
6. CONFIGURATIONS.....	61
6.1. Result Validation.....	67
6.2. Configuration 1	71
6.2.1. Cost Calculation	72
6.2.2. Results	72
6.3. Configuration 2	73
6.3.1. Configuration 2-1	74
6.3.2. Configuration 2-2	77
6.3.2.1. Optimization Procedure.....	82
6.3.2.2. Results.....	85
6.4. Configuration 3	89
6.4.1. Configuration 3-1	89
6.4.1.1. Optimization Procedure.....	93
6.4.1.2. Results.....	94
6.4.2. Configuration 3-2	103

6.4.2.1. Optimization Procedure	106
6.4.2.2. Results	107
6.5. Configuration 4.....	117
6.5.1. Results.....	122
6.6. Monthly cost of selected Configurations.....	129
7. CONCLUSION.....	134
7.1. Summary of thesis	134
7.2. Main Conclusions.....	136
7.3. Future Works	139
REFERENCES.....	143
A. Configuration 2-2 Data	147
B. Configuration 3-1 Data	166
C. Configuration 3-2 Data	180
D. Configuration 4 Data	189
E. Validation Code	207

LIST OF TABLES

TABLES

Table 2.1. Temperature regions relevant for solar process heat integration. IPH: Industrial Process Heat [11].....	7
Table 2.2. Solar process heat for potential industrial sectors and processes [1].	11
Table 3.1. Parameters and inputs for boiler	31
Table 3.2. Parameters and inputs for Heat Exchanger (HX1)	33
Table 3.3. Parameters and inputs for Heat Exchanger (HX2)	35
Table 3.4. Parameters for Solar Collector	36
Table 3.5. Inputs for Solar Collector. Note weather data processor is Type 15 and pump is Type 3	37
Table 3.6. Parameters for Heat Storage Tank.....	39
Table 3.7. Parameters for Pump	42
Table 5.1. Cost Units and Economic Parameters	55
Table 6.1. Fuel and HDN construction cost units for Hwa Chae et al. [41] study and the thesis study.....	70
Table 6.2. Validation of system's cost based on Hwa Chae et al. [41] and the thesis methods.....	71
Table 6.3. Component's name, flow rate and temperature of streams in Figure 6.18. The constant amounts of variables are presented beside each one inside parenthesis.	81
Table 6.4. Component's name, flow rate and temperature of streams in Figure 6.24. The constant amounts of variables are presented beside each one inside the parenthesis.	92
Table 6.5. Component's name, flow rate and temperature of streams in Figure 6.36. The constant amounts of variables are presented beside each one inside parenthesis.	106

Table 6.6. Components' name, flow rate and temperature of streams in Figure 6.48. The constant amounts of variables are presented beside each one inside parenthesis.	121
Table 6.7. Selected Configurations for Section 6.6. V_s = storage tank volume, T_w = industrial waste heat temperature, A_s = solar collector area, m_s = mass flow rate to solar collector.....	129
Table 6.8. Storage tank, solar collector and fuel monthly cost for selected Configurations for February.....	130
Table 6.9. Storage tank, solar collector and fuel monthly cost for selected Configurations for June.....	132

LIST OF FIGURES

FIGURES

Figure 1.1. Total final energy consumption in 2014 [3].....	2
Figure 2.1. Possible integration points for solar process heat applications [9]	5
Figure 2.2. Solar energy integration to galvanic bath heating [5]	13
Figure 2.3. Steam generation with parabolic trough collectors for an industrial steam line [37].....	14
Figure 2.4. Map of an industrial zone. Red circles represent industrial units, blue network shows HDN and yellow circle shows the central solar field location [38]..	15
Figure 3.1. Schematic Diagram of a system in TRNSYS.....	26
Figure 3.2. Example parameter (a), input (b) and output (c) windows for TRNSYS components	27
Figure 3.3. Sample connection window between boiler and heat exchanger	28
Figure 3.4. Schematic Diagram of the heat exchanger with hot side bypass	32
Figure 3.5. Schematic Diagram of the Heat exchanger (Type 5)	34
Figure 3.6. Typical solar heat system which uses water tank as heat storage tank [49]	38
Figure 3.7. Forcing functions for boiler input water flow in (a) Unit 1, (b) Unit 2...41	
Figure 3.8. Forcing functions for solar collector pump's control signal in Units 1 and 2	42
Figure 3.9. Tee-Piece (Type 11h)	43
Figure 3.10. Flow mixer (Type 649)	44
Figure 3.11. Diverter (Type 11f)	45
Figure 4.1. Monthly Average Solar Irradiation in Izmir with different collector slopes	48
Figure 4.2. TRNSYS system for evaluating collector output temperature	49

Figure 4.3. Solar collector output temperature profile in Izmir during winter (Jan., Feb., Mar.). For the three months hours start from 1st to 2160 th hour of whole year.	50
Figure 4.4. Solar collector output temperature profile in Izmir for spring (Apr., May., June). For the three months hours start from 2160 th to 2160 th hour of whole year...50	50
Figure 4.5. Solar collector output temperature profile in Izmir for summer (July, Aug., Sep.). For the three months hours start from 4345 th to 6552 th hour of whole year...51	51
Figure 4.6. Solar collector output temperature profile in Izmir for fall (Oct., Nov., Dec.). For the three months hours start from 6553 th to 8760 th hour of whole year...51	51
Figure 5.1. Main parts of optimization in the thesis	54
Figure 5.2. Schematic Diagram of Configuration 4.....	58
Figure 6.1. Schematic Diagram of Unit 1	62
Figure 6.2. Unit 1 in TRNSYS.....	63
Figure 6.3. Flow rate profiles for Unit 1 in Feb. and June. HX1ColdOutFlow represents flow rate in Unit 1 process side, HX2ColdOutFlow shows the inlet flow rate to cold side of HX2 in Unit 1 and BoilerOutFlow shows Unit 1 supply side flow rate.....	64
Figure 6.4. Temperature profiles in Unit 1 in Feb. and June. BoilerOutTemp shows Unit 1 supply side temperature, HX1ColdOutTemp represents temperature in Unit 1 process side and HX2ColdOutTemp shows the inlet temperature to cold side of HX2 in Unit 1.	64
Figure 6.5. Schematic Diagram of Unit 2	65
Figure 6.6. Unit 2 in TRNSYS.....	65
Figure 6.7. Flow rate profile in Unit 2 in Feb. and June. BoilerOutFlow shows Unit 2 supply side flow rate, HX1ColdOutFlow represents flow rate in Unit 2 process side, HX2ColdOutFlow shows the inlet flow rate to cold side of HX2 in Unit 2. HX1ColdOutFlow coincide with HX2ColdOutFlow Diagram.....	66
Figure 6.8. Temperature profile in Unit 2 for Feb. and June. BoilerOutTemp shows Unit 2 supply side temperature, HX1ColdOutTemp represents temperature in Unit 2	

process side and HX2ColdOutTemp shows the inlet temperature to cold side of HX2 in Unit 2.	66
Figure 6.9. Optimization result by MILP method in Hwa Chae et al. study [41].	68
Figure 6.10. Comparing the Hwa Chae et al [41] case study results with the thesis results for both before and after system optimization.	70
Figure 6.11. Overall view of Configuration 1	72
Figure 6.12. Hourly cost for Unit 1 and 2 and their total cost in Feb. and June.....	73
Figure 6.13. Configuration 2-1 in basic form. Unit 1 boiler efficiency is 0.7 and for Unit 2 boiler efficiency is 0.5.	75
Figure 6.14. Schematic Diagram of Configuration 2-1.	75
Figure 6.15. Configuration 2-1 in boilers coupled form.....	76
Figure 6.16. Total cost of Configuration 2-1 in two forms (basic and boilers coupled). The title Conf2-1BTotalCost shows the basic form hourly cost and Conf2-1CTotalCost shows boilers coupled situation's hourly cost.....	77
Figure 6.17. Schematic Diagram of Configuration 2-2. Diverter 1, Diverter 3 and Diverter 6 are controlled by optimization outputs.	79
Figure 6.18. Configuration 2-2 in TRNSYS.....	80
Figure 6.19. Optimization results for three decision variables, M1,M2 and M3, and storage tank average temperature, STAvg.Temp. M1 and M2 Diagrams coincide. Storage tank volume is 1 m ³ and waste heat temperature is 100 °C.	85
Figure 6.20. The impact of waste heat temperature on total cost of Configuration 2-2. Storage tank volume is 1 m ³	86
Figure 6.21. The impact of storage tank volume on total cost of Configuration 2-2. Waste heat temperature is 100 °C.	87
Figure 6.22. MATLAB vs. TRNSYS cost for Configuration 2-2 with waste heat temperature 100 °C and storage tank volume 1 m ³	88
Figure 6.23. Schematic Diagram of Configuration 3-1. Diverter 1 and Diverter 3 control signals are optimization outputs.	90
Figure 6.24. Configuration 3-1 in TRNSYS.....	91

Figure 6.25. Optimization results for two Diverters, M1 and M2, the storage tank average temperature (STAvg.Temp), the process side temperature (THX2) and the boiler feed water temperature (T2, Div1) for Configuration 3-1 in February. Storage tank volume is 1 m ³ and solar collector area is 20 m ²	95
Figure 6.26. Optimization results for two Diverters, M1 and M2, the storage tank average temperature (STAvg.Temp), the process side temperature (THX2) and the boiler feed water temperature (T2, Div1) for Configuration 3-1 in June . Storage tank volume is 1 m ³ and solar collector area is 20 m ²	96
Figure 6.27. Total cost for Configuration 3-1 with different collector areas AS=20, 30 and 60 m ² vs. total cost of Unit 1 in Configuration 1 (Conf1Total Cost) in February. Storage tank volume was assumed 1 m ³	98
Figure 6.28. Magnified view to Figure 6.27.	98
Figure 6.29. Total cost for Configuration 3-1 with different collector areas AS=20, 30 and 60 m ² vs. total cost of Unit 1 in Configuration 1 (Conf1Total Cost) in June. Storage tank volume was assumed 1 m ³	99
Figure 6.30. Magnified view to Figure 6.29.	99
Figure 6.31. Configuration 3-1 total cost with different storage tank volumes vs. Unit 1 cost in Configuration 1 for February. Storage tank volume is assumed: VS= 1, 2 and 5 m ³ and solar collector area is 20 m ²	100
Figure 6.32. Configuration 3-1 total cost with different storage tank volumes vs. Unit 1 cost in Configuration 1 for June. Storage tank volume is assumed: VS= 1, 2 and 5 m ³ and solar collector area is 20 m ²	101
Figure 6.33. MATLAB vs. TRNSYS calculated the hourly cost for Configuration 3-1 in February.	102
Figure 6.34. MATLAB vs. TRNSYS calculated the hourly cost for Configuration 3-1 in June.	102
Figure 6.35. Schematic Diagram of Configuration 3-2. Diverter 1 control signal is optimization output.	104
Figure 6.36. Configuration 3-2 in TRNSYS.	105

Figure 6.37. Configuration 3-2 diverter control signal, M1, vs storage tank average temperature, STAvg.Temp, and HX2 source side out temperature, HX2OutTemp for February. The collector area is 20 m² and storage tank volume is 1 m³..... 108

Figure 6.38. Configuration 3-2 diverter control signal, M1, vs. storage tank average temperature, STAvg.Temp, and HX2 source side out temperature, HX2OutTemp for June. The collector area is 20 m² and storage tank volume is 1 m³..... 108

Figure 6.39. Unit 2 total cost in Configuration 1 vs. Unit 2 total cost in Configuration 3-2 with different flat plate collector areas (AS=20, 30, 60 m²) and constant storage tank volume, 1m³, in February. 110

Figure 6.40. Unit 2 total cost in Configuration 1 vs. Unit 2 total cost in Configuration 3-2 with different flat plate collector areas (AS=20, 30, 60 m²) and constant storage tank volume 1m³ in June..... 110

Figure 6.41. Unit 2 total cost in the Configuration 1 vs. Unit 2 total cost in Configuration 3-2 with different storage tank volumes, VS=1, 2, 5 m³ and 20 m² solar collector area in February. 112

Figure 6.42. Storage tank average temperature profile for tanks with 1, 2 and 5 m³ volumes and 20 m² collector areas in Configuration 3-2 for February. 112

Figure 6.43. Unit 2 total cost in the Configuration 1 vs. Unit 2 total cost in Configuration 3-2 with different storage tank volumes, VS=1, 2, 5 m³ and 20 m² solar collector area in June. 114

Figure 6.44. Storage tank average temperature profile for tanks with 1, 2 and 5 m³ volumes and 20 m² collector areas in Configuration 3-2 for the June..... 114

Figure 6.45. Configuration 3-2 total cost by MATLAB vs. TRNSYS in February. 116

Figure 6.46. Configuration 3-2 total cost by MATLAB vs. TRNSYS in June. 116

Figure 6.47. Schematic Diagram of Configuration 4. Diverter 1, Diverter 3 and Diverter 6 are the diverters which are controlled by optimization outputs. 119

Figure 6.48. Configuration 4 in TRNSYS 120

Figure 6.49. Configuration 4 diverters' control signals, M1 (a), M2 (b) and M3(c), vs. storage tank average temperature, STAvg.Temp., for February. Solar collector area is 100 m² and storage tank volume is 1m³. 123

Figure 6.50. Configuration 4 diverters' control signals, M1 (a), M2 (b) and M3(c), vs. storage tank average temperature, STAvg.Temp., for June. Solar collector area is 100 m ² and storage tank volume is 1 m ³	124
Figure 6.51. Configuration 1 vs. Configuration 4 total hourly cost for February with different solar field's collector areas, AS=100, 120 and 150 m ² . Storage tank volume is 1 m ³	125
Figure 6.52. Configuration 1 vs. Configuration 4 total hourly cost for June with different solar field's collector areas, AS=100, 120 and 150 m ² . Storage tank volume is 1 m ³	126
Figure 6.53. Configuration 1 vs. Configuration 4 total hourly cost for February with different storage tank volumes, VS=1, 2 and 5 m ³ . Solar collector area is 100 m ² . 127	
Figure 6.54. Configuration 1 vs. Configuration 4 total hourly cost for June with different storage tank volumes, VS=1, 2 and 5 m ³ . Solar collector area is 100 m ² . 127	
Figure 6.55. Configuration 4 total cost by MATLAB and TRNSYS in February. Solar collector area is 100 m ² and storage tank volume is 1 m ³	128
Figure 6.56. Configuration 4 total cost by MATLAB and TRNSYS in June. Solar collector area is 100 m ² and storage tank volume is 1 m ³	128
Figure 6.57. Storage tank, solar collector and fuel monthly cost for selected Configurations for February.....	130
Figure 6.58. Storage tank, solar collector and fuel monthly cost for selected Configurations for June.....	132
Figure A.1. Total hourly fuel consumption for Configuration 1 and Configuration 2-2 for both February and June. Waste heat temperature is 100°C and storage tank volume is 1 m ³	147

LIST OF ABBREVIATIONS

CRF	Capital Recovery Factor
CHP	Combined Heat and Power
Div1	Diverter 1
Div3	Diverter 3
Div6	Diverter 6
EIP	Eco Industrial Park
HDN	Heat Distribution Network
HTF	Heat Transfer Fluid
IEA	International Energy Agency
INSHIP	Integrating National Research Agendas on Solar Heat for Industrial Processes
MILP	Mixed Integer Linear Programming
SHIP	Solar Heat for Industrial Processes

LIST OF SYMBOLS

\dot{Q}_{need}	Boiler energy requirement
\dot{Q}_{in}	Boiler inlet energy
$\dot{Q}_{\text{max}}/\dot{Q}_{\text{min}}$	Boiler max./min. capacity
n	Component life span
C	Cost
M	Diverter control signal
Q_{HX}	Energy transfer across heat exchanger
$T_{\text{eva.}}$	Fluid evaporation temperature
C_p	Fluid heat capacity
$\Delta H_{\text{ev.}}$	Fluid latent heat of vaporization
T_{in}	Inlet temperature
i	Interest rate
\dot{m}	Mass flow rate
UA	Overall heat transfer coefficient
CS_p	Pump control signal
T_{set}	Set point temperature
A_s	Solar collector area
UA_s	Storage tank loss coefficient
V_t	Storage tank volume

GREEK SYMBOLS

$\eta_{\text{boiler,combustion}}$	Boiler combustion efficiency
η_{boiler}	Boiler efficiency
γ	Bypassed fraction of fluid in hot-side of HX1 heat exchanger
ε	Heat exchanger effectiveness

CHAPTER 1

INTRODUCTION

Concerns about sustainable industrial development, greenhouse gas emissions, global warming, and decrement of fossil fuel reserves are featuring the importance of renewable energy sources more and more. Solar energy as an abundant renewable energy source has proven a huge potential to satisfy energy demand in both residential and industrial sectors.

Solar energy utilization for residential units has been investigated thoroughly and related technologies have been matured, but what has not been addressed sufficiently is the industrial application of solar energy.

Most energy in industries is consumed to provide low, medium or high temperature flows to be used in processes which are known as process heat. Industries use fossil fuels to provide their process heat, however solar thermal energy potential to replace or reduce fossil fuel consumption has been neglected in industrial sectors [1].

Just 0.3% of all installed solar thermal capacity is used for providing industrial process heat while among all solar heating and cooling applications, solar process heat has the highest potential [2]. Regarding the potential contribution of solar energy in industrial sectors and the gap in the research and development of this field, European Union defined the INSHIP (Integrating National Research Agendas on Solar Heat for Industrial Processes) project. INSHIP aims to create a synergistic framework between EU major research institutes to collaborate effectively and share structures in the solar process heat research and development field. In addition, INSHIP with some industrial partners' cooperation tackles the technological challenges to penetrate more solar process heat in different industrial sectors [2].

Industries and manufacturing sectors consume a major portion of total energy consumption. Figure 2 shows percentages of heat demand in the world. More than half of industrial heat is consumed as low and medium temperature flows which are most potential ones to be provided by solar energy [3].

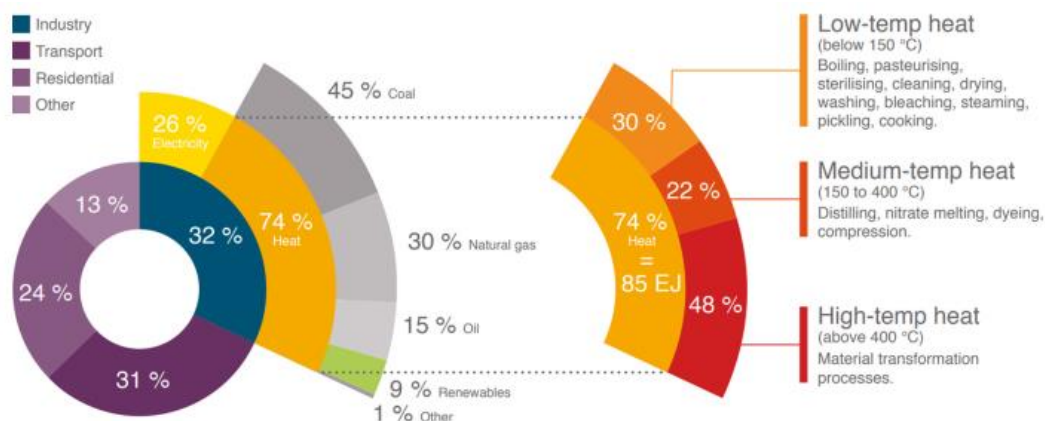


Figure 1.1. Total final energy consumption in 2014 [3]

Solar energy usage in industries could create more added values in comparison with residential applications. More importantly, renewable energy integration and sharing materials and energy between industrial units emerge eco-industrial parks (EIP) concept which could actualize sustainable industrial development [4].

Besides the potentials, regarding the high expense of high-temperature production with solar energy and difficulty of satisfying energy demand of industries, because of solar energy variation, nowadays few large scale industrial applications of solar thermal systems are operational. In addition, industries benefit from lower energy cost than that of residential units and solar heat integration needs machinery modification. All these factors make solar energy integration more difficult. [5,6,7].

Turkey is facing a rapidly growing population and economy and the country needs the energy to keep up with this sustainable development. In this regard, Industrial parks play a crucial role in the economic growth of countries, especially for developing and emerging economies such as Turkey [4]. In addition, Turkey strongly depends on

imported energy sources (oil and natural gas) and this highlights the energy security issues for Turkey while it profits from unique geographical location with rich solar potential. By considering all of these factors, solar energy could be a promising potential energy source for future Turkey energy demand [8].

CHAPTER 2

SURVEY OF LITERATURE AND OBJECTIVES

2.1. Literature Review

Industrial sectors have different layout and structures. Therefore, the first step in integrating solar thermal systems in industries is determining integration point, where solar energy will be integrated into industries' thermal system [5]. This could include an optimization procedure to choose proper integration point for the best energy efficiency of the system. Figure 1 summarizes the varied integration points in industries.

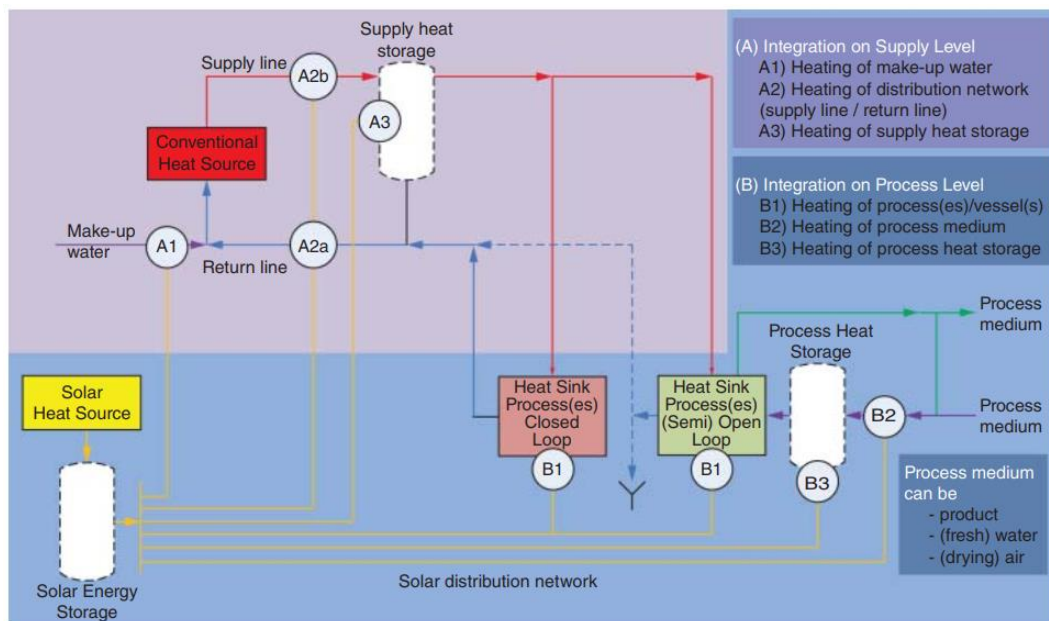


Figure 2.1. Possible integration points for solar process heat applications [9]

Generally, all integration points could be classified into two categories: Supply side and process side integration points [9]. Supply-side solar energy integration means

using solar energy in central energy supply system which includes heating a make-up water, central energy storage, the return flow to the conventional heat source or direct heat transfer to supply line (direct steam generation.) [5,10].

When solar energy is used locally in a process inside the industry energy system, it has been used in the process side. Supply-side or process side integration depends on industry process specifications. Heating process medium, process vessel and process heat storage are general categories of process side solar energy integration [9]. Generally, the integration point in different industries depends strongly on the temperature level in the process and the type of collector that could be used.

Collector accumulates heat energy from incident radiation and transfers it to the working fluid such as oil, air or water. There are different types of collectors which are applicable to produce outlet temperature range 80-250°C. Flat plate collectors, evacuated tube collector and small parabolic trough collector are the most common ones for different operating temperatures [5].

Flat plate collector is the most used type of collector in installed SHIP (Solar Heat for Industrial Processes) projects. Their popularity comes from high absorbance efficiency and their lower capital cost. In evacuated tube collectors, absorber plate has been placed inside evacuated cylindrical glass tubes to prevent heat loss by convection. Their cost is higher than that of flat plate collectors, but they could produce higher output temperature.

By parabolic trough collector, high temperature such as 400°C for output temperature is achievable. They primarily reflect incoming irradiation and then concentrate it on a solar absorber. Unlike flat plat and evacuated tube collectors which are stationary collectors, parabolic trough collectors always track the sun to work in maximum efficiency. The temperature grade that is necessary in the process, space availability, available solar energy and economic feasibility are main factors in collector type selection [1].

Kurup and Turchi [11] categorized solar process applications according to heat transfer fluid (HTF), the temperature range and the collector technology in Table 2.1.

Table 2.1. *Temperature regions relevant for solar process heat integration. IPH: Industrial Process Heat [11]*

Temperature range	Solar collector type	HTF	Applications
< 80 °C	Flat plate Non-tracking compound parabolic Solar pond	Water	Hot water Space heating
80–200 °C	Parabolic trough Linear Fresnel	Water/steam	Hot water or steam for IPH (Industrial Process Heat)
200–300 °C	Parabolic trough Linear Fresnel	Mineral oil	Steam for IPH
300–400 °C	Parabolic trough Linear Fresnel	Synthetic oil	Steam for IPH

Numerous studies surveyed different industries with different processes to recognize solar energy utilization potential in them. Most of these studies used the same methodology. Initially, they introduced temperature ranges in different processes. Then, some studies identified most qualified industries, some recognized best industrial processes and some presented both for solar process heat integration.

Schweiger et al. [12] studied the solar process heat potential of industries in different countries such as U.S.A, Switzerland, Germany, U.K, Japan, Portugal, and Spain. They concluded industrial heat demand forms 15% of total energy demand in Europe and more than half of this energy demand is in a temperature range lower than 250 °C. Authors introduced food industry (66%), chemical industry (58%) and textile industry (30%) as best industries to integrate solar energy. The percentage amounts show the fraction of industry energy which could be provided by solar energy. Specially, they presented brewing refrigeration, milk sterilization industry (110 – 150 °C), drying

processes for textile industry (120 – 220°C) and paper industry (180°C) as best processes for solar energy utilization.

The potential of Cyprus industries to use solar energy was studied by Kalogirou [13]. Again the author recognized food industries, especially milk and meat industries and breweries as industries with the great potential to couple solar heat with their process heat systems.

The report of task 49 of IEA Solar Heat and Cooling by Krummenacher and Muster indicates 19% of Europe total heat demand is in medium temperature range (100–400 C). According to this report, chemical, food, drink, tobacco, and paper industries have the highest demands at medium temperature [14].

Vannoni et al. showed the results of ECOHEATCOOL project which analyzed heat demand in industrial sectors of 32 countries (EU25+Bulgaria, Romania, Turkey, Croatia, Iceland, Norway, and Switzerland). Similar to Solar Heat for Industry study [3], The ECOHEATCOOL demonstrated that 30% of the industrial heat demand is below 100 °C, 27% is at medium temperature range (100–400°C) and 43% at high temperature range (over 400 °C) [15].

Kurup and Turchi [11] also made an evaluation of the potential integration of concentrated (Parabolic Trough Collectors and Linear Fresnel) solar heat in industrial processes, in the state of California. They concluded that the most common range of temperatures of industrial steam was between 120 and 220 °C, and usually below 260 °C. Food, paper, petroleum, chemicals, and primary metals are five industries identified by the authors based on previous research, which used more steam at less than 260 °C.

Farjann et al. [1] have done a thorough study of solar process heat. They tried to give a comprehensive view about the current and future situation of industrial applications of solar energy. Their study could be divided into two main parts. First, they discussed the potential processes that can adopt solar process heating. In the second part, they

present the most compatible industries for solar heat integration. The authors' work has been summarized in Table 2.2.

According to their study, the processes of water heating, drying, preheating, steam heating, pasteurization and sterilization and washing are the most applicable processes in various industrial sectors that solar heat has been integrated. Most of the mentioned processes use temperature grades lower than 150 °C, which makes them suitable to integrate solar energy.

Actually, water heating is the most applied industrial process with solar heat integration. SHIP plants report [16] illustrates the main industrial sectors using solar water heating, the collector type and their operational temperature range. According to this report, breweries and food industries already installed highest number of solar water heating units.

For the drying process, moisture should be extracted from material by heating. The material which could be fruit, plants, textile and mineral materials. The heat media for drying is generally warm air [1]. Pirasteh et al. reviewed industrial and agricultural applications of the solar drying process. They analyzed the energy consumption capacity of different solar drying technologies [17].

Solar thermal energy is the ideal energy source for preheating processes with low grade temperature applications. Typical examples are water preheating and boiler feed water preheating [1]. Steam heating process is usually actualized with parabolic trough collectors. This is among the solar process heat applications with the highest capital cost. Valenzuela et al. [18] numerically examined the performance of direct steam production by parabolic trough collector under different design conditions.

Some of energy-intensive processes in food industries are pasteurization and sterilization processes. These processes are mostly utilized in dairy industries. Different studies examined solar pasteurizer and solar sterilizer applications [19, 20, 21]. Furthermore, in the industrial washing process, there is a need for mass of warm water which provides excellent opportunity to use solar heating. Washing bottles,

barrels, and containers in the food industry, metal surface treatment such as galvanizing and varnishing, textile industries and laundries are potential industrial applications of solar integrated washing process [1,22].

Table 2.2 [1] presents a comprehensive list of potential solar process applicable industrial sectors, the related industrial processes and their temperature ranges which could be a good guideline to choose proper process with suitable collector technology to provide necessary temperature range. Table 2.2 indicates food and beverage industries have many processes with low process temperature which nominates these industries as most potential ones for solar process heat integration.

According to task 33 of IEA-ETSAP report, 51% of all installed solar process heating systems in industries were used for water heating and washing processes, 14% of systems were used for heating of bathes and vessels, 6% for drying and 29% for other applications such as car washing [10]. Similarly, the mentioned processes have been distinguished as the most potential processes in almost many studies [23,24,25,26].

Table 2.2. *Solar process heat for potential industrial sectors and processes [1].*

Sector	Process	Temperature Range (°C)	
Chemicals	Biochemical reaction	20 – 60	
	Distillation	100–200	
	Compression	105–165	
	Cooking	80–100	
	Thickening	110–130	
Foods & beverages	Blanching	60–100	
	Scalding	45–90	
	Evaporating	40–130	
	Cooking	70–120	
	Pasteurization	60–145	
	Smoking	20–85	
	Cleaning	60–90	
	Sterilization	100–140	
	Tempering	40–80	
	Drying	40–200	
	Washing	30–80	
	Paper	Bleaching	40–150
		De-inking	50–70
Cooking		110–180	
Drying		95–200	
Fabricated Metal	Pickling	40–150	
	Chroming	20–75	
	Degreasing	20–100	
	Electroplating	30–95	
	Phosphating	35–95	
	Purging	40–70	
	Drying	60–200	
	Textiles	Bleaching	40–100
Coloring		40–130	
Drying		60–90	
Washing		50–100	
Fixing		160–180	
Wood	Pressing	80–100	
	Steaming	70–90	
	Pickling	40–70	
	Compression	120–170	
	Cooking	80–90	
Dairy	Drying	40–150	
	Pressurization	60–80	
	Sterilization	100–120	
	Drying	120–180	
	Concentrates	60–80	
Tinned food	Boiler feed water	60–90	
	Sterilization	110–120	
	Pasteurization	60–80	
	Cooking	60–90	
Meat	Bleaching	60–90	
	Washing	60–90	
	Sterilization	60–90	
	Cooking	90–100	

In addition, a comprehensive sector-wise analysis has been done by Farjann et al. [1]. According to their study, automobile, breweries and food, paper and textile industries are most potential industries for solar process heat application. That selection of industries agrees with other reports or publications' results [5,11,12,15,23,24,25,26].

Solar process heat is used for heating water for painting operation, washing engine components and metal sheet treatment processes in the automobile industries. Uppal et al. investigated operational solar process heat systems in Indian automobile factories and categorized the processes based on process energy intensively [27].

For brewery industries, solar energy could apply for steam generation, malting process, providing heat for washing machines, air cooling and preheating the bottles. The temperature range in different malting plant processes is 25 to 120°C, which makes them suitable for solar heat utilization with flat plat collectors [28,29,30].

Many studies and reports concluded that food industries consist of the most suitable processes for solar process heat integration. Pasteurization, sterilization, hydrolyzing, drying, evaporation, distillation, cleaning and washing are some of the potential opportunities inside the scope of food industries to use solar heat. The various low graded temperature (below 150 °C) processes and the extent of this sector make the food industries as a dominant candidate to use solar process heat. The leading countries such as Mexico, USA, Greece, India, Spain and Australia already installed solar process heat units in their food industries and this is rapidly growing in other countries. In the most of operational solar heat production units, flat plate collectors and parabolic-trough collectors provide solar energy for integrated units [31,32,33,34,35,36].

As one of the solar process heat application examples, galvanic baths for metal surface treatment are one of the best options to use solar energy. Their operational temperature is 60-70 °C which makes them suitable to use flat plate collectors. Figure 2.2 shows how solar collector provides energy for a galvanic bath. By initial heat exchanger, solar energy is transferred from collector to heat storage tank. Secondary heat

exchanger uses gathered energy in a storage tank to heat galvanize bath [5]. This is one of process side solar energy integration examples.

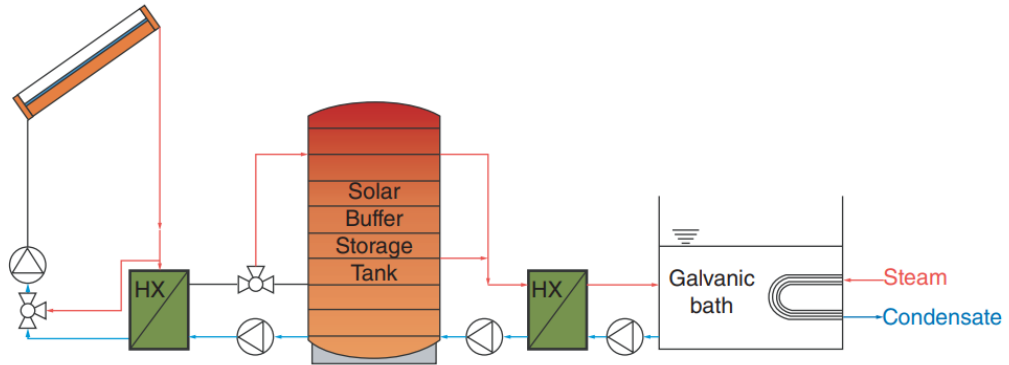


Figure 2.2. Solar energy integration to galvanic bath heating [5]

Steam boilers are most common heat supplier in industries which provide heat at a temperature up to 250°C. Regarding the heat demand of industries and available solar irradiation at the company site, direct solar steam production could be one of the concepts for solar process heat integration. Generally parabolic trough collectors are used in this technology. Figure 2.3 shows general layout of this technology. In this integration method, boiler feed water is fed to collectors and water is evaporated partially and it enters the steam drum to separate steam from liquid water. Steam is fed to main steam circuit and water is returned to the collector. Some operational plants are available now with this technology. This is one of the supply side solar energy integration examples [37].

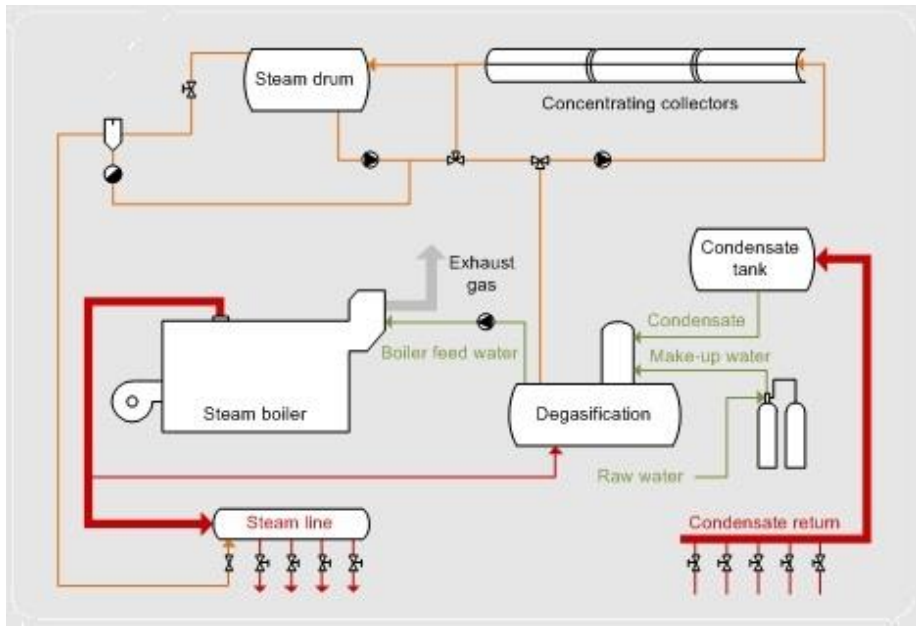


Figure 2.3. Steam generation with parabolic trough collectors for an industrial steam line [37]

Until now all the reviewed studies have investigated solar process heat integration in Unit scale. From a larger perspective, industrial zones consist of many industrial units which may do not access to sufficient or suitable space for separated solar collector areas. As a solution, researchers proposed a central solar thermal plant for an industrial zone and supplied solar heat is distributed between Units by a Heat Distribution Network (HDN).

Figure 2.4 shows a view from an industrial zone with a HDN which is fed by central solar field in Buoro et al. study [38]. Same HDN could be utilized for Units' waste heat or other energy sources sharing between industrial Units.

Hwa Chae et al. [41,42] optimized a waste heat utilization network for a petrochemical complex in South Korea with MILP method. They presented a four-step methodology for waste heat optimization in eco-industrial parks. According to their approach, energy information collection, analyzing energy data, optimization waste heat distribution network and evaluating final HDN economically and environmentally could be the steps toward optimal HDN design in each industrial zone. They reported 88% possible reduction in sink units' energy cost after HDN implementation in Yeosu national industrial complex, South Korea.

Similarly, Fichtner et al. [43] developed five-step methodology by using MILP method to design an HDN between different industries. They investigated barriers and opportunities for inter-firm connection with HDN. According to their finding, one of the most important barriers is dependency of industrial units when they are connected to each other with HDN which restricts the resource control and decision freedom for companies.

Chuan Zhang et al. [44] proposed a new methodology for waste heat recovery network design for industrial zones and studied the communities on Jurong Island of Singapore. Their method was similar to other studies' method but they eliminated non-feasible connections between units before optimization which reduced process time. In addition, they tackled the discontinuity problem in waste heat and they demonstrated that this could significantly influence optimization outcome.

Buoro et al. [45,46] have done many studies about HDN application for both residential and industrial Units energy supply. More importantly, they are among the few research groups that investigated central solar thermal plant function in energy production for an industrial zone. Again in most of their publications, MILP has been used for HDN optimization. They modeled a superstructure which includes district heating network, small-scale combined heat and power (CHP) units, large centralized solar plant and thermal storage inside an industrial zone. MILP defined the optimal layout of HDN, function, and the size of each component inside superstructure. Their

final aim was to minimize overall heat and electricity cost in an examined industrial zone. They defined four main configurations which included conventional configuration (there was not any CHP or HDN and conventional boilers provide units' energy), isolated configuration (there was not HDN but units were equipped with CHP units), distributed cogeneration configuration (both CHP and HDN were involved in model) and finally distributed renewable configuration (besides CHP units and HDN, the central solar thermal plant was entered into model).

Similar to other HDN design studies, they assumed constant temperature inside HDN. They concluded that the lowest cost is obtainable in a distributed renewable configuration which includes district heating network, thermal storage, and solar field. They obtained the optimum solar plant area and thermal storage volume. According to their results, the optimal solar thermal plant could provide 55-60% of industrial Units heat demand.

In another study [47], Buoro et al. performed a multi-objective optimization to minimize both energy cost and CO₂ emission. In that study, their final objective function was the sum of two functions, economic and environmental objective functions. These two functions with weight coefficients were related linearly to the final objective function.

2.2. Motivation and Objectives

Based on literature, the motivation of this thesis is modelling and optimizing of solar energy integration into two industrial Units' thermal system. In most studies, solar process heat just has been addressed from only unit scale or industrial zone scale. There is not a double-sided look. In the unit scale, the potential industrial sectors and processes have been identified for solar energy integration. The food industry has been opted as the best industrial sector to use solar process heat by many publications. Those studies, based on collectors' output temperature and process heat demand, suggested process side or supply side solar energy integration but collector output

temperature always changes. Therefore, hybrid integration (sometimes process side and sometimes supply side integration) could be an effective method to use the solar resource more efficiently. The hybrid solar process heat integration has not been studied in any research work.

In the industrial zone scale, studies have concentrated on the optimal HDN design for distributing industrial waste heat or solar energy between industrial units. Most of the studies tried to use linear optimization methods such as MILP to design optimal HDN layout. For this linearization, they assumed constant temperature inside HDN which could not be a credible assumption because solar energy and industrial waste heat could show variation in their temperature. This variation could significantly affect optimal results and it has not been studied completely. Previous studies are strong from the optimization point of view but weak from the thermal system modeling aspect. For this, a model should be developed to investigate solar energy integration in both unit scale and industrial clusters scale. Also, Fausto et al. [5] indicate the importance of these kind models for future solar process heat integrations.

TRNSYS is one of most powerful software for dynamic simulation of energy systems. Although TRNSYS provides different component libraries to model any system but it is weak from optimization point of view. MATLAB could provide powerful tools for optimization while using it for dynamic simulation of energy systems is really difficult and time consuming. With considering both software capabilities, the system simulation and system optimization was divided between TRNSYS and MATLAB respectively.

Thus, in the context of work package 5 of INSHIP project and tasks 5.3 (Hybrid energy supply systems) and 5.4 (Industry parks and heat distribution networks) [2] and regarding the mentioned gaps in hybrid integration of solar process heat and temperature variation inside HDN, the objectives for this research could be summarized as:

- Construction a thermal system model for two food industry units in Izmir within TRNSYS with different configurations which could use conventional boilers, solar energy or waste heat as an energy source. It will be possible to integrate solar process heat in supply side or process side or both based on an optimization results.
- Modeling the units' total energy cost by a non-linear objective function and minimizing the function with non-linear minimization method with MATLAB.
- Linking MATLAB to TRANSYS for controlling units in optimal condition with minimum cost.

2.3. Thesis Scope

In this thesis the energy cost in an industrial complex with two food industry units will be minimized by integrating solar energy and industrial waste heat. Numerous factors could affect the final cost. Detailed process simulation of industrial units, maximize solar energy gain and detailed study on the design of the solar field, HDN piping and cost calculation and long-term heat storage simulation is outside the scope of this thesis. Boilers fuel, solar collectors and thermal storage tank will be considered as main cost sources. Solar collector area, storage tank volume and waste heat temperature influence on final cost will be examined in this study. For this, different configurations will be modeled and investigated. In some configurations solar energy and for some others waste heat will be an energy source. Conventional boilers will exist in all configurations as backup energy suppliers.

All mathematical models of used components in Configurations are presented in Chapter 3. Chapter 4 discusses available solar energy in Izmir. Chapter 5 explains optimization procedure generally. Configurations thermal systems Diagrams and their

variables are shown in Chapter 6 and applied mathematical Equations for optimizing each Configuration are discussed in the thesis Appendices.

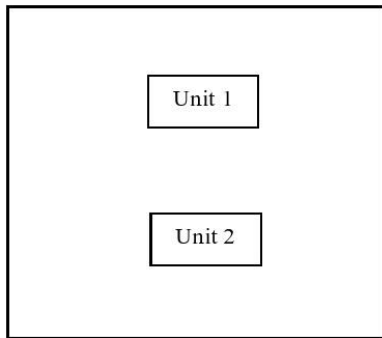
Figure 2.5 shows schematic Diagram of studied four different Configurations. Unit 1 and Unit 2 represent two industrial Units in the Configurations. Unit 1 works in just weekdays during the day and it is closed at night and weekends while Unit 2 operates continuously in day and night in all weekdays and weekends. Both Units have one boiler as main energy source and two heat exchangers to form their supply side and process side loops. Unit 1 and Unit 2 components are described in Chapter 3 and their thermal systems are discussed in Chapter 6 in more detail. In Figure 2.5, Configuration 1 is basic Configuration which boilers provide energy for Units. In Configuration 2-1, Unit 1 benefits from more efficient boiler than that for Unit 2. When Unit 1 is non-operational, it provides energy for Unit 2. In Configuration 2-2, an industrial waste heat stream is fed to a heat storage to share energy with Units. In Configuration 3-1, Unit 1 is equipped with separated solar collector and a heat storage and Configuration 3-2 simulates same condition for Unit 2. In final Configuration, Configuration 4, there is a large central solar field and a heat storage to integrate solar energy into both Units' thermal systems. The solar collector area in Configuration 4 is larger than that for Configuration 3-1 and Configuration 3-2 in separated collector condition.

The main assumption for different Configurations' modelling are:

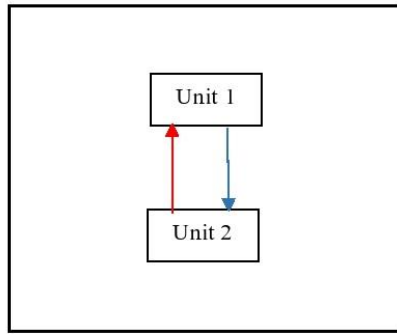
- Unit 1 works just in daytime in weekdays and it is closed at night and weekends.
- Unit 2 operates continuously 7/24.
- Unit 1 produces and consumes steam which could be used for pasteurization or cooking and because of contamination, it could not be reused.
- Waste heat for Configuration 2-2 is provided freely without any cost.
- Only boiler' fuel cost, heat storage tank and solar collectors' cost were assumed as main cost sources.
- Waste heat and boilers feed water streams were assumed in fixed temperature.
- Izmir was assumed as location in all simulations.

- Water was assumed as heat medium in all Configurations.

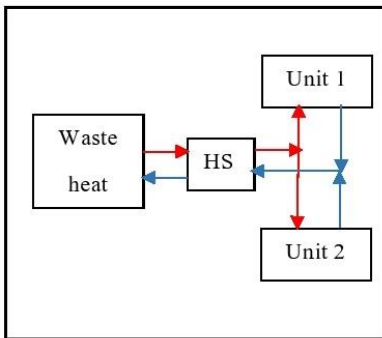
The main aim of this study is to show potential contribution of industrial waste heat and solar process heat to reduce total energy cost in industrial zones. This has been done with new approach which unlike former studies, thermal system modeling and optimization procedure have been divided between TRNSYS and MATLAB software respectively. This could create a simple benchmark model which is able to investigate solar process heat and industrial waste heat integration in various industrial processes conveniently.



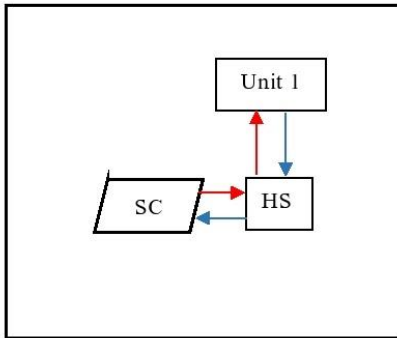
(a)



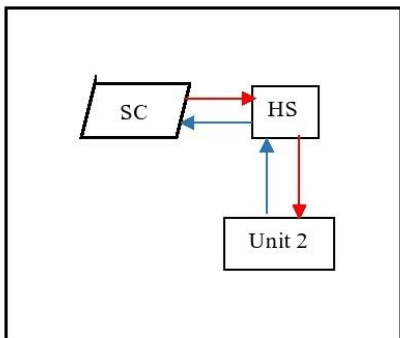
(b)



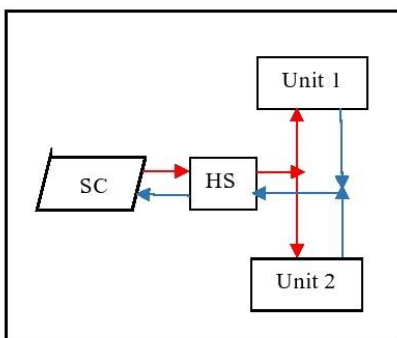
(c)



(d)



(e)



(f)

Figure 2.5. Studied Configurations: (a) Configuration 1 (b) Configuration 2-1 (c) Configuration 2-2 (d) Configuration 3-1 (e) Configuration 3-2 (f) Configuration 4. HS: Heat Storage. SC: Solar Collector.

CHAPTER 3

TRNSYS COMPONENTS MATHEMATICAL MODELS

This Chapter initially presents a brief introduction to TRNSYS. Then, the mathematical models of all used components in the thesis configurations are introduced.

3.1. TRNSYS

TRNSYS is a powerful simulation environment for transient simulation of thermal systems. A TRNSYS model is composed of several components, called Types. These components are connected to each other to simulate a complete system. TRNSYS types could exchange data and streams through connections among each other. Each type of component is described by a mathematical model in the TRNSYS simulation engine which is discussed in this section [48]. Figure 3.1 shows a system which has been simulated in TRNSYS. It includes most of the components which are used in the thesis Configurations such as boiler, heat exchanger, solar flat plate collector and heat storage tank. The colorful solid lines and dashed lines show flow and data transmission, respectively.

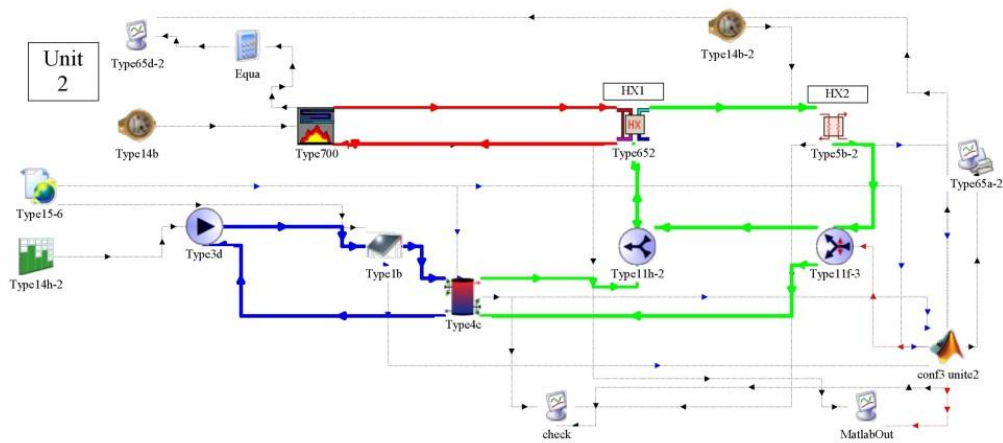


Figure 3.1. Schematic Diagram of a system in TRNSYS

The software and documentation for TRNSYS contain numerous examples and tutorials for how to develop energy models of simple energy systems, and interested readers are referred to this software and documentation for introductory information on how to use TRNSYS [48].

For specifying the variables of each type, three separated windows; parameters, inputs, and outputs windows are available. The user could set physical characteristics for each Type in its parameter window. Each parameter has a default value and if there is not any specification by user, its value will be fixed on its default value. The types could be linked together to get inputs or send outputs to other components.

Input window shows all inputs which are determined by other types' output or the ones that could be specified by user. Output window shows the output parameters which could be used as inputs for other components and it is used just for informatics purpose. As an example, Figure 3.2 shows screenshot of all three windows for a boiler (Type 700).

Parameter **Input** Output Comment

		Name	Value	Unit	More	Macro
1		Rated Capacity	470000.0	kJ/hr	More...	<input checked="" type="checkbox"/>
2		Fluid Specific Heat	4.190	kJ/kg.K	More...	<input checked="" type="checkbox"/>
3		Minimum Turn-Down Ratio	0.02	-	More...	<input checked="" type="checkbox"/>

(a)

Parameter **Input** Output Comment

		Name	Value	Unit	More	Macro
1		Inlet Fluid Temperature	20.0	C	More...	<input checked="" type="checkbox"/>
2		Inlet Fluid Flowrate	1000	kg/hr	More...	<input checked="" type="checkbox"/>
3		Input Control Signal	1	-	More...	<input checked="" type="checkbox"/>
4		Set Point Temperature	120.0	C	More...	<input checked="" type="checkbox"/>
5		Boiler Efficiency	0.78	Fraction	More...	<input checked="" type="checkbox"/>
6		Combustion Efficiency	0.85	Fraction	More...	<input checked="" type="checkbox"/>

(b)

Parameter **Input** Output Comment

		Name	Unit	More	Macro	Print
1		Outlet Fluid Temperature	C	More...	<input checked="" type="checkbox"/>	<input type="checkbox"/>
2		Outlet Fluid Flowrate	kg/hr	More...	<input checked="" type="checkbox"/>	<input type="checkbox"/>
3		Fluid Energy	kJ/hr	More...	<input checked="" type="checkbox"/>	<input type="checkbox"/>
4		Losses to Surroundings	kJ/hr	More...	<input checked="" type="checkbox"/>	<input type="checkbox"/>
5		Exhaust Energy	kJ/hr	More...	<input checked="" type="checkbox"/>	<input type="checkbox"/>
6		Required Boiler Energy Input	kJ/hr	More...	<input checked="" type="checkbox"/>	<input type="checkbox"/>
7		Part Load Ratio	-	More...	<input checked="" type="checkbox"/>	<input type="checkbox"/>

(c)

Figure 3.2. Example parameter (a), input (b) and output (c) windows for TRNSYS components

An important step in simulations is linking the variables which are output(s) of one component and input(s) for another component simultaneously. By double-clicking on the link, a graphical user interface (GUI) appears through which user could specify these variables. Figure 3.3 shows a sample connection window between boiler and heat exchanger. The user connects outputs of the first component (left-side) to necessary inputs of the second component (right-side).

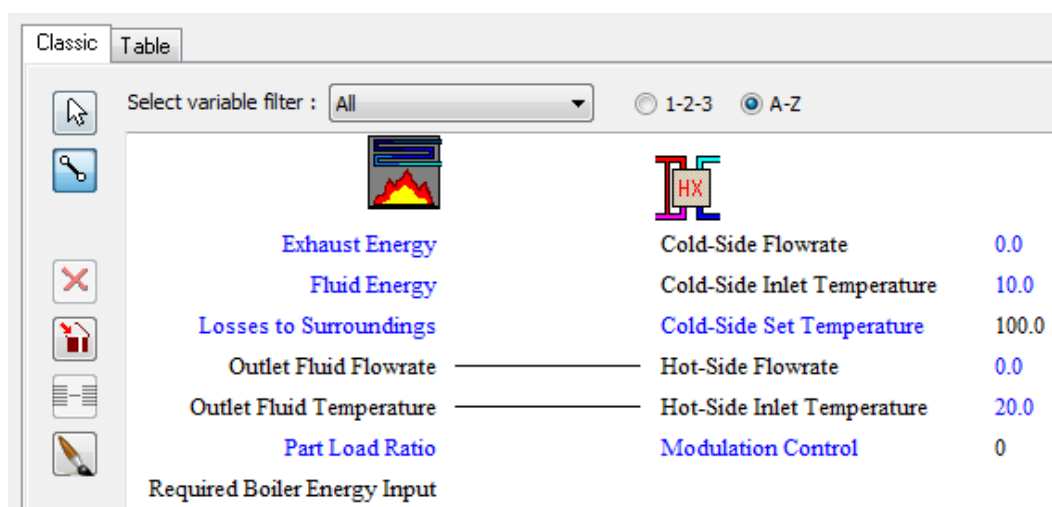


Figure 3.3. Sample connection window between boiler and heat exchanger

3.2. TRNSYS Components Mathematical Models

This section discusses mathematical models of all main components which have been used in the thesis Configurations. These mathematical models have been resulted from energy balance Equations for each component. All of these models have been used in the optimization procedure to drive objective functions. In addition, components' parameters and inputs are introduced in this section. The presented parameters will be constant in all configurations except when the effect of a variable on the total function of a Configuration is necessary to be investigated. The interested reader could refer to TRNSYS mathematical reference for detailed information [48].

3.2.1. Boiler (Type 700)

A simple steam boiler (Type 700) has been used in all Configurations as the main energy source. The boiler overall efficiency, boiler combustion efficiency, and boiler set point temperature are supplied as inputs to the model. Boiler set point temperature, T_{set} determines boiler output flow temperature. Because the heat media is water in all configurations, boiler uses Equation 3.1 to calculate the energy requirement, \dot{Q}_{need} if boiler inlet temperature, T_{in} , is higher than 100 °C. Otherwise, boiler will use Equations 3.2 to 3.5 to calculate, \dot{Q}_{need} , to elevate the temperature of the liquid from its inlet value to the set point value.

$$\dot{Q}_{need} = \dot{m}_{fluid} C_{p,water} (T_{set} - T_{in}) \quad (3.1)$$

$$\dot{Q}_{need} = \dot{Q}_1 + \dot{Q}_2 + \dot{Q}_3 \quad (3.2)$$

$$\dot{Q}_1 = \dot{m}_{fluid} C_{p,water} (T_{eva.} - T_{in}) \quad (3.3)$$

$$\dot{Q}_2 = \dot{m}_{fluid} \Delta H_{eva.} \quad (3.4)$$

$$\dot{Q}_3 = \dot{m}_{fluid} C_{p,steam} (T_{set} - T_{eva.}) \quad (3.5)$$

Where:

\dot{m}_{fluid} : Boiler inlet fluid mass flow rate

$T_{eva.}$: Boiler inlet fluid evaporation temperature ($T_{eva.} = 100$ °C for water)

T_{in} : Boiler inlet fluid temperature

$C_{p,water}$: Boiler inlet water specific heat capacity in liquid form

$C_{p,steam}$: Boiler inlet water specific heat capacity in vapor form

$\Delta H_{eva.}$: Boiler inlet fluid latent heat of vaporization

T_{set} : Boiler outlet fluid set point temperature

The boiler constant overall efficiency, η_{boiler} , is calculated by Equation 3.6 where \dot{Q}_{in} is total inlet energy to boiler.

$$\eta_{\text{boiler}} = \frac{\dot{Q}_{\text{need}}}{\dot{Q}_{\text{in}}} \quad (3.6)$$

The \dot{Q}_{need} is limited by the device capacity (specified as rated capacity, \dot{Q}_{max}). \dot{Q}_{max} is maximum heat that boiler could provide for inlet fluid to raise it to the set point temperature.

In addition, the boiler has a minimum operational capacity, \dot{Q}_{min} , which means boiler should work at least in this capacity. The \dot{Q}_{need} should be between \dot{Q}_{max} and \dot{Q}_{min} . The \dot{Q}_{max} and \dot{Q}_{min} are related by minimum turn-down ratio:

$$\text{Minimum turn - down ratio} = \frac{\dot{Q}_{\text{min}}}{\dot{Q}_{\text{max}}} \quad (3.7)$$

In this study \dot{Q}_{min} and \dot{Q}_{max} have been defined in values that boiler could actualize the output flow with the desired set point temperature.

In TRNSYS, when inlet flow to the boiler is zero, boiler sets outlet flow temperature on initial assumption of boiler's inlet temperature which could be non-zero amount. This could be confusing sometimes because boilers when they are off and inlet flow rate is zero, they show non-zero outlet flow temperature.

The boiler rated capacity, boiler input fluid specific heat and minimum turn - down ratio are the parameters of boiler. Once the energy transferred to the fluid is calculated, the amount of fuel consumed by the boiler, \dot{Q}_{in} , is calculated by Equation 3.6. Table 3.1 shows the parameters and inputs for boiler respectively.

Table 3.1. *Parameters and inputs for boiler*

	Variable	Value	Unit
Parameter			
Rated Capacity	Q_{\max}	470000	kJ/hr
Fluid Specific Heat	C_p	4.19	kJ/(kg K)
Minimum Turn-Down Ratio	-	0.02	-
Input			
Set point Temperature	T_{set}	120	°C
Boiler Efficiency	η_{boiler}	0.78	-
Combustion Efficiency	$\eta_{\text{boiler,combustion}}$	0.85	-

3.2.2. Heat Exchanger with Hot-Side Bypass (HX1)

Another main component is a counter flow heat exchanger (Type 652) which is able to keep its cold side outlet temperature in a user-specified set point temperature with automatically bypassing extra hot side flow around the heat exchanger. The cold side outlet set point temperature is an input for this component. This heat exchanger is named HX1 in all Configurations. Figure 3.4 shows the schematic Diagram of the heat exchanger and its hot side and cold side specifications.

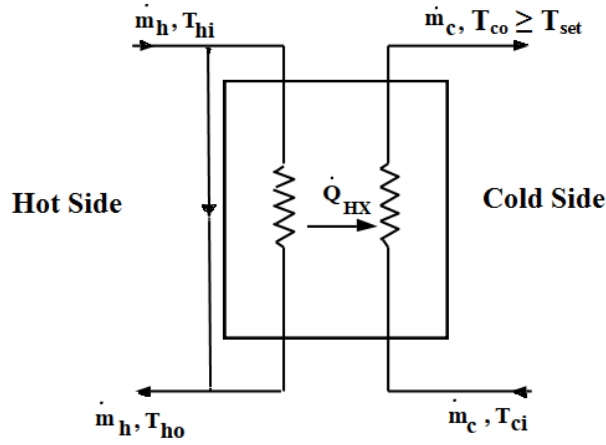


Figure 3.4. Schematic Diagram of the heat exchanger with hot side bypass

Specific heat of hot-side fluid, $C_{p,Hot}$, and Specific heat of cold-side fluid, $C_{p,Cold}$, are used to determine the hot-side fluid flow capacitance, $C_{HotSide}$, and cold-side fluid flow capacitance, $C_{ColdSide}$. The capacitances of each side are computed based on:

$$C_{HotSide} = \dot{m}_{fluid} C_{p,Hot} (1 - \gamma) \quad (3.8)$$

$$C_{ColdSide} = \dot{m}_{fluid} C_{p,Cold} \quad (3.9)$$

Where γ is the fraction of the hot-side fluid that is bypassed by the heat exchanger.

The energy transferred across the heat exchanger, Q_{HX1} , is given by:

$$Q_{HX1} = \varepsilon_1 C_{min} (T_{hot,in} - T_{cold,in}) \quad (3.10)$$

Where ε_1 is user-specified heat exchanger's effectiveness and the minimum capacitance (C_{min}) is minimum of $C_{HotSide}$ and $C_{ColdSide}$. The temperature of fluid leaving the cold side ($T_{cold,out}$) and hot-side ($T_{hot,HXout}$) before any remixing with bypassed fluid are given by:

$$T_{hot,HXout} = T_{hot,in} - \frac{Q_{HX}}{C_{HotSide}} \quad (3.11)$$

$$T_{cold,out} = T_{cold,in} + \frac{Q_{HX}}{C_{ColdSide}} \quad (3.12)$$

The hot-side outlet temperature after it has been remixed with the bypass fluid is given by Equation 3.13.

$$T_{\text{hot,out}} = \gamma T_{\text{hot,in}} + (1 - \gamma) T_{\text{hot,HXout}} \quad (3.13)$$

Table 3.2 presents the parameters and inputs for the heat exchanger.

Table 3.2. *Parameters and inputs for Heat Exchanger (HX1)*

	Variable	Value	Unit
Parameter			
Effectiveness of Heat Exchanger	ϵ_1	0.65	-
Specific Heat of Hot-Side Fluid	$C_{p,\text{Hot}}$	4.19	kJ/(kg K)
Specific Heat of Cold-Side Fluid	$C_{p,\text{Cold}}$	4.19	kJ/(kg K)
Input			
Cold-Side Set point Temperature	$T_{\text{set,Cold}}$	100	°C

3.2.3. Counterflow Heat Exchanger (HX2)

A zero capacitance sensible heat exchanger (Type 5) is modeled in counterflow heat exchanger with HX2 name in all configurations. For this heat exchanger, given the hot and cold side inlet temperatures and flow rates, the effectiveness is calculated for a given fixed value of the overall heat transfer coefficient.

This heat exchanger relies on an effectiveness minimum capacitance approach to model a heat exchanger. Under this assumption, the user is asked to provide the heat exchanger's overall heat transfer coefficient (UA) and inlet conditions. The model then determines whether the cold (load) or the hot (source) side is the minimum capacitance side and calculates effectiveness based upon the specified flow configuration and on UA. The heat exchanger outlet conditions are then computed. Source and load are merely convenient designations; energy will be transferred from

the source side to the load side if the source side is hotter than the load side. A schematic Diagram of the heat exchanger is shown in Figure 3.5.

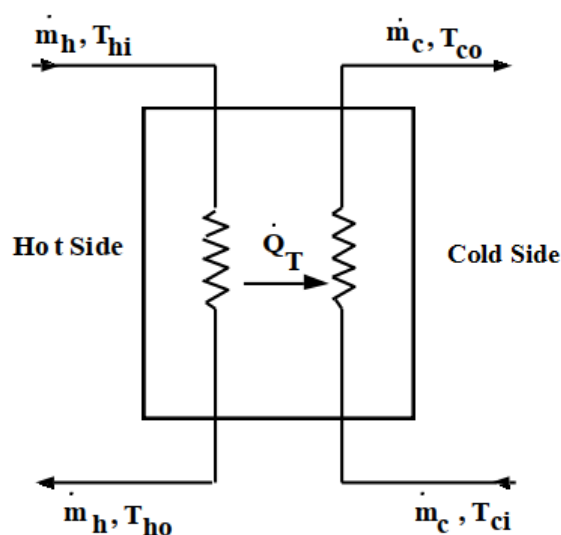


Figure 3.5. Schematic Diagram of the Heat exchanger (Type 5)

The capacitance of each side of the heat exchanger is calculated according to the Equations 3.14 to 3.17.

$$C_{\text{cold}} = \dot{m}_{\text{cold}} C_{p,\text{cold}} \quad (3.14)$$

$$C_{\text{hot}} = \dot{m}_{\text{hot}} C_{p,\text{hot}} \quad (3.15)$$

$$C_{\text{max}} = \max(C_{\text{cold}}, C_{\text{hot}}) \quad (3.16)$$

$$C_{\text{min}} = \min(C_{\text{cold}}, C_{\text{hot}}) \quad (3.17)$$

Cold subscripted variables show the heat exchanger cold side flow properties and hot subscripted ones show the same for heat exchanger hot side flow.

Equation 3.18 indicates the expression used to calculate the heat exchanger effectiveness, ε_2 , at each time step depending upon heat exchanger configuration.

$$\varepsilon_2 = \frac{1 - \exp\left[-\frac{UA}{C_{\min}}\left(1 - \frac{C_{\min}}{C_{\max}}\right)\right]}{1 - \left(\frac{C_{\min}}{C_{\max}}\right) \exp\left[-\frac{UA}{C_{\min}}\left(1 - \frac{C_{\min}}{C_{\max}}\right)\right]} \quad (3.18)$$

Where UA is heat exchanger overall heat transfer coefficient and C_{\max} and C_{\min} are calculated by Equations 3.16 and 3.17, respectively. The energy transferred across the heat exchanger, Q_{HX2} is given by:

$$Q_{HX2} = \varepsilon_2 C_{\min}(T_{\text{hot,in}} - T_{\text{cold,in}}) \quad (3.19)$$

Table 3.3 presents the parameters and inputs for the heat exchanger (HX2).

Table 3.3. *Parameters and inputs for Heat Exchanger (HX2)*

	Variable	Value	Unit
Parameter			
Specific Heat of Hot-Side Fluid	$C_{p,\text{Hot}}$	4.19	kJ/(kg K)
Specific Heat of Cold-Side Fluid	$C_{p,\text{Cold}}$	4.19	kJ/(kg K)
Input			
Source Side Flow Rate	\dot{m}_{cold}	100	kJ/(kg K)
Load Side Inlet Temperature	T_{ci}	30	°C
Load Side Flow Rate	\dot{m}_{e}	100	kJ/(kg K)
Overall Heat Transfer Coefficient of Exchanger	UA	320	kJ/(hr K)

For HX2, the inlet temperature on load side has been fixed at 30°C, which is common in industrial Units.

3.2.4. Solar Collector (Type 1b)

This component models the thermal performance of a flat-plate solar collector which was used in some configurations to integrate solar energy in the thermal system of processes. It is called Type 1b inside TRNSYS. There are many parameters and inputs which determine the performance of collector, but thermal analysis of collectors is out of the scope of this thesis. The interested reader could find detailed descriptions of solar collector and Equations in TRNSYS component mathematical model document. The most important parameters were shown in Table 3.4.

Table 3.4. *Parameters for Solar Collector*

	Variable	Value	Unit
Parameter			
Collector Area	A_s	20	m^2
Fluid Specific Heat	C_p	4.19	$kJ/(kg\ K)$

The user could define the collector area with collector area parameter. In some configurations, the effect of solar collector area on system function will be investigated, so the collector area will be set on different values and it will not be fixed on $20\ m^2$. In all collectors the heat medium is water. Most of the inputs for solar collector are determined by the weather data processor (Type 15) and pump (Type 3) output data. Table 3.5 shows the inputs to the collector from these components. In Chapter 4, solar collector performance will be investigated in Izmir, Turkey.

Table 3.5. *Inputs for Solar Collector. Note weather data processor is Type 15 and pump is Type 3*

	Output	Solar Collector Input
From	Parameter	
Weather Data	Dry Bulb Temperature	Ambient Temperature
Weather Data	Total Tilted Surface Radiation for Surface	Incident Radiation
Weather Data	Total Horizontal Radiation	Total Horizontal Radiation
Weather Data	Total Diffuse Radiation on the Horizontal	Horizontal Diffuse Radiation
Weather Data	Ground Reflectance	Ground Reflectance
Weather Data	Angle of Incidence for Surface	Incidence Angle
Weather Data	Slop of Surface	Collector Slop
Pump	Outlet Flow Rate	Inlet Flow Rate
Pump	Outlet Flow Temperature	Inlet Temperature

3.2.5. Heat Storage Tank (Type 4) [49]

Solar energy is a time-dependent energy source and if solar energy is to meet substantial portions of industrial process heat, the heat storage is necessary. For many solar systems, water is an ideal medium to store heat. The thermal performance of a fluid-filled sensible energy storage tank subject to thermal stratification can be modeled by assuming that the tank consists of N fully-mixed equal volume segments. The degree of stratification is determined by the value of N . In this thesis, N is equal to 1 which means the storage tank is modeled as a fully-mixed and uniform temperature tank without any stratification effect. Energy is added to and removed from the heat storage tank by transporting the storage medium, water. A typical system which uses a water tank as a heat storage tank and circulates water through the collector to add solar energy is shown in Figure 3.6. A similar system was used in this thesis.

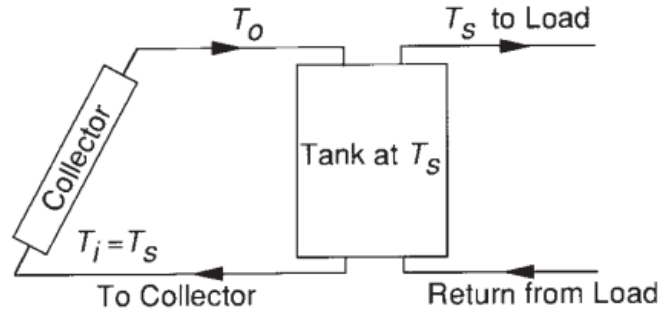


Figure 3.6. Typical solar heat system which uses water tank as heat storage tank [49]

For an unstratified tank, an energy balance on tank yields:

$$(mC_p)_s \frac{dT_s}{dt} = \dot{Q}_u - \dot{L}_s - (UA)_s(T_s - T_a) \quad (3.20)$$

Where \dot{Q}_u and \dot{L}_s are the rates of addition and removal of energy from storage tank by the collector, and load respectively, m_s is mass of water in tank, T_s is initial temperature in storage tank in the beginning of a cycle, $(UA)_s$ is storage tank loss coefficient-area product, $\frac{dT_s}{dt}$ is tank temperature change during one cycle period and T_a is the ambient temperature for tank. By integrating the Equation 3.20 over one cycle time, the storage tank temperature at the end of the cycle (T_s^+) is:

$$T_s^+ = T_s + \frac{\Delta t}{(mC_p)_s} [\dot{Q}_u - \dot{L}_s - (UA)_s(T_s - T_a)] \quad (3.21)$$

Δt is one cycle time span which was assumed to be 1 hour in all simulations in this thesis.

The storage tank inputs are defined by other components and they are changed according to configuration structure. The parameters are shown in Table 3.6.

Table 3.6. Parameters for Heat Storage Tank

	Variable	Value	Unit
Parameter			
Tank Volume	V_t	1	m^3
Tank Loss Coefficient	U_t	2.5	$\text{kJ}/(\text{hr } m^2 \text{ K})$
Height of Node	h_t	0.1	m

Because whole of storage tank was assumed as one node, the height of node parameter shows the tank height. In some configurations, the influence of storage tank volume on configuration performance is examined. Therefore, different values are used for tank volume parameter. Aligned with the thesis scope; the heat storage tank will act such as a short-term storage tank which makes solar energy or industrial waste heat available for next few hours for simulated systems.

3.2.6. MATLAB Link

TRNSYS simulation environment could be connected to MATLAB by Type 155, MATLAB link component. As it was mentioned in the thesis scope section, MATLAB gets data from TRNSYS simulation environment, based on input data, it does an optimization and then, it sends results to components in TRNSYS to operate the system at minimum cost. All this procedure is actualized by Type 155. Parameters, inputs, and outputs of this component are changed according to each Configuration structure. This component function is discussed in Chapter 5 in more detail.

3.2.7. Weather Data Processor

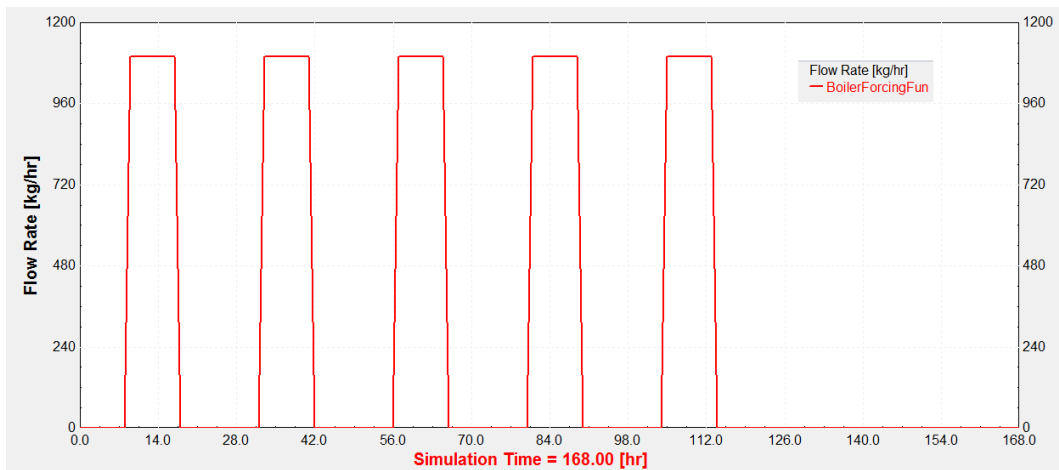
This component serves the purpose of reading data at regular time intervals from an external weather data file, interpolating the data (including solar radiation for tilted surfaces) at time steps of less than one hour, and making it available to other TRNSYS components. In this thesis, weather data processor (Type 15) provides inputs mainly for solar collector component which are displayed in Table 3.5.

3.2.8. Forcing Function

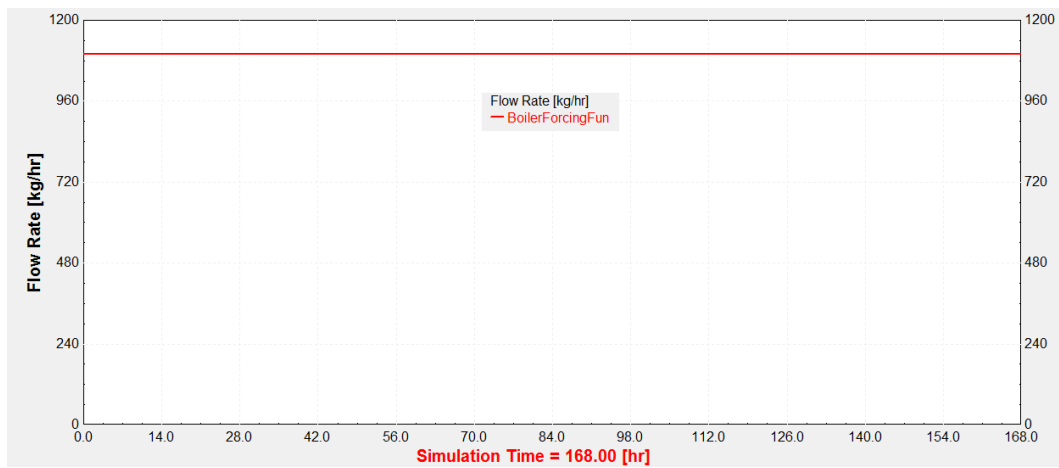
In a transient simulation, it is sometimes necessary to employ a time-dependent forcing function which has a behavior characterized by a repeated pattern. The need to use forcing functions arises from discontinuity in Unit 1 and solar collector operations. Unit 1 in this thesis simulates an industrial unit which operates just from 8:00 AM to 6:00 PM in work days of week and it is closed at the weekend. Therefore, the boiler in Unit 1 should be active in operational time intervals. In addition, the solar collector is always active in daytime from 8:00 AM to 6:00 PM, so the feeder pump should work during the specified time span.

Two kinds of forcing function components are applied for boilers and collector pumps: Type14b for boiler and Type14h for the pump. The pattern of the forcing function is established by a set of discrete data points indicating the value of the function at various times throughout one cycle. The cycle will repeat every N hours, where N is the last value of time specified.

While the code of Type14b is entirely general, this version of the component uses units of kg/hr so as to be more readily useful for creating water draw forcing functions. Type 14b controls input water flow to boiler and Type14h controls solar collector pump control signal. When control signal is 1, the pump is on and when it is 0, the pump is off. Figure 3.7 shows boiler input water flow for Units 1 and 2 in thesis configurations for one week (168 hours). Unit 1 operates discontinuously and Unit 2 works continuously. When the boiler is on, forcing function provides 1100 kg/hr feed water. Figure 3.8 shows weekly forcing function pattern for collector feeder pump. The patterns in Figures 3.7 and 3.8 are repeated for a longer simulation time span.



(a)



(b)

Figure 3.7. Forcing functions for boiler input water flow in (a) Unit 1, (b) Unit 2

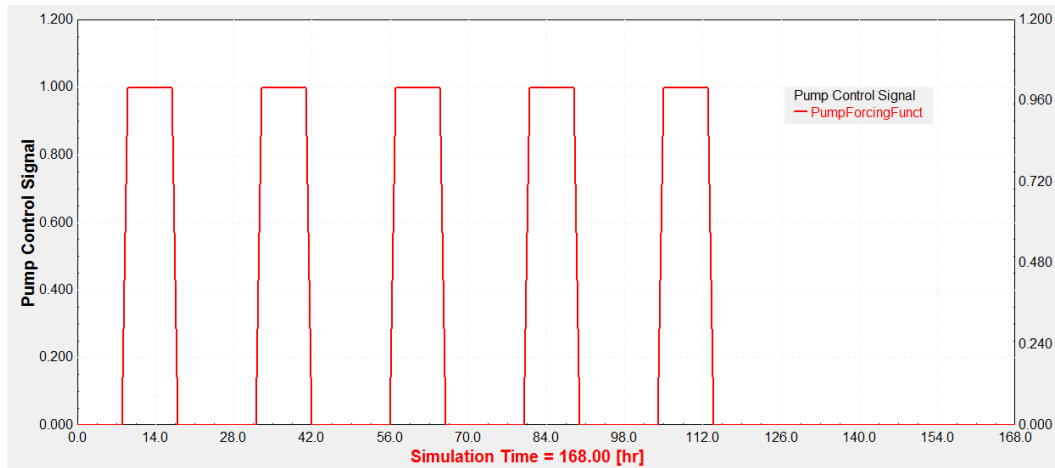


Figure 3.8. Forcing functions for solar collector pump’s control signal in Units 1 and 2

3.2.9. Pump (Type 3d)

This component as a single speed pump (Type 3d) sets the flow rate for the rest of the components in the flow loop by using a variable control signal, which could have a value between 1 and 0, and a fixed (user-specified) maximum flow rate. Pump outlet mass flow rate is computed by Equation 3.22.

$$\dot{m}_p = (\dot{m}_{p,max})(CS_p) \quad (3.22)$$

Where \dot{m}_p is the pump output flow rate, $\dot{m}_{p,max}$ pump maximum flow rate and CS_p pump control signal. A user-specified portion of the pump power is converted to fluid thermal energy which has been named conversion coefficient as input. Table 3.7 shows parameters for the pump.

Table 3.7. Parameters for Pump

	Variable	Value	Unit
Parameter			
Maximum Flow Rate	$\dot{m}_{p,max}$	100	kg/hr
Maximum Power	-	60	kJ/hr
Conversion Coefficient	-	0.05	-

3.2.10. Tee-Piece, Flow Mixer and Flow Diverter

The use of Tee-Pieces, Flow Mixers, and Flow Diverters, which are subject to external control, is often necessary for thermal systems. In a Tee-Piece (Type 11h) two inlet streams of the same fluid at different temperatures and flow rates are completely mixed. Tee-piece is actually a flow mixer with two inlets. Figure 3.9 shows the schematic Diagram of a Tee-Piece and Equations 3.22 and 3.23 calculate its outlet flow and temperature.

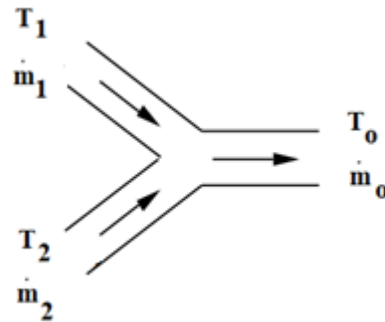


Figure 3.9. Tee-Piece (Type 11h)

$$T_o = \frac{\dot{m}_1 T_1 + \dot{m}_2 T_2}{\dot{m}_1 + \dot{m}_2} \quad (3.23)$$

$$\dot{m}_o = \dot{m}_1 + \dot{m}_2 \quad (3.24)$$

Similar to Tee-Piece, Flow Mixer (Type 649) mixes three flows with different temperature and flow rates with together. Figure 3.10 shows the schematic Diagram of the Flow Mixer and Equations 3.24 and 3.25 calculates mixer's output temperature and flow rate, respectively.

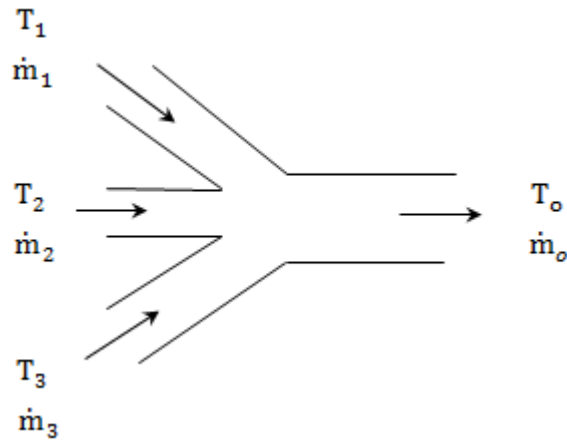


Figure 3.10. Flow mixer (Type 649)

$$T_o = \frac{\dot{m}_1 T_1 + \dot{m}_2 T_2 + \dot{m}_3 T_3}{\dot{m}_1 + \dot{m}_2 + \dot{m}_3} \quad (3.25)$$

$$\dot{m}_o = \dot{m}_1 + \dot{m}_2 + \dot{m}_3 \quad (3.26)$$

In addition, a flow could be split proportionally between two possible outlets via a flow Diverter. Type 11f simulates the operation of a Flow Diverter. The outlet flows are controlled by M, an input control function as shown in Figure 3.11. Equations 3.26 to 3.29 show the outlet flows' temperature and mass flow rates. M could get a value between 0 and 1. In the thesis, M is the optimization result which is provided by the MATLAB optimization code.

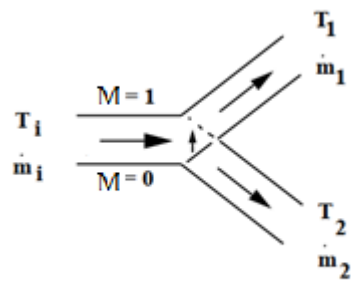


Figure 3.11. Diverter (Type 11f)

$$T_1 = T_i \quad (3.27)$$

$$\dot{m}_1 = \dot{m}_i (1 - M) \quad (3.28)$$

$$T_2 = T_i \quad (3.29)$$

$$\dot{m}_2 = \dot{m}_i M \quad (3.30)$$

CHAPTER 4

IZMIR AND SOLAR ENERGY

Izmir is located on Turkey's Aegean coast with 38.42 °N latitude and 27.14 °E longitude geographical coordinates. Izmir as the second largest economic center of Turkey produces 9.3% of total industrial production of the country. In addition, the production of food products ranks second with a 15.5% share when the sectorial distribution of the industrial businesses in Izmir are examined. Rich solar energy resource and well developed food industrial sectors make Izmir an ideal option to use industrial solar energy [50]. Izmir was chosen as location for all simulations for all Configurations in this study. Izmir solar energy data is available in TRNSYS weather data processor dataset.

4.1. Solar Collectors' Inclination and Azimuth Angles

As discussed in Chapter 2, the main contribution of this work is the novel integration of TRNSYS and MATLAB models to yield a new method to optimize the HDNs' design with solar and waste heat feeds. A detailed study on the design of the solar field is outside the scope of this work, and herein non-tracking collectors with nominal values for collector azimuth and tilt are assumed based on the following analysis.

All effective factors on collector output temperature and solar gain will not be examined in Configurations but a rough estimation was made on collector tilt and azimuth angles with Meteonorm software. Azimuth angle assumed zero in all simulations which means that collectors always face south. Different collector slopes are examined in Meteonorm 7.2 software [51] to identify the slope with maximum monthly average incident solar energy. Figure 4.1 shows the results.

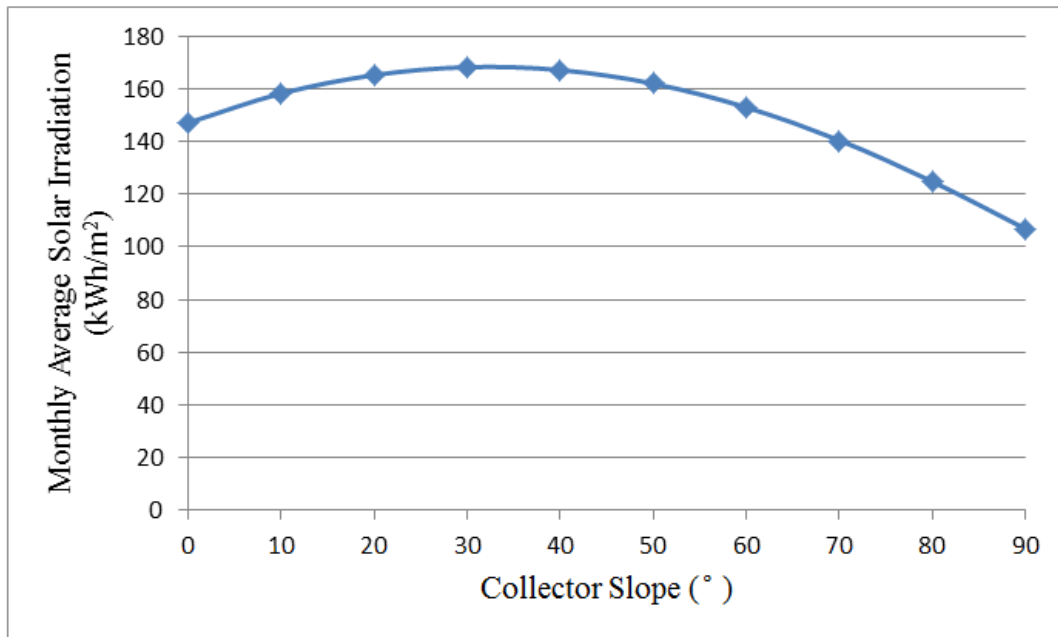


Figure 4.1. Monthly Average Solar Irradiation in Izmir with different collector slopes

The collector with 30° slop receives highest monthly average irradiation about 168.2 kWh/m² and this angle was set as collector tilt angle for all solar collectors in all Configurations. Overall this result is expected. Assuming clear sky conditions, a surface tilted at the latitude and facing due south maximizes solar resources on the equinoxes, which is the “average” day over the year in terms of solar geometries. Because summer days are longer and clearer, tilting the collector slightly less than latitude increases summer resources more than it decreases winter resources, and therefore maximizes annual resources. Izmir latitude is 38.42° and 30° tilt angle is an acceptable assumption for maximum solar energy.

4.2. Selection of time periods to simulate

In this section solar collector output temperature is examined for Izmir to determine simulation time periods. The whole of the year includes 8760 hours and doing simulation for all of these hours will be time-consuming. Instead of it, simulating of systems in selected hours which represent others, not only reduces simulation time but also could result in a comprehensive view of system annual function.

Figure 4.2 shows the simulated system to obtain collector output temperature in TRNSYS. The main purpose of this simulation is to find when maximum and minimum collector output temperatures happen. Collector was assumed a 5 m² flat plate collector and it is fed with a constant 20 °C temperature and 100 kg/hr flow rate stream by a pump. As discussed in Chapter 3, the collector gets all inputs from the weather data processor and pump and it works just in the daytime from 8:00 AM to 6:00 PM .

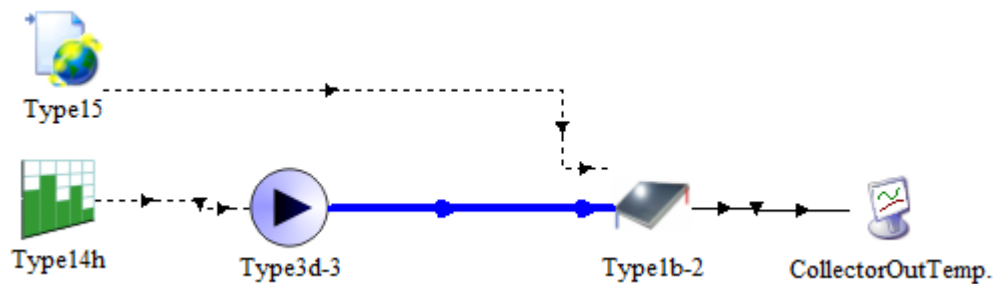


Figure 4.2. TRNSYS system for evaluating collector output temperature

Figure 4.3 to Figure 4.6 show collector output temperature for the 4 seasons of Izmir for a 5 m² flat plate collector. According to them the maximum and minimum output temperatures happen in June and February, respectively. June starts from 3625th hour and it ends in 4344th hour of a year and for February timespan is between 745th to 1416th hour. The outlet temperature for all other hours could be put between these two time intervals.

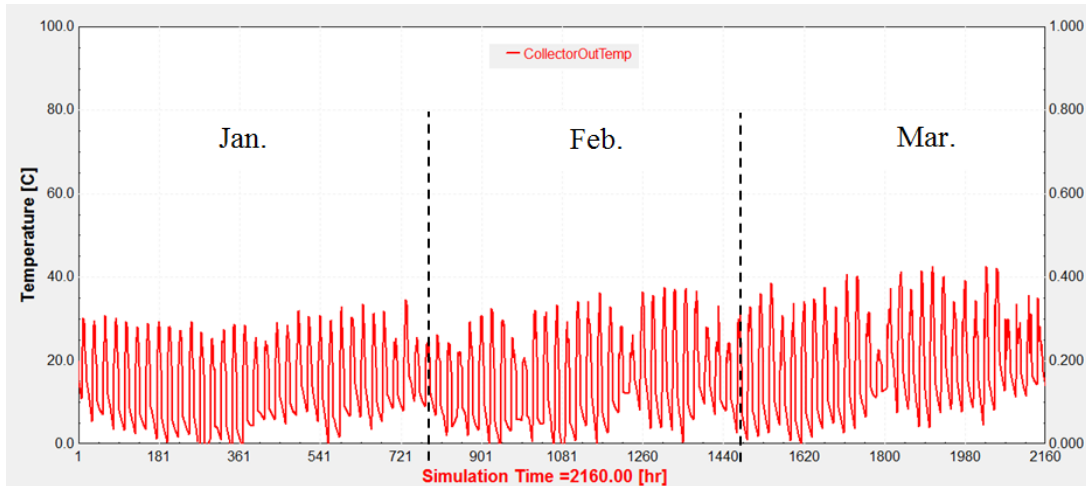


Figure 4.3. Solar collector output temperature profile in Izmir during winter (Jan., Feb., Mar.). For the three months hours start from 1st to 2160th hour of whole year.

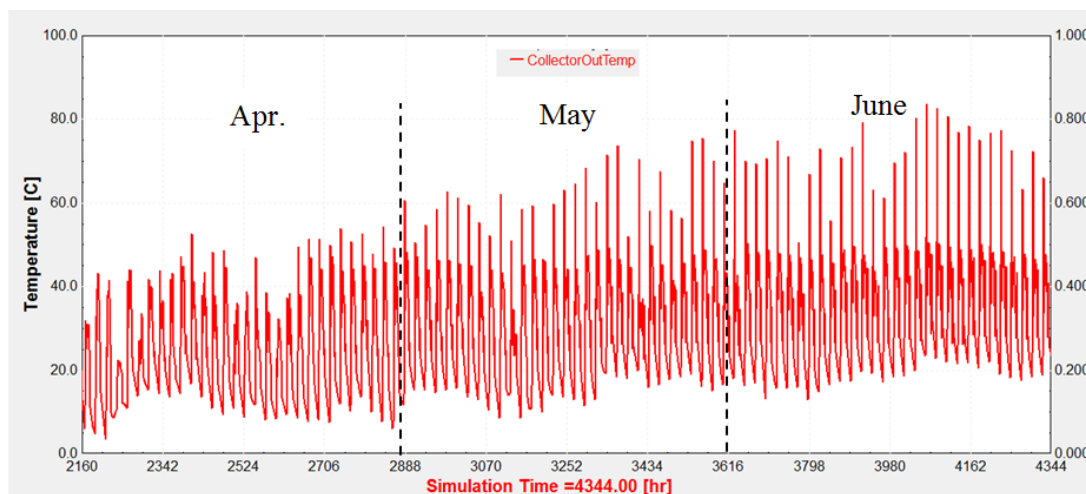


Figure 4.4. Solar collector output temperature profile in Izmir for spring (Apr., May., June). For the three months hours start from 2160th to 2160th hour of whole year.

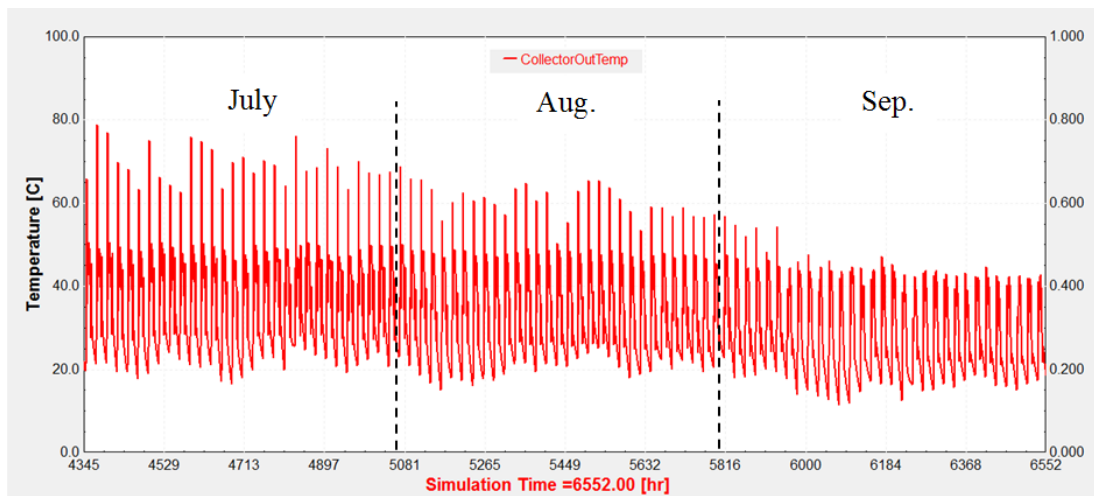


Figure 4.5. Solar collector output temperature profile in Izmir for summer (July, Aug., Sep.). For the three months hours start from 4345th to 6552th hour of whole year.

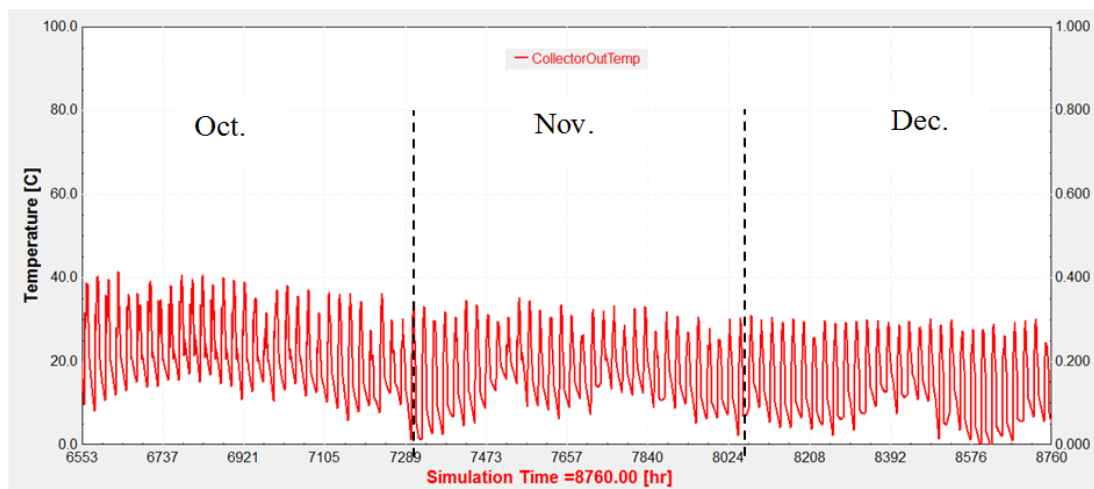


Figure 4.6. Solar collector output temperature profile in Izmir for fall (Oct., Nov., Dec.). For the three months hours start from 6553th to 8760th hour of whole year.

CHAPTER 5

COST OPTIMIZATION AND ECONOMIC PARAMETERS

In this Chapter, the optimization procedure in MATLAB is discussed generally. Then the important cost units are introduced and finally optimization procedure for one of studied Configurations is discussed.

5.1. Optimization Procedure

First of all, for optimization, all TRNSYS components' mathematical models in Chapter 3 which are extracted directly from TRNSYS volume 4, mathematical reference named document [48], are used to derive each Configuration objective function in terms of decision variables.

The objective function calculates total fuel consumption in Configurations' boiler(s). In fact, all of the Configurations' fuel cost is showed with one Equation based on decision variable(s). Decision variables are output flow rate of diverter(s). The objective function is a nonlinear Equation and fmincon function of MATLAB, a nonlinear optimization method, is used for objective function minimization. The optimization purpose in the thesis is to minimize fuel consumption and fuel cost in each simulation time step.

Besides the Configurations' mathematical models, MATLAB receives data such as T_s , average temperature of storage tank, T_{coll} , solar collector output temperature and T_a , the ambient temperature, from TRNSYS in each simulation time step. T_s , T_{coll} and T_a are used to form objective function.

Based on received data, MATLAB manages energy sources such as boiler, industrial waste heat or solar energy in a way that boiler fuel consumption is minimized. Finally, Diverter(s)' outputs are determined and proper orders about diverters' functions are

sent to TRNSYS. According to the Configuration's structure, MATLAB adds solar collector or storage tank cost to minimized fuel cost and it obtains configuration total cost.

All of this procedure was repeated for each hour, namely simulation time interval. Actually a system simulation and optimization is done simultaneously.

Four main parts of each optimization in this thesis is shown in Figure 5.1 flowchart.

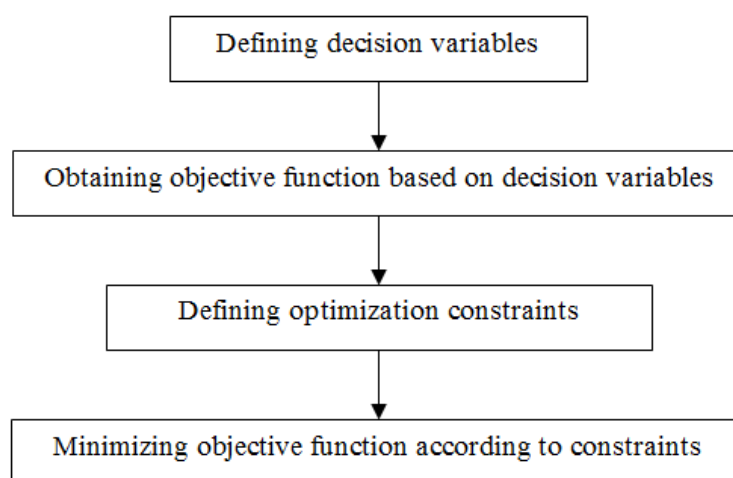


Figure 5.1. Main parts of optimization in the thesis

Before any optimization, these parts should be defined properly and they are discussed in detail in the following paragraphs.

Decision variables actually are optimization outputs. These outputs could be integer or continuous values. For this thesis, decision variables are output flow rate of Flow Diverters which are used to calculate diverters' control signals. These control signals actually are splitting ratio in flow Diverters which are defined as M in Chapter 3. Actually, M determines how much of system energy should be satisfied by boiler or other energy sources such as solar energy or waste heat.

In the second stage, for each Configuration, an objective function was obtained by using mathematical models of components in Chapter 3. The mathematical models relate the output of one component to the input of another one and by replacing the temperatures and flows, a function which gains Configuration total fuel consumption is achieved.

In this thesis, each Configuration according to its structure and used components has a unique objective function. The objective functions for each Configuration will be discussed in detail in Chapter 6.

As mentioned in the thesis objectives, boiler fuel, solar collector and storage tank costs are three main costs in this study. Based on the interest rate (i) and component life span (n), capital recovery factor, CRF, was calculated for both collectors and storage tank by Equation 5.1. If total capital cost of a component multiply by related component CRF, the annual cost of that is calculated.

$$CRF(i, n) = \frac{i(1 + i)^n}{(1 + i)^n - 1} \quad (5.1)$$

The interest rate, component life span and cost units have been adopted from the literature for the European Union zone and they are shown in Table 5.1 [38,52].

Table 5.1. *Cost Units and Economic Parameters*

	Variable	Value	Unit
Fuel Cost	C_{fuel}	0.06	€/kWh
Solar Collector Cost	C_{solar}	220	€/m ²
Storage Tank Cost	C_{tank}	180	€/m ³
Interest Rate	i	0.017	-
Solar Collector Life Span	n_1	20	Year
Storage Tank Life Span	n_2	40	Year

Simulation time step in this thesis is 1 hour and optimization and system total cost is calculated for each hour. Storage tank and solar collectors have a capital cost which is multiplied by capital recovery factor (CRF) to obtain their annual cost. Each year consists of 8760 hours which if annual cost of components is divided by 8760, the hourly cost share of components is obtained. For estimating system total cost, the system hourly fuel cost which is calculated by objective function, is sum up with components hourly cost. Equation 5.2 shows the general form of total cost Equation in which F represents the objective function and total fuel consumption in boilers for each configuration.

$$C_{\text{total}} = C_{\text{fuel}}F + \frac{f_s C_{\text{solar}}A_s + f_t C_{\text{tank}} V_t}{8760} \quad (5.2)$$

C_{total} is the total cost of a Configuration in each time step, C_{fuel} , C_{solar} and C_{tank} are fuel, solar collector and heat storage tank cost units ,respectively. f_s and f_t are capital recovery factors for solar collector and storage tank volume, respectively. Capital recovery factor has not been considered for fuel cost. A_s is the solar collector area and V_t is used storage tank volume.

Constraints in this study consist of energy balance for each component, components' capacity limitations and variables' upper and lower bounds.

Finally, a minimization function in MATLAB was chosen to minimize obtained objective functions. Because the aim of this thesis is cost optimization of different configurations, optimization and minimization have the same meaning in the thesis text and these two terms could be used interchangeably. The linearity or nonlinearity of objective function and function's variables determine the minimization method that should be used. As it is discussed in the literature review Chapter, because linear optimization methods are well developed and studied, most studies tried to linearize their objective functions by some simplifying assumptions such as constant

temperature inside Heat Distribution Network (HDN). These assumptions could cause inaccuracy in systems simulations. In this thesis, unlike previous studies, the temperature inside Heat Distribution Network (HDN) and processes' thermal systems was assumed as a variable which made all objective functions nonlinear.

MATLAB has some functions for nonlinear optimization. The "fmincon" function was chosen for objective functions' minimization. The interested reader can find a detailed discussion of this function's capabilities in [53] reference.

For clarifying, how optimization calculates system total cost in each hour, one of studied Configurations, Configuration 4, is chosen as an example and optimization stages are described for it. All other Configurations' optimization follows the same procedure. Configuration 4 is one of the most complex Configurations in this thesis. Figure 5.2 shows the schematic Diagram of Configuration 4. Units are connected to storage tank which is fed by central solar field, a central solar thermal plant. Each Unit uses its boiler as backup energy source. The provided solar energy is managed by MATLAB optimization to minimize fuel consumption in boilers.

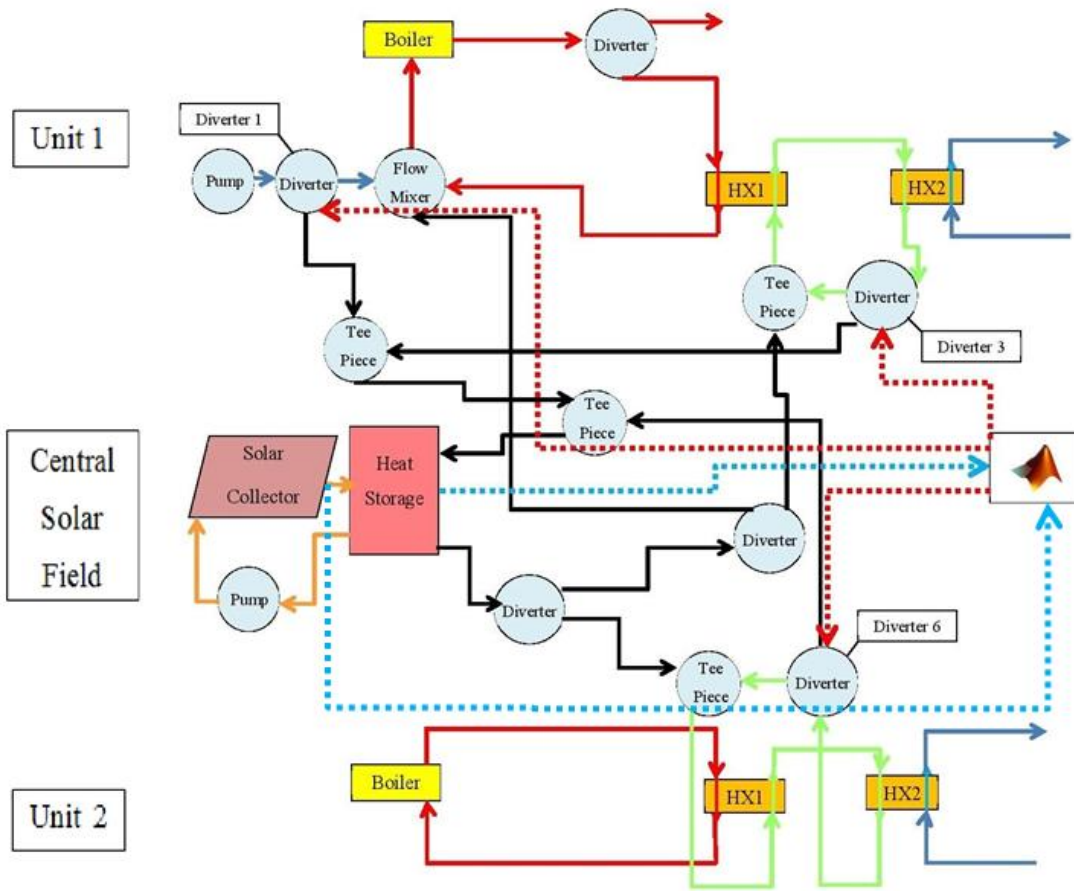


Figure 5.2. Schematic Diagram of Configuration 4

The time interval for all simulations in this thesis is 1 hour. This means MATLAB optimization and system data transfer between TRANSYS and MATLAB happens in each hour and all variables are assumed constant during each hour. 1 hour simulation time interval is common between most of solar energy related researches because solar radiation data is available mostly in 1 hour time steps. Furthermore, as discussed in Chapter 4, doing simulation and optimization for all hours of a year is so time consuming and according to Chapter 4 findings, February and June are chosen as this thesis simulation time periods. It means simulation and optimization is done for each hour of these two months.

According to Figure 5.2, three options are defined for integrating solar energy into both Units' thermal systems which include: Unit 1 supply-side, Unit 1 process-side and Unit 2 process-side. Based on three options three decision variables should be defined. Decision variables are three diverters' output flow rates. Diverters are shown with Diverter 1, Diverter 3 and Diverter 6 names in Figure 5.2 and decision variables are named $\dot{m}_{2,Div1}$, $\dot{m}_{2,Div3}$ and $\dot{m}_{2,Div6}$.

MATLAB uses some information such as storage tank average temperature in last simulation time step, T_s , and solar collector outlet temperature, T_{coll} , to form objective function. The blue dashed lines in Figure 5.2 represent data transfer from TRANSYS to MATLAB. In addition, MATLAB uses TRNSYS component mathematical models which are described in Chapter 3 to obtain objective function according to defined decision variables. Objective function calculates the hourly fuel consumption in boilers and fuel cost in Configuration.

Equation 5.3 shows a part of Configuration 4 objective function, O.F.4. Red rectangles show the decision variables and red circles show the data that MATLAB receives from TRNSYS environment. Because related function is so long, just a part of it is shown.

$$\begin{aligned}
 \text{O.F.4} = & \left(\frac{419 \dot{m}_{2,Div1}}{5} \right) + (502800 \left(\left(\frac{6969 \dot{m}_{2,Div3}}{100} \right) - (\dot{m}_{2,Div3} T_s) + (20 \dot{m}_{2,Div1} - \right. \\
 & 500 T_{coll} + \left. \left(6969 \frac{\dot{m}_{2,Div3}}{100} \right) + \left(6969 \frac{\dot{m}_{2,Div6}}{100} \right) + (100 (T_a - T_s)) (50 V_{st} + \right. \\
 & \left. \left. 5 \left(\frac{(157 \frac{V_{st}}{500})^{\frac{1}{2}}}{\dot{m}_{2,Div1} + \dot{m}_{2,Div3}} \right) \right) + \dots \right) \quad (5.3)
 \end{aligned}$$

After calculating objective function, fmincon function in MATLAB minimizes obtained objective function. By using Equation 5.2, the Configuration total hourly cost could be estimated. As it was mentioned, each optimization includes some constraints. For Figure 5.2, energy balance and mass balance Equations for components especially for Diverters form optimization constraints.

As it is obvious in Equation 5.3, objective function respect to decision variables is a nonlinear function. fmincon function is suitable optimizer for nonlinear functions. After minimizing the objective function, decision variables are determined and they are used to calculate control signals of related diverters.

Equation 5.4 shows how control signal of Diverter 1, M1, is calculated where $\dot{m}_{in,Div1}$ is inlet flow rate to Diverter 1. Other control signals are calculated by similar Equations. Control signals are analog and they could take values between 0 and 1. In fact, a diverter control signal determines splitting ration for that diverter which mean when it is 1 the diverter guides all inlet flow to outlet 1 and when it is 0 the inlet flow is guided to outlet 2 of diverter. For values between 0 and 1, inlet flow is divided between two outlets proportionally.

$$M1 = \frac{\dot{m}_{2,Div1}}{\dot{m}_{in,Div1}} \quad (5.4)$$

Diverters' control signals are actually optimization outputs and MATLAB sends them to TRNSYS diverters to operate system in minimum fuel consumption in boilers. The red dashed lines in Figure 5.2 shows the data transfer from MATLAB to TRNSYS diverters. All of these procedure repeats in each simulation time interval, 1 hour.

CHAPTER 6

CONFIGURATIONS

This Chapter discusses four different Configurations with different components and working profiles. Each Configuration involves two food industry Units. Unit 1 works just in daytime and it is non-operational at night and weekends, whereas Unit 2 operates continually all the time. As it is prevalent in food industry units, Unit 1 produces and consumes steam in its process which could be used for pasteurization or cooking and this steam is not recycled because of contaminations [54]. Configurations' energy could be provided by three energy sources: conventional boilers, industrial waste heat or solar energy. In accordance with the thesis objectives, the main aim of Chapter 6 is to investigate how solar energy and industrial waste heat application could affect each Configuration's total cost. In all Configurations, boilers are auxiliary energy sources except Configuration 1 and natural gas is assumed as their fuel. In the thesis, Configuration 1 simulates Units in a conventional form in which only boilers satisfy Units' energy demand and there is not an industrial waste heat or solar energy integration. Actually, Configuration 1 will be a benchmark to be compared with other Configurations' results. In Configuration 2, Units are connected to each other by a Heat Distribution Network (HDN) and industrial waste heat could be shared between them by this network. Configuration 3 simulates the condition in which Units are equipped with separated solar collectors and heat storage tanks. Finally, in Configuration 4, Units are linked to each other and they benefit from central solar field heat via HDN.

The thermal system of the four Configurations was simulated in TRNSYS based on information in reference [1] food industries' processes' temperature ranges, in reference [55] different solar energy integration points in industrial Units and finally

in reference [37] industrial process indicators database and suggested solar energy integrated structures in the food industry.

There are different processes inside an industrial Unit from the early stage of production like raw material entrance to the last phase of production where the final product emerges. Each of these processes needs a specific temperature and flow rate. Instead of producing energy in a wide range of temperatures, a central heat production Unit is installed to produce energy for a central loop. In most food industries, this central loop uses high-temperature steam as heat medium and it is named supply-side heat production line or briefly supply-line. Different processes could be linked to supply line to extract their needed amount of energy by a subsidiary loop which is known as process-side loop. According to industrial Units' process, usually, they have one central supply-side line and some process-side lines. Temperature in supply-side loop is fixed while process-side loops could have various temperatures. In the thesis, all simulated Units in Configurations, have one supply-side loop and one process-side loop. Supply loop is shown with red and process loop is shown with light green in all Configurations. Supply-side temperature has been fixed at 120°C and process side has 100°C temperatures. Both Units include one boiler and two heat exchangers which form supply side and process side loops. Figure 6.1 shows schematic Diagram of Unit 1 and Figure 6.2 shows Unit 1 in TRNSYS simulation environment.

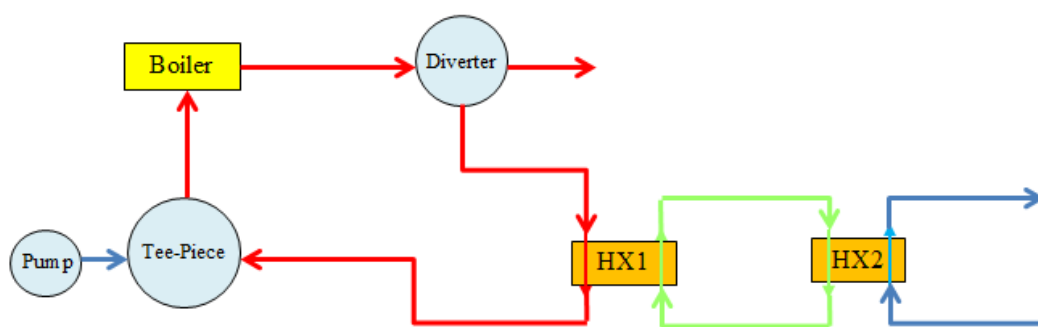


Figure 6.1. Schematic Diagram of Unit 1

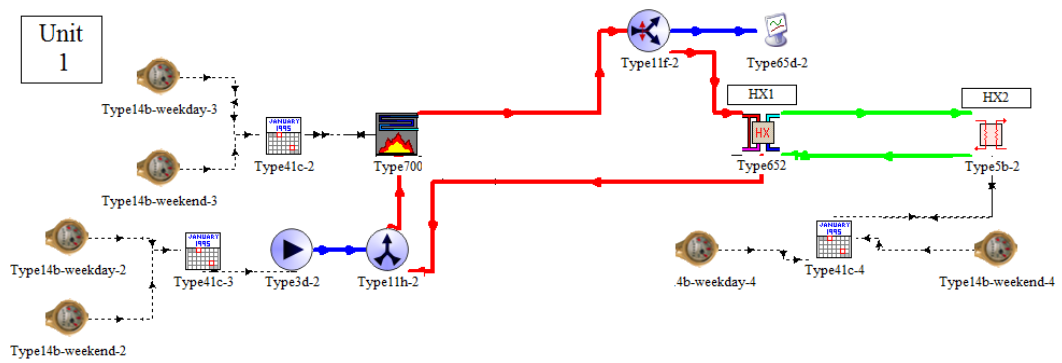


Figure 6.2. Unit 1 in TRNSYS

Figure 6.3 shows the flow rate profile in both supply side and process side of Unit 1 for February and June. Flow rate amount in load side and source side of the heat exchanger HX2 is the same as 100 kg/hr and for this, flow rate profile of cold side in HX1 and HX2 in Figure 6.3, blue and red Diagrams, coincide with each other. As expected from Unit 1 operation profile, the flow rate is like a square wave which is zero on weekends. The temperature profile in supply side and process side of Unit 1 is like Figure 6.4. According to the description in Section 3.2.1 when input flow to a boiler or heat exchanger is zero, TRNSYS puts output temperature the same as initial assumption of inlet temperatures. Therefore, according to Figure 6.4, at the weekend flows have non-zero temperature while flow rate is zero.

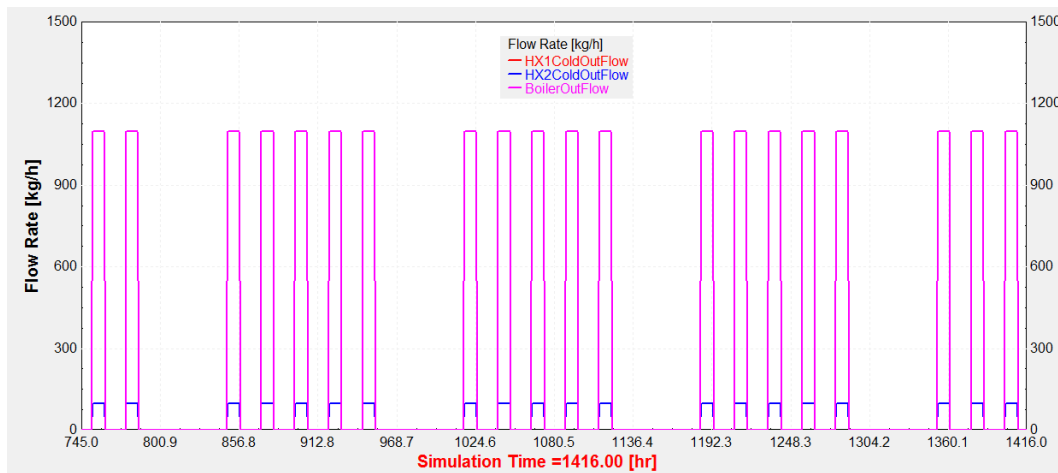


Figure 6.3. Flow rate profiles for Unit 1 in Feb. and June. HX1ColdOutFlow represents flow rate in Unit 1 process side, HX2ColdOutFlow shows the inlet flow rate to cold side of HX2 in Unit 1 and BoilerOutFlow shows Unit 1 supply side flow rate.

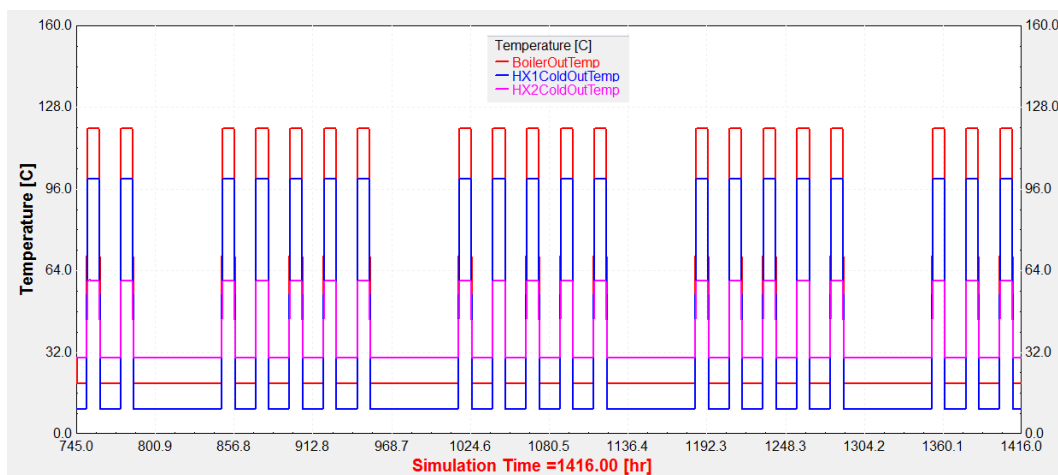


Figure 6.4. Temperature profiles in Unit 1 in Feb. and June. BoilerOutTemp shows Unit 1 supply side temperature, HX1ColdOutTemp represents temperature in Unit 1 process side and HX2ColdOutTemp shows the inlet temperature to cold side of HX2 in Unit 1.

Unit 2 schematic Diagram and simulated system in TRNSYS are shown in Figure 6.5 and Figure 6.6, respectively. It works continuously and its continuous flow rate and temperature profiles for February and June are shown in Figure 6.7 and Figure 6.8,

respectively. In Figure 6.7, Diagram of flow rate in Unit 2 process side coincides with Diagram of inlet flow rate to cold side of HX2 in Unit 2.

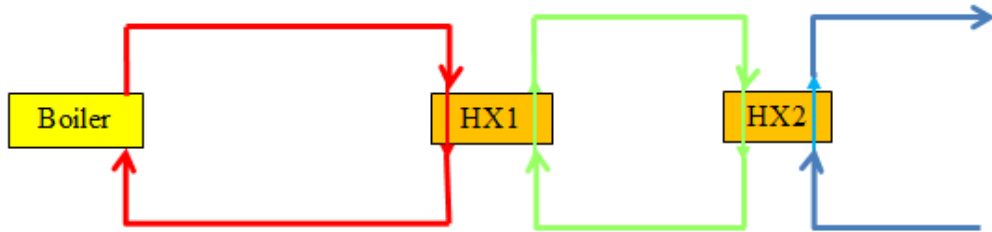


Figure 6.5. Schematic Diagram of Unit 2

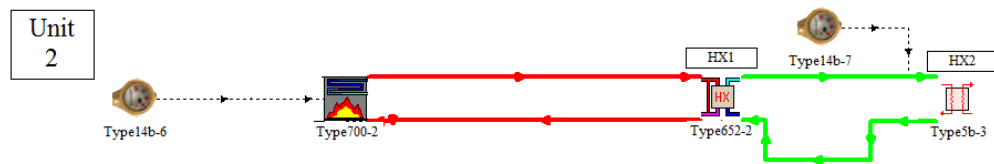


Figure 6.6. Unit 2 in TRNSYS

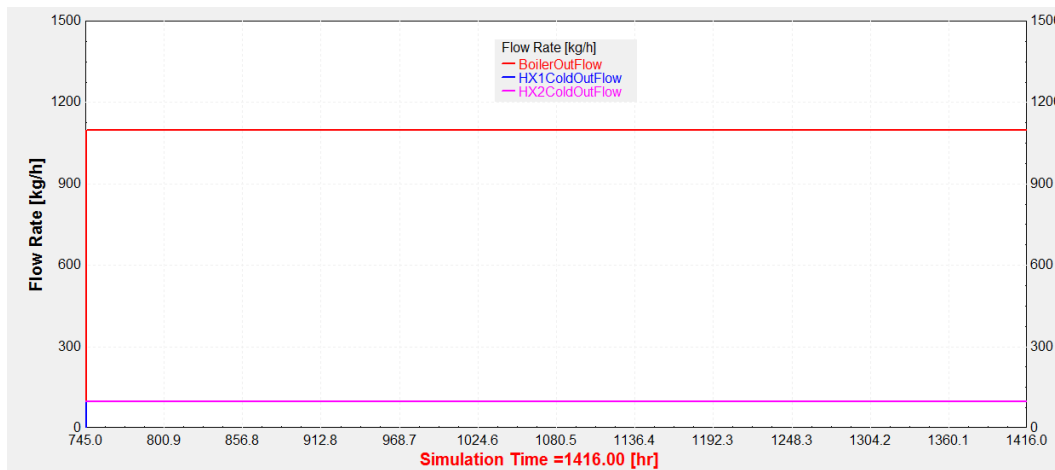


Figure 6.7. Flow rate profile in Unit 2 in Feb. and June. BoilerOutFlow shows Unit 2 supply side flow rate, HX1ColdOutFlow represents flow rate in Unit 2 process side, HX2ColdOutFlow shows the inlet flow rate to cold side of HX2 in Unit 2. HX1ColdOutFlow coincide with HX2ColdOutFlow Diagram.

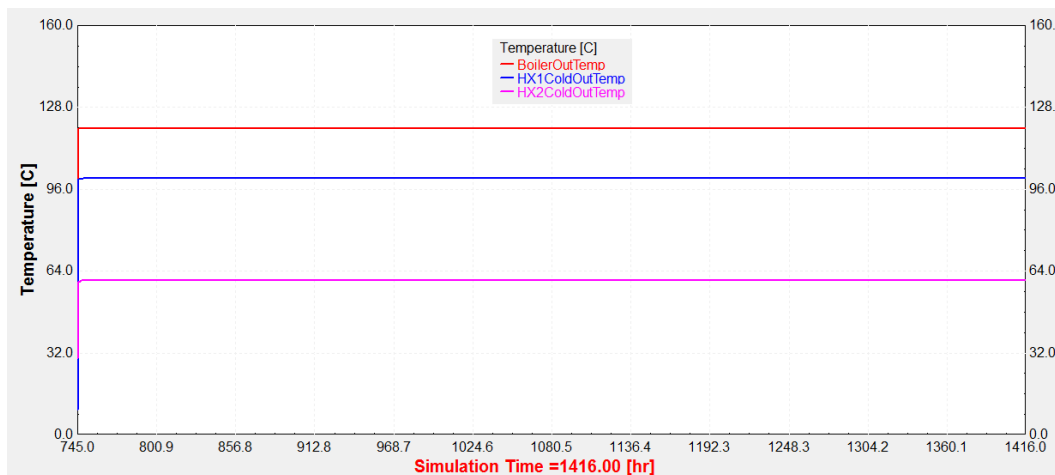


Figure 6.8. Temperature profile in Unit 2 for Feb. and June. BoilerOutTemp shows Unit 2 supply side temperature, HX1ColdOutTemp represents temperature in Unit 2 process side and HX2ColdOutTemp shows the inlet temperature to cold side of HX2 in Unit 2.

MATLAB as an optimizer in all simulated structures is coupled with TRNSYS components to minimize the Configurations' fuel consumption by using solar energy or industrial waste heat as a secondary energy source. Each Configuration's fuel consumption is estimated with an objective function. All necessary Equations and mathematical models are introduced to gain final unique objective function for each

Configuration. Optimization procedure includes minimizing an objective function as described generally in Chapter 5 and will be discussed for each Configuration in more detail in this Chapter. Finally, the hourly cost profile of all optimized systems will be assessed to identify solar energy or industrial waste heat contribution impact on systems' total cost. Because radiation data are usually available on hourly basis, the time interval in the thesis Configurations' simulations is one hour.

Instead of discussing each Configuration in separated Chapters, a Section was assigned for each one. By this, following up between different Configurations from the simplest one to the most complex will be easier. To make thesis' results credible and acceptable, before any Configuration discussion, the thesis methodology was validated by another case study data. In Configurations' Sections, initially, introductory information is presented for each Configuration. Some of the Configurations include sub-Configurations which are discussed in sub-Sections. If Configuration includes optimization, objective function obtaining procedure and all related Equations which are adopted from component mathematical models in Chapter 3, will be discussed in related Appendices and finally hourly cost profiles will be analyzed for each Configuration.

6.1. Result Validation

To make the thesis results acceptable, result validation is essential. Finding a research work which exactly matches with this study is impossible. Therefore, this Section concentrates on applied methodology validation. As it was mentioned in literature review Section, most studies used linear optimization methods while the main contribution of this study is using a nonlinear method for different Configurations' optimization. In addition, those studies do not present all used data for their optimization. Based on different optimization algorithms, any insignificant difference in input data could create big variations in final results. Considering all of these facts, a paper by Song Hwa Chae et al. [41] was chosen for validation. They did a case study

in an existing petrochemical complex in Yeosu, South Korea. They initially defined 5 waste heat source nodes and 8 Units which needed energy as sink nodes. Then, the authors used Mixed Integer Linear Programming (MILP) method to create an HDN between nodes to link source nodes to sink nodes to minimize the complex annual energy cost. According to their results, total energy cost of sink nodes could be reduced more than 88% from the present value. Figure 6.9 shows the optimization results and optimal HDN by Hwa Chae et al. the left side is the heat source and the right side is the heat sink nodes.

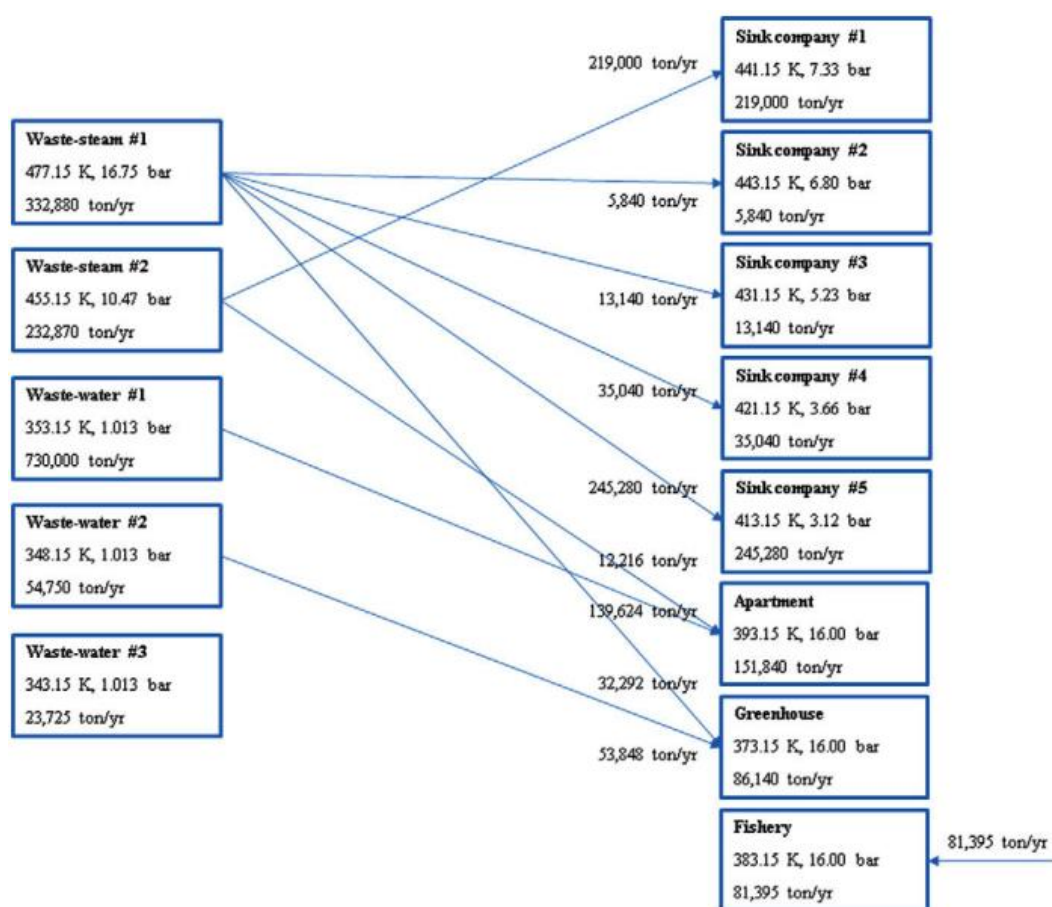


Figure 6.9. Optimization result by MILP method in Hwa Chae et al. study [41].

They reported the total cost for before and after optimization just for sink nodes. After understanding the optimization constraints, variables upper and lower bands and

analyzing the waste heat streams' structure completely, the MATLAB `fmincon` function was applied to optimize the Song Hwa Chae et al. system and the results were compared with the paper results. The used code is shown in Appendix E. Figure 6.10 compares Hwa Chae et al. results by MILP method with the thesis results which are obtained by MATLAB `fmincon` function. All the results are categorized into two groups: before optimization and after optimization. Four main factors which strongly affect the optimization results are: Units thermal system, fuel unit cost (\$/GJ), HDN construction cost (\$/(yr km)) and the optimization method used. During the validation of results, it was tried to minimize Units' initial condition, the fuel unit cost and HDN construction cost's effect on final optimal results as much as possible and the main aim was to investigate the optimization method influence on the final results. For this, in the thesis, fuel cost unit was assumed value that before optimization system total cost became almost equal with the Hwa Chae et al. results.

The fuel and HDN construction cost units are presented in Table 6.1. Before optimization, just fuel cost determines system total cost. For pre-optimization, there are two important points. First, because there was not presented detailed information about modeled Configuration in Hwa Chae et al. paper, the thermal structure of the studied Configuration was approximated. Second, the exact fuel cost unit could be extracted from the validation paper. Because the main aim of result validation is to show used methodology reliability, the fuel cost unit was changed in a way to minimize Configuration structure inaccuracy effect on optimization final results. Because of this, there is a big difference between fuel cost unit for the paper and that for the thesis method. Therefore, with this assumption, the validation of optimization procedure was done.

The HDN construction cost unit of Hwa Chae et al. was used directly in the thesis method. In conclusion, the difference between optimal results of Hwa Chae et al. and the thesis method could be attributed to the difference in optimization methods. All system total cost for both before optimization and after optimization is shown in Table 6.2. There is a 5.1% difference between two methods' results before optimization and

17.76% difference after optimization. In other words, 5.1% of 17.76% difference after optimization could be attributed to results' difference before optimization. 12.66% remaining difference originates from after optimization effective parameters such as optimization method and HDN construction cost unit. It is possible to reduce differences between results if more detailed data are available from simulated system in Hwa Chae et al. case study.

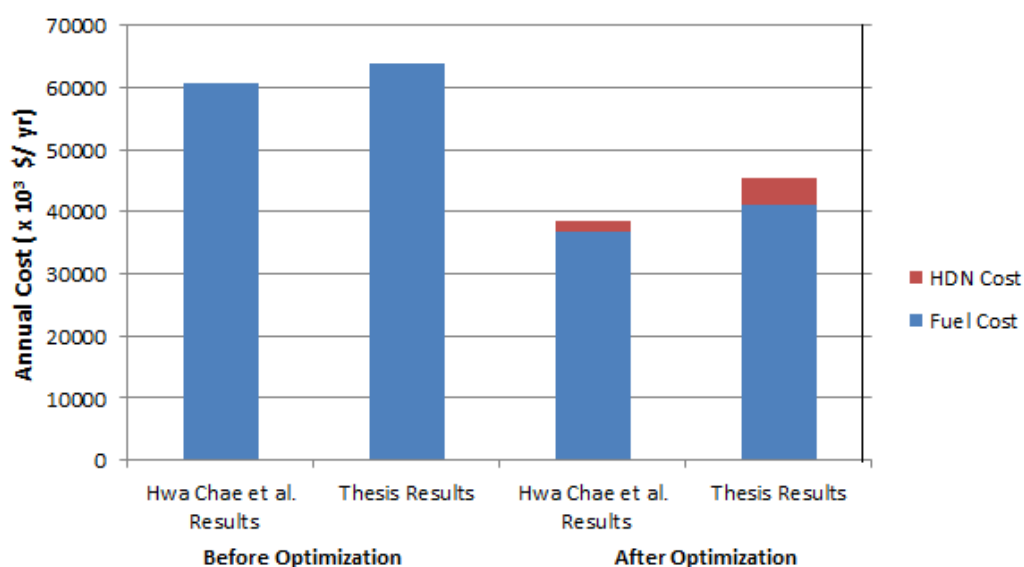


Figure 6.10. Comparing the Hwa Chae et al [41] case study results with the thesis results for both before and after system optimization.

Table 6.1. Fuel and HDN construction cost units for Hwa Chae et al. [41] study and the thesis study.

	Fuel Cost (\$/GJ)	HDN construction cost ¹ (\$/(yr km))
In Hwa Chae et al.	17.74	152585.5
In The Thesis	9.07	152585.5

¹ Ten year depreciation of investment cost was applied

Table 6.2. Validation of system's cost based on Hwa Chae et al. [41] and the thesis methods.

		Total Fuel Cost ($\times 10^3$ \$/yr)	Total HDN Construction Cost ($\times 10^3$ \$/yr)	Total Cost (Fuel + HDN costs) ($\times 10^3$ \$/yr)
Befor Optimization	Hwa Chae et al. Results	60780	0	60780
	Thesis Results	63820	0	63820
After Optimization	Hwa Chae et al. Results	36664	1918	38582
	Thesis Results	41033.98	4403.6	45437.58

6.2. Configuration 1

In Configuration 1, there is no solar energy or industrial waste heat integration and Units are not connected with Heat Distribution Network (HDN). Conventional boilers supply Units' energy demand and this Configuration is used as a benchmark for other Configurations' results interpretation. In fact, Configuration 1 shows two Units in basic form. Based on Configuration 1 structure, boiler fuel cost is the only cost source and because this Configuration does not use any other secondary energy source, there will not be any optimization.

As it was determined in Chapter 4, February and June were chosen as simulation time intervals in all simulations but because in Configuration 1 there is not any solar collector and ambient temperature negligible effect on system function, all temperatures, flows and hourly costs Diagrams will be the same for both months. Thus, results are shown just for February. Figure 6.11 presents the overall view of Configuration 1 in TRNSYS environment.

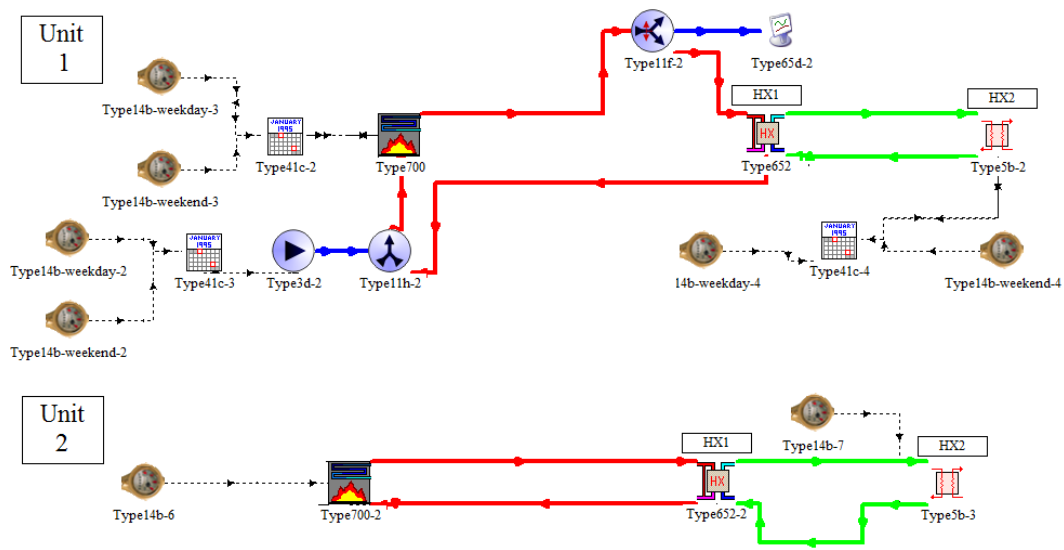


Figure 6.11. Overall view of Configuration 1

6.2.1. Cost Calculation

In Configuration 1, no optimization was done and the main cost in this Configuration is boilers' fuel cost. Therefore, by Equation 6.1 the boilers' input energy (kJ/hr) data which is received directly from TRNSYS and fuel unit cost (€/kWh) in Table 5.1, C_{fuel} are used to calculate each boiler total hourly fuel cost (€/hr). Finally, two boilers fuel costs are added to obtain system total cost.

$$\text{Fuel Cost} = \frac{(\text{boiler input energy from TRNSYS})(C_{fuel})}{3600} \quad (6.1)$$

6.2.2. Results

Figure 6.12 shows the hourly fuel cost of both Units separately and total cost in Configuration 1. As described previously, Figure 6.12 is valid for both February and June.

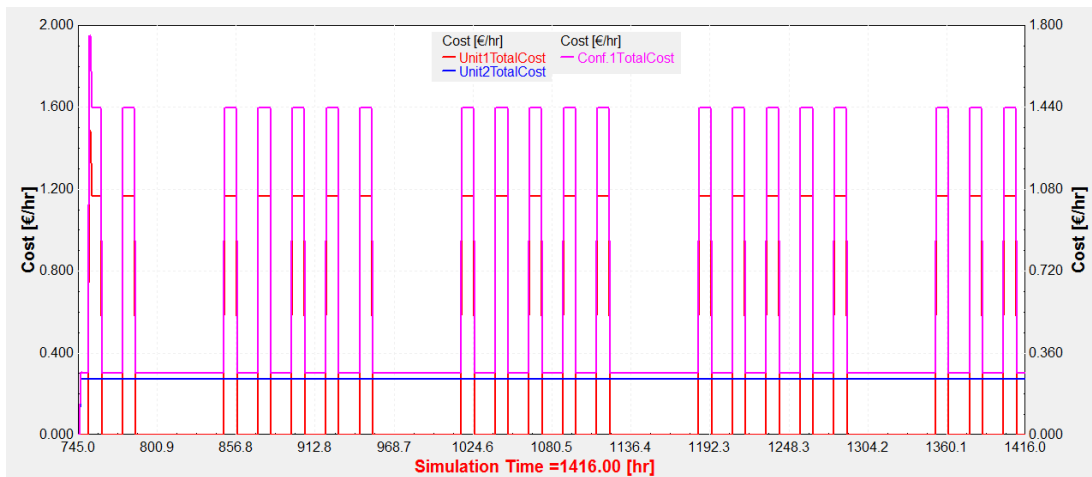


Figure 6.12. Hourly cost for Unit 1 and 2 and their total cost in Feb. and June.

As expected, hourly cost of Unit1 is higher than that of Unit 2 because Unit 1 produces steam, so it consumes more fuel. Hourly cost for Unit 1 is zero at night and weekend while it is constant for Unit 2 in all hours because it works continuously. The total cost, the purple Diagram in Figure 6.12, is the sum of both Units' costs and on weekdays it reaches its maximum and at night and weekend, it approaches to Unit 2 cost profile because Unit 1 is shut down. Figure 6.12 will be used as a basic Diagram to compare with other Configurations cost profiles to determine if optimization of industrial waste heat or solar energy integration reduces Configurations' cost or not.

6.3. Configuration 2

In this Configuration, a Heat Distribution Network (HDN) was installed between Units. Configuration 2 consists of two sub-Configurations. In the first one, boilers have different efficiencies and more efficient boiler shares output with lower one. In the second sub-Configuration, Units have the same boilers but they could use industrial waste heat with HDN. Generally, Configuration 2 examines two important subjects. 1) How could the sharing more efficient boilers with other industrial Units affect Configurations' total cost? 2) Could sharing industrial waste heat with different

temperatures be economic for a system? Each sub Configuration tries to answer one of these questions. Solar energy has not been integrated to Units' processes, therefore, the results for February and June will be the same and all simulations and the results are presented for February.

6.3.1. Configuration 2-1

In this sub-Configuration, the system is the same as Configuration 1 but Unit 1 uses a boiler with 70% ($\eta_{\text{boiler}} = 0.7$) efficiency and for Unit 2, boiler efficiency is 50% ($\eta_{\text{boiler}} = 0.5$). As it was assumed, Unit 1 works 10 hours a day but Unit 2 works all the time. The question that was intended to be answered is this: is it possible to use Unit 1 efficient boiler when Unit 1 is closed at night and weekends for providing energy for Unit 2? If yes, how much it will be affordable?

Figure 6.13 shows the basic form for sub-Configuration 2-1. It is the same as Configuration 1 structure just with different boilers efficiencies. Figure 6.14 and Figure 6.15 show schematic Diagram and TRNSYS simulation of Configuration 2-1 respectively, when two Units' boilers are connected in a way that Unit 1 boiler provides energy for Unit 2 from 6:00 PM to 8:00 AM and during weekend. Diverters 1 and 2 guide Unit 1 boiler output to heat exchanger HX 1 in Unit 2 and in this time span Unit 2 boiler is closed. Actually, Unit 1 boiler provides energy for supply side of Unit 2. In conclusion, Unit 1 boiler will work continuously and at night and weekend, it will provide energy for Unit 2. Again there is not any optimization and system total cost has been calculated by Equation 6.1 and direct data from TRNSYS.

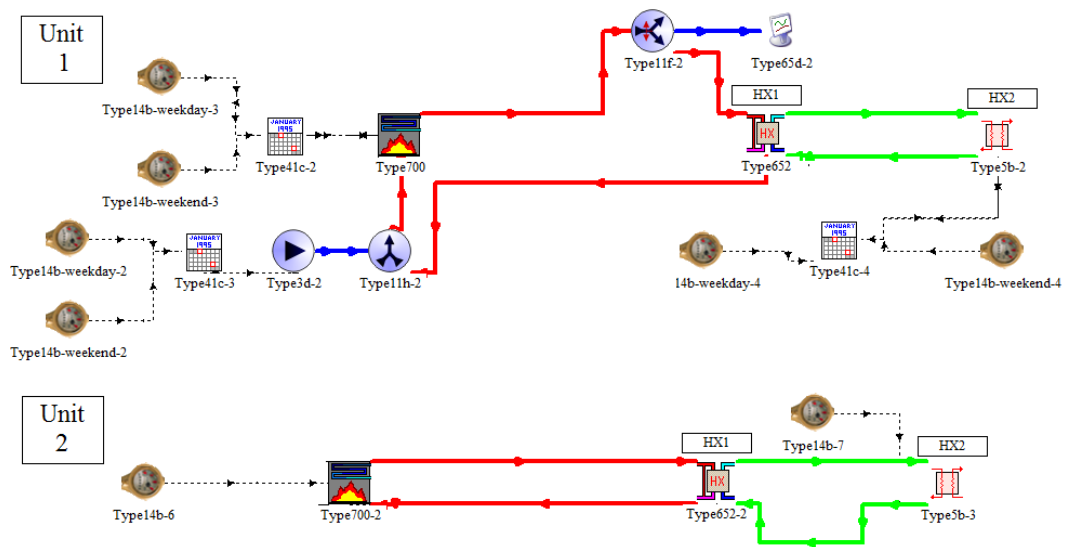


Figure 6.13. Configuration 2-1 in basic form. Unit 1 boiler efficiency is 0.7 and for Unit 2 boiler efficiency is 0.5.

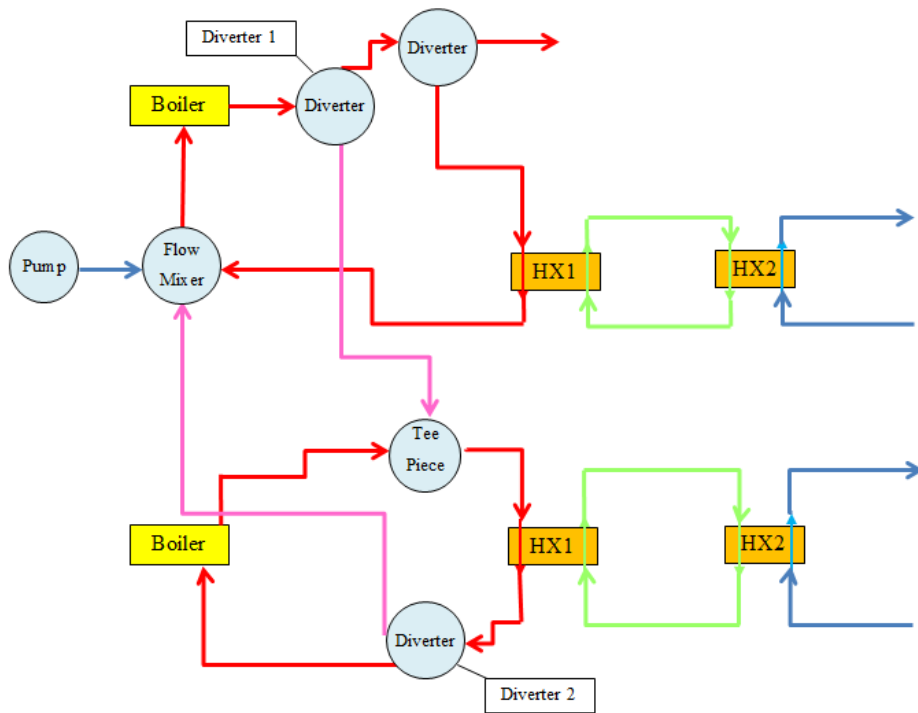


Figure 6.14. Schematic Diagram of Configuration 2-1.

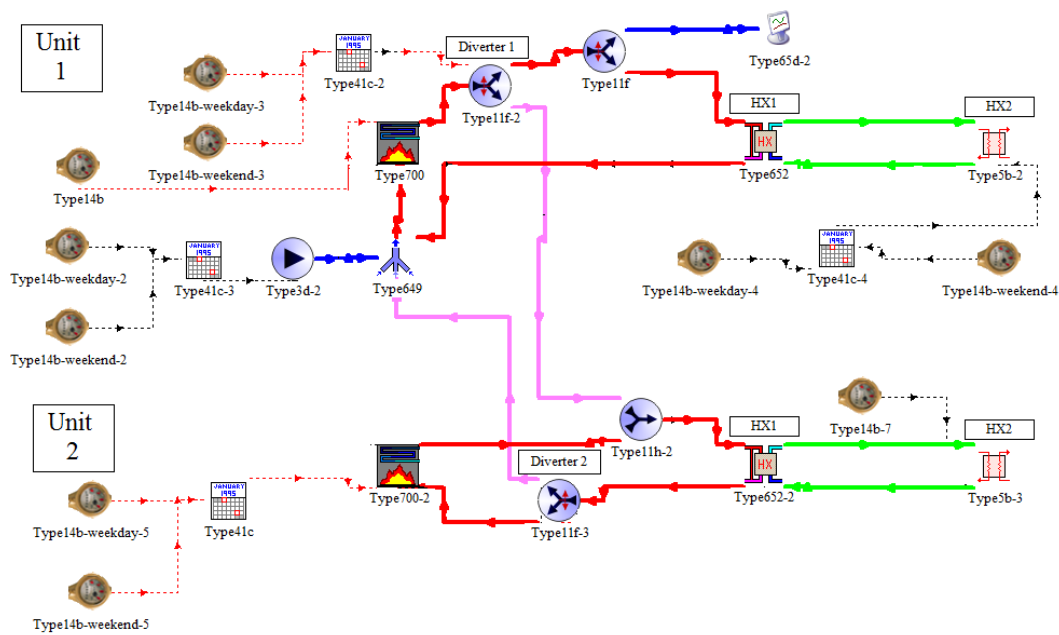


Figure 6.15. Configuration 2-1 in boilers coupled form

Figure 6.16 shows total cost of Configuration 2-1 in basic form and when two boilers have been coupled. As it was expected, the total cost in boilers coupled situation is lower than basic form in all simulation time intervals and this is because of reduction in Unit 2 fuel consumption. Unit 1 with its more efficient boiler reduces Unit 2 boiler workload, which results in reduction in total fuel consumption and total cost.

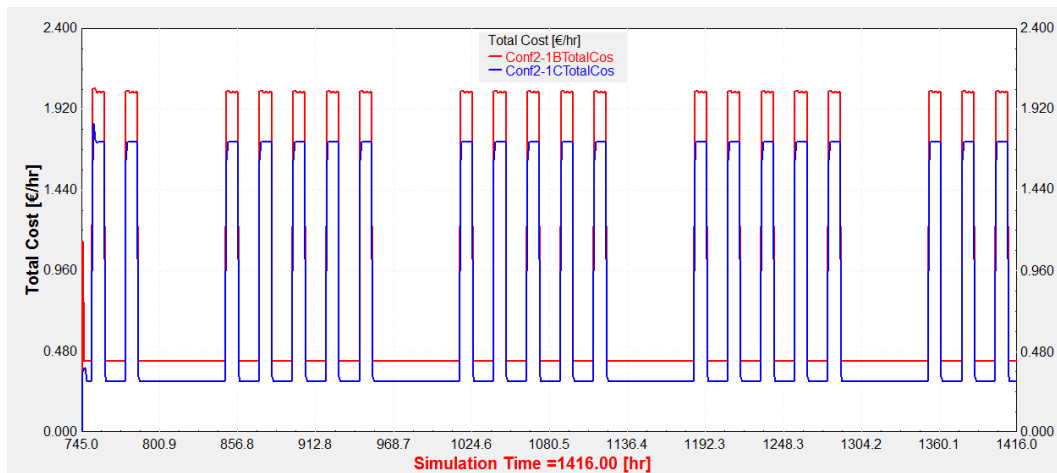


Figure 6.16. Total cost of Configuration 2-1 in two forms (basic and boilers coupled). The title Conf2-1BTotalCost shows the basic form hourly cost and Conf2-1CTotalCost shows boilers coupled situation's hourly cost.

6.3.2. Configuration 2-2

It was assumed that inside an industrial zone some Units have waste heat and Configuration 2-2 investigates the possibilities and effect of using this waste heat on the total cost of two industrial Units. In this sub-Configuration both Units have boilers with the same efficiency ($\eta_{\text{boiler}} = 0.78$), but there is an industrial waste heat stream which is fed to the storage tank and it could be shared between Units by HDN. Therefore, there are two energy sources to satisfy Units' energy demand: boilers and industrial waste heat. The waste heat stream has a 500 kg/hr continuous flow rate. Industrial waste heat temperature and storage tank volume are the variables which their influence on total cost were evaluated in this Section. Three different options, which include: Unit 1 supply-side, Unit 1 process-side and Unit 2 process-side have been introduced to use this heat source. An optimization was done to choose the best option with minimum fuel cost.

Figure 6.17 shows a schematic Diagram of the Configuration 2-2 in which simple blocks represent TRNSYS types and arrows show the flows between the components. Diverter 1, Diverter 3 and Diverter 6 control signals in Figure 6.17 are optimization outputs.

Figure 6.18 demonstrates the Configuration 2-2 thermal system and used Types inside the TRNSYS simulation environment. Between Figure 6.17 and Figure 6.18, matching colors for flows are respected to make relating two Figures to each other easier.

In Figure 6.18, a number is devoted for each component and flow which Table 6.3 clarifies each number's flowrate, temperature, and specifications. In Figure 6.18, flow streams are shown with solid colored lines and dashed lines show data transfer lines.

Again because there is not any solar energy as energy source for Units, February and June results are equal and just February results are presented in this Section. The following Section will discuss optimization procedure.

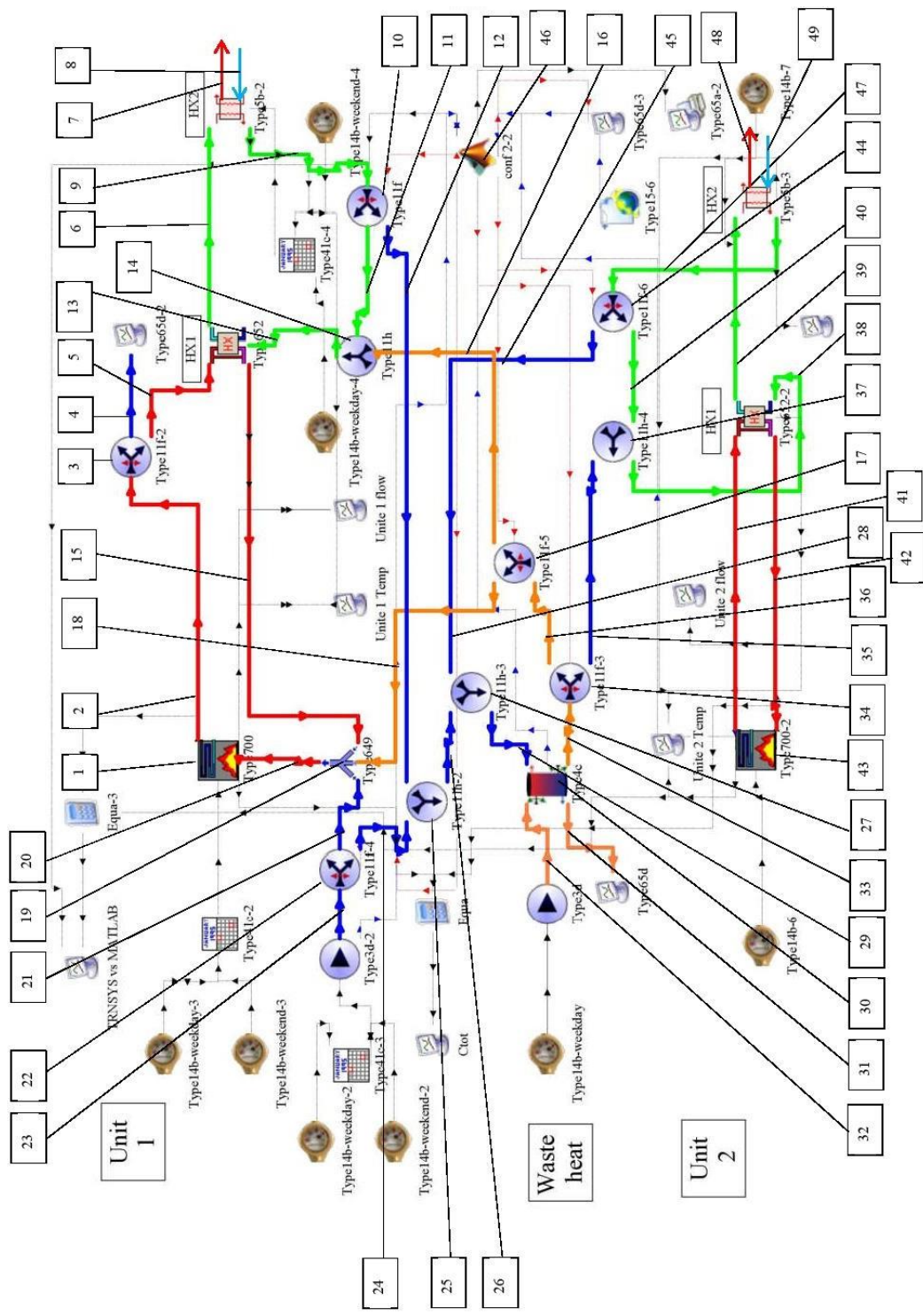


Figure 6.18. Configuration 2-2 in TRNSYS

Table 6.3. Component's name, flow rate and temperature of streams in Figure 6.18. The constant amounts of variables are presented beside each one inside parenthesis.

No.	Flow Rate (kg/hr)	Temperature (°C)	No.	Flow Rate (kg/hr)	Temperature (°C)
2	$\dot{m}_{b,U1}$ (1100)	$T_{b,U1}$ (120)	36	$\dot{m}_{1,Div5}$	$T_{1,Div5}$
4	$\dot{m}_{1,Div4}$ (100)	$T_{1,Div4}$ (120)	38	\dot{m}_{Mix5} (100)	T_{Mix5}
5	$\dot{m}_{2,Div4}$ (1000)	$T_{2,Div4}$ (120)	39	$\dot{m}_{1,HX1,U2}$ (100)	$T_{1,HX1,U2}$ (100)
6	$\dot{m}_{1,HX1,U1}$ (100)	$T_{1,HX1,U1}$ (100)	40	$\dot{m}_{1,Div6}$	$T_{1,Div6}$
7	$\dot{m}_{out,U1}$ (100)	$T_{out,U1}$	41	$\dot{m}_{b,U2}$ (1100)	$T_{b,U2}$ (120)
8	$\dot{m}_{in,U1}$ (100)	$T_{in,U1}$ (30)	42	$\dot{m}_{2,HX1,U2}$ (1100)	$T_{2,HX1,U2}$
9	$\dot{m}_{HX2,U1}$ (100)	$T_{HX2,U1}$	45	$\dot{m}_{2,Div6}$	$T_{2,Div6}$
11	$\dot{m}_{1,Div3}$	$T_{1,Div3}$	47	$\dot{m}_{HX2,U2}$ (100)	$T_{HX2,U2}$
12	$\dot{m}_{2,Div3}$	$T_{2,Div3}$	48	$\dot{m}_{out,U2}$ (100)	$T_{out,U2}$
13	\dot{m}_{Mix2} (100)	T_{Mix2}	49	$\dot{m}_{in,U2}$ (100)	$T_{in,U2}$ (30)
15	$\dot{m}_{2,HX1,U1}$ (1000)	$T_{2,HX1,U1}$	Components' Name		
16	$\dot{m}_{2,Div2}$	$T_{2,Div2}$	1	Boiler 1	
18	$\dot{m}_{1,Div2}$	$T_{1,Div2}$	3	Div4	
20	\dot{m}_{Mix1} (1100)	T_{Mix1}	10	Div3	
21	$\dot{m}_{1,Div1}$	$T_{1,Div1}$ (20)	14	Mix2	
23	$\dot{m}_{in,Div1}$ (100)	$T_{in,Div1}$ (20)	17	Div2	
24	$\dot{m}_{2,Div1}$	$T_{2,Div1}$ (20)	19	Mix1	
26	\dot{m}_{Mix3}	T_{Mix3}	22	Div1	
28	$\dot{m}_{2,Div6}$	$T_{2,Div6}$	25	Mix3	
29	\dot{m}_{Mix4}	T_{Mix4}	27	Mix4	
30	m_s	T_s	34	Div5	
31	$\dot{m}_{2,ST}$	$T_{2,ST}$	37	Mix5	
32	\dot{m}_w (500)	T_w (100)	43	Boiler 2	
33	$\dot{m}_{1,ST}$	$T_{1,ST}$	44	Div6	
35	$\dot{m}_{2,Div5}$	$T_{2,Div5}$	46	MATLAB optimizer	

6.3.2.1. Optimization Procedure

Configuration 2-2 uses optimization to manage industrial waste heat and boilers' output energy between two industrial Units in optimum form. The optimization procedure for Configuration 2-2 follows the discussed stages in Chapter 5.

Decision variables in Configuration 2-2 are output flow rate of three Diverters which are named Div1, Dive3 and Dive6 in Table 6.3 and Figure 6.17. Optimization is done by fmincon function of MATLAB and three diverters' outputs are determined to minimize the objective function. Finally, proper orders about Diverters' functions are sent to TRNSYS. All of this procedure was repeated for each hour, namely simulation time interval.

Three control signals: M1, M2 and M3 control the output of Div1, Div3 and Div6 Diverters, respectively. Equations 6.2 to 6.4 show how diverters' control signals is calculated based on three decision variables.

$$M1 = \frac{\dot{m}_{2,Div1}}{\dot{m}_{in,Div1}} \quad (6.2)$$

$$M2 = \frac{\dot{m}_{2,Div3}}{\dot{m}_{HX2,U1}} \quad (6.3)$$

$$M3 = \frac{\dot{m}_{2,Div6}}{\dot{m}_{HX2,U2}} \quad (6.4)$$

As it was described in Chapter 3, diverters' control signal is analog and it could get a value between 0 and 1. MATLAB optimizer decides the amount of three decision values. Then it uses Table 6.3 values in the denominator of three Equations to calculate three diverters' control signals. Finally, MATLAB sends M1, M2 and M3 values to related diverters in TRNSYS to operate the system based on the optimized condition.

The main focus in this Section will be on showing the objective function obtaining procedure by components' mathematical models and Table 6.3 variables. Initially, the fuel consumption in boilers was determined. As discussed in Chapter 5, in each optimization, objective function should be in terms of decision variables and in this Section, boilers' fuel consumption was derived according to three diverters' outputs.

The detailed Equations for obtaining the objective function of Configuration 2-2, are presented in Appendix A. By replacing all Equations A.1 to A.12 and Equations A.14 to A.19 of Appendix A in Equation 6.5 and Equation 6.6 respectively, the boilers' fuel consumption could be obtained based on the decision variable.

For Unit 1 calculating $\dot{Q}_{need,1}$:

$$\dot{Q}_{need,1} = (\dot{m}_{b,U1})C_p(T_{b,U1} - T_{Mix1}) \quad (6.5)$$

For Unit 2 calculating $\dot{Q}_{need,2}$:

$$\dot{Q}_{need,2} = (\dot{m}_{b,U2})C_p(T_{b,U2} - T_{2,HX1,U2}) \quad (6.6)$$

$\dot{Q}_{need,1}$ and $\dot{Q}_{need,2}$ are the amount of energy (kJ/hr) which boilers in Unit 1 and Unit 2 respectively transfer to fluid to acquire boilers' output set point temperature. By boilers' efficiency, the amount of fuel which should enter each boiler is calculated.

By replacing related Equations in Equation 6.5 and Equation 6.6, the $\dot{Q}_{need,1}$ and $\dot{Q}_{need,2}$ are defined based on three optimization decision variables: $\dot{m}_{2,Div1}$, $\dot{m}_{2,Div3}$ and $\dot{m}_{2,Div6}$. Optimization part in MATLAB decides the amount of these decision variables to make fuel consumption minimum.

The objective function is the sum of two boilers' energy ($\dot{Q}_{\text{need,total}} = \dot{Q}_{\text{need,1}} + \dot{Q}_{\text{need,2}}$) which is entered to fluid. The cumulative amount of fuel that both boilers consume is calculated by:

$$F_{\text{boiler}} = \frac{\dot{Q}_{\text{need,total}}}{3600 \eta_{\text{boiler}}} \quad (6.7)$$

F_{boiler} (kWh/hr) is the total amount of inlet fuel to both boilers in the Configuration. η_{boiler} is boilers' efficiency ($\eta_{\text{boiler}} = 0.78$) and $\dot{Q}_{\text{need,total}}$ (kJ/hr) is the total amount of energy which boilers transfer to fluid.

Therefore, with the minimization of $\dot{Q}_{\text{need,total}}$, the minimum amount of boilers' fuels could be calculated. In addition to boilers' fuel cost, there is storage tank cost for Configuration 2-2. By considering these costs for Configuration 2-2, the Equation 6.8 based on Equation 5.2, for total cost calculation is used.

$$C_{\text{total}} = C_{\text{fuel}}F + \frac{f_t C_{\text{tank}} V_t}{8760} \quad (6.8)$$

All the variables in Equation 6.8 are described in Chapter 5 and F equals the F_{boiler} in Equation 6.7. Because all simulations have been done in 1 hour, the annual cost of storage tank should be divided to all hours of one year, 8760 to obtain hourly share of storage tank cost.

6.3.2.2. Results

In this Section the MATLAB optimizer outputs and effect of some factors such as industrial waste heat temperature and storage tank volume on total hourly cost of Configuration 2-2, C_{total} in Equation 6.8, are investigated.

Figure 6.19 shows MATLAB optimizer results and storage tank average temperature for Configuration 2-2.

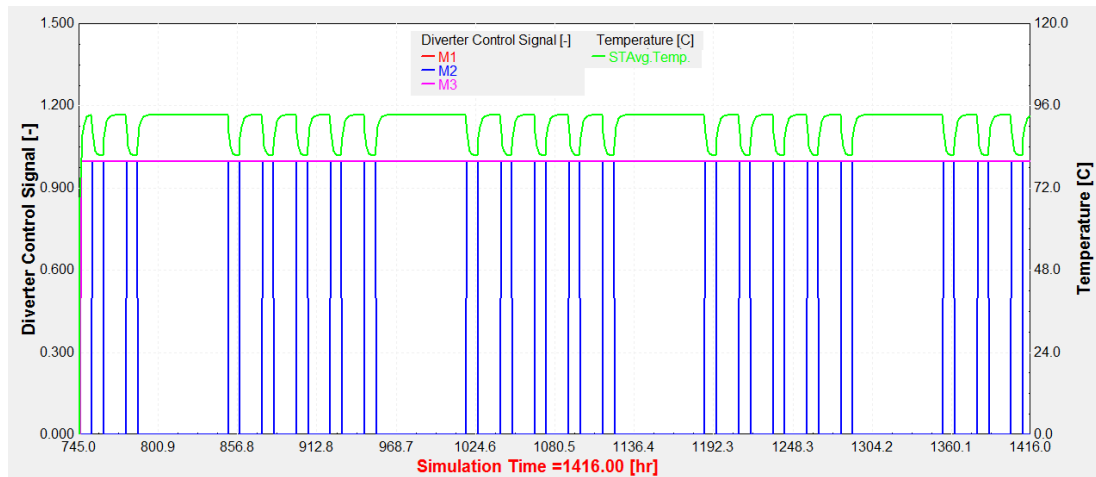


Figure 6.19. Optimization results for three decision variables, M1, M2 and M3, and storage tank average temperature, STAvg.Temp. M1 and M2 Diagrams coincide. Storage tank volume is 1 m^3 and waste heat temperature is 100°C .

From Figure 6.19, the control signal for Dive6 is always 1, which means the process-side flow in Unit 2 is always preheated by waste heat stream. When Unit 1 starts to work, both Div1 and Dive3 have control signal 1, and both supply-side and process-side in Unit 1 use industrial waste heat as a preheater. Because of this, M1 and M2 Diagrams in Figure 6.19 coincide. According to Figure 6.19, when all diverters have control signals 1, three flows are sent to the storage tank to use its heat and this reduces storage tank average temperature to 81.53°C . Again when Unit 1 is closed, because just one flow enters the storage tank, its temperature increases to 93.45°C .

Figure 6.20 shows impact of waste heat temperature on system total cost where it compares total cost for Configuration 1 as basic Configuration with Configuration 2-

2 when there are industrial waste heat streams with 500 kg/hr flow rate and different temperatures.

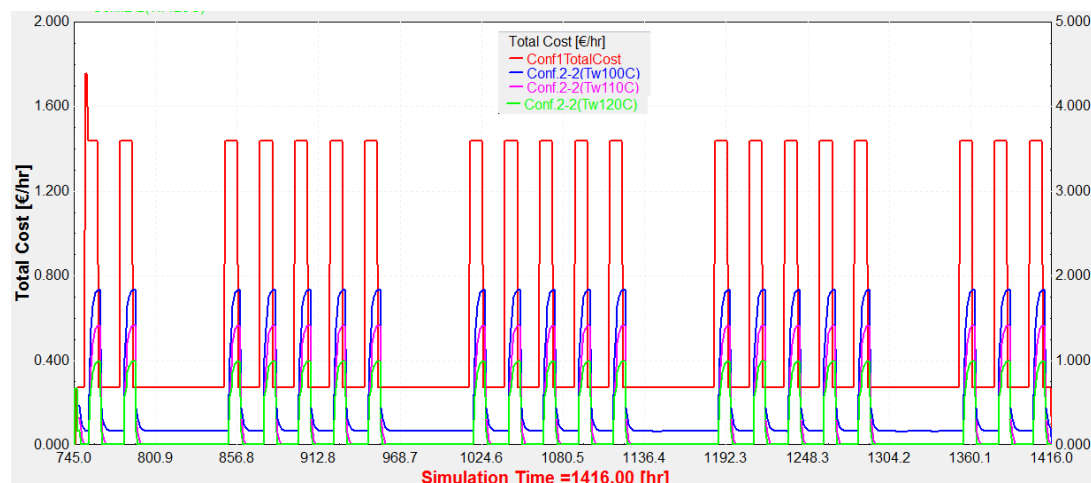


Figure 6.20. The impact of waste heat temperature on total cost of Configuration 2-2. Storage tank volume is 1 m³.

As waste heat temperature increases, total cost decreases. The total cost was shown for three waste heat temperatures, 100, 110 and 120°C. The storage tank volume is fixed on 1 m³ constant. On average, each 10°C increase in temperature decreases total hourly cost by 26% when both Units are active. When just Unit 2 is active, waste heat with 110°C or 120°C covers most of the energy demand of Unit 2. Thus increasing temperature from 110°C to 120°C has not any effect on Unit 2 total cost.

Figure 6.21 investigates the effect of storage tank volume on Configuration 2-2 hourly total cost. A bigger storage tank could store more energy, but on the contrary, its cost will be higher. Three tank volumes, 1, 2 and 5 m³, are chosen for investigation. The waste heat temperature remained constant in 100°C.

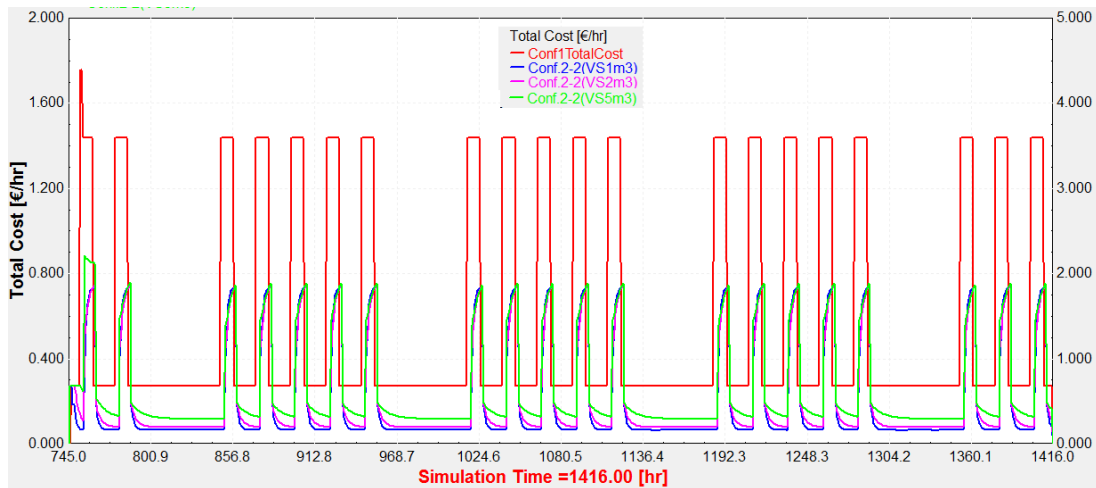


Figure 6.21. The impact of storage tank volume on total cost of Configuration 2-2. Waste heat temperature is 100 °C.

As storage tank volume increases, the cost of it will increase and this could increase hourly cost. When both Units are active the larger tank provides more liquid mass and this means storage tank could save more energy for a longer time. When both Units are working, Unit 1 hourly cost occupies a large share of Configuration total cost and any factor which could reduce fuel consumption in its boiler, could really reduce total cost. In conclusion, when both Units work, a larger storage tank provides more energy for the system especially for Unit 1 and this reduces fuel consumption in Unit 1 significantly and results in the reduction of the system's total cost. This cost reduction compensates for the larger storage tank capital cost increment. Therefore, when both Units are active, the larger storage tank's positive and negative impacts on total hourly cost result in almost the same hourly cost for three different storage tank volumes. When just Unit 2 is working, total cost is reduced which makes it more sensitive to components' cost such as storage tank capital cost and with larger storage tank the system's hourly total cost will increase. In fact, the negative effect of a larger storage tank is stronger than its positive effect in this condition. In conclusion, for a system with Configuration 2-2 structure and industrial waste heat equal to 100 °C, the storage tank with 1 m³ among studied tanks is optimum storage tank volume.

In this thesis, components' mathematical models are used in MATLAB to derive objective functions and optimization is done to minimize them. MATLAB and TRNSYS have different views to thermal systems. Some intrinsic differences between these two software cause difference in their results.

One of those intrinsic differences is that MATLAB operates immediately while TRNSYS operates gradually. For example if it is necessary to make one of the diverters' outputs zero, it could be done by setting the diverter control signal to proper amount in MATLAB code and it is done immediately inside MATLAB environment. Now if that control signal is sent to a diverter inside TRNSYS environment via MATLAB link component, the diverter output will not be immediately but gradually zero.

Figure 6.22 shows how intrinsic difference of two software affects results. For Configuration 2-2 when waste heat temperature is 100 °C and flow rate is 500 kg/hr and storage tank volume is 1 m³, the Configuration total cost was calculated one time with MATLAB and one time directly by TRNSYS. Based on Figure 6.22, by considering intrinsic differences between MATLAB and TRNSYS, the results show consistency.

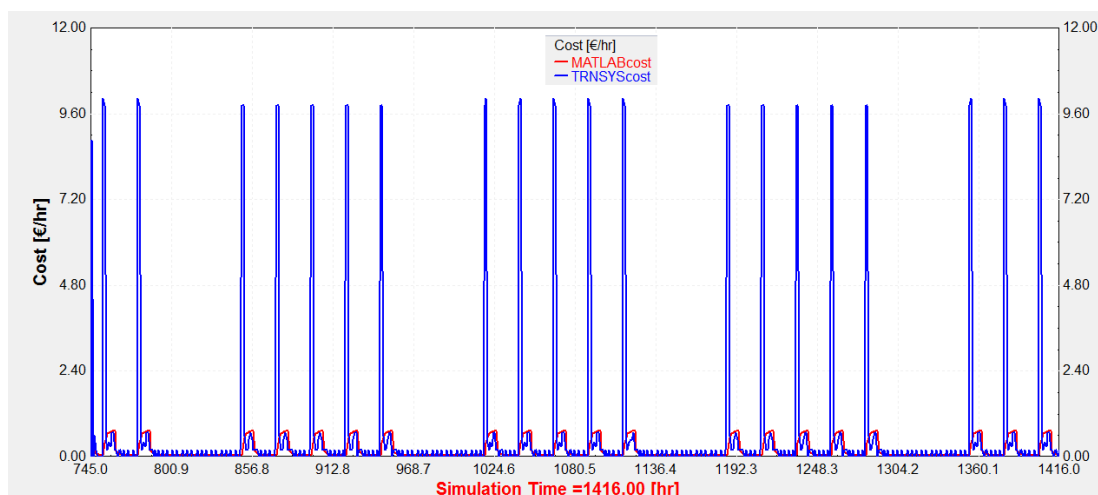


Figure 6.22. MATLAB vs. TRNSYS cost for Configuration 2-2 with waste heat temperature 100 °C and storage tank volume 1 m³

6.4. Configuration 3

In this Configuration, each Unit equipped with flat plate solar collector and a heat storage tank. There is not any network between Units and each Unit provides its required energy by the boiler or separated solar collector independently. Configuration 3 was divided into two sub-Configurations, Configuration 3-1 and Configuration 3-2 in which Configuration 3-1 evaluates Unit 1 and Configuration 3-2 simulates Unit 2 with solar energy integration. Flat plate collector area and heat storage tank volume are the main factors that their effects on systems' total hourly cost are considered. Based on Chapter 4, all solar collectors are considered in 30° declination angle and 0° azimuth angle in Izmir location. For each Unit, an optimization is done to determine how to use solar energy inside Units. Optimization procedure and related Equations are presented in each sub Configuration's Appendix. Because of integrating solar energy and available solar energy is different in February and June, results are discussed for both February and June.

6.4.1. Configuration 3-1

This sub Configuration examines Unit 1 when flat plate solar collector and a heat storage tank are integrated into its thermal system. Optimization is done to manage solar energy inside Unit 1. Solar energy could be used in the Unit's process-side or supply-side.

Figure 6.23 shows a schematic Diagram of the Configuration 3-1 in which simple blocks represent TRNSYS types and arrows show the flow between the components. Diverter 1 and Diverter 3 that their control signals are optimization outputs are demonstrated in Figure 6.23.

Figure 6.24 demonstrates the Configuration 3-1 thermal system and used Types inside the TRNSYS simulation environment. Between Figures 6.23 and 6.24, matching colors for flows are respected to make relating two Figures to each other easier.

In Figure 6.24, a number is devoted for each component and flow which Table 6.4 clarifies each number's flowrate, temperature, and its specifications. In Figure 6.24, flow streams are shown with solid colored lines and dashed lines show data transfer lines.

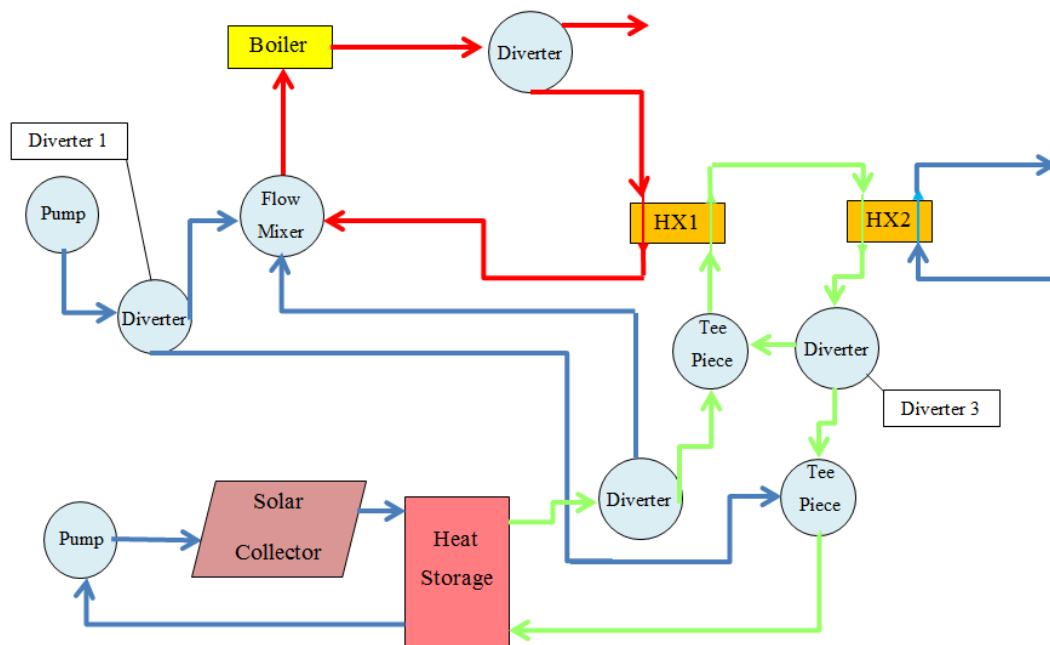


Figure 6.23. Schematic Diagram of Configuration 3-1. Divorter 1 and Divorter 3 control signals are optimization outputs.

Table 6.4. Component's name, flow rate and temperature of streams in Figure 6.24. The constant amounts of variables are presented beside each one inside the parenthesis.

No.	Flow Rate (kg/hr)	Temperature (°C)	No.	Flow Rate (kg/hr)	Temperature (°C)
2	\dot{m}_{boiler} (1100)	T_{boiler} (120)	25	\dot{m}_{coll} (100)	T_{coll}
4	$\dot{m}_{2,\text{Div4}}$ (1000)	$T_{2,\text{Div4}}$ (120)	27	$\dot{m}_{2,\text{ST}}$	$T_{2,\text{ST}}$
5	$\dot{m}_{1,\text{Div4}}$ (100)	$T_{1,\text{Div4}}$ (120)	28	$\dot{m}_{1,\text{ST}}$	$T_{1,\text{ST}}$
6	$\dot{m}_{1,\text{HX1}}$ (100)	$T_{1,\text{HX1}}$ (100)	30	$\dot{m}_{2,\text{Div2}}$	$T_{2,\text{Div2}}$
7	\dot{m}_{out} (100)	T_{out}	31	$\dot{m}_{1,\text{Div2}}$	$T_{1,\text{Div2}}$
8	\dot{m}_{in} (100)	T_{in} (30)	Components' Name		
9	\dot{m}_{HX2} (100)	T_{HX2}	1	Boiler 1	
11	$\dot{m}_{1,\text{Div3}}$	$T_{1,\text{Div3}}$	3	Div4	
13	\dot{m}_{Mix2} (100)	T_{Mix2}	10	Div3	
14	$\dot{m}_{2,\text{HX1}}$ (1000)	$T_{2,\text{HX1}}$	12	Mix2	
15	\dot{m}_{Mix1} (1100)	T_{Mix1}	16	Mix1	
17	$\dot{m}_{1,\text{Div1}}$	$T_{1,\text{Div1}}$ (20)	18	Div1	
19	$\dot{m}_{\text{in,Div1}}$ (100)	$T_{\text{in,Div1}}$ (20)	21	Mix3	
20	$\dot{m}_{2,\text{Div1}}$	$T_{2,\text{Div1}}$ (20)	26	Flat Plate Collector	
22	\dot{m}_{Mix3}	T_{Mix3}	29	Div2	
23	$\dot{m}_{2,\text{Div3}}$	$T_{2,\text{Div3}}$	32	MATLAB Optimizer	
24	m_s	T_s			

6.4.1.1. Optimization Procedure

Configuration 3-1 uses optimization to manage boiler's energy and solar energy to satisfy Unit 1 energy demand. Supplying all the energy with flat plate collector is not possible, so the boiler will be an auxiliary energy source. In this Configuration, two options for solar energy integration are defined. The first option is preheating the boiler feed water called $\dot{m}_{in,Div1}$ in Table 6.4 with solar energy and the second one is using solar energy to preheat the process side stream called \dot{m}_{HX2} in Table 6.4. $\dot{m}_{2,Div1}$ and $\dot{m}_{2,Div3}$ are decision variables in the Configuration 3-1.

Because solar energy is a variable energy source, the optimization results could be changed in each time interval. Based on two decision variables, $\dot{m}_{2,Div1}$ and $\dot{m}_{2,Div3}$ in the Configuration 3-1, two diverters' control signals are defined as optimization outputs, M1 for Diverter 1 (Div1) and M2 for Diverter 3 (Div3) controlling. Equation 6.9 and Equation 6.10 show how these variables are calculated.

$$M1 = \frac{\dot{m}_{2,Div1}}{\dot{m}_{in,Div1}} \quad (6.9)$$

$$M2 = \frac{\dot{m}_{2,Div3}}{\dot{m}_{HX2}} \quad (6.10)$$

The denominator of Equations 6.9 and 6.10 are constant and presented in Table 6.4. Diverters' control signal is analog and can vary between 0 and 1.

The detailed Equations for obtaining the objective function of Configuration 3-1, are presented in Appendix B. By replacing all Equations B.1 to B.10 of Appendix B in Equation 6.11, the Unit 1 boiler's fuel consumption could be obtained based on the decision variable.

Calculating $\dot{Q}_{need,1}$:

$$\dot{Q}_{need,1} = (\dot{m}_{boiler})C_p(T_{boiler} - T_{mix1}) \quad (6.11)$$

$\dot{Q}_{need,1}$ (kJ/hr) is the amount of energy which Unit 1 boiler transfers to fluid to acquire boiler output set point temperature and it represents objective function in this Configuration. By boilers' efficiency, Equation 6.12, the amount of fuel which should enter the boiler is calculated.

$$F_{boiler1} = \frac{\dot{Q}_{need,1}}{3600 \eta_{boiler1}} \quad (6.12)$$

$F_{boiler1}$ (kWh/hr) is the total amount of inlet fuel to boiler 1 in the Configuration. η_{boiler} is boilers efficiency ($\eta_{boiler} = 0.78$) and $\dot{Q}_{need,1}$ (kJ/hr) is the amount of energy which boiler 1 transfers to fluid.

Therefore, with minimization of $\dot{Q}_{need,1}$, the minimum amount of boiler 1 fuel consumption is calculated. In addition to boilers' fuel cost, there is the storage tank and the solar collector capital cost for Configuration 3-1. Equation 6.13 is used directly to calculate total hourly cost for this Configuration.

$$C_{total} = C_{fuel}F + \frac{f_s C_{solar}A_s + f_t C_{tank} V_t}{8760} \quad (6.13)$$

All the variables in Equation 6.13 are described in Chapter 5 and F equals the $F_{boiler1}$ in Equation 6.12.

6.4.1.2. Results

In this Section, the MATLAB optimizer outputs and effect of solar collector area and storage tank volume on total hourly cost of Configuration 3-1, C_{total} in Equation 6.13 are examined.

Figure 6.25 shows the optimization results for two diverters, M1 and M2, in February. The storage tank volume was assumed 1 m^3 and solar collector area was fixed on 20 m^2 . Moreover, in the same Figure the storage tank average temperature (STAvg.Temp), the process side temperature (T_{HX2}) and the boiler feed water temperature ($T_{2,Div1}$) are shown. In some time steps, storage tank average temperature is higher than both temperatures, T_{HX2} and $T_{2,Div1}$, and optimization determines which option minimizes the total fuel consumption by using solar energy. According to Figure 6.25, the best option for solar energy usage is preheating the boiler feed water, and always M1 is 1 and M2 is zero in February.

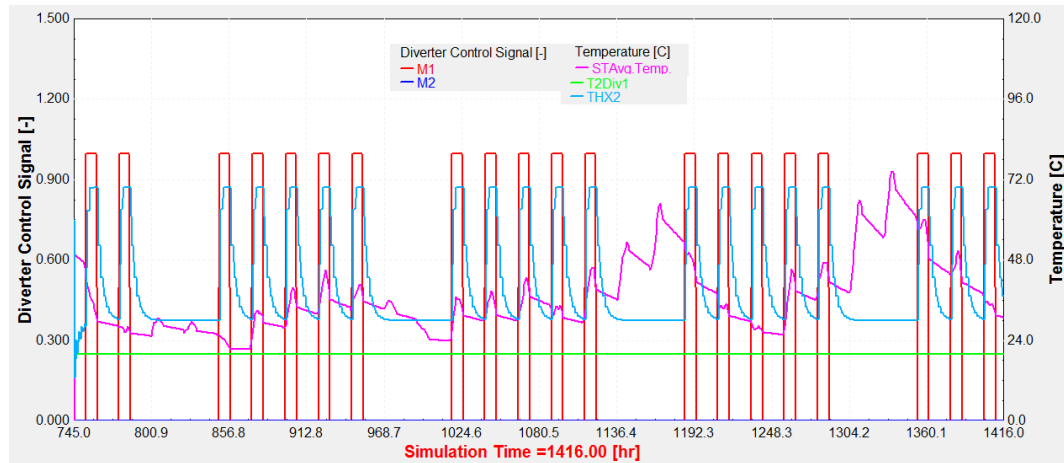


Figure 6.25. Optimization results for two Diverters, M1 and M2, the storage tank average temperature (STAvg.Temp), the process side temperature (T_{HX2}) and the boiler feed water temperature ($T_{2,Div1}$) for Configuration 3-1 in February. Storage tank volume is 1 m^3 and solar collector area is 20 m^2 .

Figure 6.26 shows similar results for Configuration 3-1 for June. In June, available solar energy is maximized, and storage tank temperature is higher in comparison with February temperature profile. Again, using the solar energy for heating boiler feed water (M1) is better option to minimize fuel consumption, but because of higher solar energy availability, sometimes it is used to preheat the flow in process side (M2).

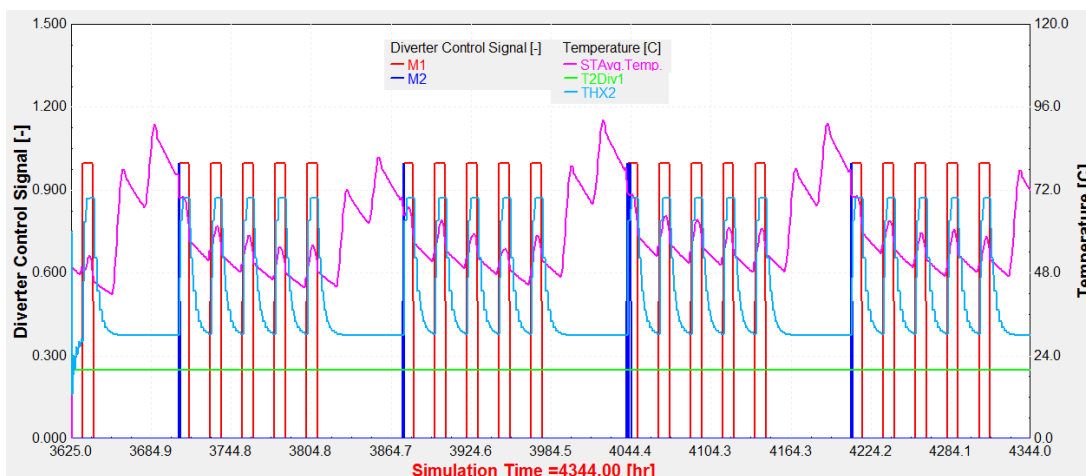


Figure 6.26. Optimization results for two Diverters, M1 and M2, the storage tank average temperature (STAvg.Temp), the process side temperature (T_{HX2}) and the boiler feed water temperature ($T_{2,Div1}$) for Configuration 3-1 in June . Storage tank volume is 1 m^3 and solar collector area is 20 m^2 .

In Figure 6.27 and Figure 6.29, the total cost of Unit 1 in Configuration 3-1 with different collector areas is compared with Unit 1 cost in Configuration 1 as basic Configuration in the February and June, respectively. In fact, In Figure 6.27 and Figure 6.29, the effect of collector area on Configuration 3-1 total cost is investigated.

The storage tank volume is fixed on 1 m^3 but collectors with 20, 30 and 60 m^2 areas are modeled. Generally, when Unit 1 is operational, the collector area increment does not change the Configuration total hourly cost significantly because the larger collector area could provide more solar energy, but it increases collector capital cost, simultaneously. Actually positive and negative effects of larger collector area counteract each other. A magnified view to Figure 6.27 and Figure 6.29 are shown in Figure 6.28 and Figure 6.30, respectively which show the general effect of different collector areas on Configuration 3-1 total cost in February and June, respectively. Using solar collector in June reduces the total cost more than that in February because of more available solar energy. When Unit 1 is non-operational, larger collector area imposes higher collector cost, which increases total cost. It could be concluded that

because larger collector area could not decrease the Configuration total cost during its operational time significantly and in the meanwhile, a large collector area causes higher total cost when Unit 1 is inactive; collector with 20 m² area among examined collectors is an optimum collector for Configuration 3-1 in both February and June.

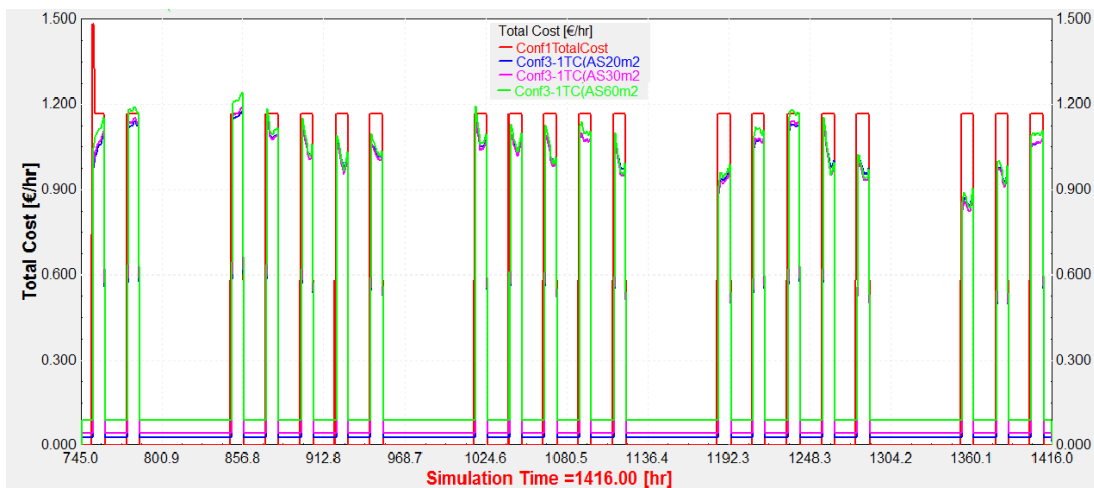


Figure 6.27. Total cost for Configuration 3-1 with different collector areas $AS=20, 30$ and 60 m^2 vs. total cost of Unit 1 in Configuration 1 (Conf1Total Cost) in February. Storage tank volume was assumed 1 m^3 .

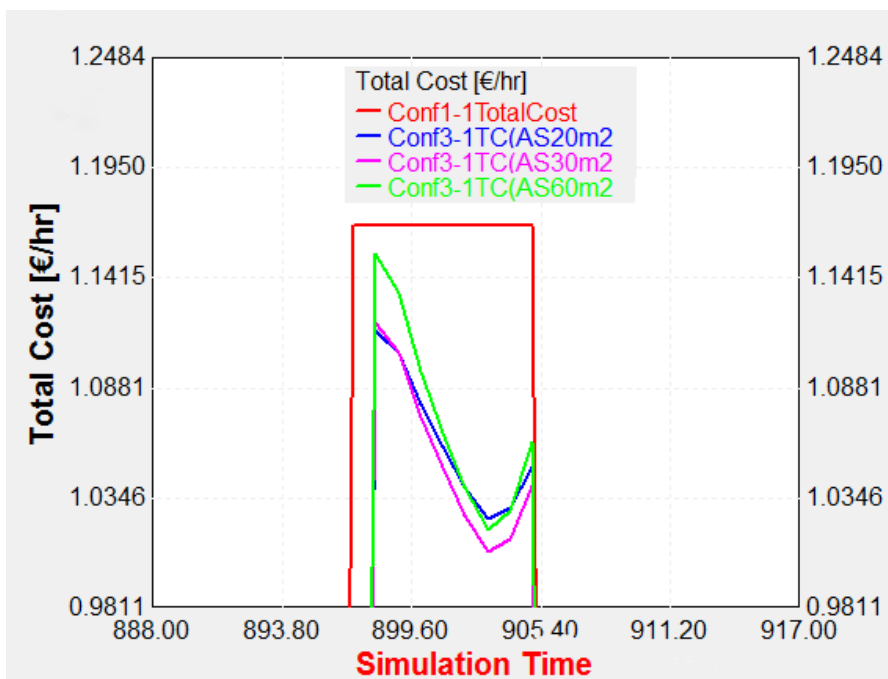


Figure 6.28. Magnified view to Figure 6.27.

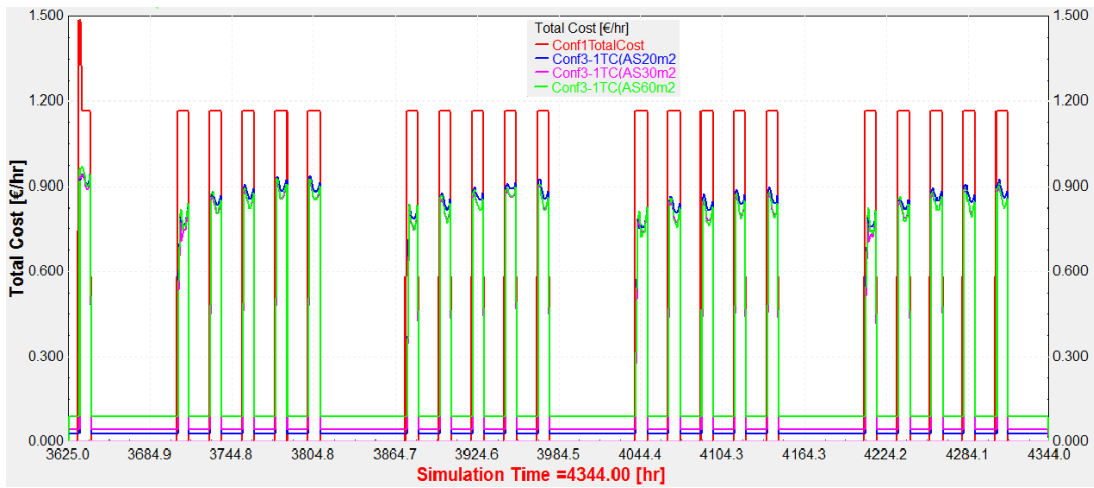


Figure 6.29. Total cost for Configuration 3-1 with different collector areas AS=20, 30 and 60 m² vs. total cost of Unit 1 in Configuration 1 (Conf1Total Cost) in June. Storage tank volume was assumed 1 m³.

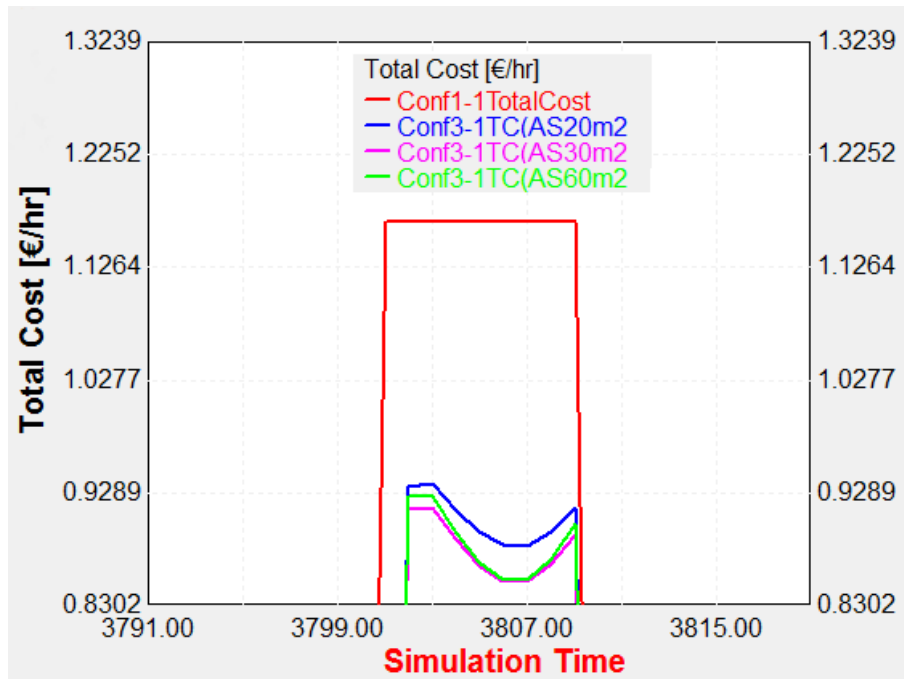


Figure 6.30. Magnified view to Figure 6.29.

The effect of storage tank volume on Configuration 3-1 total cost is examined in Figure 6.31 and Figure 6.32 for February and June, respectively. The collector area is fixed on 20 m², and storage tank volume is considered 1, 2 and 5 m³. The larger storage tank could store more energy, but again it could increase total cost negatively. According to Figure 6.31 and Figure 6.32, the negative effect of the larger storage tank volume is stronger than its positive effect in both February and June. During the operation time of Unit 1, the larger storage tank has a higher total capital cost. The positive effect of storage tank usage is more obvious for June than that of February because in the summer, there is more solar energy to be stored and used. When Unit 1 is inactive, different storage tank volume Diagrams almost coincide with each other. Therefore, considering the negative effect of the larger storage tank on total cost and its neutral effect when Unit 1 is inactive, the 1 m³ storage tank among studied storage tanks is optimal for Configuration 3-1 in both February and June.

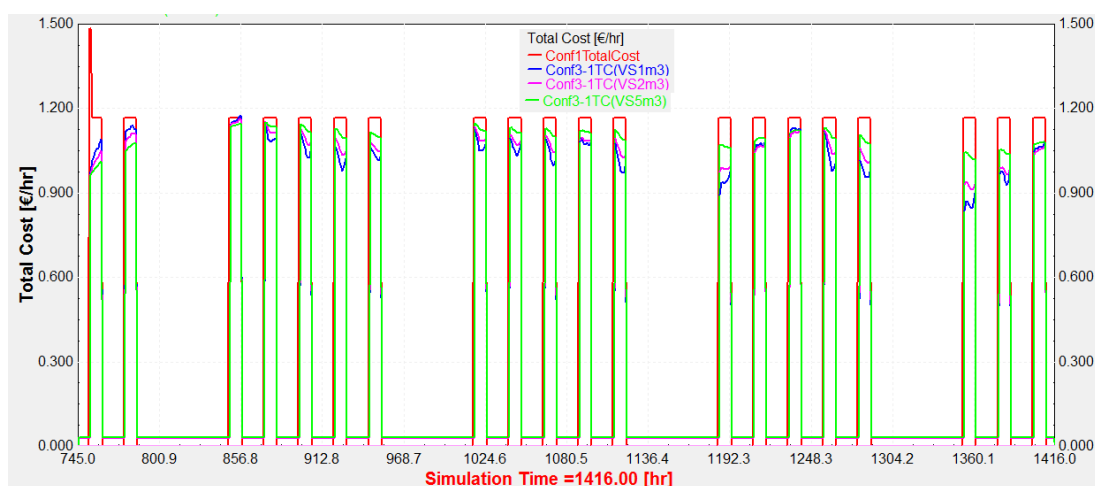


Figure 6.31. Configuration 3-1 total cost with different storage tank volumes vs. Unit 1 cost in Configuration 1 for February. Storage tank volume is assumed: VS= 1, 2 and 5 m³ and solar collector area is 20 m².

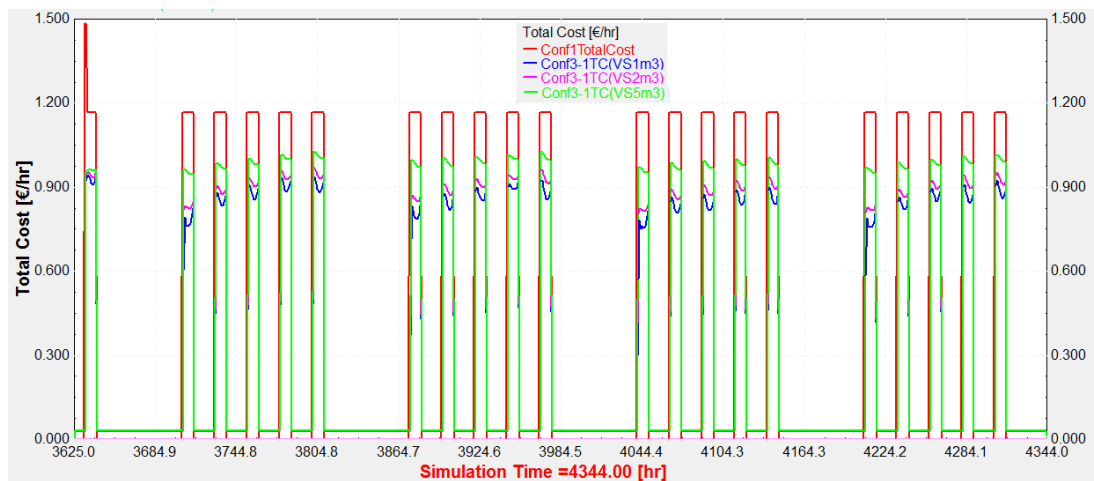


Figure 6.32. Configuration 3-1 total cost with different storage tank volumes vs. Unit 1 cost in Configuration 1 for June. Storage tank volume is assumed: VS= 1, 2 and 5 m³ and solar collector area is 20 m².

Figure 6.33 and Figure 6.34 show the Configuration 3-1 total cost with 20 m² solar collector area and 1 m³ storage tank volume. The cost was calculated using MATLAB and TRNSYS, separately. Because of some intrinsic differences between MATLAB and TRNSYS, there are some differences between the two Diagrams in Figure 6.33 and Figure 6.34, but generally, they are consistent with each other. It could be concluded that used objective function in MATLAB describes TRNSYS simulated models correctly.

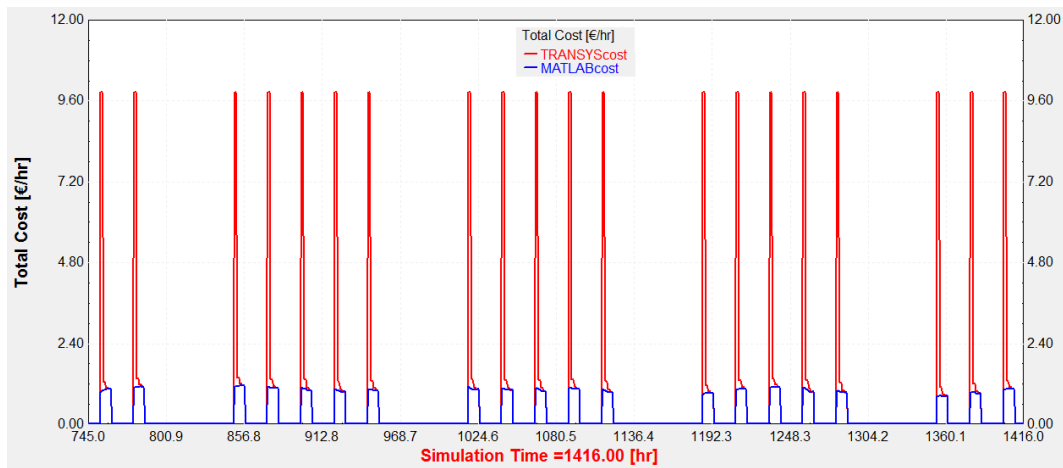


Figure 6.33. MATLAB vs. TRNSYS calculated the hourly cost for Configuration 3-1 in February.

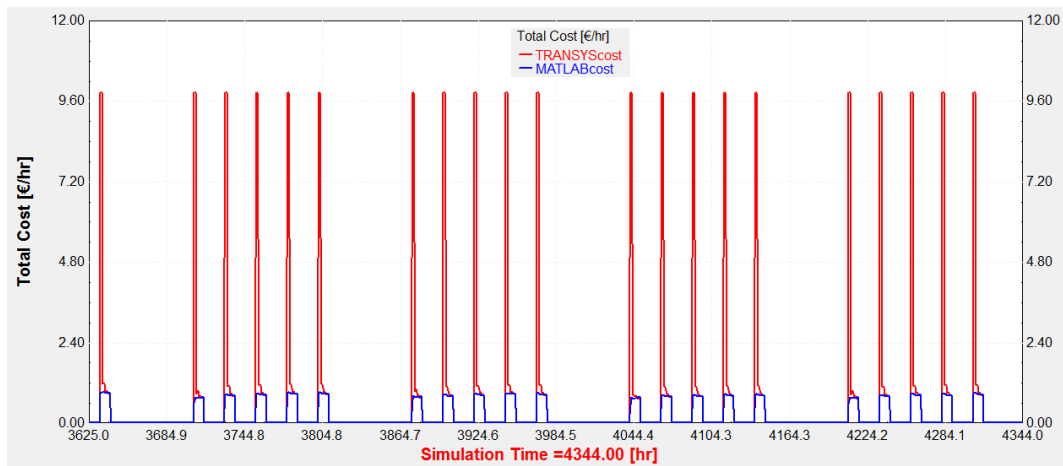


Figure 6.34. MATLAB vs. TRNSYS calculated the hourly cost for Configuration 3-1 in June.

6.4.2. Configuration 3-2

In This sub-Configuration Unit 2 is equipped with flat plate collector and heat storage tank. Optimization is done to manage solar energy inside Unit 2. However in Unit 2 there is not steam production, so solar energy just is used in the process-side. Therefore, the optimization part acts more like a controller in the Configuration 3-2. Because of solar energy, similar to Configuration 3-1, results are displayed for both February and June.

Figure 6.35 shows a schematic Diagram of the Configuration 3-2 in which simple blocks represent TRNSYS types and arrows show the flow between the components. Diverter 1 control signal is optimization output and it is demonstrated in Figure 6.35. Figure 6.36 demonstrates the Configuration 3-2 thermal system and used Types inside the TRNSYS simulation environment. In Figure 6.35 and Figure 6.36, flows colors are correspondent to make relating two Figures to each other easier. In Figure 6.36, a number is devoted to each component and flow and Table 6.5 shows each number's flowrate, temperature, and its specifications. In Figure 6.36, flow streams are shown with solid colorful lines and dashed lines show data transfer lines. Solar collector area and storage tank volume are the main variables, and their influence on total cost is analyzed.

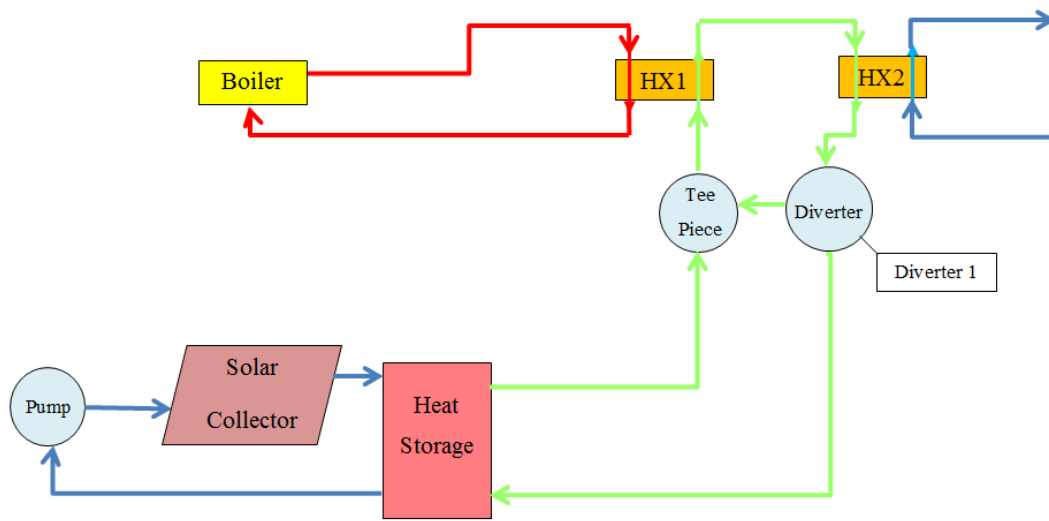


Figure 6.35. Schematic Diagram of Configuration 3-2. Diverter 1 control signal is optimization output.

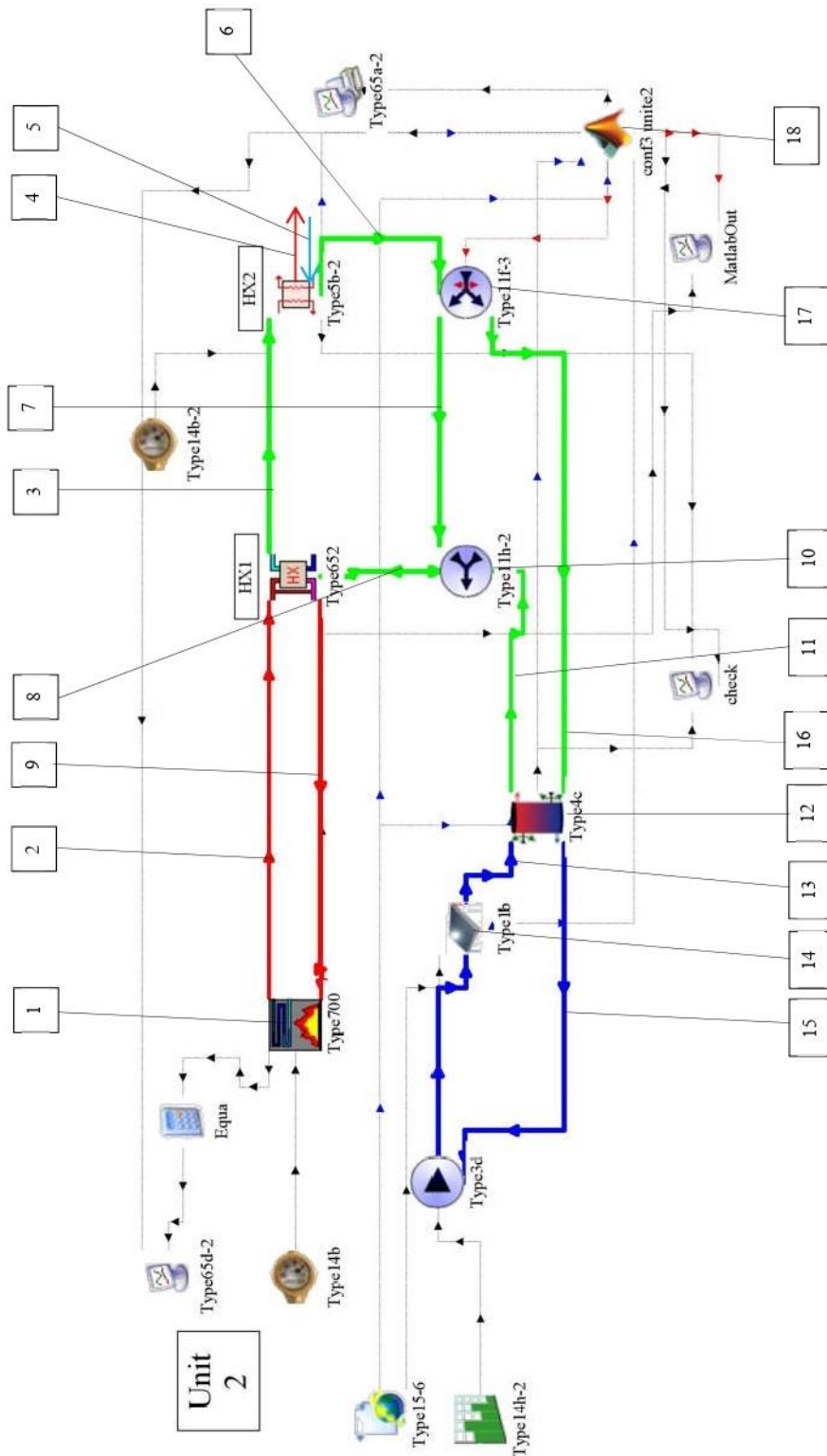


Figure 6.36. Configuration 3-2 in TRNSYS.

Table 6.5. Component's name, flow rate and temperature of streams in Figure 6.36. The constant amounts of variables are presented beside each one inside parenthesis.

No.	Flow Rate (kg/hr)	Temperature (°C)	No.	Flow Rate (kg/hr)	Temperature (°C)
2	\dot{m}_{ob} (1100)	T_{ob} (120)	13	\dot{m}_{coll} (100)	T_{coll}
3	$\dot{m}_{1,HX1}$ (100)	$T_{1,HX1}$ (100)	15	$\dot{m}_{2,ST}$ (100)	$T_{2,ST}$
4	$\dot{m}_{o,HX2}$ (100)	$T_{o,HX2}$	16	$\dot{m}_{2,Div1}$	$T_{2,Div1}$
5	$\dot{m}_{i,HX2}$ (100)	$T_{i,HX2}$ (30)	Components' Name		
6	$\dot{m}_{2,HX2}$ (100)	$T_{2,HX2}$			
7	$\dot{m}_{1,Div1}$	$T_{1,Div1}$	1	Boiler 1	
8	\dot{m}_{Mix1} (100)	T_{Mix1}	10	Mix1	
9	\dot{m}_{ib} (1100)	T_{ib}	14	Flat Plate Collector	
11	$\dot{m}_{1,ST}$	$T_{1,ST}$	17	Div1	
12	m_s	T_s	18	MATLAB optimizer	

6.4.2.1. Optimization Procedure

In Configuration 3-2, boiler energy and solar energy are managed to provide Unit 2 energy demand. Solar energy in Configuration 3-2 could be applied to preheat Unit's process-side flow, $\dot{m}_{2,HX2}$. There is just one decision variable, $\dot{m}_{2,Div1}$ which controls Div1 diverter outflows by M1. Equation 6.14 shows how optimizer calculates M1. M1 is analog and could take a value between 0 and 1.

$$M1 = \frac{\dot{m}_{2,Div1}}{\dot{m}_{2,HX2}} \quad (6.14)$$

Again, the objective function calculates the total fuel consumption in Unit 2. Minimizing fuel consumption is achieved with solar energy integrating. The detailed Equations for obtaining the objective function of Configuration 3-2, are presented in Appendix C. By replacing all Equations C.1 to C.6 of Appendix C in Equation 6.15, the objective function could be obtained based on the decision variable, $\dot{m}_{2,Div1}$. Optimization part in MATLAB decides the amount of the variable to make fuel consumption minimum.

$$\dot{Q}_{\text{need},2} = (\dot{m}_{\text{ob}})C_p(T_{\text{ob}} - T_{\text{ib}}) \quad (6.15)$$

$\dot{Q}_{\text{need},2}$ (kJ/hr) is the amount of energy which Unit 2 boiler transfers to fluid to acquire boiler output set point temperature and it represents objective function in this Configuration. By boilers' efficiency, Equation 6.16, the amount of fuel which should enter the boiler is calculated.

$$F_{\text{boiler}2} = \frac{\dot{Q}_{\text{need},2}}{3600 \eta_{\text{boiler}}} \quad (6.16)$$

$F_{\text{boiler}2}$ (kWh/hr) is the total amount of inlet fuel to boiler 2 in the Configuration. η_{boiler} is boiler efficiency ($\eta_{\text{boiler}} = 0.78$) and $\dot{Q}_{\text{need},2}$ (kJ/hr) is the amount of energy which boiler 2 transfers to fluid.

Therefore, with minimization of $\dot{Q}_{\text{need},2}$, the minimum amount of boiler 2 fuel consumption is calculated. In addition to boilers' fuel cost, there is the storage tank and the solar collector cost for Configuration 3-2. Equation 6.17 is used directly to calculate total hourly cost for this Configuration.

$$C_{\text{total}} = C_{\text{fuel}}F + \frac{f_s C_{\text{solar}}A_s + f_t C_{\text{tank}} V_t}{8760} \quad (6.17)$$

All the variables in Equation 6.17 are described in Chapter 5 and F equals the $F_{\text{boiler}2}$ in Equation 6.16.

6.4.2.2. Results

Figure 6.37 and Figure 6.38 display the decision variable, $M1$ in left y-axis and storage tank average temperature, $ST_{\text{Avg.Temp}}$ and HX2 hot-side out temperature, $HX2_{\text{OutTemp}}$, in right y-axis for February and June, respectively. The solar collector area is fixed on 20 m^2 and 1 m^3 is assumed as storage tank volume. In Configuration 3-2 just when $ST_{\text{Avg.Temp}}$ is higher than $HX2_{\text{OutTemp}}$, the solar energy is used for

preheating and in February, according to Figure 6.37, this happens only four times. Storage tank stores solar energy which is provided by flat plate collectors and in February there is not so much solar energy. Figure 6.38 shows the results for June. Because of so much available solar energy the storage tank average temperature is higher and M1 continuously operates to use stored solar energy in Unit 2 process side.

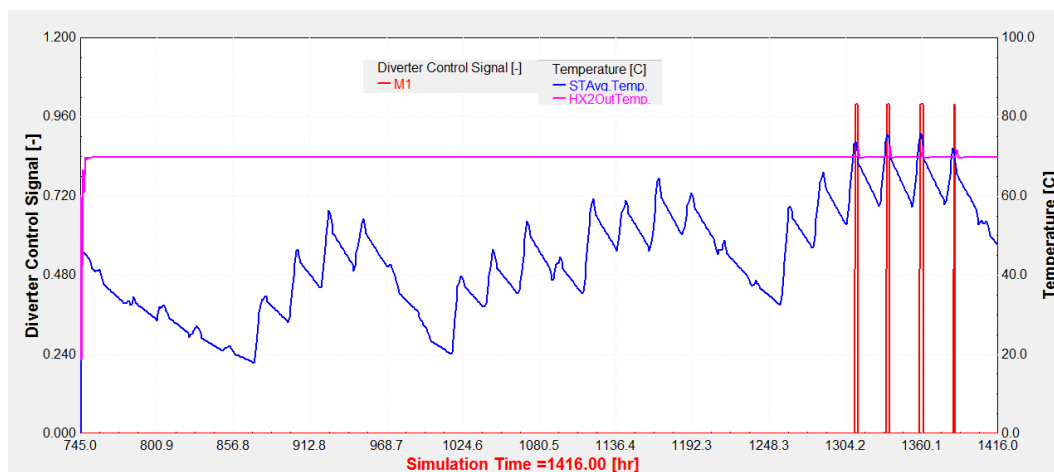


Figure 6.37. Configuration 3-2 diverter control signal, M1, vs storage tank average temperature, STAvg.Temp, and HX2 source side out temperature, HX2OutTemp for February. The collector area is 20 m² and storage tank volume is 1 m³.

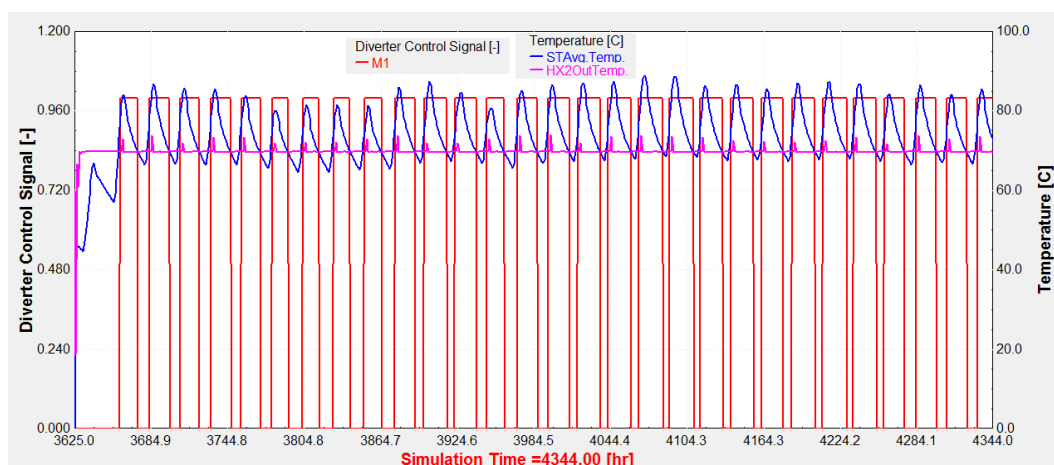


Figure 6.38. Configuration 3-2 diverter control signal, M1, vs. storage tank average temperature, STAvg.Temp, and HX2 source side out temperature, HX2OutTemp for June. The collector area is 20 m² and storage tank volume is 1 m³.

Figure 6.39 and Figure 6.40 compare the total cost of Configuration 3-2 with different collector areas with Unit 2 cost in Configuration 1 as a basic configuration for February and June, respectively. In fact, Figure 6.39 and Figure 6.40 examine the effect of solar collector area on Configuration 3-2 total cost. The solar collector area is assumed 20, 30 and 60 m² and the storage tank volume is assumed constant in 1m³. Generally, collector area increment increases total cost except when Diverter 1 incorporates solar energy in Unit 2 process side in both February and June. In fact, a larger solar collector area provides more solar energy but it increases collector cost, simultaneously. Because in February, Unit 2 could not benefit from so much solar energy, according to Figure 6.39, the larger solar collector area just increases total cost negatively. In Figure 6.40, Unit 2 uses solar energy continuously so the larger solar collector area could be beneficial for cost reduction. Actually according to Figure 6.40, when Unit 2 uses solar energy, the larger solar collector area reduces total cost while when it does not use solar energy, a larger collector area increases the total cost.

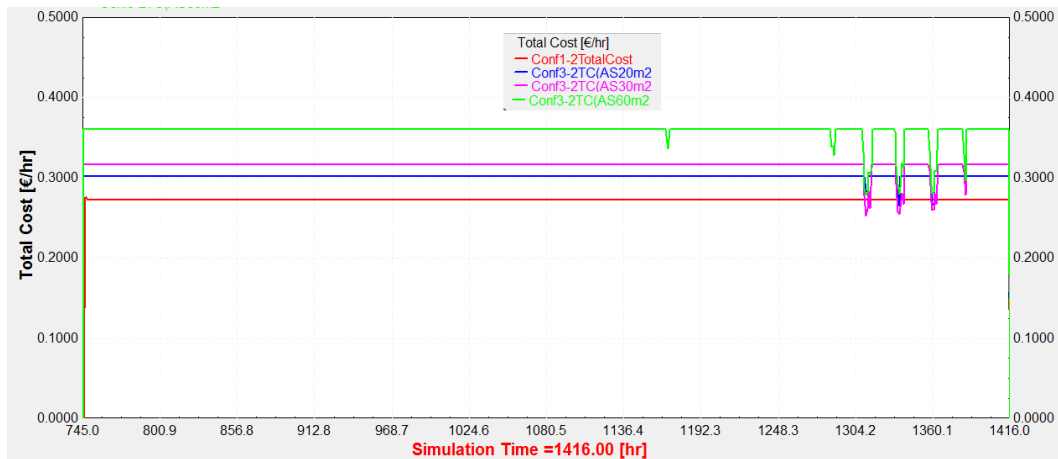


Figure 6.39. Unit 2 total cost in Configuration 1 vs. Unit 2 total cost in Configuration 3-2 with different flat plate collector areas ($AS=20, 30, 60 \text{ m}^2$) and constant storage tank volume, 1 m^3 , in February.

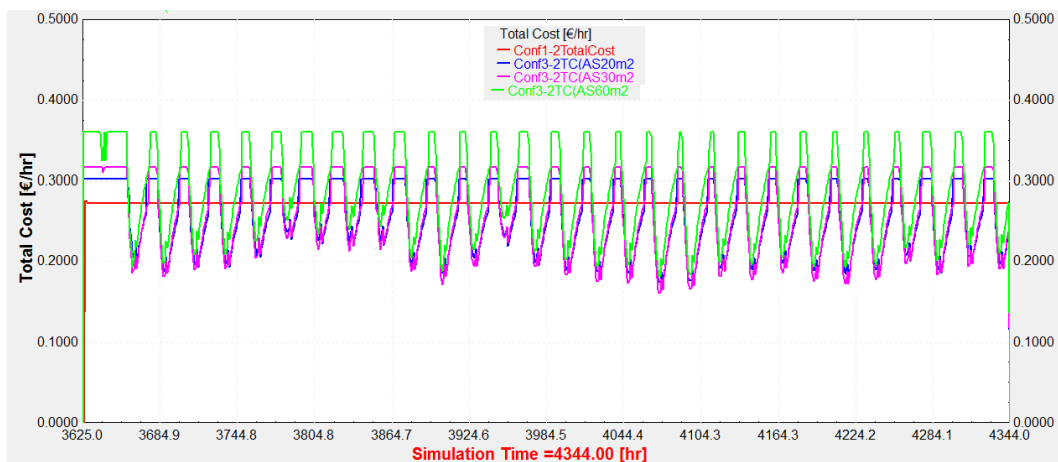


Figure 6.40. Unit 2 total cost in Configuration 1 vs. Unit 2 total cost in Configuration 3-2 with different flat plate collector areas ($AS=20, 30, 60 \text{ m}^2$) and constant storage tank volume 1 m^3 in June.

The effect of storage tank volume on Configuration 3-2 total cost is considered in Figure 6.41 and Figure 6.43 for February and June, respectively. The solar collector area is fixed on 20 m^2 and $1, 2$ and 5 m^3 storage tank volumes are applied in the model. According to Figure 6.41, different storage tanks' volumes provide almost equal total

cost except for storage tank with 1 m³ volume which shows some reductions when solar energy is integrated to Unit 2. Other storage tanks with 2 and 5 m³ volumes show almost equal and constant total cost without any variation. In fact, when storage tank volume is increased, the energy storage capacity of the tank is also increased and it could store more energy for a longer time, but its average temperature is decreased. The storage tank average temperature profiles are shown in Figure 6.42 in February. As it is obvious in Figure 6.42, tank with 1m³ volume shows a higher average temperature in comparison with other volumes and sometimes it exceeds the HX2 hot-side outlet temperature, HX2OutTemp. This creates an opportunity to preheat HX2 hot side outlet flow with stored solar energy in the storage tank. Because of this, in Figure 6.41, between studied storage tanks just storage tank with 1 m³ volume reduces total cost in some hours. In conclusion, for Unit 2 with 20 m² solar collector area, storage tank with 1 m³ volume is the best choice among examined storage tanks in February.



Figure 6.41. Unit 2 total cost in the Configuration 1 vs. Unit 2 total cost in Configuration 3-2 with different storage tank volumes, VS=1, 2, 5 m³ and 20 m² solar collector area in February.

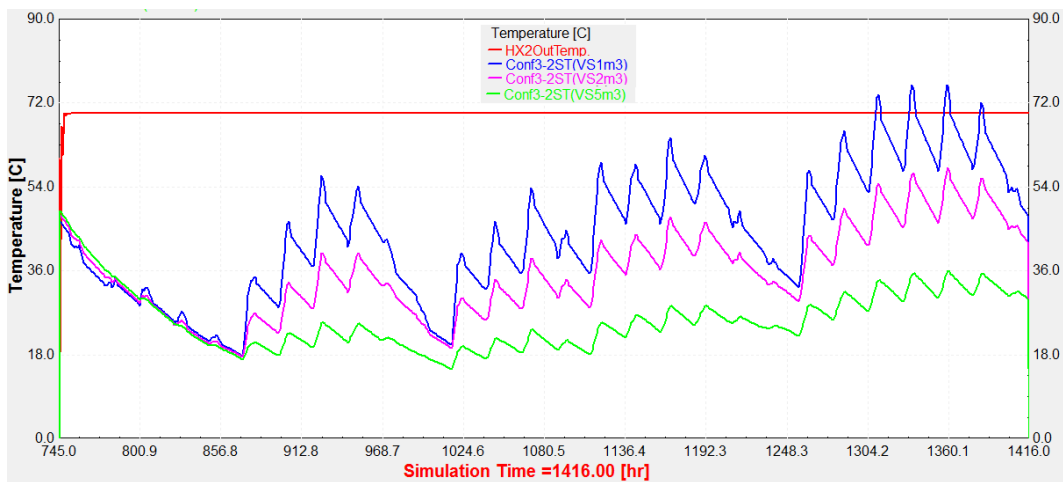


Figure 6.42. Storage tank average temperature profile for tanks with 1, 2 and 5 m³ volumes and 20 m² collector areas in Configuration 3-2 for February.

Figure 6.43 investigates the Unit 2 total cost with different storage tank volumes in June. Solar collector area again is fixed on 20 m² and 1, 2 and 5 m³ are considered as tank's volumes. Figure 6.43 shows that tank volumes with 1 and 2 m³ reduce total cost but 5 m³ tank does not cause any variation on the system's total cost. In addition, 1 m³

tank reduces total cost more than 2 m³ tank. Again according to the same reasoning for Figure 6.41, the larger storage tank shows a lower average temperature which prohibits it to be used as energy source for high-temperature streams. Figure 6.44 shows storage tank average temperature profile for three different tank volumes for June. The average temperature of tanks with 1 and 2 m³ volumes sometimes exceeds the HX2OutTemp which means solar energy could be used as a preheater but the temperature of tank with 5 m³ volume remains always lower than HX2OutTemp which means it could not provide energy to be used as a preheater energy source. According to Figure 6.41 and Figure 6.43, for Unit 2 in both February and June, 1 m³ tank is the best option to integrate solar energy.

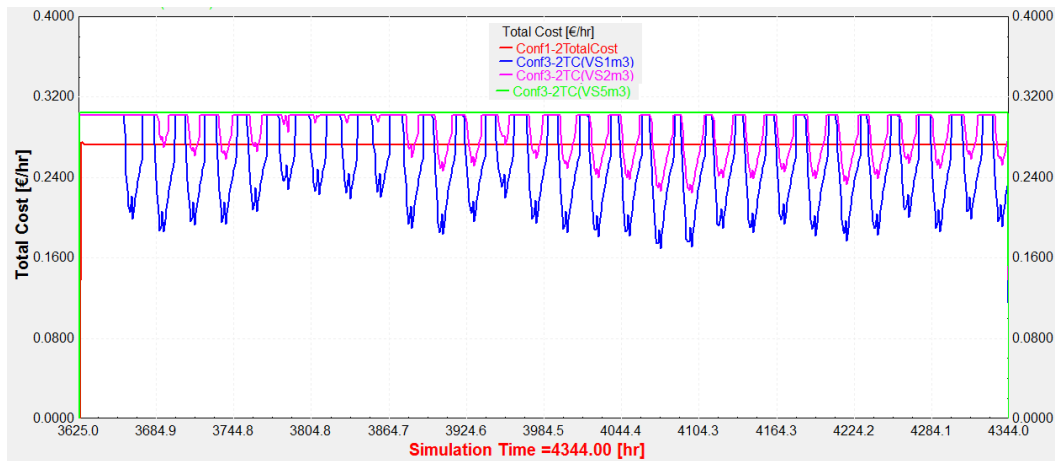


Figure 6.43. Unit 2 total cost in the Configuration 1 vs. Unit 2 total cost in Configuration 3-2 with different storage tank volumes, VS=1, 2, 5 m³ and 20 m² solar collector area in June.

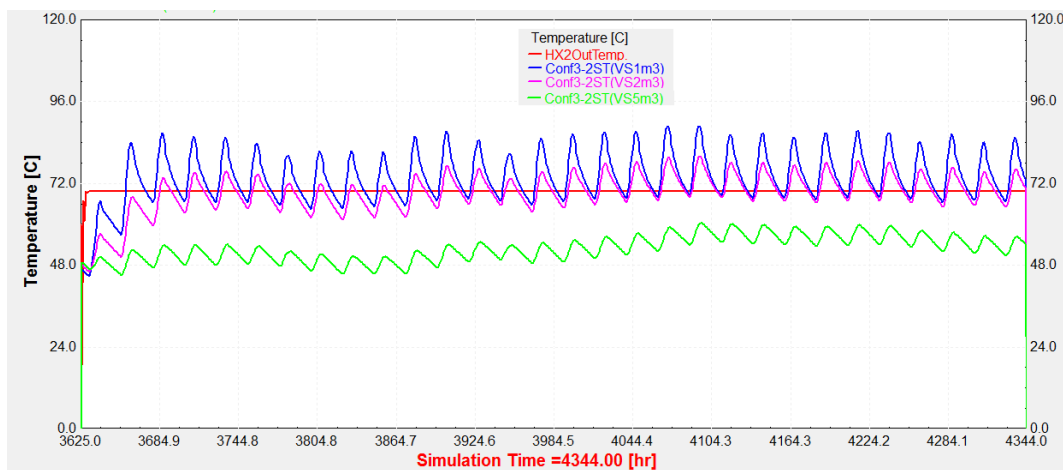


Figure 6.44. Storage tank average temperature profile for tanks with 1, 2 and 5 m³ volumes and 20 m² collector areas in Configuration 3-2 for the June.

Figure 6.45 and Figure 6.46 show the Configuration 3-2 total cost which is calculated using MATLAB and TRNSYS separately for February and June, respectively. The solar collector area and storage tank volume are assumed to be 20 m² and 1 m³, respectively. Figure 6.45 and Figure 6.46 show the consistency between MATLAB and TRNSYS results. This consistency shows that to calculating the Configuration's

total cost MATLAB uses the components' models which are the same as the models which TRNSYS uses in the simulations.

The Figures similar to Figure 6.45 and Figure 6.46 are used as debugging tools during validating all used Equations' accuracy. During simulating Configurations 3-2, initially the MATLAB and TRNSYS results had significant deviations, and significant time was spent to identify the cause, which ultimately associated with a typo in a MATLAB Equation. After correcting this typo the results matched, which increases the confidence in my MATLAB model. Briefly, if one of the Equations inside MATLAB is different from components' mathematical models in TRNSYS, there will be a big difference between MATLAB and TRNSYS calculated total hourly cost.

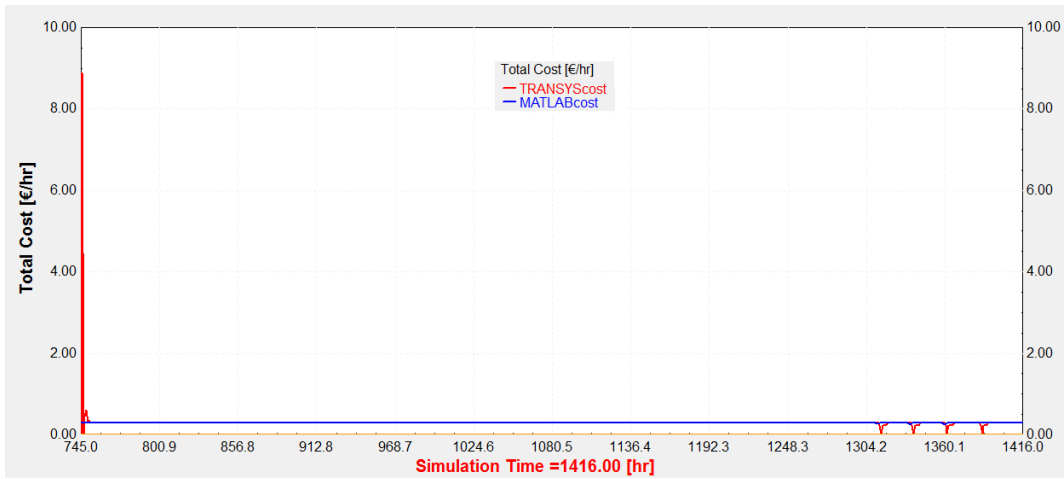


Figure 6.45. Configuration 3-2 total cost by MATLAB vs. TRNSYS in February.

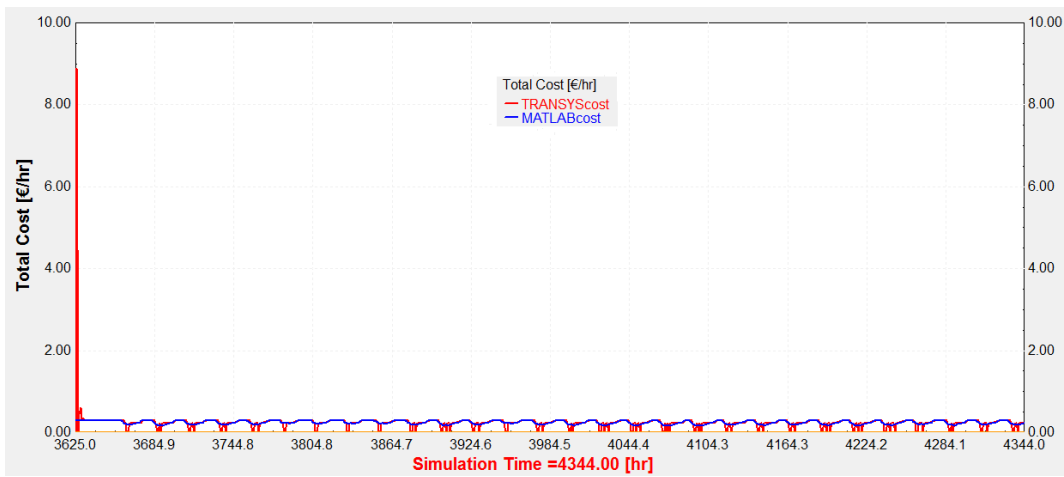


Figure 6.46. Configuration 3-2 total cost by MATLAB vs. TRNSYS in June.

6.5. Configuration 4

Configuration 4 investigates the effect of solar energy integration on the total cost of both Unit 1 and Unit 2 but unlike Configuration 3, the solar energy is provided by a central solar field. The central solar field uses same flat plate collectors with the same collector orientation in Configuration 3 and because of a larger available area, the solar collector area in the central solar field is larger than that for separated collectors. Again water is used to extract heat from collectors and solar field inlet water flow rate is fixed on 500 kg/hr in all simulations. In Configuration 4, the effect of the solar collector area and storage tank volume with different values on the Configuration's total cost, are studied.

Configuration 4 and Configuration 2-2 are so similar from structure and streams' specification points with the same flow rates and temperatures' names, but instead of industrial waste heat, the heat storage tank in Configuration 4 is fed by central solar collectors. The provided solar energy could be shared between Units by HDN. As a matter of fact, the only difference between Configuration 4 and Configuration 2-2 is using a central solar field outlet flow rate/temperature (m_{coll}/ T_{coll}) in Configuration 4 instead of industrial waste heat flow rate/temperature (m_w/ T_w) in Configuration 2-2. The MATLAB optimizer is used to manage central solar thermal energy and boilers' output energy between Units in optimum form for Configuration 4.

Because Configuration 4 and Configuration 2-2 are parallel, the optimization procedure, the objective function and decision variables in Configuration 4 are adopted from Configuration 2-2 and this Section mainly focuses on presenting results for Configuration 4. The used decision variables and Equations for optimization in Configuration 4 are discussed in Appendix D in more detail. The main aim of Configuration 4 is to assess the influence of the central solar field instead of separated solar collectors for each Unit, on the Configuration's total cost.

Figure 6.47 presents the schematic Diagram of Configuration 4 with simple blocks instead of components and arrows represent flows between the components. Figure

6.48 shows Configuration 4 in TRNSYS simulation environment with used Types, flow or data transfer lines between them. For clarifying the components and flows' names and specifications, a number is devoted to each one in Figure 6.48 and Table 6.6 expresses the related information for each number. The applied colors for flows between components in Figure 6.47 and Figure 6.48 are consistent.

Figure 6.47, Figure 6.48 and Table 6.6 are all adopted from Configuration 2-2 Section with a minor change in storage tank feeder flow which is replaced with central solar collector outlet flow.

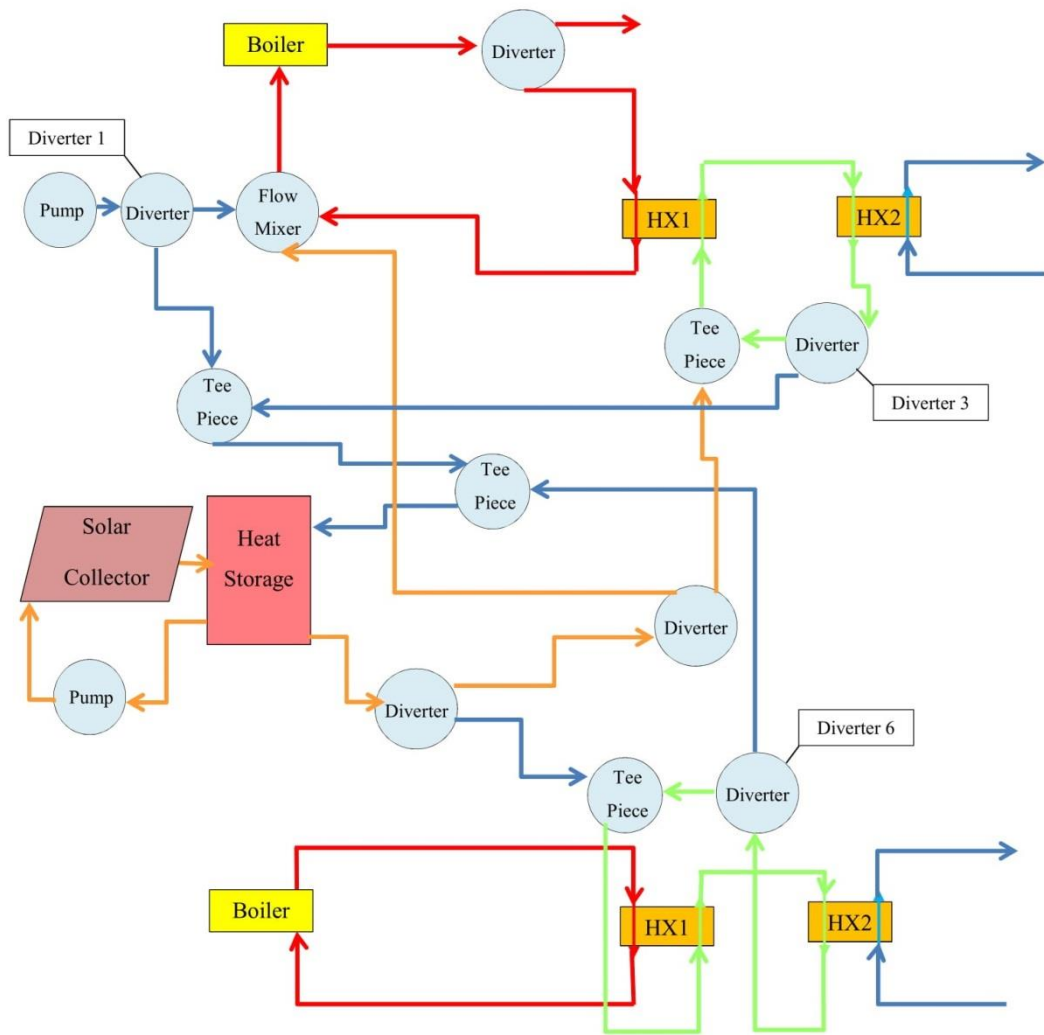


Figure 6.47. Schematic Diagram of Configuration 4. Diverter 1, Diverter 3 and Diverter 6 are the diverters which are controlled by optimization outputs.

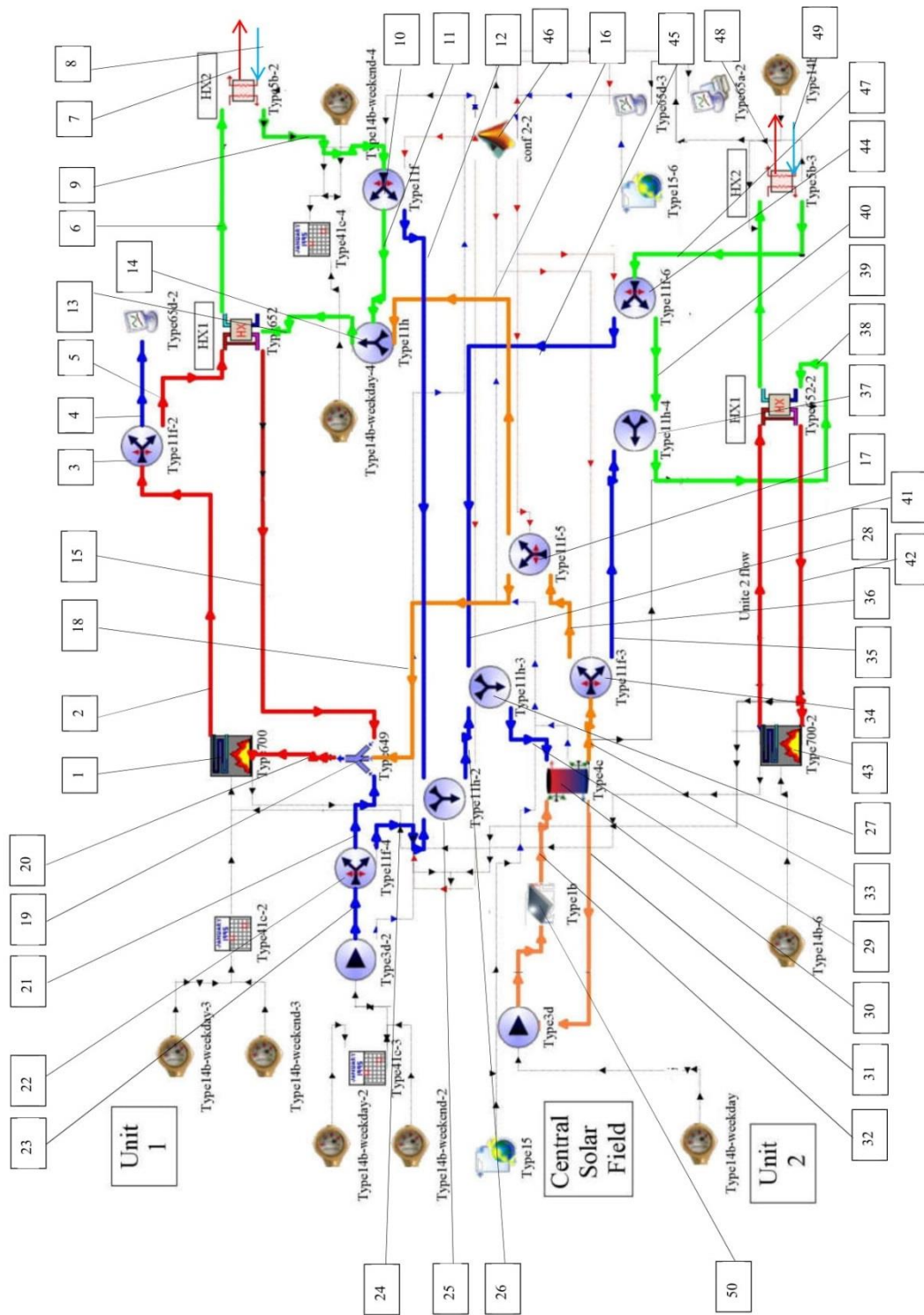


Figure 6.48. Configuration 4 in TRNSYS

Table 6.6. Components' name, flow rate and temperature of streams in Figure 6.48. The constant amounts of variables are presented beside each one inside parenthesis.

No.	Flow Rate (kg/hr)	Temperature (°C)	No.	Flow Rate (kg/hr)	Temperature (°C)
2	$\dot{m}_{b,U1}$ (1100)	$T_{b,U1}$ (120)	38	\dot{m}_{Mix5} (100)	T_{Mix5}
4	$\dot{m}_{1,Div4}$ (100)	$T_{1,Div4}$ (120)	39	$\dot{m}_{1,HX1,U2}$ (100)	$T_{1,HX1,U2}$ (100)
5	$\dot{m}_{2,Div4}$ (1000)	$T_{2,Div4}$ (120)	40	$\dot{m}_{1,Div6}$	$T_{1,Div6}$
6	$\dot{m}_{1,HX1,U1}$ (100)	$T_{1,HX1,U1}$ (100)	41	$\dot{m}_{b,U2}$ (1100)	$T_{b,U2}$ (120)
7	$\dot{m}_{out,U1}$ (100)	$T_{out,U1}$	42	$\dot{m}_{2,HX1,U2}$ (1100)	$T_{2,HX1,U2}$
8	$\dot{m}_{in,U1}$ (100)	$T_{in,U1}$ (30)	45	$\dot{m}_{2,Div6}$	$T_{2,Div6}$
9	$\dot{m}_{HX2,U1}$ (100)	$T_{HX2,U1}$	47	$\dot{m}_{HX2,U2}$ (100)	$T_{HX2,U2}$
11	$\dot{m}_{1,Div3}$	$T_{1,Div3}$	48	$\dot{m}_{out,U2}$ (100)	$T_{out,U2}$
12	$\dot{m}_{2,Div3}$	$T_{2,Div3}$	49	$\dot{m}_{in,U2}$ (100)	$T_{in,U2}$ (30)
13	\dot{m}_{Mix2} (100)	T_{Mix2}	Components' Name		
15	$\dot{m}_{2,HX1,U1}$ (1000)	$T_{2,HX1,U1}$	1	Boiler 1	
16	$\dot{m}_{2,Div2}$	$T_{2,Div2}$	3	Div4	
18	$\dot{m}_{1,Div2}$	$T_{1,Div2}$	10	Div3	
20	\dot{m}_{Mix1} (1100)	T_{Mix1}	14	Mix2	
21	$\dot{m}_{1,Div1}$	$T_{1,Div1}$ (20)	17	Div2	
23	\dot{m}_{inDiv1} (100)	$T_{in,Div1}$ (20)	19	Mix1	
24	$\dot{m}_{2,Div1}$	$T_{2,Div1}$ (20)	22	Div1	
26	\dot{m}_{Mix3}	T_{Mix3}	25	Mix3	
28	$\dot{m}_{2,Div6}$	$T_{2,Div6}$	27	Mix4	
29	\dot{m}_{Mix4}	T_{Mix4}	34	Div5	
30	m_s	T_s	37	Mix5	
31	$\dot{m}_{2,ST}$	$T_{2,ST}$	43	Boiler 2	
32	\dot{m}_{coll} (500)	T_{coll}	44	Div6	
33	$\dot{m}_{1,ST}$	$T_{1,ST}$	46	MATLAB optimizer	
35	$\dot{m}_{2,Div5}$	$T_{2,Div5}$	50	Solar Collector	
36	$\dot{m}_{1,Div5}$	$T_{1,Div5}$			

6.5.1. Results

In this Section, the MATLAB optimizer outputs and the effect of the solar field's collector area and storage tank volume on total hourly cost of Configuration 4 are investigated.

Figure 6.49 and Figure 6.50 show the optimization outputs, three Diverters' control signals which are named M1, M2, and M3 for Configuration 4 in February and June, respectively. M1, M2, and M3 control the output of Div1, Div3 and Div6 Diverters as shown in Figure 6.47, respectively.

In Figure 6.49, the Diverters' control signals and storage tank average temperature are shown in the left and right y-axis respectively for February. In most of the time steps, M1 is 1 which means solar energy mostly is used to preheat Unit 1 boiler feed water. Solar energy rarely is used in Unit 1 process-side. In some hours, solar energy is used to preheat the flow in Unit 2 process-side. In Figure 6.49, the solar collector area is assumed to be 100 m^2 and storage tank volume is fixed on 1 m^3 .

Figure 6.50 displays Configuration 4 diverters' controls signal versus storage tank average temperature for June. Because of more available solar energy in June, storage tank average temperature is higher than that for February and solar energy is used in all three options in both Units in Configuration 4.

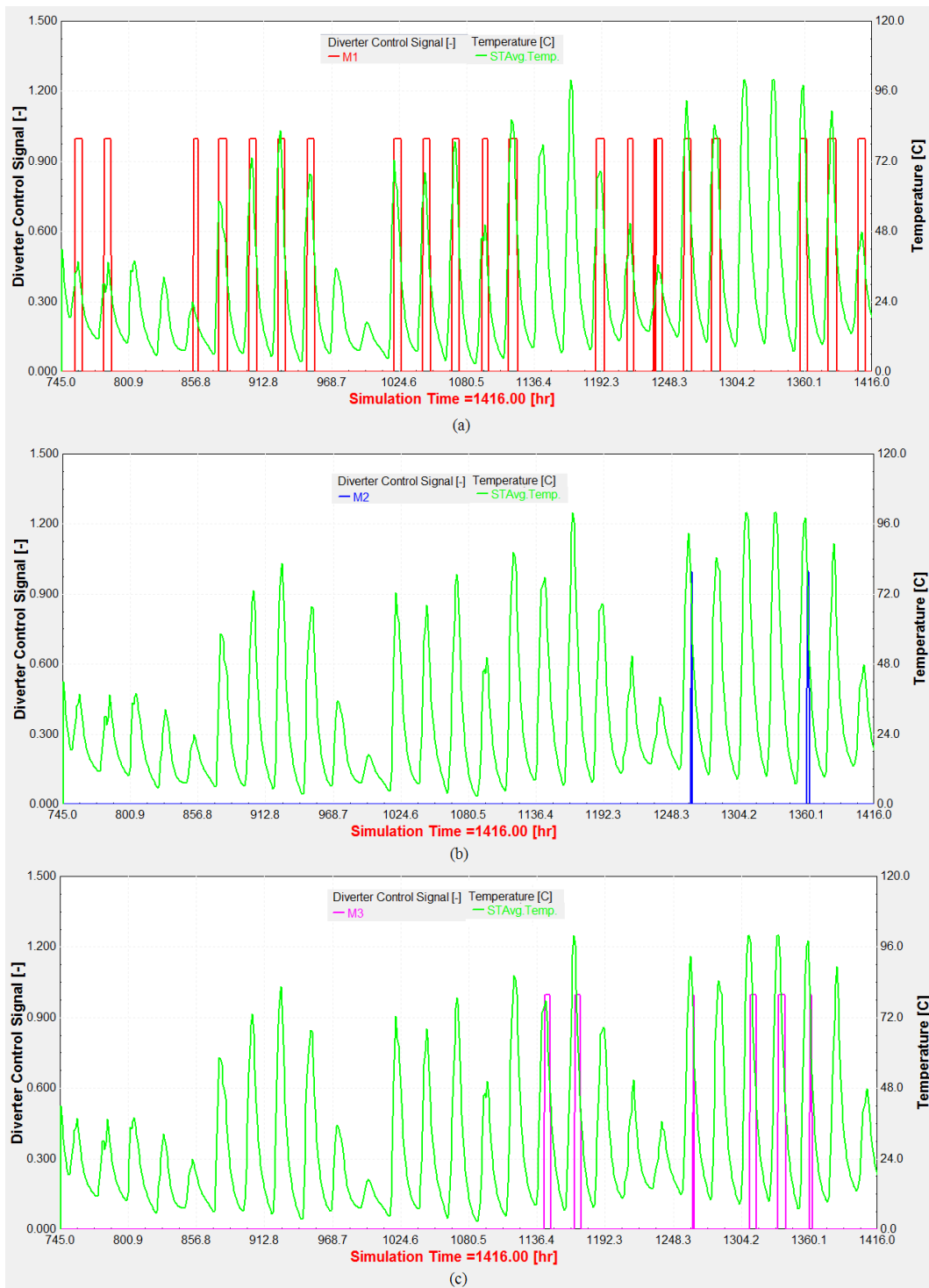


Figure 6.49. Configuration 4 diverters' control signals, M1 (a), M2 (b) and M3(c), vs. storage tank average temperature, STAvg.Temp., for February. Solar collector area is 100 m² and storage tank volume is 1m³.

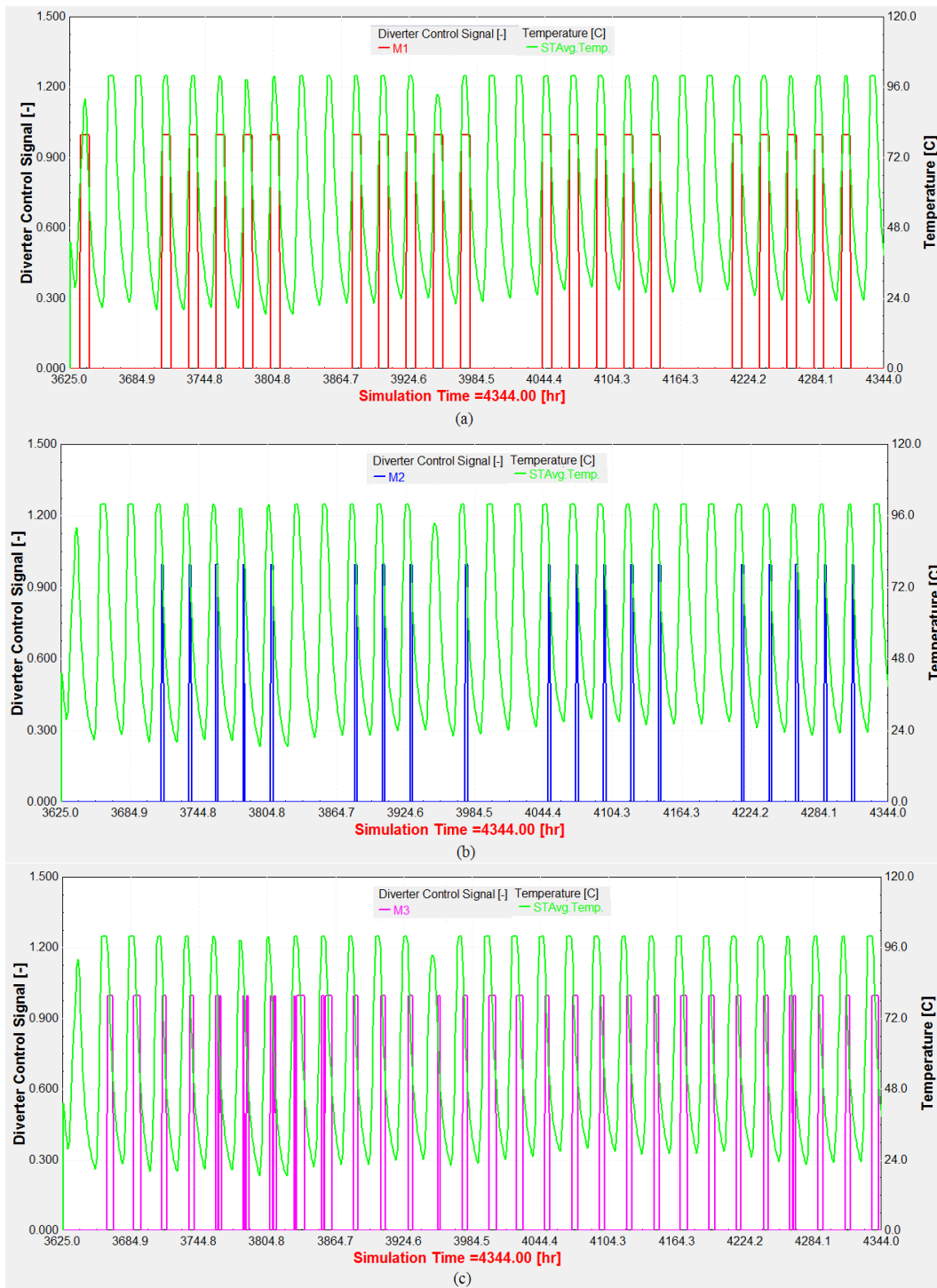


Figure 6.50. Configuration 4 diverters' control signals, M1 (a), M2 (b) and M3(c), vs. storage tank average temperature, STAvg.Temp., for June. Solar collector area is 100 m² and storage tank volume is 1m³.

Figure 6.51 and Figure 6.52 show the Configuration 1 vs. Configuration 4 total cost with different central solar field collector area for February and June, respectively. In fact, Figure 6.51 and Figure 6.52 show the effect of central solar field's collector area impact on Configuration 4 total hourly cost.

The collector area is investigated with 100, 120 and 150 m² total collector areas and storage tank volume is 1 m³ for this analysis. Generally, a larger collector area causes a higher capital cost which increases the Configuration total hourly cost. There are some decrements in total cost with larger collector areas. These decrements match the hours which solar energy is used in Units' thermal systems. Again because of more available solar energy in June, cost decrements are more common in comparison with results for February. By comparing the cost Diagrams of different collector areas with each other for both February and June, the collector area with 100 m² shows the best performance among studied collector areas.

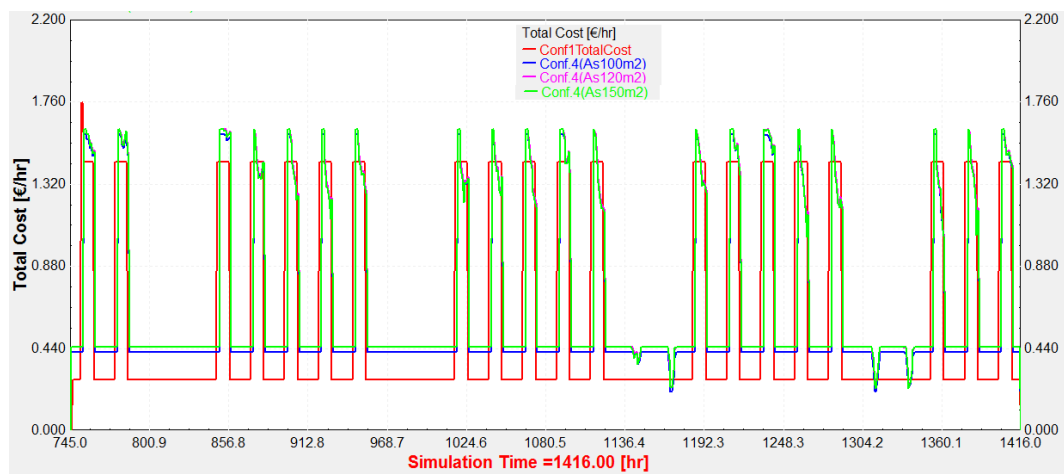


Figure 6.51. Configuration 1 vs. Configuration 4 total hourly cost for February with different solar field's collector areas, AS=100, 120 and 150 m². Storage tank volume is 1 m³.

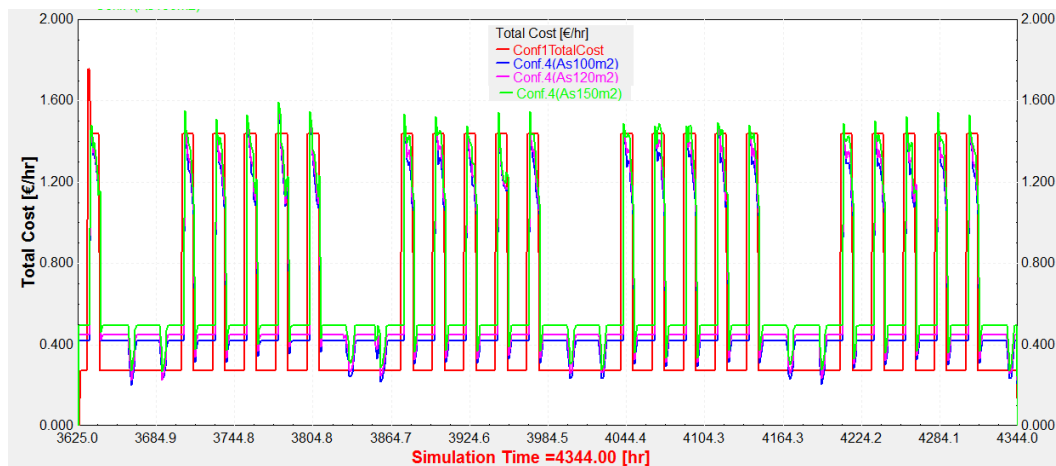


Figure 6.52. Configuration 1 vs. Configuration 4 total hourly cost for June with different solar field's collector areas, AS=100, 120 and 150 m². Storage tank volume is 1 m³.

Figure 6.53 and Figure 6.54 show the influence of storage tank volume on Configuration 4 total hourly cost for February and June, respectively. The storage tank is investigated with 1, 2 and 5 m³ volumes. The central solar field's area is fixed on 100 m². As much as storage tank volume increases, the tank's thermal storage capacity is increased but, its average temperature decreases. A storage tank with a lower average temperature could not be a suitable energy source to preheat the streams with higher temperature. In fact, storage tank volume increment improves its long-term function, which means the tank could store more energy for a longer period.

The larger storage tank's function is obvious in Figure 6.63 and Figure 6.64 where the cost Diagram for a storage tank with 5 m³ shows minimum variation because this tank has a lower average temperature in all simulation time intervals. Except for the cost decrement moments in both Diagrams, three cost Diagrams for three tank volumes almost coincide. In conclusion, among all studied storage tanks, the 1 m³ tank shows the optimal performance.

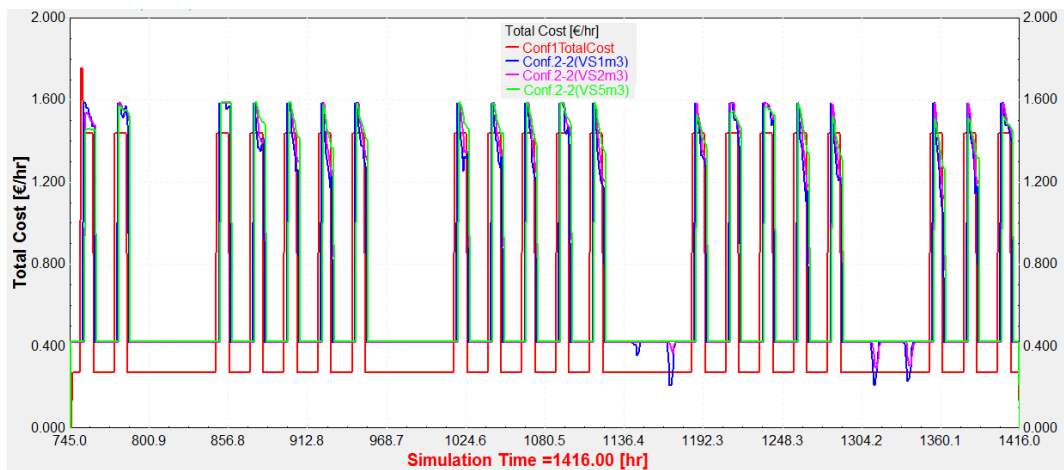


Figure 6.53. Configuration 1 vs. Configuration 4 total hourly cost for February with different storage tank volumes, VS=1, 2 and 5 m³. Solar collector area is 100 m².

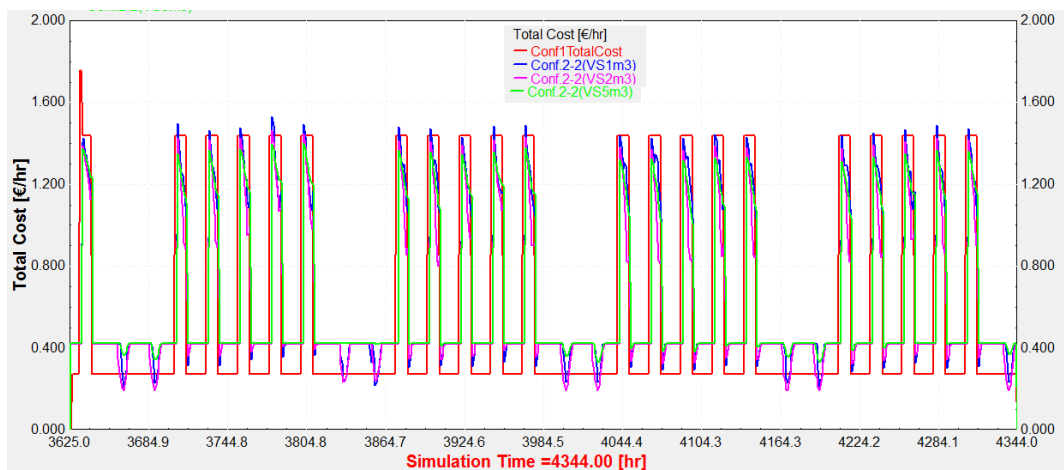


Figure 6.54. Configuration 1 vs. Configuration 4 total hourly cost for June with different storage tank volumes, VS=1, 2 and 5 m³. Solar collector area is 100 m².

Figure 6.55 and Figure 6.56 present Configuration 4 total cost which is calculated by MATLAB and TRNSYS separately. The two software results are consistent in both February and June.

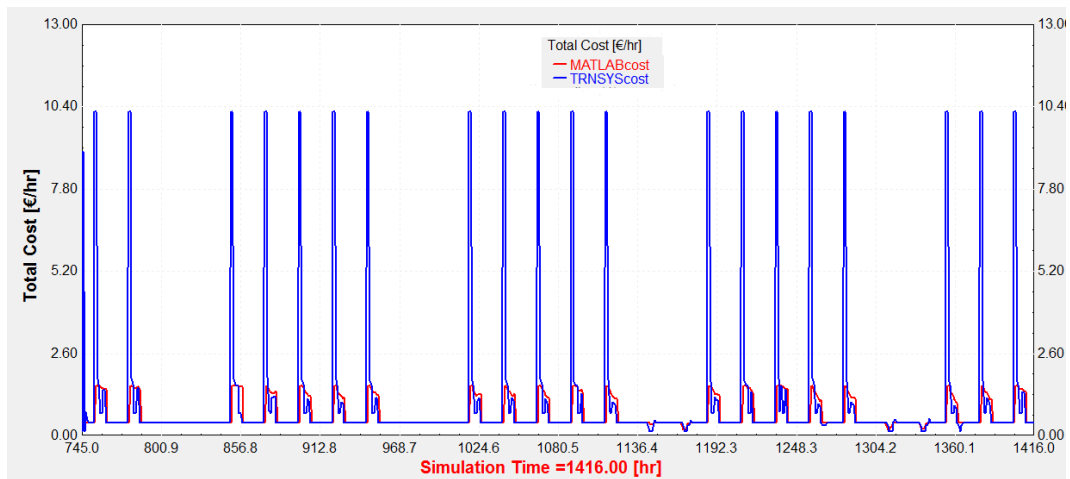


Figure 6.55. Configuration 4 total cost by MATLAB and TRNSYS in February. Solar collector area is 100 m² and storage tank volume is 1 m³.

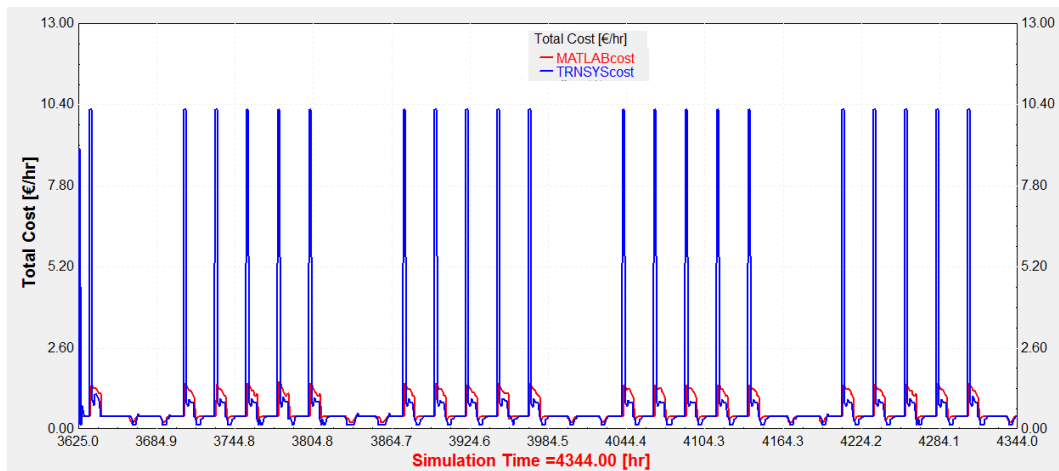


Figure 6.56. Configuration 4 total cost by MATLAB and TRNSYS in June. Solar collector area is 100 m² and storage tank volume is 1 m³.

6.6. Monthly cost of selected Configurations

In this Section, the accumulated hourly cost of selected Configurations in studied months, February and June which results in Configurations' total monthly cost are presented. Monthly total cost is necessary to highlight results, and these results reflect an overall view of industrial waste heat or solar energy integration into different Configurations.

The waste heat temperature, solar collector area, and storage tank volume were the main variables whose influence on hourly total cost was evaluated. Some Configurations whose variables show the best performance among considered variables are chosen to be discussed in this Section as Cases, and they are shown in Table 6.7. In fact, this Section's main aim is to make conclusions more obvious. Totally seven Configurations are selected. Case A is basic Configuration and Case B and Case C consider industrial waste heat, Case D to Case F consider separated solar collector area and Case G examines central solar field effect on total monthly cost.

Table 6.7. Selected Configurations for Section 6.6. V_s = storage tank volume, T_w = industrial waste heat temperature, A_s = solar collector area, \dot{m}_s = mass flow rate to solar collector

Case	Configuration
A	Conf. 1
B	Conf. 2-2 ($V_s=1 \text{ m}^3$, $T_w=100^\circ\text{C}$)
C	Conf. 2-2 ($V_s=1 \text{ m}^3$, $T_w=120^\circ\text{C}$)
D	Conf. 3-1 ($V_s=1 \text{ m}^3$, $A_s=20 \text{ m}^2$, $\dot{m}_s=100 \text{ kg/hr}$) + Conf. 3-2 ($V_s=1 \text{ m}^3$, $A_s=20 \text{ m}^2$, $\dot{m}_s=100 \text{ kg/hr}$)
E	Conf. 3-1 ($V_s=1 \text{ m}^3$, $A_s=20 \text{ m}^2$, $\dot{m}_s=100 \text{ kg/hr}$) + Conf. 3-2 ($V_s=1 \text{ m}^3$, $A_s=30 \text{ m}^2$, $\dot{m}_s=100 \text{ kg/hr}$)
F	Conf. 3-1 ($V_s=1 \text{ m}^3$, $A_s=20 \text{ m}^2$, $\dot{m}_s=100 \text{ kg/hr}$) + Conf. 3-2 ($V_s=1 \text{ m}^3$, $A_s=60 \text{ m}^2$, $\dot{m}_s=100 \text{ kg/hr}$)
G	Conf. 4 ($V_s=1 \text{ m}^3$, $A_s=100 \text{ m}^2$, $\dot{m}_s=500 \text{ kg/hr}$)

Table 6.8 and Table 6.9 show the quantitative amounts of costs and Figure 6.57 and Figure 6.58 present costs in Diagram form for February and June, respectively. The results are presented in both Table and Figure format because storage tank cost is such a small part of total cost that it does not appear in Figures. In addition, in Figure 6.57 and Figure 6.58, the total cost of some Configurations are so close to each other that

it was necessary to present them as Tables so that interested reader could distinguish the cheapest and the most expensive ones from Tables.

In both February and June, the Configurations which benefit from free industrial waste heat show the minimum total cost. According to Figure 6.57 and Figure 6.58, the Fuel cost occupies the biggest share of Configurations' total cost.

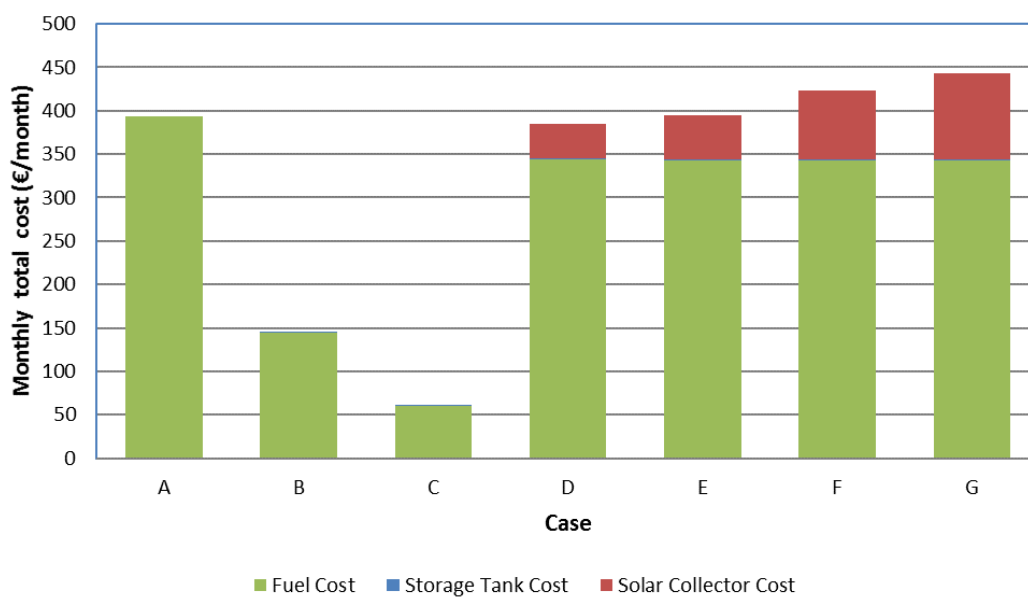


Figure 6.57. Storage tank, solar collector and fuel monthly cost for selected Configurations for February

Table 6.8. Storage tank, solar collector and fuel monthly cost for selected Configurations for February

Cost (€/month)	Case						
	A	B	C	D	E	F	G
Storage Tank Cost	0	0,478	0,478	0,956	0,956	0,956	0,478
Solar Collector Cost	0	0	0	40,02	50,03	80,06	100,09
Fuel Cost	393,71	144,89	60,41	343,95	343,32	342,78	343,11
Total Cost	393,71	145,368	60,888	384,926	394,306	423,796	443,678

In Figure 6.57 for February, the Configuration 2-2 with 120 °C industrial waste heat temperature has a minimum total cost. The second Configuration with the lowest total cost again is Configuration 2-2 with 100 °C waste heat temperature, therefore it would not be wrong to propose that using free waste heat reduces total cost dramatically. The Configurations with Cases D and E which represent the Units when they are equipped with separated solar collectors and storage tanks, have almost equal total cost with Case A as basic configuration. The reason for this is adding solar collector to Units' thermal system reduces the total fuel cost, however, on the contrary, the capital cost of solar collectors itself increases the cost which makes total cost almost equal to the condition in which there is not any solar collector. The solar collector high capital cost causes total cost of Configurations with Cases F and G to be higher than Case A. Because there is not so much solar energy in February, the positive influence of solar collector application inside Configurations is not viable and in the most of times, it affects Configurations' total cost negatively. Cases D to G show the same fuel cost because in February there is not so much solar energy to be used and increasing solar collector area just increases Configuration total cost.

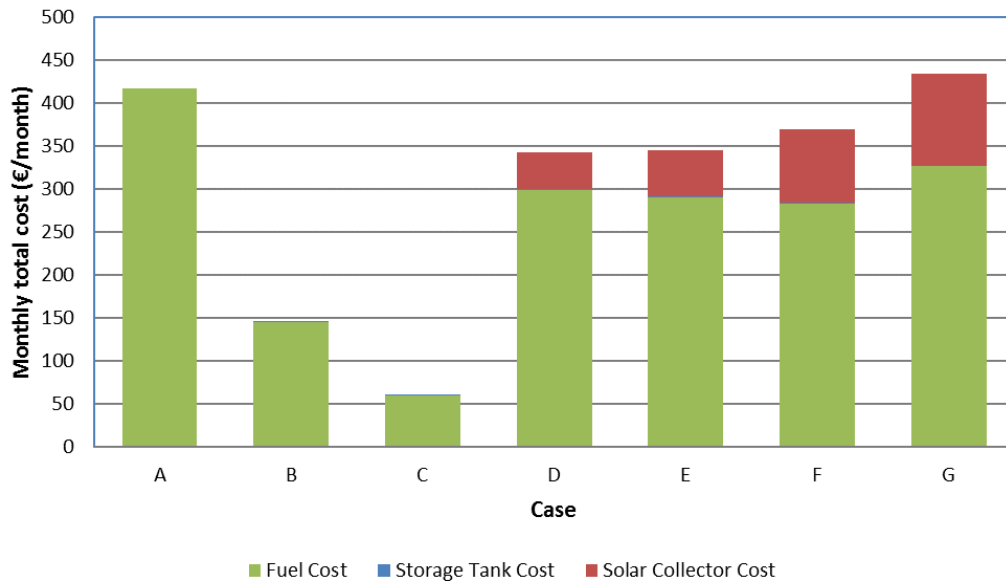


Figure 6.58. Storage tank, solar collector and fuel monthly cost for selected Configurations for June

Table 6.9. Storage tank, solar collector and fuel monthly cost for selected Configurations for June

Cost (€/month)	Case						
	A	B	C	D	E	F	G
Storage Tank Cost	0	0,512	0,512	1,024	1,024	1,024	0,512
Solar Collector Cost	0	0	0	42,9	53,62	85,8	107,25
Fuel Cost	417,03	144,85	60,37	299,56	290,86	283,02	326,63
Total Cost	417,03	145,362	60,882	343,484	345,504	369,844	434,392

Figure 6.58 presents selected Configurations' total cost for June. Cases C and D show the minimum total cost respectively because they benefit from free industrial waste heat. Because of more solar energy availability in June, the fuel cost is reduced in all Configurations which use solar collectors, Cases D to G. Case D, Case E and Case F show gradual increments in total cost which indicate that 20 m² collector area shows the best performance in comparison with other studied collector areas inside Unit 2 thermal system. On the contrary, the total fuel cost decreases gradually from Case D to Case F. The reason behind this is an increment in Unit 2 solar collector area which reaches 60 m² from 20 m². According to Table 6.7, the inlet water flow rate to both Units' solar collectors is 100 kg/hr in Case D to Case F. For fixed solar irradiation

energy on a collector, as much as the collector inlet fluid flow rate to unit area decreases, the outlet temperature increases. For Unit 2 with fixed collector inlet fluid flow rate, when collector area increases from 20 m² to 60 m², the inlet flow rate to collector unit area decreases from 5 kg/(hr m²) ($\frac{100 \text{ kg/hr}}{20 \text{ m}^2}$) to 1.66 kg/(hr m²) ($\frac{100 \text{ kg/hr}}{60 \text{ m}^2}$) which increases the collector outlet temperature. A solar collector with higher outlet temperature could replace more boilers energy with solar energy and results in a reduction in Configuration fuel cost. In conclusion, for Case D to Case F in June, when solar collector area is constant for Unit 1, 20 m², the solar collector area increment for Unit 2 decreases the fuel cost while increases total cost because of high capital cost of solar collectors.

Despite using a large solar collector area in Case G, because of the high capital cost of solar collectors, the total monthly cost of Case 7 is higher than that for Case A.

CHAPTER 7

CONCLUSION

In this Chapter, a summary of the thesis is given (Section 7.1), followed by the main conclusions (Section 7.2) and future work (Section 7.3).

7.1. Summary of thesis

In the context of European Union INSHIP (Integrating National Research Agendas on Solar Heat for Industrial Process) project and aligned with its task 5.3 (Hybrid energy supply system) and task 5.4 (Industry parks and heat distribution network), solar energy and industrial waste heat integration into two food industry Units are simulated and optimized in this study. Units' thermal systems' simulation was done in TRNSYS while MATLAB linked to TRNSYS to optimize systems simultaneously. Simulation and optimization time interval is chosen 1 hour and Izmir, Turkey is determined as location in this study. Four different Configurations are defined and investigated in separated Sections in Chapter 6, to simulate Units with different solar energy or industrial waste heat integration options.

Configuration 1, as basic Configuration, simulates Units in the conventional form with only boilers as energy sources, Configuration 2 examined the industrial waste heat application; and Configuration 3 and Configuration 4 evaluated solar energy integrations into Units in separated and central solar fields, respectively.

Instead of doing all the simulation and optimization procedure for all hours of year, two months, February and June, are chosen as time period of study. Simulated Units' supply-side and process-side are defined as different integration options for solar or

industrial waste heat integration, and MATLAB optimization decides the best option(s) to minimize Configurations total cost.

Inside an industrial Unit, double-sided look to waste heat or solar energy integration was applied. Double-sided look means supply-side or process-side energy integration which is defined as hybrid solar energy integration in the thesis objective Section. Previous studies just examine one of the mentioned options in their investigations. An optimization which chooses the best option to minimize total cost was studied rarely in previous studies. This is first novelty of this study.

MATLAB estimates Configurations' total fuel consumption by an objective function. In each hour, initially based on TRNSYS component mathematical models and exchanged data between MATLAB and TRNSYS, MATLAB forms a specific objective function for each Configuration. All obtained objective functions are nonlinear so a nonlinear optimization function in MATLAB is utilized. After optimization, MATLAB sends proper orders to TRNSYS components to operate Units in optimal condition with minimum cost.

The waste heat temperature, solar collector area, and storage tank volume were the main variables whose influence on hourly total cost of different Configurations, were evaluated.

Aligned with the thesis scope, the studied Configurations cover both industrial unit scale and industrial zone scale investigation of an industrial Unit's function. Previous studies examine different energy integrations into one specific Unit separately or in the form of numbers of Units in an industrial zone, but this study considers each industrial Unit inside an industrial zone in a way that its function affects the overall functionality of whole industrial zone. This new view toward industrial Unit's function was a gap in past research works. This could be named second novelty of this thesis.

Doing both thermal system simulation and optimization of two industrial Units' operation with different energy sources by TRNSYS and MATLAB respectively is

third novelty of this work. TRNSYS and MATLAB are strong in the field of their assigned tasks in this thesis and utilizing advantages of each one make the used method as a new approach to energy systems' modeling. In fact, modeling and optimizing a system by different software simultaneously create a benchmark to other studies and provides a new method to model and optimize complex energy systems in a more convenient way and lesser time. By the applied method in this study, a user could change any variable in TRNSYS simulation environment, and he could define it as input to MATLAB. Therefore, without any need to change optimization code, he could evaluate easily the changed variable impact on Configuration overall function.

Finally, based on previous research in solar energy integration into industrial Unit(s), the solar collectors are considered either separated solar collector for each Unit or central solar field for whole of an industrial zone. This study examined both separated and central solar collectors in Configuration 3 and Configuration 4 respectively, to clarify the effect of each one on Configurations' total cost which could be named another novelty of this thesis. This is forth novelty of this modelling work.

This thesis tackles some gaps in previous research, and four mentioned novelties distinguish this study from other studies. Actually, this study attempts to strengthen the solar energy integration models from thermal system modeling aspect instead of optimization aspect which has been addressed numerously in past studies.

7.2. Main Conclusions

In this study, different Configurations with different energy sources are simulated for the assumed inputs and then their results are benchmarked with respect to Configuration 1 as basic Configuration. In this Section, the hourly cost and total monthly cost of Configurations is reviewed to create a broad perspective from solar energy or industrial waste heat integration into examined two industrial Units.

In the industrial zones, some Units operate under their nominal capacity continuously or they are non-operational in some periods. Those Units' boiler could be used as an energy source for other Units. Configuration 2-1 models the condition when one industrial Unit has high efficient boiler ($\eta_{\text{boiler}}=0.7$) with discontinuous operation pattern and its boiler's output could be shared with another Unit ($\eta_{\text{boiler}}=0.5$). In boilers coupled condition in Configuration 2-1, total hourly cost decreased by about 21.5%. This Configuration highlights the effect of Using HDN for sharing energy between industrial Units. Configuration 2-1 presents unused boilers' capacity of some Units as an opportunity to provide energy for other Units.

Configuration 2-2 simulates system when industrial waste heat is used as an energy source for both Units beside boilers energy. Industrial waste heat integration into the Units' thermal system could cover a significant part of energy demand and reduces total cost dramatically. Based on examined factors, industrial waste heat temperature is a strong effective factor on Configuration's total hourly cost. 10 °C increment in waste heat temperature decreases Configuration total cost by about %26. 1 m³ storage tank shows the best performance among studied storage volumes in Configuration 2-2. In addition, according to Figure 6.57 and Figure 6.58, because waste heat is provided freely for the Configuration, Configuration 2-2 shows the minimum total monthly cost in both February and June among selected Configurations.

Configuration 3-1 and Configuration 3-2 examined the solar energy integration into Unit 1 and Unit 2, respectively. Solar collector integration could reduce total cost by replacing boilers energy with solar energy but on the contrary, it could also increase total cost because of its high capital cost. As it is expected, because of more solar energy availability in June than that of February, solar collectors are more effective in June.

In both Configuration 3-1 and Configuration 3-2, 1 m³ storage tank shows better performance among studied storage tanks' volumes. 20 m², 30 m² and 60 m² are assumed as solar collector area for both Configurations. Because of lower capital cost

and based on Figure 6.57 and Figure 6.58, collector with 20 m² shows the best performance in both Units among studied collectors. With 20 m² collector area and 1 m³ storage tank in February for Configuration 3-1, solar energy integration reduces total hourly cost 11% while for Configuration 3-2, solar collector installation increases total hourly cost by about 10.7%.

With the same structure for June, solar energy reduces Configuration 3-1 total hourly cost by about 27.8%. For Configuration 3-2, solar energy reduces total hourly cost by about 16%. As an important point, solar energy integration has a more positive effect on Configuration 3-1 total hourly cost than Configuration 3-2 while both Configurations have same boiler outlet flowrate and set-point temperature. The reason behind this is low-temperature boiler feed water existence in Configuration 3-1 which create an opportunity for solar energy to be used as a preheater energy source in most hours. Because of higher solar energy availability in June, cost reduction for both Configurations is more obvious in June. Because of high capital cost of solar collectors, solar energy increases total hourly cost of Configuration 3-2 in February.

According to Figure 6.57 and Figure 6.58, Cases C, D and E represent Configuration 3 (Conf. 3-1+ Conf. 3-2) total monthly cost for February and June, respectively. In February, generally solar collector installation has not any positive effect and it increases total cost. In June, because more solar energy is accessible, solar collector decreases monthly fuel cost but because of high capital cost, it increases monthly total cost.

For Configuration 4 which investigates central solar field integration effect on total cost, 100, 120 and 150 m² solar collector areas are examined for central solar field. Among examined variables 100 m² collector area and 1 m³ storage tank showed better performance in Configuration 4 thermal system. According to Figure 6.57 and Figure 6.58, again because solar collectors are expensive components, in both February and June, central solar field increases Configuration's total monthly cost.

In conclusion, integrating free industrial waste heat by a Heat Distribution Network (HDN) inside Units' thermal systems could be the best option to reduce total monthly cost of studied Configurations. Using solar collectors in Units during February does not have any positive effect on Units' total cost decrements because of lack of sufficient solar energy. Integrating solar collectors and heat storage tank in Configurations show a more positive effect in June.

Considering all results for February and June, it could be concluded that storage tank in different Configurations forms an insignificant part of total costs. In addition, among considered volumes for a storage tank, the 1 m³ tank shows the best performance, and this demonstrates that eliminating storage tank completely from Configurations' thermal system and using solar energy or industrial waste heat directly could be considered as another Configuration for future work. In fact, because of small volume of storage tanks, they act more like a heat exchanger with zero resistance between hot-side and cold-side flows instead of storing energy component in the evaluated Configurations.

Solar collectors have high capital cost which prohibits central solar field from reducing total cost significantly and studied storage tanks could not play an effective role in storing energy for next time interval. Consequently, it could be concluded that between examined Configurations, the separated solar collectors show lower total cost than that of central solar field with larger collector area.

7.3. Future Works

The following suggestions could be considered as recommendations for future works to investigate solar energy or industrial waste heat integration into industrial Units in more depth. As future work a sensitivity analysis would help to determine the extent to mentioned results are generalizable versus being a result of the assumed inputs and other assumed inputs would yield different conclusions.

- Modeling more Units inside industrial zone with various working pattern and energy consumption profile.
- Matching the Units' flowrate and temperature specifications with real data from similar food industry Units.
- Evaluating different solar collector technologies' influence such as parabolic trough collectors on the overall function of units.
- Considering piping, pumping and HDN maintenance cost during calculating Configurations' hourly cost.
- Optimizing Heat Distribution Network (HDN) specifications to find out optimal pipeline diameter and pumping power.
- Evaluating Configurations when there is no storage tank and solar energy is integrated directly into the Units' thermal system.
- Evaluating boilers' efficiency variation effect during Units on-off periods on Configuration total cost
- Sensitivity analysis of major inputs
- Integrating larger storage tank with monthly charging and discharging period into Configuration 4 to store excess solar energy in summer for next months.
- Controlling the inlet flow temperature into solar collectors in Configuration 3 and Configuration 4 to prevent solar energy wasting.
- Calculating Configurations hourly cost with different storage tank volumes and different solar collector areas to find optimum values.

REFERENCES

- [1] S. H. Farjana, N. Huda, M. A. P. Mahmud, and R. Saidur, “Solar process heat in industrial systems – A global review,” *Renewable and Sustainable Energy Reviews*. 2018.
- [2] “<http://www.inship.eu/index.php>.” .
- [3] German Solar Association, “Solar Heat for Industry,” 2017.
- [4] An International Framework for Eco-Industrial Parks. 2018.
- [5] F. Gallucci and M. Van Sint Annaland, *Process Intensification for Sustainable Energy Conversion*. 2015.
- [6] C. Brunner, B. Slawitsch, K. Giannakopoulou, and H. Schnitzer, “Industrial Process Indicators and Heat Integration in Industries,” *Joanneum Res. Graz, Austria*, 2008.
- [7] W. Platzer, “Potential studies on solar process heat worldwide,” p. 17, 2015.
- [8] H. Benli, “Potential application of solar water heaters for hot water production in Turkey,” *Renewable and Sustainable Energy Reviews*. 2016.
- [9] B. Ilyes Ben Hassine, Annabell Helmke, Stefan Heß, Pierre Krummenacher and H. S. Muster, Bastian Schmitt, “Solar process heat for production and advanced applications,” *Sol. Process Heat Prod. Adv. Appl.*, 2012.
- [10] R. Kempener, J. Burch, C. Brunner, C. Navntoft, and D. Mugnier, “Solar heat for industrial processes: Technology Brief,” *IEA-ETSAP IRENA Technol. Br. E21*, vol. 17, no. January, pp. 216–260, 2015.
- [11] P. Kurup and C. Turchi, “Initial Investigation into the Potential of CSP Industrial Process Heat for the Southwest United States,” 2015.
- [12] C. M. Schweiger H, Mendes JF, Benz N, Hennecke K, Prieto G, “The potencial of solar heat in industrial processes. A estate of the art review for Spain and Portugal,” *Eurosun*, no. April 2014, pp. 19–22, 2000.
- [13] S. Kalogirou, “The potential of solar industrial process heat applications,” *Appl. Energy*, 2003.
- [14] P. Bettina, Muster-Slawitsch- Krummenacher, “Methodologies and software tools for integrating solar heat into industrial processes,” 2014.
- [15] C. Vannoni, R. Battisti, and S. Drigo, “Potential for solar heat in indutrial processes. IEA SHC Task 33 and and SolarPACES Task IV: Solar heat for industrial processes.,” *Iea*, pp. 1–21, 2008.

- [16] “<http://ship-plants.info/solar-thermal-plants>.” .
- [17] G. Pirasteh, R. Saidur, S. M. A. Rahman, and N. A. Rahim, “A review on development of solar drying applications,” *Renewable and Sustainable Energy Reviews*. 2014.
- [18] L. Valenzuela, D. Hernández-Lobón, and E. Zarza, “Sensitivity analysis of saturated steam production in parabolic trough collectors,” in *Energy Procedia*, 2012.
- [19] O. M. Bany Mousa and R. A. Taylor, “A Broad Comparison of Solar Photovoltaic and Thermal Technologies for Industrial Heating Applications,” *J. Sol. Energy Eng.*, 2018.
- [20] R. Zahira, H. Akif, N. Amin, M. Azam, and Zia-ul-Haq, “Fabrication and performance study of a solar milk pasteurizer,” *Pakistan J. Agric. Sci.*, 2009.
- [21] E. Aiken, N. Lacroix, and K. Bucher, “Development of a Solar Water Pasteurizer With Integral Heat Exchanger (Spihx),” 2007.
- [22] G. Yuan, L. Hong, X. Li, L. Xu, W. Tang, and Z. Wang, “Experimental Investigation of a Solar Dryer System for Drying Carpet,” in *Energy Procedia*, 2015.
- [23] A. Crespo, C. Barreneche, M. Ibarra, and W. Platzer, “Latent thermal energy storage for solar process heat applications at medium-high temperatures – A review,” *Solar Energy*, 2018.
- [24] C. Lauterbach, B. Schmitt, U. Jordan, and K. Vajen, “The potential of solar heat for industrial processes in Germany,” *Renewable and Sustainable Energy Reviews*. 2012.
- [25] S. Hess, A. Oliva, M. Hermann, G. Stryi-Hipp, and V. Hanby, “Solar Process Heat – System Design for Selected Low-Temperature Applications in the Industry,” no. January, pp. 1–12, 2016.
- [26] M. Stewart and J. Petrie, “A process systems approach to life cycle inventories for minerals: South African and Australian case studies,” *J. Clean. Prod.*, 2006.
- [27] A. Uppal, J. P. Kesari, and M. Zunaid, “Designing of solar process heating system for indian automobile industry,” *Int. J. Renew. Energy Res.*, 2016.
- [28] C. Lauterbach, B. Schmitt, K. Vajen, and U. Jordan, “Solar Process Heat in Breweries - Potential and Barriers of a New Application Area,” *Renew. Energy*, pp. 645–647, 2009.
- [29] F. Mauthner, “Solar Heat for Industrial Applications Design study part II Aim of the session (part II),” 2014.
- [30] F. Mauthner, M. Hubmann, C. Brunner, and C. Fink, “Manufacture of malt and beer with low temperature solar process heat,” in *Energy Procedia*, 2014.

- [31] C. Palaniappan, "Perspectives of solar food processing in India," *Processing*, pp. 1–11, 2009.
- [32] A. R. Eswara and M. Ramakrishnarao, "Solar energy in food processing - A critical appraisal," *Journal of Food Science and Technology*. 2013.
- [33] A. Frein, M. Calderoni, and M. Motta, "Solar thermal plant integration into an industrial process," in *Energy Procedia*, 2014.
- [34] D. D. Desai, J. B. Raol, S. Patel, and I. Chauhan, "Application of Solar energy for sustainable Dairy Development," *Eur. J. Sustain. Dev.*, 2013.
- [35] B. Norton, "Industrial and agricultural applications of solar heat," in *Comprehensive Renewable Energy*, 2012.
- [36] A. K. Sharma, C. Sharma, S. C. Mullick, and T. C. Kandpal, "Carbon mitigation potential of solar industrial process heating: Paper industry in India," *J. Clean. Prod.*, 2016.
- [37] "http://wiki.zero-emissions.at/index.php?title=Subsection_DA_food." [Online]. Available: http://wiki.zero-emissions.at/index.php?title=Subsection_DA_food.
- [38] D. Buoro, P. Pinamonti, and M. Reini, "Optimization of a Distributed Cogeneration System with solar district heating," *Appl. Energy*, 2014.
- [39] T. Falke, S. Kregel, A. K. Meinerzhagen, and A. Schnettler, "Multi-objective optimization and simulation model for the design of distributed energy systems," *Appl. Energy*, 2016.
- [40] D. Chinese, "Optimal size and layout planning for district heating and cooling networks with distributed generation options," *Int. J. Energy Sect. Manag.*, 2008.
- [41] S. H. Chae, S. H. Kim, S. G. Yoon, and S. Park, "Optimization of a waste heat utilization network in an eco-industrial park," *Appl. Energy*, 2010.
- [42] S. H. Kim, S. G. Yoon, S. H. Chae, and S. Park, "Economic and environmental optimization of a multi-site utility network for an industrial complex," *J. Environ. Manage.*, 2010.
- [43] W. Fichtner, M. Frank, and O. Rentz, "Inter-firm energy supply concepts: An option for cleaner energy production," *J. Clean. Prod.*, 2004.
- [44] C. Zhang et al., "A novel methodology for the design of waste heat recovery network in eco-industrial park using techno-economic analysis and multi-objective optimization," *Appl. Energy*, 2016.
- [45] D. Buoro, M. Casisi, P. Pinamonti, and M. Reini, "Optimal Lay-Out and Operation of District Heating and Cooling Distributed Trigeration Systems," 2011.

- [46] D. Buoro, M. Casisi, P. Pinamonti, and M. Reini, "Optimization of Distributed Trigenation Systems Integrated with Heating and Cooling Micro-grids," *Distrib. Gener. Altern. Energy J.*, vol. 26, no. 2, pp. 7–34, 2011.
- [47] D. Buoro, M. Casisi, A. De Nardi, P. Pinamonti, and M. Reini, "Multicriteria optimization of a distributed energy supply system for an industrial area," *Energy*, 2013.
- [48] TRNSYS, "TRNSYS mathematical reference- TRNSYS help document, volume 4." .
- [49] J. A. Duffie and W. A. Beckman, *Solar Engineering of Thermal Processes: Fourth Edition*. 2013.
- [50] "<http://www.investinizmir.com>." .
- [51] "<https://meteonorm.com/>." .
- [52] "https://ec.europa.eu/eurostat/statistics-explained/index.php/Natural_gas_price_statistics." .
- [53] "<https://www.mathworks.com/help/optim/ug/fmincon.html>." .
- [54] "http://wiki.zero-emissions.at/index.php?title=Cooking_in_food_industry." .
- [55] U. E. Finder, "Solar Process Heat for Production and Advanced Applications Updated Efficiency Finder," no. December 2014, pp. 1–11, 2015.

APPENDICES

A. Configuration 2-2 Data

In this Appendix, initially fuel consumption Diagram in Configuration 2-2 is presented. Then, all applied mathematical models of components during Configuration's optimization is shown and finally optimization MATLAB code is inserted.

Figure A.1 compares total hourly fuel consumption in Configuration 1 (basic Configuration) with Configuration 2-2 when waste heat temperature is 100 °C and storage tank volume is 1 m³. Figure A.1 provides useful information about the environmental beneficiary of the industrial waste heat integration into Configuration 2-2 with lessening fuel consumption.

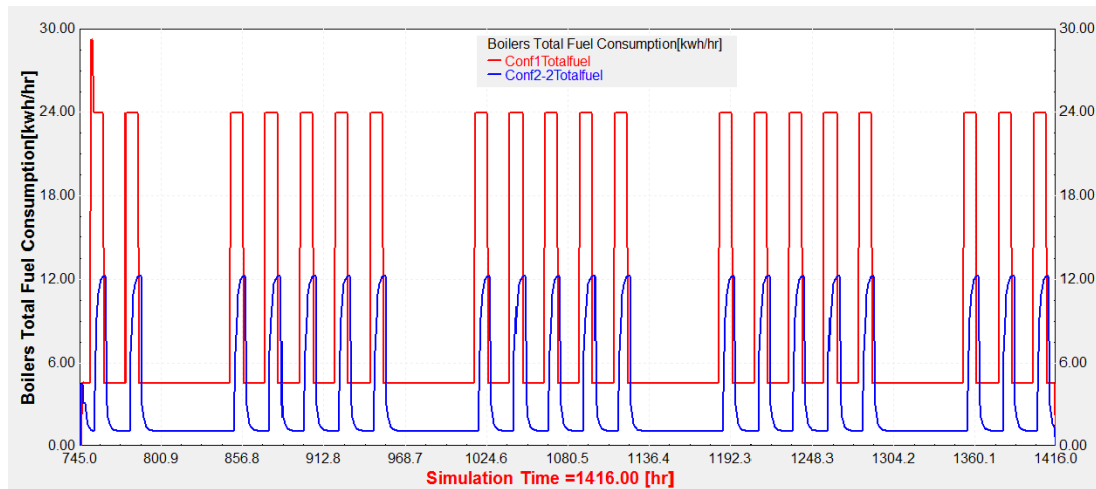


Figure A.1. Total hourly fuel consumption for Configuration 1 and Configuration 2-2 for both February and June. Waste heat temperature is 100 °C and storage tank volume is 1 m³

As it is expected, using waste heat reduces fuel consumption in both boilers. As it was mentioned in the thesis scope, the main aim of this work is cost optimization but it

will be valuable if Configurations are evaluated from an environmental view point. The main source of pollution in all Configurations is boilers' stack gas, so lower fuel consumption means lower pollutant. When both boilers are working, using waste heat reduces fuel consumption from 24.00 to 12.05 kWh/hr, or by about 50%. During just Unit 2 working time, the fuel consumption is reduced from 4.54 to 1.108 kWh/hr by approximately 75%. 75% fuel consumption reduction means when just boiler 2 works and it uses waste heat stream, it just provides 25% of energy demand in Unit 2 and the rest of it is provided by industrial waste heat.

In the following, all Equations which are used to obtain objective function for Configuration 2-2 are presented. For each Equation, the related Equation in Chapter 3 and the related component in the corresponding Unit are mentioned. By replacing Equations A.1 to A.12 and Equations A.14 to A.19 In Equations A.13 and A.20, respectively. The boilers output energy is calculated based on three decision variables, $\dot{m}_{2,Div1}$, $\dot{m}_{2,Div3}$ and $\dot{m}_{2,Div6}$.

In the following Equations, the amount of energy which each boiler transfers to process fluid was calculated for both Unit 1 and Unit 2.

For Unit1:

Obtaining storage tank average temperature ($T_{1,ST}$) at the end of each hour:

From Eqn.(3.19) for HX2 in Unit 1:

$$T_{HX2,U1} = T_{1,HX1,U1} - \frac{(\varepsilon_2)(\dot{m}_{in,U1})(T_{1,HX1,U1} - T_{in,U1})}{\dot{m}_{1,HX1,U1}} \quad (A.1)$$

From Eqn.(3.23) for Tee-Piece (Mix3) :

$$T_{\text{Mix3}} = \frac{(\dot{m}_{2,\text{Div1}})(T_{\text{in,Div1}}) + (\dot{m}_{2,\text{Div3}})(T_{\text{HX2,U1}})}{(\dot{m}_{2,\text{Div1}} + \dot{m}_{2,\text{Div3}})} \quad (\text{A. 2})$$

From Eqn.(3.19) for HX2 in Unit 2:

$$T_{\text{HX2,U2}} = T_{1,\text{HX1,U2}} - \left(\frac{\varepsilon_2}{\dot{m}_{1,\text{HX1,U2}}} \right) \left(\frac{C_{\text{min1}}}{C_p} \right) (T_{1,\text{HX1,U2}} - T_{\text{in,U2}}) \quad (\text{A. 3})$$

From Eqn.(3.23) for Tee-Piece (Mix4) :

$$T_{\text{Mix4}} = \frac{(\dot{m}_{2,\text{Div1}} + \dot{m}_{2,\text{Div3}})(T_{\text{Mix3}}) + (\dot{m}_{2,\text{Div6}})(T_{\text{HX2,U2}})}{(\dot{m}_{2,\text{Div1}} + \dot{m}_{2,\text{Div3}} + \dot{m}_{2,\text{Div6}})} \quad (\text{A. 4})$$

From Eqn.(3.21) for Heat Storage Tank :

$$T_{1,\text{ST}} = \frac{[T_s - \left(\frac{1}{\dot{m}_s} \right) ((\dot{m}_w)(T_w) - (\dot{m}_{2,\text{Div1}} + \dot{m}_{2,\text{Div3}} + \dot{m}_{2,\text{Div6}})(T_{\text{Mix4}}) + \frac{(\text{UAs})(T_s - T_a)}{C_p})]}{[1 + \left(\frac{1}{\dot{m}_s} \right) (\dot{m}_{2,\text{Div1}} + \dot{m}_{2,\text{Div3}} + \dot{m}_{2,\text{Div6}} - \dot{m}_w)]} \quad (\text{A. 5})$$

From Eqn.(3.27) for Diverter (Div2 and Div5) :

$$T_{1,\text{Div2}} = T_{1,\text{ST}} \quad (\text{A. 6})$$

Calculating hot-side outlet temperature ($T_{2,\text{HX1,U1}}$) of HX1 heat exchanger in Unit 1:

From Eqn.(3.27) for Diverter (Div5) and Eqn.(3.29) for Diverter (Div2) :

$$T_{2,\text{Div2}} = T_{1,\text{ST}} \quad (\text{A. 7})$$

From Eqn.(3.27) for Diverter (Div3) :

$$T_{1,Div3} = T_{HX2,U1} \quad (A. 8)$$

From Eqn.(3.23) for Tee-Piece (Mix2):

$$T_{Mix2} = \frac{(\dot{m}_{1,Div3})(T_{1,Div3}) + (\dot{m}_{2,Div2})(T_{2,Div2})}{(\dot{m}_{1,Div3} + \dot{m}_{2,Div2})} \quad (A. 9)$$

From Eqn.(3.12) for HX1 in Unit 1:

$$\gamma_1 = 1 - \frac{(T_{1,HX1,U1} - T_{Mix2})(\dot{m}_{Mix2})}{(\varepsilon_1)(\dot{m}_{2,Div4})(T_{2,Div4} - T_{Mix2})} \quad (A. 10)$$

From Eqn.(3.13) for HX1 in Unit 1:

$$T_{2,HX1,U1} = (\gamma_1)(T_{2,Div4}) + (1 - \gamma_1)(T_{2,Div4} - (\varepsilon_1)(T_{2,Div4} - T_{Mix2})) \quad (A. 11)$$

Calculating $\dot{Q}_{need,1}$:

From Eqn.(3.25) for Flow Mixer (Mix1):

$$T_{Mix1} = \frac{(\dot{m}_{in,Div1} - \dot{m}_{2,Div1})(T_{1,Div1}) + (\dot{m}_{2,Div1})(T_{1,Div2}) + (\dot{m}_{2,HX1,U1})(T_{2,HX1,U1})}{(\dot{m}_{in,Div1} + \dot{m}_{2,HX1,U1})} \quad (A. 12)$$

From Eqn.(3.1) for Boiler in Unit 1:

$$\dot{Q}_{\text{need},1} = (\dot{m}_{b,U1})C_p(T_{b,U1} - T_{\text{Mix}1}) \quad (\text{A. 13})$$

For Unit 2:

From Eqn.(3.29) for Flow Diverter (Div5):

$$T_{2,\text{Div}5} = T_{1,\text{ST}} \quad (\text{A. 14})$$

From Eqn.(3.19) for HX2 in Unit 2:

$$T_{\text{HX}2,\text{U}2} = T_{1,\text{HX}1,\text{U}2} - \left(\frac{\varepsilon_2}{\dot{m}_{1,\text{HX}1,\text{U}2}} \right) \left(\frac{C_{\text{min}1}}{C_p} \right) (T_{1,\text{HX}1,\text{U}2} - T_{\text{in},\text{U}2}) \quad (\text{A. 15})$$

From Eqn.(3.27) for Flow Diverter (Div6):

$$T_{1,\text{Div}6} = T_{\text{HX}2,\text{U}2} \quad (\text{A. 16})$$

From Eqn.(3.23) for Tee-Piece (Mix5):

$$T_{\text{Mix}5} = \frac{(\dot{m}_{1,\text{Div}6})(T_{1,\text{Div}6}) + (\dot{m}_{2,\text{Div}5})(T_{2,\text{Div}5})}{(\dot{m}_{1,\text{Div}6} + \dot{m}_{2,\text{Div}5})} \quad (\text{A. 17})$$

From Eqn.(3.12) for HX1 in Unit 2:

$$\gamma_2 = 1 - \frac{(T_{1,HX1,U2} - T_{Mix5})(\dot{m}_{Mix5})}{(\epsilon_1)(\dot{m}_{b,U2})(T_{b,U2} - T_{Mix5})} \quad (A. 18)$$

From Eqn.(3.13) for HX1 in Unit 2:

$$T_{2,HX1,U2} = (\gamma_2)(T_{2,U2}) + (1 - \gamma_2)(T_{b,U2} - (\epsilon_1)(T_{b,U2} - T_{Mix5})) \quad (A. 19)$$

Calculating $\dot{Q}_{need,2}$:

From Eqn.(3.1) for Boiler in Unit 2:

$$\dot{Q}_{need,2} = (\dot{m}_{b,U2})C_p(T_{b,U2} - T_{2,HX1,U2}) \quad (A. 20)$$

As final part, the used optimization code in MATLAB for Configuration 2-2 is presented. This code uses all aforementioned Equations and fmincon function to minimize total fuel consumption in Configuration 2-2.

```
%this project is for configuration 2-2

% --- Process Inputs -----
% -----
% -----

Ts      = trnInputs(1);
Ta      = trnInputs(2);
U1      = trnInputs(3); % pump output flow rate in unit1, if U1>0
(U1=100 kg/hr) it means Unit 1 operates
U2      = trnInputs(4); % boiler output flow rate in unit2, if U2>0
(U2=1100 kg/hr) it means Unit 2 operates
%% mFileErrorCode = 120      % After processing inputs

% --- First call of the simulation: initial time step (no iterations)
% -----
% -----

% (note that Matlab is initialized before this at the info(7) = -1
call, but the m-file is not called)
```

```

if ( (trnInfo(7) == 0) & (trnTime-trnStartTime < 1e-6) )

    % This is the first call (Counter will be incremented later for
this very first call)
    nCall = 0;

    % This is the first time step
    nStep = 1;

    % Initialize history of the variables for plotting at the end of
the simulation
    nTimeSteps = (trnStopTime-trnStartTime)/trnTimeStep + 1;

    history.Ts      = zeros(nTimeSteps,1);
    history.Ta      = zeros(nTimeSteps,1);

    history.Ctot    = zeros(nTimeSteps,1);

    % No return, we will calculate the solar collector performance
during this call
    %% mFileErrorCode = 130      % After initialization

end

% --- Very last call of the simulation (after the user clicks "OK"):
Do nothing -----
% -----
-----

if ( trnInfo(8) == -1 )

    %% mFileErrorCode = 1000;

    mFileErrorCode = 0; % Tell TRNSYS that we reached the end of the
m-file without errors
    return

end

% --- Post convergence calls: store values -----
% -----
-----

if (trnInfo(13) == 1)

    %% mFileErrorCode = 140;    % Beginning of a post-convergence call

```

```

    history.Ts(nStep)      = Ts;
    history.Ta(nStep)      = Ta;

    mFileErrorCode = 0; % Tell TRNSYS that we reached the end of the
m-file without errors
    return % Do not update outputs at this call

end

% --- All iterative calls -----
% -----
% -----

% --- If this is a first call in the time step, increment counter --
-

if ( trnInfo(7) == 0 )
    nStep = nStep+1;
end
%% mFileErrorCode = 145;
% --- Get TRNSYS Inputs ---

nI = trnInfo(3);    % For bookkeeping
nO = trnInfo(6);    % For bookkeeping

mFileErrorCode = 147
    %% mFileErrorCode = 140;    % Beginning of a post-convergence
call

    history.Ts(nStep)      = Ts;
    history.Ta(nStep)      = Ta;

    mFileErrorCode = 0; % Tell TRNSYS that we reached the end of the
m-file without errors
    return % Do not update outputs at this call

end

% --- All iterative calls -----
% -----
% -----

% --- If this is a first call in the time step, increment counter --
-

if ( trnInfo(7) == 0 )

```



```

Tmix3 = (m2Div1*Tindiv1 + m2Div3 * THX2U1)/(m2Div1+m2Div3)
THX2U2 = T1HX1U2 - (ep2/m1HX1U2)*(Cmin1/Cp)*(T1HX1U2-TinU2)

Tmix4 = ((m2Div1+m2Div3)*Tmix3 + m2Div6 *
THX2U2)/(m2Div1+m2Div3+m2Div6)
T1ST=(Ts-(1/mS)*(mw*Tw-(m2Div1+m2Div3+m2Div6)* Tmix4+(U*AS)*(Ts-
Ta)/Cp))/(1+(1/mS)*(m2Div1+m2Div3+m2Div6-mw))
T1Div2=T1ST
%%%%%%%%%%%%%%%%%%%%%%%%%%%%%%%%%%%%%%%%%%%%%%%%%%%%%%%%%%%%%%%%%%%%%%%%

```

%% T2HX1U1 finding %%%

```

T2Div2=T1ST
T1Div3 = THX2U1
Tmix2=(m1Div3*T1Div3 + m2Div2 * T2Div2)/(m1Div3 + m2Div2 )
Gama1=1-(((T1HX1U1-Tmix2)*mMix2)/(ep1*m2Div4*(T2Div4-Tmix2)));
T2HX1U1= Gama1*T2Div4 + (1-Gama1)*(T2Div4-ep1*(T2Div4-Tmix2))

```

%%

```

Tmix1= ((mindiv1-m2Div1)* T1div1 + m2Div1 * T1Div2 + m2HX1U1 *
T2HX1U1) / (mindiv1+m2HX1U1)
m2Div1=0

```

Ptin1=mbU1*Cp*(TbU1-Tmix1)

```

%%%%%%%%%%%%%%%%%%%%%%%%%%%%%%%%%%%%%%%%%%%%%%%%%%%%%%%%%%%%%%%%%%%%%%%%
%%%%%%%%%%%%%%%%%%%%%%%%%%%%%%%%%%%%%%%%%%%%%%%%%%%%%%%%%%%%%%%%%%%%%%%%
%%%%%%%%%%%%%%%%%%%%%%%%%%%%%%%%%%%%%%%%%%%%%%%%%%%%%%%%%%%%%%%%%%%%%%%% Ptin2
%%%%%%%%%%%%%%%%%%%%%%%%%%%%%%%%%%%%%%%%%%%%%%%%%%%%%%%%%%%%%%%%%%%%%%%%
%%%%%%%%%%%%%%%%%%%%%%%%%%%%%%%%%%%%%%%%%%%%%%%%%%%%%%%%%%%%%%%%%%%%%%%%
%%%%%%%%%%%%%%%%%%%%%%%%%%%%%%%%%%%%%%%%%%%%%%%%%%%%%%%%%%%%%%%%%%%%%%%%

```

```

T2div5= T1ST
THX2U2 = T1HX1U2 - (ep2/m1HX1U2)*(Cmin1/Cp)*(T1HX1U2-TinU2)
T1div6= THX2U2

```

```

Tmix5 = (m1Div6*T1div6 + m2Div5 * T2div5)/(m1Div6+m2Div5)
Gama2=1-(((T1HX1U2-Tmix5)*mMix5)/(ep1*mbU2*(TbU2-Tmix5)));
T2HX1U2=Gama2*TbU2 + (1-Gama2)*(TbU2-ep1*(TbU2-Tmix5))

```

Ptin2=mbU2*Cp*(TbU2-T2HX1U2)

```

%%%%%%%%%%%%%%%%%%%%%%%%%%%%%%%%%%%%%%%%%%%%%%%%%%%%%%%%%%%%%%%%%%%%%%%%
%%%%%%%%%%%%%%%%%%%%%%%%%%%%%%%%%%%%%%%%%%%%%%%%%%%%%%%%%%%%%%%%%%%%%%%% optimization part %%%%%%%%%%%%%%%%%%%%%%%%%%%%%%%%%%%%%%%%%%%%%%%%%%%%%%%%%%%%%%%%%%%%%%%%%
%%%%%%%%%%%%%%%%%%%%%%%%%%%%%%%%%%%%%%%%%%%%%%%%%%%%%%%%%%%%%%%%%%%%%%%%

```

if U1 > 0

```

A = [0 0 1;0 1 0;1 0 0 ]
b = [100;100;100]
lb= [0,0,0]
ub= [100,100,100]
x0=[0,0,0]

```

```
PtinC = Ptin1 + Ptin2
```

```

fun = @(x) (419*x(1))/5 + (502800*((6969*x(2))/100 -
(x(2))*((1857797655504137*Ta)...
/1179380152417648640 + (1177522354762144503*Ts)/1179380152417648640
+ x(1)/400 + ...
(6969*x(2))/800000 + (6969*x(3))/800000 - 25/4))/(x(1)/8000 +
x(2)/8000 + ...
x(3)/8000 + 15/16) + 3031))/((90597*x(2))/200 -
(13*x(2))*((1857797655504137*Ta)...
/1179380152417648640 + (1177522354762144503*Ts)/1179380152417648640
+ x(1)/400 + ...
(6969*x(2))/800000 + (6969*x(3))/800000 - 25/4))/(2*(x(1)/8000 +
x(2)/8000 + ...
x(3)/8000 + 15/16)) + 65403/2) -
(419*x(1))*((1857797655504137*Ta)/1179380152417648640 ...
+ (1177522354762144503*Ts)/1179380152417648640 + x(1)/400 +
(6969*x(2))/800000 + ...
(6969*x(3))/800000 - 25/4))/(100*(x(1)/8000 + x(2)/8000 + x(3)/8000
+ 15/16)) - ...
(4190*((6969*x(2))/100 -
(x(2))*((1857797655504137*Ta)/1179380152417648640 + ...
(1177522354762144503*Ts)/1179380152417648640 + x(1)/400 +
(6969*x(2))/800000 + ...
(6969*x(3))/800000 - 25/4))/(x(1)/8000 + x(2)/8000 + x(3)/8000 +
15/16) + 3031)...
*( (13*x(2))*((1857797655504137*Ta)/1179380152417648640 +
(1177522354762144503*Ts)/...
1179380152417648640 + x(1)/400 + (6969*x(2))/800000 +
(6969*x(3))/800000 - 25/4))...
/(2000*(x(1)/8000 + x(2)/8000 + x(3)/8000 + 15/16)) -
(90597*x(2))/200000 + ...
174597/2000))/((90597*x(2))/200 -
(13*x(2))*((1857797655504137*Ta)/1179380152417648640 ...
+ (1177522354762144503*Ts)/1179380152417648640 + x(1)/400 +
(6969*x(2))/800000 + ...
(6969*x(3))/800000 - 25/4))/(2*(x(1)/8000 + x(2)/8000 + x(3)/8000
+...
15/16)) + 65403/2) + 41900 ...
+...
(553080*((6969*x(3))/100 -
(x(3))*((1857797655504137*Ta)/1179380152417648640 ...
+ (1177522354762144503*Ts)/1179380152417648640 + x(1)/400 +
(6969*x(2))/800000 ...

```

```

+ (6969*x(3))/800000 - 25/4))/(x(1)/8000 + x(2)/8000 + x(3)/8000 +
15/16)...
+ 3031))/((996567*x(3))/2000 -
(143*x(3))*((1857797655504137*Ta)/1179380152417648640 ...
+ (1177522354762144503*Ts)/1179380152417648640 + x(1)/400 +
(6969*x(2))/800000 + ...
(6969*x(3))/800000 - 25/4))/(20*(x(1)/8000 + x(2)/8000 + x(3)/8000 +
15/16)) + ...
719433/20) - (4609*((6969*x(3))/100 -
(x(3))*((1857797655504137*Ta)/1179380152417648640 ...
+ (1177522354762144503*Ts)/1179380152417648640 + x(1)/400 +
(6969*x(2))/800000 + ...
(6969*x(3))/800000 - 25/4))/(x(1)/8000 + x(2)/8000 + x(3)/8000 +
15/16) + 3031)...
*(13*x(3))*((1857797655504137*Ta)/1179380152417648640 +
(1177522354762144503*Ts)/1179380152417648640 ...
+ x(1)/400 + (6969*x(2))/800000 + (6969*x(3))/800000 -
25/4))/(2000*(x(1)/8000 + x(2)/8000 ...
+ x(3)/8000 + 15/16)) - (90597*x(3))/200000 +
174597/2000))/((996567*x(3))/2000 - ...
(143*x(3))*((1857797655504137*Ta)/1179380152417648640 +
(1177522354762144503*Ts)/1179380152417648640 ...
+ x(1)/400 + (6969*x(2))/800000 + (6969*x(3))/800000 -
25/4))/(20*(x(1)/8000 + x(2)/8000 ...
+ x(3)/8000 + 15/16)) + 719433/20)

```

```
x = fmincon(fun,x0,A,b,[],[],lb,ub)
```

```
mFileErrorCode = 110
```

```

m2Div1=x(1)
m2Div3=x(2)
m2Div6=x(3)

```

```

m2Div5 = m2Div6
m1ST = m2Div1 + m2Div3 + m2Div6

```

```

m2Div2 = m2Div3
m1Div5 = m2Div3 + m2Div1

```

```

M4 = (m2Div5)/(m1ST)
M5 = (m2Div2)/(m1Div5)

```

$$\begin{aligned}
\text{PtinC} = & (419*m2\text{Div}1)/5 + (502800*((6969*m2\text{Div}3)/100 - \\
& (m2\text{Div}3*((1857797655504137*Ta) \dots \\
& /1179380152417648640 + (1177522354762144503*Ts)/1179380152417648640 \\
& + m2\text{Div}1/400 + \dots \\
& (6969*m2\text{Div}3)/800000 + (6969*m2\text{Div}6)/800000 - 25/4))/ (m2\text{Div}1/8000 + \\
& m2\text{Div}3/8000 + \dots \\
& m2\text{Div}6/8000 + 15/16) + 3031))/ ((90597*m2\text{Div}3)/200 - \\
& (13*m2\text{Div}3*((1857797655504137*Ta) \dots \\
& /1179380152417648640 + (1177522354762144503*Ts)/1179380152417648640 \\
& + m2\text{Div}1/400 + \dots \\
& (6969*m2\text{Div}3)/800000 + (6969*m2\text{Div}6)/800000 - 25/4))/ (2*(m2\text{Div}1/8000 \\
& + m2\text{Div}3/8000 + \dots \\
& m2\text{Div}6/8000 + 15/16)) + 65403/2) - \\
& (419*m2\text{Div}1*((1857797655504137*Ta)/1179380152417648640 \dots \\
& + (1177522354762144503*Ts)/1179380152417648640 + m2\text{Div}1/400 + \\
& (6969*m2\text{Div}3)/800000 + \dots \\
& (6969*m2\text{Div}6)/800000 - 25/4))/ (100*(m2\text{Div}1/8000 + m2\text{Div}3/8000 + \\
& m2\text{Div}6/8000 + 15/16)) - \dots \\
& (4190*((6969*m2\text{Div}3)/100 - \\
& (m2\text{Div}3*((1857797655504137*Ta)/1179380152417648640 + \dots \\
& (1177522354762144503*Ts)/1179380152417648640 + m2\text{Div}1/400 + \\
& (6969*m2\text{Div}3)/800000 + \dots \\
& (6969*m2\text{Div}6)/800000 - 25/4))/ (m2\text{Div}1/8000 + m2\text{Div}3/8000 + \\
& m2\text{Div}6/8000 + 15/16) + 3031) \dots \\
& * ((13*m2\text{Div}3*((1857797655504137*Ta)/1179380152417648640 + \\
& (1177522354762144503*Ts)/ \dots \\
& 1179380152417648640 + m2\text{Div}1/400 + (6969*m2\text{Div}3)/800000 + \\
& (6969*m2\text{Div}6)/800000 - 25/4)) \dots \\
& / (2000*(m2\text{Div}1/8000 + m2\text{Div}3/8000 + m2\text{Div}6/8000 + 15/16)) - \\
& (90597*m2\text{Div}3)/200000 + \dots \\
& 174597/2000))/ ((90597*m2\text{Div}3)/200 - \\
& (13*m2\text{Div}3*((1857797655504137*Ta)/1179380152417648640 \dots \\
& + (1177522354762144503*Ts)/1179380152417648640 + m2\text{Div}1/400 + \\
& (6969*m2\text{Div}3)/800000 + \dots \\
& (6969*m2\text{Div}6)/800000 - 25/4))/ (2*(m2\text{Div}1/8000 + m2\text{Div}3/8000 + \\
& m2\text{Div}6/8000 + \dots \\
& 15/16)) + 65403/2) + 41900 \dots \\
& + \dots \\
& (553080*((6969*m2\text{Div}6)/100 - \\
& (m2\text{Div}6*((1857797655504137*Ta)/1179380152417648640 \dots \\
& + (1177522354762144503*Ts)/1179380152417648640 + m2\text{Div}1/400 + \\
& (6969*m2\text{Div}3)/800000 \dots \\
& + (6969*m2\text{Div}6)/800000 - 25/4))/ (m2\text{Div}1/8000 + m2\text{Div}3/8000 + \\
& m2\text{Div}6/8000 + 15/16) \dots \\
& + 3031))/ ((996567*m2\text{Div}6)/2000 - \\
& (143*m2\text{Div}6*((1857797655504137*Ta)/1179380152417648640 \dots \\
& + (1177522354762144503*Ts)/1179380152417648640 + m2\text{Div}1/400 + \\
& (6969*m2\text{Div}3)/800000 + \dots \\
& (6969*m2\text{Div}6)/800000 - 25/4))/ (20*(m2\text{Div}1/8000 + m2\text{Div}3/8000 + \\
& m2\text{Div}6/8000 + 15/16)) + \dots
\end{aligned}$$

```

719433/20) - (4609*((6969*m2Div6)/100 -
(m2Div6*((1857797655504137*Ta)/1179380152417648640 ...
+ (1177522354762144503*Ts)/1179380152417648640 + m2Div1/400 +
(6969*m2Div3)/800000 + ...
(6969*m2Div6)/800000 - 25/4))/ (m2Div1/8000 + m2Div3/8000 +
m2Div6/8000 + 15/16) + 3031)...
*((13*m2Div6*((1857797655504137*Ta)/1179380152417648640 +
(1177522354762144503*Ts)/1179380152417648640 ...
+ m2Div1/400 + (6969*m2Div3)/800000 + (6969*m2Div6)/800000 -
25/4))/ (2000*(m2Div1/8000 + m2Div3/8000 ...
+ m2Div6/8000 + 15/16)) - (90597*m2Div6)/200000 +
174597/2000))/ ((996567*m2Div6)/2000 - ...
(143*m2Div6*((1857797655504137*Ta)/1179380152417648640 +
(1177522354762144503*Ts)/1179380152417648640 ...
+ m2Div1/400 + (6969*m2Div3)/800000 + (6969*m2Div6)/800000 -
25/4))/ (20*(m2Div1/8000 + m2Div3/8000 ...
+ m2Div6/8000 + 15/16)) + 719433/20)

```

Fboiler=(1/(3600*boilereff))* PtinC % kg fuel inlet boiler

```

%%%%%%%%%%%%%%%%%%%%%%%%%%%%%%%%%%%%%%%%%%%%%%%%%%%%%%%%%%%%%%%%%%%%%%%% Fboiler2 calculation
%%%%%%%%%%%%%%%%%%%%%%%%%%%%%%%%%%%%%%%%%%%%%%%%%%%%%%%%%%%%%%%%%%%%%%%%

```

```

Ptin2=(553080*((6969*m2Div6)/100 - (m2Div6*(m2Div1/400 +
(6969*m2Div3)/800000 ...
+ (6969*m2Div6)/800000 +
389820887896086347/4398046511104000))/ (m2Div1/8000 ...
+ m2Div3/8000 + m2Div6/8000 + 15/16) + 3031))/ ((996567*m2Div6)/2000
- ...
(143*m2Div6*(m2Div1/400 + (6969*m2Div3)/800000 +
(6969*m2Div6)/800000 ...
+ 389820887896086347/4398046511104000))/ (20*(m2Div1/8000 +
m2Div3/8000 ...
+ m2Div6/8000 + 15/16)) + 719433/20) - (4609*((6969*m2Div6)/100 -
...
(m2Div6*(m2Div1/400 + (6969*m2Div3)/800000 +
(6969*m2Div6)/800000 ...
+ 389820887896086347/4398046511104000))/ (m2Div1/8000 +
m2Div3/8000 ...
+ m2Div6/8000 + 15/16) + 3031))* ((13*m2Div6*(m2Div1/400 + ...
(6969*m2Div3)/800000 + (6969*m2Div6)/800000 +
389820887896086347 ...
/4398046511104000))/ (2000*(m2Div1/8000 + m2Div3/8000 +
m2Div6/8000 ...
+ 15/16)) - (90597*m2Div6)/200000 +
174597/2000))/ ((996567*m2Div6)/2000 ...
- (143*m2Div6*(m2Div1/400 + (6969*m2Div3)/800000 +
(6969*m2Div6)/800000 ...
+ 389820887896086347/4398046511104000))/ (20*(m2Div1/8000 +
m2Div3/8000 ...
+ m2Div6/8000 + 15/16)) + 719433/20)

```

```

Fboiler2=(1/(3600*boilereff))* Ptin2
%subs(Fboiler2, [m2Div1,m2Div3,m2Div6], [100,100,100])
%%%%%%%%%%%%%%%%%%%%%%%%%%%%%%%%%%%%%%%%%%%%%%%%%%%%%%%%%%%%%%%%%%%%%%%%

%fat*Cstortank*Vst  is cost which we must pay each year for 40 years
for
%storage tank but our simulation is for 1 hr so we should divide
this to
%365x24 to obtain the cost of storage tank for each hour

    Ctot= Fboiler * Cfboiler + fat*Cstortank*Vst /(365*24)

else

A = [0 0 1;0 1 0;1 0 0 ]
b = [100;100;100]
lb= [0,0,0]
ub= [0,0,100]
x0= [0,0,0]

%x(1)=0
%x(2)=0

fun = @(x) (553080*((6969*x(3))/100 -
(x(3))*((1857797655504137*Ta)/1179380152417648640 ...
+ (1177522354762144503*Ts)/1179380152417648640 + x(1)/400 +
(6969*x(2))/800000 ...
+ (6969*x(3))/800000 - 25/4))/(x(1)/8000 + x(2)/8000 + x(3)/8000 +
15/16)...
+ 3031))/((996567*x(3))/2000 -
(143*x(3))*((1857797655504137*Ta)/1179380152417648640 ...
+ (1177522354762144503*Ts)/1179380152417648640 + x(1)/400 +
(6969*x(2))/800000 + ...
(6969*x(3))/800000 - 25/4))/(20*(x(1)/8000 + x(2)/8000 + x(3)/8000 +
15/16)) + ...
719433/20) - (4609*((6969*x(3))/100 -
(x(3))*((1857797655504137*Ta)/1179380152417648640 ...
+ (1177522354762144503*Ts)/1179380152417648640 + x(1)/400 +
(6969*x(2))/800000 + ...
(6969*x(3))/800000 - 25/4))/(x(1)/8000 + x(2)/8000 + x(3)/8000 +
15/16) + 3031)...
*((13*x(3))*((1857797655504137*Ta)/1179380152417648640 +
(1177522354762144503*Ts)/1179380152417648640 ...
+ x(1)/400 + (6969*x(2))/800000 + (6969*x(3))/800000 -
25/4))/(2000*(x(1)/8000 + x(2)/8000 ...
+ x(3)/8000 + 15/16)) - (90597*x(3))/200000 +
174597/2000))/((996567*x(3))/2000 - ...
(143*x(3))*((1857797655504137*Ta)/1179380152417648640 +
(1177522354762144503*Ts)/1179380152417648640 ...

```

```

+ x(1)/400 + (6969*x(2))/800000 + (6969*x(3))/800000 -
25/4))/(20*(x(1)/8000 + x(2)/8000 ...
+ x(3)/8000 + 15/16)) + 719433/20)

x = fmincon(fun,x0,A,b,[],[],lb,ub)

m2Div1=x(1)
m2Div3=x(2)
m2Div6=x(3)

m2Div5 = m2Div6
m1ST = m2Div1 + m2Div3 + m2Div6

M4 = (m2Div5)/(m1ST)
M5 = 0

% PtinC=Ptin2 because Ptin1 is shut down

PtinC =(553080*((6969*m2Div6)/100 -
(m2Div6*((1857797655504137*Ta)/1179380152417648640 ...
+ (1177522354762144503*Ts)/1179380152417648640 + m2Div1/400 +
(6969*m2Div3)/800000 ...
+ (6969*m2Div6)/800000 - 25/4))/(m2Div1/8000 + m2Div3/8000 +
m2Div6/8000 + 15/16)...
+ 3031))/((996567*m2Div6)/2000 -
(143*m2Div6*((1857797655504137*Ta)/1179380152417648640 ...
+ (1177522354762144503*Ts)/1179380152417648640 + m2Div1/400 +
(6969*m2Div3)/800000 + ...
(6969*m2Div6)/800000 - 25/4))/(20*(m2Div1/8000 + m2Div3/8000 +
m2Div6/8000 + 15/16)) + ...
719433/20) - (4609*((6969*m2Div6)/100 -
(m2Div6*((1857797655504137*Ta)/1179380152417648640 ...
+ (1177522354762144503*Ts)/1179380152417648640 + m2Div1/400 +
(6969*m2Div3)/800000 + ...
(6969*m2Div6)/800000 - 25/4))/(m2Div1/8000 + m2Div3/8000 +
m2Div6/8000 + 15/16) + 3031)...
*((13*m2Div6*((1857797655504137*Ta)/1179380152417648640 +
(1177522354762144503*Ts)/1179380152417648640 ...
+ m2Div1/400 + (6969*m2Div3)/800000 + (6969*m2Div6)/800000 -
25/4))/(2000*(m2Div1/8000 + m2Div3/8000 ...
+ m2Div6/8000 + 15/16)) - (90597*m2Div6)/200000 +
174597/2000))/((996567*m2Div6)/2000 - ...
(143*m2Div6*((1857797655504137*Ta)/1179380152417648640 +
(1177522354762144503*Ts)/1179380152417648640 ...
+ m2Div1/400 + (6969*m2Div3)/800000 + (6969*m2Div6)/800000 -
25/4))/(20*(m2Div1/8000 + m2Div3/8000 ...
+ m2Div6/8000 + 15/16)) + 719433/20)

Fboiler=(1/(3600*boilereff))* PtinC % kg fuel inlet boiler

```

```

%%%%%%%%%%%%%%%%%%%%%%%%%%%%%%%%%%%%%%%%%%%%%%%%%%%%%%%%%%%%%%%%%%%%%%%%555 Fboiler2 calculation %%%%%%%%%%%%%%%%%%%%%%%%%%%%%%%%%%%%%%%%%%%%%%%%%%%%%%%%%%%%%%%%%%%%%%%%%
Ptin2=(553080*((6969*m2Div6)/100 - (m2Div6*(m2Div1/400 +
(6969*m2Div3)/800000 ...
+ (6969*m2Div6)/800000 +
389820887896086347/4398046511104000))/(m2Div1/8000 ...
+ m2Div3/8000 + m2Div6/8000 + 15/16) + 3031))/((996567*m2Div6)/2000
- ...
(143*m2Div6*(m2Div1/400 + (6969*m2Div3)/800000 +
(6969*m2Div6)/800000 ...
+ 389820887896086347/4398046511104000))/(20*(m2Div1/8000 +
m2Div3/8000 ...
+ m2Div6/8000 + 15/16)) + 719433/20) - (4609*((6969*m2Div6)/100 -
...
(m2Div6*(m2Div1/400 + (6969*m2Div3)/800000 +
(6969*m2Div6)/800000 ...
+ 389820887896086347/4398046511104000))/(m2Div1/8000 +
m2Div3/8000 ...
+ m2Div6/8000 + 15/16) + 3031)*((13*m2Div6*(m2Div1/400 + ...
(6969*m2Div3)/800000 + (6969*m2Div6)/800000 +
389820887896086347 ...
/4398046511104000))/(2000*(m2Div1/8000 + m2Div3/8000 +
m2Div6/8000 ...
+ 15/16)) - (90597*m2Div6)/200000 +
174597/2000))/((996567*m2Div6)/2000 ...
- (143*m2Div6*(m2Div1/400 + (6969*m2Div3)/800000 +
(6969*m2Div6)/800000 ...
+ 389820887896086347/4398046511104000))/(20*(m2Div1/8000 +
m2Div3/8000 ...
+ m2Div6/8000 + 15/16)) + 719433/20)

```

```
Fboiler2=(1/(3600*boilereff))* Ptin2
```

```

%fat*Cstortank*Vst is cost which we must pay each year for 40
years for
%storage tank but our simulation is for 1 hr so we should divide
this to
%365x24 to obtain the cost of storage tank for each hour

```

```
Ctot= Fboiler * Cfboiler + fat*Cstortank*Vst /(365*24)
```

```
end
```

```
%% mFileErrorCode = 95;
```

```
% --- Set outputs ---

M1 = m2Div1 / mindiv1
M2 = m2Div3 / mHX2U1
M3 = m2Div6 / mHX2U2

trnOutputs(1) = M1; % inlet steam production fluid controller
trnOutputs(2) = M2 ;% HX2 source side outlet fluid controller
trnOutputs(3) = M3 ;%
trnOutputs(4) = M4 ;% Div5 control signal
trnOutputs(5) = M5 ;% Div2 control signal
trnOutputs(6) = Ctot ;
trnOutputs(7) = Fboiler ;

%% mFileErrorCode = 90;

mFileErrorCode = 0;
```

B. Configuration 3-1 Data

In this Appendix, initially fuel consumption Diagram in Configuration 3-1 is presented. Then, all applied mathematical models of components during Configuration's optimization is shown and finally optimization MATLAB code is inserted.

Figure B.1 and Figure B.2 show the effect of solar energy application on Unit 1 boiler fuel consumption in February and June, respectively. Fuel consumption reduction is more in June because Unit 1 uses more solar energy. Flat plate collector installation in Configuration 3-1 could reduce total fuel consumption by about 15% in February while this reduction is 30 % in June.

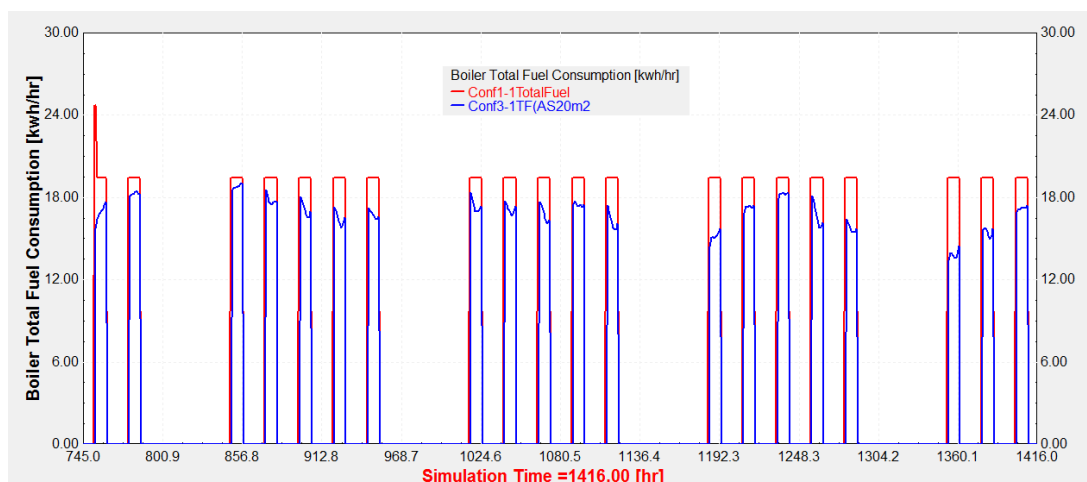


Figure B.1. Unit 1 total fuel consumption in Configuration 1 vs. Configuration 3-1 with 20 m² solar collector area and 1 m³ storage tank volume for the February.

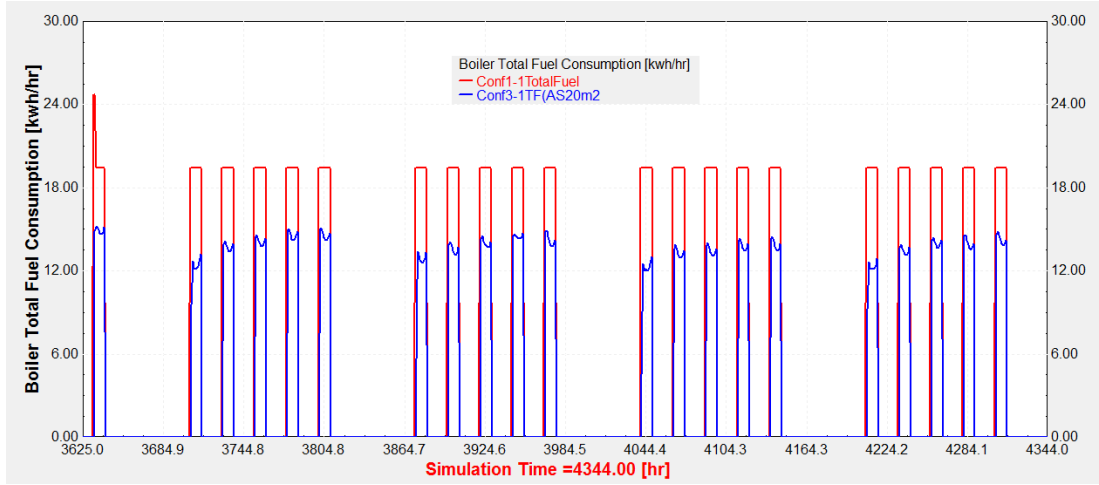


Figure B.2. Unit 1 total fuel consumption in Configuration 1 vs. Configuration 3-1 with 20 m² solar collector area and 1 m³ storage tank volume for the June.

Following Equations describe how to derive an objective function for Configuration 3-1. For subsequent Equations, the related Equation in Chapter 3, the related component name and investigated Unit are mentioned.

Obtaining storage tank average temperature ($T_{1,ST}$) at the end of each hour:

From Eqn. (3.19) for HX2 in Unit 1:

$$T_{HX2} = T_{1,HX1} - (\varepsilon_2) \left(\frac{\dot{m}_{1,HX1}}{\dot{m}_{1,HX1}} \right) (T_{1,HX1} - T_{in}) \quad (B.1)$$

From Eqn.(3.29) for Diverter (Div3):

$$T_{2,Div3} = T_{HX2} \quad (B.2)$$

From Eqn. (3.23) for Tee-Piece (Mix3):

$$T_{\text{Mix3}} = \frac{(\dot{m}_{2,\text{Div1}})(T_{\text{in,Div1}}) + (\dot{m}_{2,\text{Div3}})(T_{2,\text{Div3}})}{(\dot{m}_{2,\text{Div1}} + \dot{m}_{2,\text{Div3}})} \quad (\text{B. 3})$$

From Eqn. (3.21) for heat storage tank:

$$T_{1,\text{ST}} = \frac{[T_s - \left(\frac{1}{\dot{m}_s}\right)((\dot{m}_{\text{coll}})(T_{\text{coll}}) - (\dot{m}_{2,\text{Div1}} + \dot{m}_{2,\text{Div3}})(T_{\text{Mix3}}) + \frac{(\text{UAs})(T_s - T_a)}{C_p})]}{[1 + \left(\frac{1}{\dot{m}_s}\right)(\dot{m}_{2,\text{Div1}} + \dot{m}_{2,\text{Div3}} - \dot{m}_{\text{coll}})]} \quad (\text{B. 4})$$

From Eqn.(3.29) for Diverter (Div2):

$$T_{2,\text{Div2}} = T_{1,\text{ST}} \quad (\text{B. 5})$$

Calculating hot-side outlet temperature ($T_{2,\text{HX1}}$) of HX1 heat exchanger:

From Eqn. (3.27) for Diverter (Div3):

$$T_{1,\text{Div3}} = T_{\text{HX2}} \quad (\text{B. 6})$$

From Eqn. (3.23) for Tee-Piece (Mix2):

$$T_{\text{Mix2}} = \frac{(\dot{m}_{1,\text{Div3}})(T_{1,\text{Div3}}) + (\dot{m}_{2,\text{Div2}})(T_{2,\text{Div2}})}{(\dot{m}_{1,\text{Div3}} + \dot{m}_{2,\text{Div2}})} \quad (\text{B. 7})$$

From Eqn. (3.12) for HX1 in Unit 1:

$$\gamma_1 = 1 - \frac{(T_{1,\text{HX1}} - T_{\text{Mix2}})(\dot{m}_{\text{Mix2}})}{(\varepsilon_1)(\dot{m}_{2,\text{Div4}})(T_{2,\text{Div4}} - T_{\text{Mix2}})} \quad (\text{B. 8})$$

From Eqn. (3.13) for HX1 in Unit 1:

$$T_{2,HX1} = (\gamma_1)(T_{2,Div4}) + (1 - \gamma_1) \left(T_{2,Div4} - (\varepsilon_1)(T_{2,Div4} - T_{Mix2}) \right) \quad (B. 9)$$

From Eqn. (3.25) for Flow Mixer (Mix1):

$$T_{Mix1} = \frac{(\dot{m}_{in,Div1} - \dot{m}_{2,Div1})(T_{1,Div1}) + (\dot{m}_{2,Div1})(T_{1,Div2}) + (\dot{m}_{2,HX1})(T_{2,HX1})}{(\dot{m}_{in,Div1} + \dot{m}_{2,HX1})} \quad (B. 10)$$

Calculating $\dot{Q}_{need,1}$:

From Eqn. (3.1) for Boiler in Unit 1:

$$\dot{Q}_{need,1} = (\dot{m}_{boiler})C_p(T_{boiler} - T_{mix1}) \quad (B. 11)$$

The following code is used MATLAB code for Configuration 3-1 optimization.

```
i=0.017% 17% turkey interest rate
n1=20 % life span of solar collector
n2=40 % life span of storage tank
fas=(i*(1+i)^n1) /(((1+i)^n1)-1)
fat=(i*(1+i)^n2) /(((1+i)^n2)-1)

Csolar = 220 % E/M^2 solar collector cost
Cstortank = 180 % E/M^3 storage tank cost
Cfboiler = 0.06 % E/kwh natural gaz cost

Asp= 20 % m^2 solar collector area
Vst= 1 % m^3 storage tank volume

Hi=50000 % kj/kg natural gas lower heat value
boilereff=0.78
```

```
%%%%%%%%%%%%%%%%%%%%%%%%%%%%%%%%%%%%%%%%%%%%%%%%%%%%%%%%%%%%%%%%%%%%%%%%
%%%%%%%%%%%%%%%%%%%%%%%%%%%%%%%%%%%%%%%%%%%%%%%%%%%%%%%%%%%%%%%%%%%%%%%%5555
```

```
syms m2Div1 m2Div3 Ts Ta Tcoll Vst
```

```
mFileErrorCode = 3;
```

```
ro=1000 % kg/m3 water density
%VS=1 % storage tank volume [m3]
hS=0.1 % storage tank hight [m]
AS=(2*Vst/hS)+2*(Vst*3.14*hS)^0.5 % storage tank surface [m2]
mS=ro*Vst
mColl= 100 % kg/hr solar collector inlet flow rate
U=2.5 % Tank Loss Coefficient [kj/(hr.m2.k)]
Cp = 4.19 % for water kj/(kg.k)
ep1= 0.65 % heat exchanger effectiveness of HX1
ep2= 0.433 % heat exchanger effectiveness of HX2
```

```
Cmin1=min(100*4.19,1100*4.19)
% always Cmin1=419
mindiv1=100
Tindiv1=20
```

```
mboiler=1100 % kg/hr
```

```
m2HX1= 1000 % kg/hr
m2Div4 = m2HX1
```

```
mcoll = 100 % kg/hr
```

```
T1div1=Tindiv1
T1HX1 = 100 % oC
```

```
min = 100 % kg/hr
m1HX1 = 100 % kg/hr
mHX2 = m1HX1
mMix2 = m1HX1
```

```
Tin=30 % oC
Tboiler=120 % oC
```

```
T2Div4 = Tboiler
```

```
m1Div3 = mHX2 - m2Div3
m2Div2 = m2Div3
```



```

% trnStopTime (1x1)      : TRNSYS Simulation Stop time
% trnTimeStep (1x1)     : TRNSYS Simulation time step
% mFileErrorCode (1x1) : Error code for this m-file. It is set to 1
by TRNSYS and the m-file should set it to 0 at the
%                          end to indicate that the call was
successful. Any non-zero value will stop the simulation
% trnOutputs (nOx1)     : TRNSYS outputs
%
%
% Notes:
% -----
%
% You can use the values of trnInfo(7), trnInfo(8) and trnInfo(13)
to identify the call (e.g. first iteration, etc.)
% Real-time controllers (callingMode = 10) will only be called once
per time step with trnInfo(13) = 1 (after convergence)
%
% The number of inputs is given by trnInfo(3)
% The number of expected outputs is given by trnInfo(6)
% WARNING: if multiple units of Type 155 are used, the variables
passed from/to TRNSYS will be sized according to
%          the maximum required by all units. You should cope with
that by only using the part of the arrays that is
%          really used by the current m-File. Example: use "nI =
trnInfo(3); myInputs = trnInputs(1:nI);"
%
%                                     rather than
"MyInputs = trnInputs;"
%
% Please also note that all m-files share the same
workspace in Matlab (they are "scripts", not "functions") so
%          variables like trnInfo, trnTime, etc. will be overwritten
at each call.
%
% -----
% -----
% This example implements a very simple solar collector model. The
component is iterative (should be called at each
% TRNSYS call)
%
% trnInputs
% -----
%
% trnInputs(1) : T1, Heat Exchanger source side outlet temperature
% trnInputs(2) : T2, fluid for steam production inlet temperature
% trnInputs(3) : T3, Average Tanke Temperature
% trnInputs(4) : Qin, boiler energy to fluid
%
%
% trnOutputs
% -----
%
% trnOutputs(1) : M1, inlet steam production fluid controller
% trnOutputs(2) : M2, HX2 source side outlet fluid controller
% trnOutputs(3) : Ctot, total cost of system
%

```

```

%
% SK, November 2018
% -----
-----

% TRNSYS sets mFileErrorCode = 1 at the beginning of the M-File for
error detection
% This file increments mFileErrorCode at different places. If an
error occurs in the m-file the last succesful step will
% be indicated by mFileErrorCode, which is displayed in the TRNSYS
error message
% At the very end, the m-file sets mFileErrorCode to 0 to indicate
that everything was OK

% --- Process Inputs -----
-----
% -----
-----

T1    = trnInputs(1);
T2    = trnInputs(2);
Ts    = trnInputs(3);
Qin   = trnInputs(4);
%Ts   = trnInputs(5);
Tcoll = trnInputs(5);
S1    = trnInputs(6);
Ta    = trnInputs(7);

%% mFileErrorCode = 120    % After processing inputs

% --- First call of the simulation: initial time step (no
iterations) -----
% -----
-----

% (note that Matlab is initialized before this at the info(7) = -1
call, but the m-file is not called)

if ( (trnInfo(7) == 0) & (trnTime-trnStartTime < 1e-6) )

    % This is the first call (Counter will be incremented later for
this very first call)
    nCall = 0;

    % This is the first time step
    nStep = 1;

    % Initialize history of the variables for plotting at the end of
the simulation
    nTimeSteps = (trnStopTime-trnStartTime)/trnTimeStep + 1;

```

```

    history.T1      = zeros(nTimeSteps,1);
    history.T2      = zeros(nTimeSteps,1);

    history.Ctot    = zeros(nTimeSteps,1);

    % No return, we will calculate the solar collector performance
    during this call
    %% mFileErrorCode = 130      % After initialization

end

% --- Very last call of the simulation (after the user clicks "OK"):
Do nothing -----
% -----
-----

if ( trnInfo(8) == -1 )

    %% mFileErrorCode = 1000;

    mFileErrorCode = 0; % Tell TRNSYS that we reached the end of the
m-file without errors
    return

end

% --- Post convergence calls: store values -----
-----
% -----
-----

if (trnInfo(13) == 1)

    %% mFileErrorCode = 140;      % Beginning of a post-convergence
call

    history.T1(nStep)      = T1;
    history.T2(nStep)      = T2;

    mFileErrorCode = 0; % Tell TRNSYS that we reached the end of the
m-file without errors
    return % Do not update outputs at this call

end

```


B=1

```
A = [0 1;1 0]
b = [100;100]
lb= [0;0]
ub= [100;100]
x0=[0,0]
```

```
fun = @(x) (419*x(1))/5 + (502800*((6969*x(2))/100 - (x(2)*(Ts +
...
(20*x(1) - 100*Tcoll + (6969*x(2))/100 + (100*(Ta - Ts)*(50*Vst +
...
5*((157*Vst)/500)^(1/2)))/419)/(8000*Vst)))/((x(1) + x(2) -
100)/...
(8000*Vst) + 1) + 3031))/((90597*x(2))/200 - (13*x(2)*(Ts + (20*x(1)
...
- 100*Tcoll + (6969*x(2))/100 + (100*(Ta - Ts)*(50*Vst +
5*((157*Vst)/500) ...
^(1/2)))/419)/(8000*Vst)))/(2*((x(1) + x(2) - 100)/(8000*Vst) + 1))
+ 65403/2) ...
- (4190*((6969*x(2))/100 - (x(2)*(Ts + (20*x(1) - 100*Tcoll +
(6969*x(2))/100 ...
+ (100*(Ta - Ts)*(50*Vst +
5*((157*Vst)/500)^(1/2)))/419)/(8000*Vst)))/((x(1) + x(2) ...
- 100)/(8000*Vst) + 1) + 3031)*((13*x(2)*(Ts + (20*x(1) - 100*Tcoll
+ (6969*x(2))/100 ...
+ (100*(Ta - Ts)*(50*Vst +
5*((157*Vst)/500)^(1/2)))/419)/(8000*Vst)))/(2000*((x(1) + ...
x(2) - 100)/(8000*Vst) + 1)) - (90597*x(2))/200000 +
174597/2000))/((90597*x(2))/200 ...
- (13*x(2)*(Ts + (20*x(1) - 100*Tcoll + (6969*x(2))/100 + (100*(Ta
- Ts)*(50*Vst + ...
5*((157*Vst)/500)^(1/2)))/419)/(8000*Vst)))/(2*((x(1) + x(2) -
100)/(8000*Vst) + 1)) + ...
65403/2) - (419*x(1)*(Ts + (20*x(1) - 100*Tcoll + (6969*x(2))/100 +
(100*(Ta - Ts)* ...
(50*Vst + 5*((157*Vst)/500)^(1/2)))/419)/(8000*Vst)))/(100*((x(1) +
x(2) - 100)/(8000*Vst) + 1)) + 41900
```

```
x = fmincon(fun,x0,A,b,[],[],lb,ub)
```

```
% mFileErrorCode = 130;
```

```
M1=x(1)/100
M2=x(2)/100
M3=(x(2))/(x(1)+x(2))
```

```

    Ptin = (419*x(1))/5 + (502800*((6969*x(2))/100 - (x(2)*(Ts + ...
(20*x(1) - 100*Tcoll + (6969*x(2))/100 + (100*(Ta - Ts)*(50*Vst +
...
5*((157*Vst)/500)^(1/2)))/419)/(8000*Vst)))/((x(1) + x(2) -
100)/...
(8000*Vst) + 1) + 3031))/((90597*x(2))/200 - (13*x(2)*(Ts + (20*x(1)
...
- 100*Tcoll + (6969*x(2))/100 + (100*(Ta - Ts)*(50*Vst +
5*((157*Vst)/500) ...
^(1/2)))/419)/(8000*Vst)))/(2*((x(1) + x(2) - 100)/(8000*Vst) + 1))
+ 65403/2) ...
- (4190*((6969*x(2))/100 - (x(2)*(Ts + (20*x(1) - 100*Tcoll +
(6969*x(2))/100 ...
+ (100*(Ta - Ts)*(50*Vst +
5*((157*Vst)/500)^(1/2)))/419)/(8000*Vst)))/((x(1) + x(2) ...
- 100)/(8000*Vst) + 1) + 3031)*((13*x(2)*(Ts + (20*x(1) - 100*Tcoll
+ (6969*x(2))/100 ...
+ (100*(Ta - Ts)*(50*Vst +
5*((157*Vst)/500)^(1/2)))/419)/(8000*Vst)))/(2000*((x(1) + ...
x(2) - 100)/(8000*Vst) + 1)) - (90597*x(2))/200000 +
174597/2000))/((90597*x(2))/200 ...
- (13*x(2)*(Ts + (20*x(1) - 100*Tcoll + (6969*x(2))/100 + (100*(Ta
- Ts)*(50*Vst + ...
5*((157*Vst)/500)^(1/2)))/419)/(8000*Vst)))/(2*((x(1) + x(2) -
100)/(8000*Vst) + 1)) + ...
65403/2) - (419*x(1)*(Ts + (20*x(1) - 100*Tcoll + (6969*x(2))/100 +
(100*(Ta - Ts)* ...
(50*Vst + 5*((157*Vst)/500)^(1/2)))/419)/(8000*Vst)))/(100*((x(1) +
x(2) - 100)/(8000*Vst) + 1)) + 41900

```

```

    %mFileErrorCode = 110;

```

```

Fboiler=(1/(3600*boilereff))* Ptin % kwh fuel inlet boiler

```

```

Ctot= ((fas*Csolar*Asp + fat*Cstortank*Vst)/(365*24)* B )+ Fboiler *
Cfboiler

```

```

% mFileErrorCode = 100;

```

```

    else

```

```

        B=1

```

```

        M1=0

```

```

        M2=0

```

```

        M3=0 % it is not important if M3=0 or M3=1 because Div2 input is
zero

```

```

        x(1)=0

```

```

        x(2)=0

```

```

        %M1=x(1)/100

```

```

        %M2=x(2)/100

```

```

    Ptin= (419*x(1))/5 + (502800*((6969*x(2))/100 - (x(2)*(Ts + ...
(20*x(1) - 100*Tcoll + (6969*x(2))/100 + (100*(Ta - Ts)*(50*Vst +
...
5*((157*Vst)/500)^(1/2)))/419)/(8000*Vst)))/((x(1) + x(2) -
100)/...
(8000*Vst) + 1) + 3031))/((90597*x(2))/200 - (13*x(2)*(Ts + (20*x(1)
...
- 100*Tcoll + (6969*x(2))/100 + (100*(Ta - Ts)*(50*Vst +
5*((157*Vst)/500) ...
^(1/2)))/419)/(8000*Vst)))/(2*((x(1) + x(2) - 100)/(8000*Vst) + 1))
+ 65403/2) ...
- (4190*((6969*x(2))/100 - (x(2)*(Ts + (20*x(1) - 100*Tcoll +
(6969*x(2))/100 ...
+ (100*(Ta - Ts)*(50*Vst +
5*((157*Vst)/500)^(1/2)))/419)/(8000*Vst)))/((x(1) + x(2) ...
- 100)/(8000*Vst) + 1) + 3031)*((13*x(2)*(Ts + (20*x(1) - 100*Tcoll
+ (6969*x(2))/100 ...
+ (100*(Ta - Ts)*(50*Vst +
5*((157*Vst)/500)^(1/2)))/419)/(8000*Vst)))/(2000*((x(1) + ...
x(2) - 100)/(8000*Vst) + 1)) - (90597*x(2))/200000 +
174597/2000))/((90597*x(2))/200 ...
- (13*x(2)*(Ts + (20*x(1) - 100*Tcoll + (6969*x(2))/100 + (100*(Ta
- Ts)*(50*Vst + ...
5*((157*Vst)/500)^(1/2)))/419)/(8000*Vst)))/(2*((x(1) + x(2) -
100)/(8000*Vst) + 1)) + ...
65403/2) - (419*x(1)*(Ts + (20*x(1) - 100*Tcoll + (6969*x(2))/100 +
(100*(Ta - Ts)* ...
(50*Vst + 5*((157*Vst)/500)^(1/2)))/419)/(8000*Vst)))/(100*((x(1) +
x(2) - 100)/(8000*Vst) + 1)) + 41900

```

```

    Fboiler=(1/(3600*boilereff))* Ptin

```

```

    Ctot= ((fas*C solar*Asp + fat*Cstortank*Vst) / (365*24)* B )+
Fboiler * Cfboiler
    % ( 0.0594*220*20 + 0.0347*180*1) / (365*24)

```

```

    end
%end
%
else
B=1
M1=0
M2=0
M3=0
Ctot= (fas*C solar*Asp + fat*Cstortank*Vst)/(365*24)* B % boiler is
off and cost just includes solar collector and storage tank
Ptin=0
Fboiler=0

```

```

%Ctot=S1*100

end
%}

%Ctot=U1*100
%else
  %Ctot=0
%end

%% mFileErrorCode = 95;

% --- Set outputs ---

trnOutputs(1) = M1; % inlet steam production fluid controller
trnOutputs(2) = M2 ;% HX2 source side outlet fluid controller
trnOutputs(3) = Ctot ;% total cost of system
trnOutputs(4) = Ptin ;
trnOutputs(5) = M3 ;
trnOutputs(6) = S1 ;
trnOutputs(7)= Fboiler;

```

C. Configuration 3-2 Data

Add Appendix here In this Appendix, initially fuel consumption Diagram in Configuration 3-2 is presented. Then, all applied mathematical models of components during Configuration's optimization is shown and finally optimization MATLAB code is inserted.

The fuel consumption in Configuration 3-2 with 20 m² solar collector area and 1 m³ storage tank volume is compared with a basic Configuration in Figures C.1 and C.2 for February and June, respectively. Configuration 3-2 shows fuel consumption reduction in a few hours in February while in June because of much solar energy, total fuel consumption shows a continuous reduction. In both Figure C.1 and C.2, the fuel consumption hours match with the hours which solar energy is used in the Configuration 3-2 system.

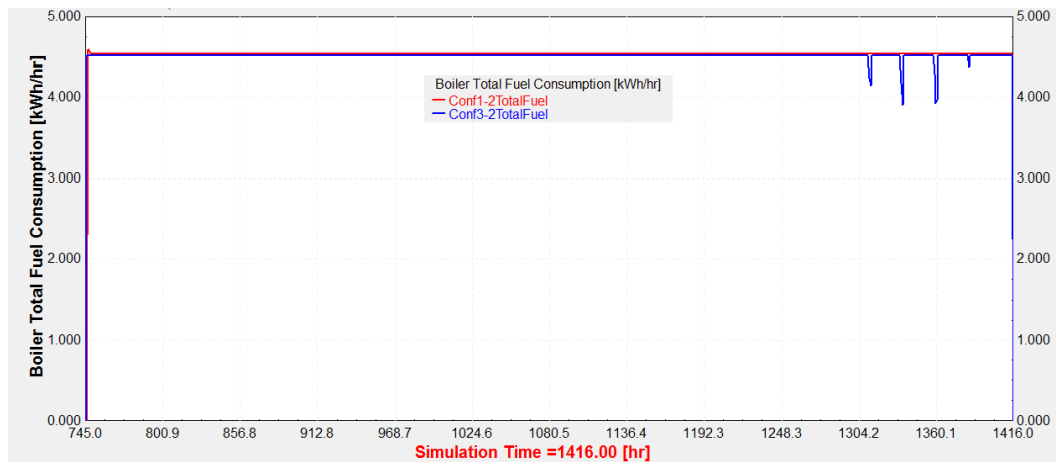


Figure C.1. Fuel consumption in Unit 2 in the Configuration 1 vs. fuel consumption in Configuration 3-2 in the February. Storage tank volume is 1 m³ and solar collector area is 20 m².

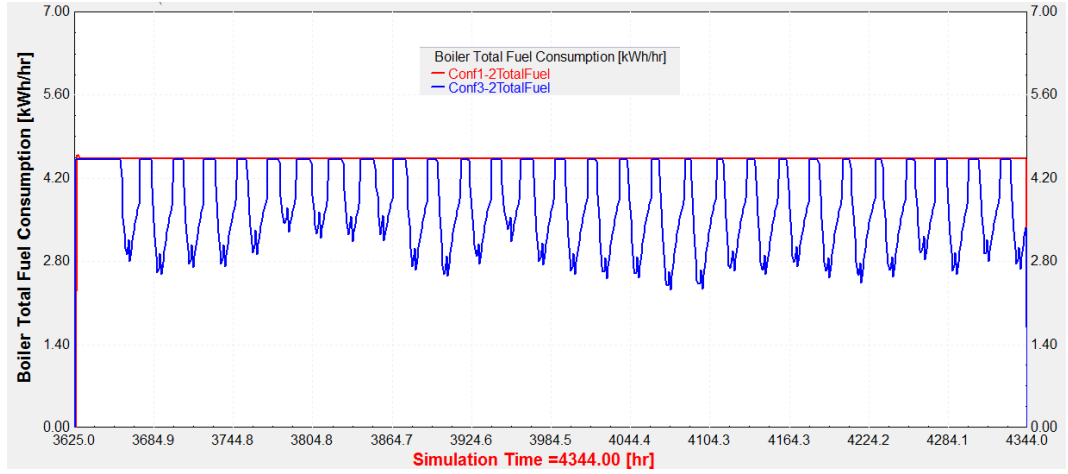


Figure C.2. Fuel consumption in Unit 2 in Configuration 1 vs. fuel consumption in Configuration 3-2 in June. Storage tank volume is 1 m³ and solar collector area is 20 m².

In this Appendix, all Equations which are used to obtain objective function for Configuration 3-2 are presented. For each Equation, the related Equation in Chapter 3 and the related component in the corresponding Unit are mentioned.

From Eqn.(3.19) for HX2 in Unit 2:

$$T_{2,HX2} = T_{1,HX1} - \left(\frac{\varepsilon_2}{\dot{m}_{1,HX1}} \right) \left(\frac{C_{\min 1}}{C_p} \right) (T_{1,HX1} - T_{i,HX2}) \quad (C.1)$$

From Eqn.(3.21) for heat storage tank:

$$T_{1,ST} = \frac{[T_s - \left(\frac{1}{\dot{m}_s} \right) ((\dot{m}_{\text{coll}})(T_{\text{coll}}) - (\dot{m}_{2,\text{Div1}})(T_{2,\text{Div1}}) + \frac{(UAs)(T_s - T_a)}{C_p})]}{[1 + \left(\frac{1}{\dot{m}_s} \right) (\dot{m}_{2,\text{Div1}} - \dot{m}_{\text{coll}})]} \quad (C.2)$$

From Eqn. (3.23) for Tee–Piece (Mix1):

$$T_{\text{Mix1}} = \frac{(\dot{m}_{1,\text{Div1}})(T_{1,\text{Div1}}) + (\dot{m}_{1,\text{ST}})(T_{1,\text{ST}})}{(\dot{m}_{\text{Mix1}})} \quad (\text{C. 3})$$

From Eqn. (3.12) for HX1 in Unit 2:

$$\gamma = 1 - \frac{(T_{1,\text{HX1}} - T_{\text{Mix1}})(C_{\text{cold-side}})}{(\varepsilon_1)(\dot{m}_{\text{ob}})C_p(T_{\text{ob}} - T_{\text{Mix1}})} \quad (\text{C. 4})$$

From Eqn. (3.8) for HX1 in Unit 2:

$$C_{\text{min}} = (\dot{m}_{\text{ob}})C_p(1 - \gamma) \quad (\text{C. 5})$$

From Eqn. (3.13) for HX1 in Unit 2:

$$T_{\text{ib}} = \gamma (T_{\text{ob}}) + (1 - \gamma) \left[T_{\text{ob}} - \frac{(\varepsilon_1)(C_{\text{min}})(T_{\text{ob}} - T_{\text{Mix1}})}{(\dot{m}_{\text{ob}})C_p(1 - \gamma)} \right] \quad (\text{C. 6})$$

Calculating $\dot{Q}_{\text{need},2}$:

From Eqn.(3.1) for boiler in Unit 2:

$$\dot{Q}_{\text{need},2} = (\dot{m}_{\text{ob}})C_p(T_{\text{ob}} - T_{\text{ib}}) \quad (\text{C. 7})$$

The following MATLAB code is used to optimize Configuration 3-2 in each hour.

```

%%%%%%%%%%%%%%%%%%%%%%%%%%%%%%%%%%%%%%%%%%%%%%%%%%%%%%%%%%%%%%%%%%%%%%%% optimization %%%%%%%%%
% --- Process Inputs -----
% -----
% -----

T1    = trnInputs(1);
Ts    = trnInputs(2);
TColl = trnInputs(3);
Ta    = trnInputs(4);

mFileErrorCode = 120    % After processing inputs

% --- First call of the simulation: initial time step (no
iterations) -----
% -----
% (note that Matlab is initialized before this at the info(7) = -1
call, but the m-file is not called)

if ( (trnInfo(7) == 0) & (trnTime-trnStartTime < 1e-6) )

    % This is the first call (Counter will be incremented later for
this very first call)
    nCall = 0;

    % This is the first time step
    nStep = 1;

    % Initialize history of the variables for plotting at the end of
the simulation
    nTimeSteps = (trnStopTime-trnStartTime)/trnTimeStep + 1;

    history.T1    = zeros(nTimeSteps,1);
    history.Ts    = zeros(nTimeSteps,1);

    history.Ctot  = zeros(nTimeSteps,1);

    % No return, we will calculate the solar collector performance
during this call
    mFileErrorCode = 130    % After initialization

end

% --- Very last call of the simulation (after the user clicks "OK"):
Do nothing -----

```

```

% -----
% -----

if ( trnInfo(8) == -1 )

    mFileErrorCode = 1000

    mFileErrorCode = 0; % Tell TRNSYS that we reached the end of
the m-file without errors
    return

end

% --- Post convergence calls: store values -----
% -----

if (trnInfo(13) == 1)

    %% mFileErrorCode = 140; % Beginning of a post-convergence
call

    history.T1(nStep)      = T1;
    history.Ts(nStep)     = Ts;

    mFileErrorCode = 0; % Tell TRNSYS that we reached the end of the
m-file without errors
    return % Do not update outputs at this call

end

% --- All iterative calls -----
% -----

% --- If this is a first call in the time step, increment counter --
-

if ( trnInfo(7) == 0 )
    nStep = nStep+1;
end
mFileErrorCode = 145

% --- Get TRNSYS Inputs ---

nI = trnInfo(3); % For bookkeeping
nO = trnInfo(6); % For bookkeeping

```

```

T1    = trnInputs(1);
Ts    = trnInputs(2);
TColl = trnInputs(3);
Ta    = trnInputs(4);

i=0.017% 1.7% Europe interest rate
n1=20 % life span of solar collector
n2=40 % life span of storage tank
fas=(i*(1+i)^n1) /(((1+i)^n1)-1)
fat=(i*(1+i)^n2) /(((1+i)^n2)-1)

mFileErrorCode = 148

Csolar    = 220 % E/M^2 solar collector cost
Cstortank = 180 % E/M^3 storage tank cost
Cfboiler  = 0.06 % E/kwh natural gaz cost
%syms m2Div1 Ts TColl Ta Vst

Asp= 20 % m^2 solar collector area
%%%%%%%%%%%%%%%%%%%%%%%%%%%%%%%%%%%%%%%%%%%%%%%%%%%%%%%%%%%%%%%%%%%%%%%%
Vst= 1 % m^3 storage tank volume
%%%%%%%%%%%%%%%%%%%%%%%%%%%%%%%%%%%%%%%%%%%%%%%%%%%%%%%%%%%%%%%%%%%%%%%%
&&&&

Hi=50000 % kj/kg natural gas lower heat value
boilereff=0.78
%%%%%%%%%%%%%%%%%%%%%%%%%%%%%%%%%%%%%%%%%%%%%%%%%%%%%%%%%%%%%%%%%%%%%%%%
%%%%%%%%%%%%%%%%%%%%%%%%%%%%%%%%%%%%%%%%%%%%%%%%%%%%%%%%%%%%%%%%%%%%%%%%5555
mFileErrorCode = 149.5

if Ts > T1

    B=1
    A = [1]
    b = [100]
    lb= [0]
    ub= [100]
    x0=[0]

    mFileErrorCode = 149.8

    mFileErrorCode = 151

fun = @(m2Div1) (553080*((2920011*m2Div1)/10000 - (419*m2Div1*(Ts +
...
((6969*m2Div1)/100 - 100*TColl + (100*(Ta - Ts)*(50*Vst +
5*((157*Vst) ...

```

```

    /500)^(1/2)))/419)/(1000*Vst)))/(100*((m2Div1 - 100)/(1000*Vst)
+ 1))...
    + 1269989/100))/((417561573*m2Div1)/200000 - (59917*m2Div1*(Ts +
...
    ((6969*m2Div1)/100 - 100*TColl + (100*(Ta - Ts)*(50*Vst +
5*((157*Vst)...
    /500)^(1/2)))/419)/(1000*Vst)))/(2000*((m2Div1 - 100)/(1000*Vst)
+ 1))...
    + 301442427/2000) - (4609*((13*m2Div1*(Ts + ((6969*m2Div1)/100 -
100*TColl...
    + (100*(Ta - Ts)*(50*Vst +
5*((157*Vst)/500)^(1/2)))/419)/(1000*Vst)))...
    /2000*((m2Div1 - 100)/(1000*Vst) + 1)) - (90597*m2Div1)/200000
+ 174597/2000)...
    *(2920011*m2Div1)/10000 - (419*m2Div1*(Ts + ((6969*m2Div1)/100
- 100*TColl + ...
    (100*(Ta - Ts)*(50*Vst +
5*((157*Vst)/500)^(1/2)))/419)/(1000*Vst)))/(100* ...
    ((m2Div1 - 100)/(1000*Vst) + 1)) +
1269989/100))/((417561573*m2Div1)/200000 ...
    - (59917*m2Div1*(Ts + ((6969*m2Div1)/100 - 100*TColl + (100*(Ta
- Ts)* ...
    (50*Vst +
5*((157*Vst)/500)^(1/2)))/419)/(1000*Vst)))/(2000*((m2Div1 - 100)...
    /1000*Vst) + 1)) + 301442427/2000)

```

```
mFileErrorCode = 153
```

```
m2Div1 = fmincon(fun,x0,A,b,[],[],lb,ub)
```

```
% mFileErrorCode = 130;
```

```
M2=m2Div1/100
```

```
M2=m2Div1/100
```

```

Ptin = (553080*((2920011*m2Div1)/10000 - (419*m2Div1*(Ts + ...
    ((6969*m2Div1)/100 - 100*TColl + (100*(Ta - Ts)*(50*Vst +
5*((157*Vst) ...
    /500)^(1/2)))/419)/(1000*Vst)))/(100*((m2Div1 - 100)/(1000*Vst)
+ 1))...
    + 1269989/100))/((417561573*m2Div1)/200000 - (59917*m2Div1*(Ts +
...
    ((6969*m2Div1)/100 - 100*TColl + (100*(Ta - Ts)*(50*Vst +
5*((157*Vst)...
    /500)^(1/2)))/419)/(1000*Vst)))/(2000*((m2Div1 - 100)/(1000*Vst)
+ 1))...

```

```

+ 301442427/2000) - (4609*((13*m2Div1*(Ts + ((6969*m2Div1)/100 -
100*TColl)...
+ (100*(Ta - Ts)*(50*Vst +
5*((157*Vst)/500)^(1/2)))/419)/(1000*Vst)))...
/(2000*((m2Div1 - 100)/(1000*Vst) + 1)) - (90597*m2Div1)/200000
+ 174597/2000)...
*((2920011*m2Div1)/10000 - (419*m2Div1*(Ts + ((6969*m2Div1)/100
- 100*TColl + ...
(100*(Ta - Ts)*(50*Vst +
5*((157*Vst)/500)^(1/2)))/419)/(1000*Vst)))/(100* ...
((m2Div1 - 100)/(1000*Vst) + 1)) +
1269989/100))/((417561573*m2Div1)/200000 ...
- (59917*m2Div1*(Ts + ((6969*m2Div1)/100 - 100*TColl + (100*(Ta
- Ts)* ...
(50*Vst +
5*((157*Vst)/500)^(1/2)))/419)/(1000*Vst)))/(2000*((m2Div1 - 100)...
/(1000*Vst) + 1)) + 301442427/2000)

```

```
Fboiler=(1/(3600*boilereff))* Ptin % kwh fuel inlet boiler
```

```
Ctot= (fas*C solar*Asp + fat*Cstortank*Vst)/(365*24)* B + Fboiler *
Cfboiler
```

```
mFileErrorCode = 100;
```

```
else
```

```
m2Div1=0
M2=m2Div1/100
```

```
B=1
```

```

Ptin = (553080*((2920011*m2Div1)/10000 - (419*m2Div1*(Ts + ...
((6969*m2Div1)/100 - 100*TColl + (100*(Ta - Ts)*(50*Vst +
5*((157*Vst) ...
/500)^(1/2)))/419)/(1000*Vst)))/(100*((m2Div1 - 100)/(1000*Vst)
+ 1))...
+ 1269989/100))/((417561573*m2Div1)/200000 - (59917*m2Div1*(Ts +
...
((6969*m2Div1)/100 - 100*TColl + (100*(Ta - Ts)*(50*Vst +
5*((157*Vst)...
/500)^(1/2)))/419)/(1000*Vst)))/(2000*((m2Div1 - 100)/(1000*Vst)
+ 1))...
+ 301442427/2000) - (4609*((13*m2Div1*(Ts + ((6969*m2Div1)/100 -
100*TColl)...
+ (100*(Ta - Ts)*(50*Vst +
5*((157*Vst)/500)^(1/2)))/419)/(1000*Vst)))...
/(2000*((m2Div1 - 100)/(1000*Vst) + 1)) - (90597*m2Div1)/200000
+ 174597/2000)...
*((2920011*m2Div1)/10000 - (419*m2Div1*(Ts + ((6969*m2Div1)/100
- 100*TColl + ...

```

```

(100*(Ta - Ts)*(50*Vst +
5*((157*Vst)/500)^(1/2)))/419)/(1000*Vst)))/(100* ...
((m2Div1 - 100)/(1000*Vst) + 1)) +
1269989/100))/((417561573*m2Div1)/200000 ...
- (59917*m2Div1*(Ts + ((6969*m2Div1)/100 - 100*TColl + (100*(Ta
- Ts)* ...
(50*Vst +
5*((157*Vst)/500)^(1/2)))/419)/(1000*Vst)))/(2000*((m2Div1 - 100)...
/(1000*Vst) + 1)) + 301442427/2000)

Fboiler=(1/(3600*boilereff))* Ptin

Ctot= (fas*Csolar*Asp + fat*Cstortank*Vst)/(365*24)* B + Fboiler
* Cfboiler

end

mFileErrorCode = 95;

% --- Set outputs ---

%trnOutputs(1) = M1; % inlet steam production fluid controller
trnOutputs(1) = M2 ;% HX2 source side outlet fluid controller
trnOutputs(2) = Ctot ;% total cost of system
trnOutputs(3) = Fboiler
mFileErrorCode = 90;

mFileErrorCode = 0;

```

D. Configuration 4 Data

In this Appendix, initially fuel consumption Diagram in Configuration 4 is presented. Then, all applied mathematical models of components during Configuration's optimization are shown and finally MATLAB code of optimization is inserted.

Figure D.1 and Figure D.2 are presented which compare total fuel consumption in boilers of Configuration 1 with that in Configuration 4 in February and June, respectively. Figure D.1 and Figure D.2 provide useful information about the environmental beneficiary of the central solar field integration into Configuration 4 with reducing fuel consumption. The fuel consumption reduction is more obvious for June because of more available solar energy.

In the following, all Equations which are used to obtain objective function for Configuration 4 are presented. For each Equation, the related Equation in Chapter 3 and the related component in the corresponding Unit are mentioned. By replacing Equations D.1 to D.12 and Equations D.14 to D.19 in Equations D.13 and D.20, respectively. The boilers output energy is calculated based on three decision variables, $\dot{m}_{2,Div1}$, $\dot{m}_{2,Div3}$ and $\dot{m}_{2,Div6}$, similar to Configuration 2-2 optimization procedure. Equation D.21 calculates the total fuel consumption in both Units in Configuration 4 and finally by Equation D.22 the total hourly cost of Configuration 4 is estimated. Equations D.23 to D.25 show how optimizer uses decision variables to calculate three diverters' control signals, M1, M2 and M3. Diverters' control signals are analog and they could get a value between 0 and 1.

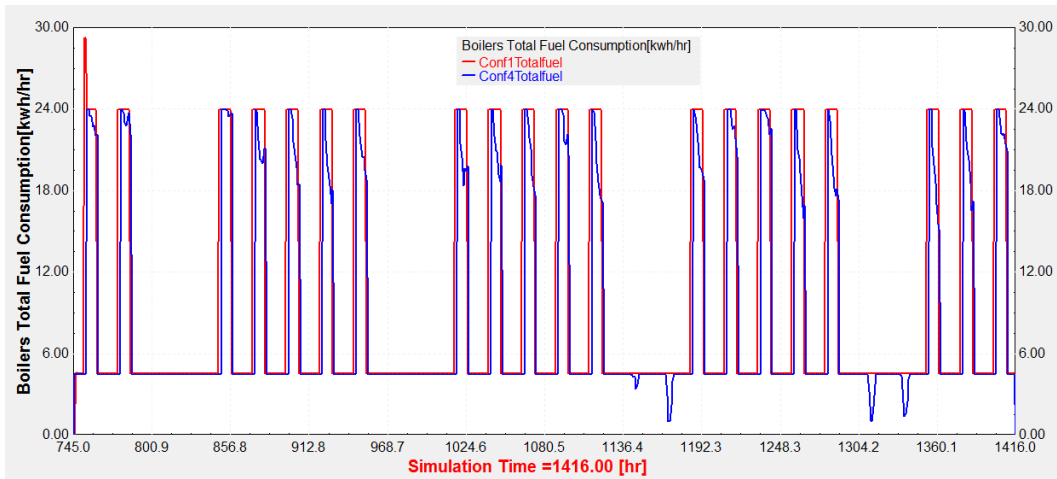


Figure D.1. Configuration 1 vs. Configuration 4 boilers' total fuel consumption in February. Solar collector area is 100 m² and storage tank volume is 1 m³.

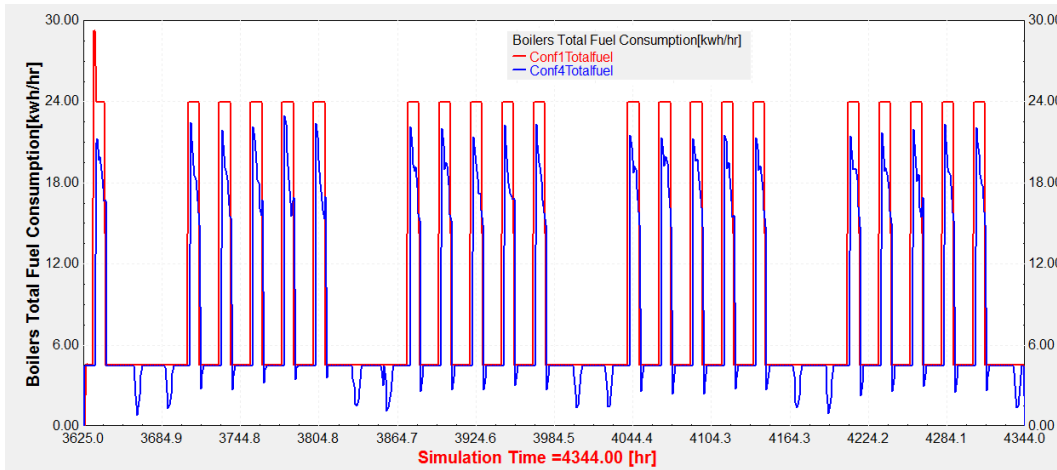


Figure D.2. Configuration 1 vs. Configuration 4 boilers' total fuel consumption in June. Solar collector area is 100 m² and storage tank volume is 1 m³.

For Unit1:

Obtaining storage tank average temperature ($T_{1,ST}$) at the end of each hour:

From Eqn.(3.19) for HX2 in Unit 1:

$$T_{HX2,U1} = T_{1,HX1,U1} - \frac{(\varepsilon_2)(\dot{m}_{in,U1})(T_{1,HX1,U1} - T_{in,U1})}{\dot{m}_{1,HX1,U1}} \quad (D. 1)$$

From Eqn.(3.23) for Tee-Piece (Mix3) :

$$T_{Mix3} = \frac{(\dot{m}_{2,Div1})(T_{in,Div1}) + (\dot{m}_{2,Div3})(T_{HX2,U1})}{(\dot{m}_{2,Div1} + \dot{m}_{2,Div3})} \quad (D. 2)$$

From Eqn.(3.19) for HX2 in Unit 2:

$$T_{HX2,U2} = T_{1,HX1,U2} - \left(\frac{\varepsilon_2}{\dot{m}_{1,HX1,U2}} \right) \left(\frac{C_{min1}}{C_p} \right) (T_{1,HX1,U2} - T_{in,U2}) \quad (D. 3)$$

From Eqn.(3.23) for Tee-Piece (Mix4) :

$$T_{Mix4} = \frac{(\dot{m}_{2,Div1} + \dot{m}_{2,Div3})(T_{Mix3}) + (\dot{m}_{2,Div6})(T_{HX2,U2})}{(\dot{m}_{2,Div1} + \dot{m}_{2,Div3} + \dot{m}_{2,Div6})} \quad (D. 4)$$

From Eqn.(3.21) for Heat Storage Tank :

$$T_{1,ST} = \frac{[T_s - \left(\frac{1}{\dot{m}_s}\right)((\dot{m}_{coll})(T_{coll}) - (\dot{m}_{2,Div1} + \dot{m}_{2,Div3} + \dot{m}_{2,Div6})(T_{Mix4}) + \frac{(UAs)(T_s - Ta)}{C_p})]}{[1 + \left(\frac{1}{\dot{m}_s}\right)(\dot{m}_{2,Div1} + \dot{m}_{2,Div3} + \dot{m}_{2,Div6} - \dot{m}_{coll})]} \quad (D. 5)$$

From Eqn.(3.27) for Diverter (Div2 and Div5) :

$$T_{1,Div2} = T_{1,ST} \quad (D. 6)$$

Calculating hot-side outlet temperature ($T_{2,HX1,U1}$) of HX1 heat exchanger in Unit 1:

From Eqn.(3.27) for Diverter (Div5) and Eqn.(3.29) for Diverter (Div2) :

$$T_{2,Div2} = T_{1,ST} \quad (D. 7)$$

From Eqn.(3.27) for Diverter (Div3) :

$$T_{1,Div3} = T_{HX2,U1} \quad (D. 8)$$

From Eqn.(3.23) for Tee-Piece (Mix2):

$$T_{Mix2} = \frac{(\dot{m}_{1,Div3})(T_{1,Div3}) + (\dot{m}_{2,Div2})(T_{2,Div2})}{(\dot{m}_{1,Div3} + \dot{m}_{2,Div2})} \quad (D. 9)$$

From Eqn.(3.12) for HX1 in Unit 1:

$$\gamma_1 = 1 - \frac{(T_{1,HX1,U1} - T_{Mix2})(\dot{m}_{Mix2})}{(\epsilon_1)(\dot{m}_{2,Div4})(T_{2,Div4} - T_{Mix2})} \quad (D. 10)$$

From Eqn.(3.13) for HX1 in Unit 1:

$$T_{2,HX1,U1} = (\gamma_1)(T_{2,Div4}) + (1 - \gamma_1) \left(T_{2,Div4} - (\varepsilon_1)(T_{2,Div4} - T_{Mix2}) \right) \quad (D. 11)$$

From Eqn.(3.25) for Flow Mixer (Mix1):

$$T_{Mix1} = \frac{(\dot{m}_{in,Div1} - \dot{m}_{2,Div1})(T_{1,Div1}) + (\dot{m}_{2,Div1})(T_{1,Div2}) + (\dot{m}_{2,HX1,U1})(T_{2,HX1,U1})}{(\dot{m}_{in,Div1} + \dot{m}_{2,HX1,U1})} \quad (D. 12)$$

Calculating $\dot{Q}_{need,1}$:

From Eqn.(3.1) for Boiler in Unit 1:

$$\dot{Q}_{need,1} = (\dot{m}_{b,U1})C_p(T_{b,U1} - T_{Mix1}) \quad (D. 13)$$

For Unit 2:

From Eqn.(3.29) for Flow Diverter (Div5):

$$T_{2,Div5} = T_{1,ST} \quad (D. 14)$$

From Eqn.(3.19) for HX2 in Unit 2:

$$T_{HX2,U2} = T_{1,HX1,U2} - \left(\frac{\varepsilon_2}{\dot{m}_{1,HX1,U2}} \right) \left(\frac{C_{min1}}{C_p} \right) (T_{1,HX1,U2} - T_{in,U2}) \quad (D. 15)$$

From Eqn.(3.27) for Flow Diverter (Div6):

$$T_{1,Div6} = T_{HX2,U2} \quad (D. 16)$$

From Eqn.(3.23) for Tee-Piece (Mix5):

$$T_{\text{Mix5}} = \frac{(\dot{m}_{1,\text{Div6}})(T_{1,\text{Div6}}) + (\dot{m}_{2,\text{Div5}})(T_{2,\text{Div5}})}{(\dot{m}_{1,\text{Div6}} + \dot{m}_{2,\text{Div5}})} \quad (\text{D. 17})$$

From Eqn.(3.12) for HX1 in Unit 2:

$$\gamma_2 = 1 - \frac{(T_{1,\text{HX1,U2}} - T_{\text{Mix5}})(\dot{m}_{\text{Mix5}})}{(\varepsilon_1)(\dot{m}_{\text{b,U2}})(T_{\text{b,U2}} - T_{\text{Mix5}})} \quad (\text{D. 18})$$

From Eqn.(3.13) for HX1 in Unit 2:

$$T_{2,\text{HX1,U2}} = (\gamma_2)(T_{2,\text{U2}}) + (1 - \gamma_2)(T_{\text{b,U2}} - (\varepsilon_1)(T_{\text{b,U2}} - T_{\text{Mix5}})) \quad (\text{D. 19})$$

Calculating $\dot{Q}_{\text{need},2}$:

From Eqn.(3.1) for Boiler in Unit 2:

$$\dot{Q}_{\text{need},2} = (\dot{m}_{\text{b,U2}})C_p(T_{\text{b,U2}} - T_{2,\text{HX1,U2}}) \quad (\text{D. 20})$$

$$F_{\text{boiler}} = \frac{\dot{Q}_{\text{need},\text{total}}}{3600 \eta_{\text{boiler}}} \quad (\text{D. 21})$$

$$C_{\text{total}} = C_{\text{fuel}}F + \frac{f_s C_{\text{solar}}A_s + f_t C_{\text{tank}}V_t}{8760} \quad (\text{D. 22})$$

$$M1 = \frac{\dot{m}_{2,Div1}}{\dot{m}_{in,Div1}} \quad (D.23)$$

$$M2 = \frac{\dot{m}_{2,Div3}}{\dot{m}_{HX2,U1}} \quad (D.24)$$

$$M3 = \frac{\dot{m}_{2,Div6}}{\dot{m}_{HX2,U2}} \quad (D.25)$$

The following MATLAB code is the used code for Configuration 4 optimization.

```
%this project is for configuration 4

% --- Process Inputs -----
% -----
% -----

Ts      = trnInputs(1);
Ta      = trnInputs(2);
U1      = trnInputs(3); % pump output flow rate in unit1, if U1>0
        (U1=100 kg/hr) it means Unit 1 operates
U2      = trnInputs(4); % boiler output flow rate in unit2, if U2>0
        (U2=1100 kg/hr) it means Unit 2 operates
Tcoll   = trnInputs(5); % solar collector output temperature
%Ts     = trnInputs(3);
%Qin    = trnInputs(4);
%Ts     = trnInputs(5);
%Tcoll  = trnInputs(5);

%% mFileErrorCode = 120      % After processing inputs

% --- First call of the simulation: initial time step (no
iterations) -----
% -----
% (note that Matlab is initialized before this at the info(7) = -1
call, but the m-file is not called)

if ( (trnInfo(7) == 0) & (trnTime-trnStartTime < 1e-6) )
```

```

    % This is the first call (Counter will be incremented later for
this very first call)
    nCall = 0;

    % This is the first time step
    nStep = 1;

    % Initialize history of the variables for plotting at the end of
the simulation
    nTimeSteps = (trnStopTime-trnStartTime)/trnTimeStep + 1;

    history.Ts      = zeros(nTimeSteps,1);
    history.Ta      = zeros(nTimeSteps,1);

    history.Ctot    = zeros(nTimeSteps,1);

    % No return, we will calculate the solar collector performance
during this call
    %% mFileErrorCode = 130    % After initialization

end

% --- Very last call of the simulation (after the user clicks "OK"):
Do nothing -----
% -----
-----

if ( trnInfo(8) == -1 )

    %% mFileErrorCode = 1000;

    mFileErrorCode = 0; % Tell TRNSYS that we reached the end of the
m-file without errors
    return

end

% --- Post convergence calls: store values -----
% -----
-----

if (trnInfo(13) == 1)

    %% mFileErrorCode = 140;    % Beginning of a post-convergence
call

    history.Ts(nStep)      = Ts;

```



```

ro=1000 % kg/m3 water density
%%%%%%%%%%%%%%%%%%%%%%%%%%%%%%%%%%%%%%%%%%%%%%%%%%%%%%%%%%%%%%%%%%%%%%%%777&7
hS=0.1 % storage tank hight [m]
AS=(2*Vst/hS)+2*(Vst*3.14*hS)^0.5 % storage tank surface [m2]
mS=ro*Vst
mColl= 100 % kg/hr solar collector inlet flow rate
U=2.5 % Tank Loss Coefficient [kj/(hr.m2.k)]
Cp = 4.19 % for water kj/(kg.k)
ep1= 0.65 % heat exchanger effectiveness of HX1
ep2= 0.433 % heat exchanger effectiveness of HX2

mFileErrorCode = 4;
Cmin1=min(100*4.19,1100*4.19)
% always Cmin1=419
mindiv1=100
Tindiv1=20

mbU1=1100 % kg/hr
mbU2 = mbU1

m2HX1U1= 1000 % kg/hr
m2Div4 = m2HX1U1

mcoll = 500 % kg/hr
T1div1=Tindiv1
T1HX1U1 = 100 % oC
T1HX1U2=T1HX1U1

minU1 = 100 % kg/hr
m1HX1U1 = 100 % kg/hr
mHX2U1 = m1HX1U1
m1HX1U2 = m1HX1U1
mMix2 = m1HX1U1
mMix5 = m1HX1U2

m1HX1U2 = m1HX1U1

TinU1=30 % oC
TinU2=TinU1

TbU1=120 % oC
TbU2 = TbU1 % oC

T2Div4 = TbU1
m1Div3 = mHX2U1 - m2Div3
m2Div2 = m2Div3
mHX2U2= mHX2U1
m1Div6 = mHX2U2 - m2Div6

m2Div5=m2Div6

mFileErrorCode = 5;

```



```
Ptin2=mbU2*Cp*(TbU2-T2HX1U2)
```

```
%%%%%%%%%%%%%%%%%%%%%%%%%%%%%%%%%%%%%%%%%%%%%%%%%%%%%%%%%%%%%%%%%%%%%%%%  
%%%%%%%%%%%%%%%%%%%%%%%%%%%%%%%%%%%%%%%%%%%%%%%%%%%%%%%%%%%%%%%%%%%%%%%% optimization part %%%%%%%%%  
%%%%%%%%%%%%%%%%%%%%%%%%%%%%%%%%%%%%%%%%%%%%%%%%%%%%%%%%%%%%%%%%%%%%%%%%
```

```
mFileErrorCode = 8;  
if U1 > 0
```

```
A = [0 0 1;0 1 0;1 0 0 ]  
b = [100;100;100]  
lb= [0,0,0]  
ub= [100,100,100]  
x0= [0,0,0]
```

```
PtinC = Ptin1 + Ptin2
```

```
fun = @(x) (419*x(1))/5 + (502800*((6969*x(2))/100 - (x(2)*(Ts +  
(20*x(1) ...  
- 500*Tcoll + (6969*x(2))/100 + (6969*x(3))/100 + (100*(Ta -  
Ts)*(50*Vst ...  
+ 5*((157*Vst)/500)^(1/2)))/419)/(1000*Vst)))/((x(1) + x(2) + x(3) -  
500)...  
/(1000*Vst) + 1) + 3031))/((90597*x(2))/200 - (13*x(2)*(Ts +  
(20*x(1) - ...  
500*Tcoll + (6969*x(2))/100 + (6969*x(3))/100 + (100*(Ta -  
Ts)*(50*Vst + ...  
5*((157*Vst)/500)^(1/2)))/419)/(1000*Vst)))/(2*((x(1) + x(2) + x(3)  
- ...  
500)/(1000*Vst) + 1)) + 65403/2) - (4190*((6969*x(2))/100 -  
(x(2)*(Ts + ...  
(20*x(1) - 500*Tcoll + (6969*x(2))/100 + (6969*x(3))/100 + (100*(Ta  
- Ts) ...  
*(50*Vst + 5*((157*Vst)/500)^(1/2)))/419)/(1000*Vst)))/((x(1) + x(2)  
+ x(3) ...  
- 500)/(1000*Vst) + 1) + 3031)*((13*x(2)*(Ts + (20*x(1) - 500*Tcoll  
+ ...  
(6969*x(2))/100 + (6969*x(3))/100 + (100*(Ta - Ts)*(50*Vst +  
5*((157*Vst)/500)...  
^(1/2)))/419)/(1000*Vst)))/(2000*((x(1) + x(2) + x(3) -  
500)/(1000*Vst) + 1))...  
- (90597*x(2))/200000 + 174597/2000))/((90597*x(2))/200 -  
(13*x(2)*(Ts + ...  
(20*x(1) - 500*Tcoll + (6969*x(2))/100 + (6969*x(3))/100 + (100*(Ta  
- Ts)* ...  
(50*Vst + 5*((157*Vst)/500)^(1/2)))/419)/(1000*Vst)))/(2*((x(1) +  
x(2) + x(3) ...  
- 500)/(1000*Vst) + 1)) + 65403/2) - (419*x(1)*(Ts + (20*x(1) -  
500*Tcoll + ...
```

```

(6969*x(2))/100 + (6969*x(3))/100 + (100*(Ta - Ts)*(50*Vst +
5*((157*Vst)/500)^(1/2)))/419)/(1000*Vst))/((x(1) + x(2) + x(3) -
500)/(1000*Vst) + 1)) + 41900 ...
+...
(553080*((6969*x(3))/100 - (x(3)*(Ts + (20*x(1) - 500*Tcoll +
(6969*x(2))/100 ...
+ (6969*x(3))/100 + (100*(Ta - Ts)*(50*Vst +
5*((157*Vst)/500)^(1/2)))/419)/(1000*Vst))) ...
/((x(1) + x(2) + x(3) - 500)/(1000*Vst) + 1) +
3031))/((996567*x(3))/2000 - ...
(143*x(3)*(Ts + (20*x(1) - 500*Tcoll + (6969*x(2))/100 +
(6969*x(3))/100 + ...
(100*(Ta - Ts)*(50*Vst +
5*((157*Vst)/500)^(1/2)))/419)/(1000*Vst)))/(20*((x(1) + ...
x(2) + x(3) - 500)/(1000*Vst) + 1)) + 719433/20) -
(4609*((6969*x(3))/100 - ...
(x(3)*(Ts + (20*x(1) - 500*Tcoll + (6969*x(2))/100 + (6969*x(3))/100
+ ...
(100*(Ta - Ts)*(50*Vst +
5*((157*Vst)/500)^(1/2)))/419)/(1000*Vst)))/((x(1) + ...
x(2) + x(3) - 500)/(1000*Vst) + 1) + 3031)*((13*x(3)*(Ts + (20*x(1)
- ...
500*Tcoll + (6969*x(2))/100 + (6969*x(3))/100 + (100*(Ta -
Ts)*(50*Vst + ...
5*((157*Vst)/500)^(1/2)))/419)/(1000*Vst)))/(2000*((x(1) + x(2) +
x(3) - ...
500)/(1000*Vst) + 1)) - (90597*x(3))/200000 +
174597/2000))/((996567*x(3))/2000 ...
- (143*x(3)*(Ts + (20*x(1) - 500*Tcoll + (6969*x(2))/100 +
(6969*x(3))/100 + ...
(100*(Ta - Ts)*(50*Vst +
5*((157*Vst)/500)^(1/2)))/419)/(1000*Vst)))/(20*((x(1) + ...
x(2) + x(3) - 500)/(1000*Vst) + 1)) + 719433/20)

```

```
x = fmincon(fun,x0,A,b,[],[],lb,ub)
```

```
mFileErrorCode = 110
```

```

m2Div1=x(1)
m2Div3=x(2)
m2Div6=x(3)

```

```

m2Div5 = m2Div6
m1ST = m2Div1 + m2Div3 + m2Div6

```

```

m2Div2 = m2Div3
m1Div5 = m2Div3 + m2Div1

```

```

M4 = (m2Div5)/(m1ST)
M5 = (m2Div2)/(m1Div5)

```

$$\begin{aligned}
P_{tinC} = & (419*m2Div1)/5 + (502800*((6969*m2Div3)/100 - (m2Div3*(Ts + \\
& (20*m2Div1 \dots \\
& - 500*Tcoll + (6969*m2Div3)/100 + (6969*m2Div6)/100 + (100*(Ta - \\
& Ts)*(50*Vst \dots \\
& + 5*((157*Vst)/500)^{(1/2)}))/419)/(1000*Vst)))/((m2Div1 + m2Div3 + \\
& m2Div6 - 500)\dots \\
& /(1000*Vst) + 1) + 3031))/((90597*m2Div3)/200 - (13*m2Div3*(Ts + \\
& (20*m2Div1 - \dots \\
& 500*Tcoll + (6969*m2Div3)/100 + (6969*m2Div6)/100 + (100*(Ta - \\
& Ts)*(50*Vst + \dots \\
& 5*((157*Vst)/500)^{(1/2)}))/419)/(1000*Vst)))/(2*((m2Div1 + m2Div3 + \\
& m2Div6 - \dots \\
& 500)/(1000*Vst) + 1)) + 65403/2) - (4190*((6969*m2Div3)/100 - \\
& (m2Div3*(Ts + \dots \\
& (20*m2Div1 - 500*Tcoll + (6969*m2Div3)/100 + (6969*m2Div6)/100 + \\
& (100*(Ta - Ts) \dots \\
& *(50*Vst + 5*((157*Vst)/500)^{(1/2)}))/419)/(1000*Vst)))/((m2Div1 + \\
& m2Div3 + m2Div6 \dots \\
& - 500)/(1000*Vst) + 1) + 3031)*((13*m2Div3*(Ts + (20*m2Div1 - \\
& 500*Tcoll + \dots \\
& (6969*m2Div3)/100 + (6969*m2Div6)/100 + (100*(Ta - Ts)*(50*Vst + \\
& 5*((157*Vst)/500)\dots \\
& ^{(1/2)}))/419)/(1000*Vst)))/(2000*((m2Div1 + m2Div3 + m2Div6 - \\
& 500)/(1000*Vst) + 1))\dots \\
& - (90597*m2Div3)/200000 + 174597/2000))/((90597*m2Div3)/200 - \\
& (13*m2Div3*(Ts + \dots \\
& (20*m2Div1 - 500*Tcoll + (6969*m2Div3)/100 + (6969*m2Div6)/100 + \\
& (100*(Ta - Ts)* \dots \\
& (50*Vst + 5*((157*Vst)/500)^{(1/2)}))/419)/(1000*Vst)))/(2*((m2Div1 + \\
& m2Div3 + m2Div6 \dots \\
& - 500)/(1000*Vst) + 1)) + 65403/2) - (419*m2Div1*(Ts + (20*m2Div1 - \\
& 500*Tcoll + \dots \\
& (6969*m2Div3)/100 + (6969*m2Div6)/100 + (100*(Ta - Ts)*(50*Vst + \\
& 5*((157*Vst)/500)^ \dots \\
& (1/2)))/419)/(1000*Vst)))/(100*((m2Div1 + m2Div3 + m2Div6 - \\
& 500)/(1000*Vst)+ 1)) + 41900 \dots \\
& + \dots \\
& (553080*((6969*m2Div6)/100 - (m2Div6*(Ts + (20*m2Div1 - 500*Tcoll + \\
& (6969*m2Div3)/100 \dots \\
& + (6969*m2Div6)/100 + (100*(Ta - Ts)*(50*Vst + \\
& 5*((157*Vst)/500)^{(1/2)}))/419)/(1000*Vst)) \dots \\
& /((m2Div1 + m2Div3 + m2Div6 - 500)/(1000*Vst) + 1) + \\
& 3031))/((996567*m2Div6)/2000 - \dots \\
& (143*m2Div6*(Ts + (20*m2Div1 - 500*Tcoll + (6969*m2Div3)/100 + \\
& (6969*m2Div6)/100 + \dots \\
& (100*(Ta - Ts)*(50*Vst + \\
& 5*((157*Vst)/500)^{(1/2)}))/419)/(1000*Vst)))/(20*((m2Div1 + \dots \\
& m2Div3 + m2Div6 - 500)/(1000*Vst) + 1)) + 719433/20) - \\
& (4609*((6969*m2Div6)/100 - \dots \\
& (m2Div6*(Ts + (20*m2Div1 - 500*Tcoll + (6969*m2Div3)/100 + \\
& (6969*m2Div6)/100 + \dots \\
& (100*(Ta - Ts)*(50*Vst + \\
& 5*((157*Vst)/500)^{(1/2)}))/419)/(1000*Vst)))/((m2Div1 + \dots
\end{aligned}$$

```

m2Div3 + m2Div6 - 500)/(1000*Vst) + 1) + 3031)*((13*m2Div6*(Ts +
(20*m2Div1 - ...
500*Tcoll + (6969*m2Div3)/100 + (6969*m2Div6)/100 + (100*(Ta -
Ts)*(50*Vst + ...
5*((157*Vst)/500)^(1/2)))/419)/(1000*Vst)))/(2000*((m2Div1 + m2Div3
+ m2Div6 - ...
500)/(1000*Vst) + 1)) - (90597*m2Div6)/200000 +
174597/2000))/((996567*m2Div6)/2000 ...
- (143*m2Div6*(Ts + (20*m2Div1 - 500*Tcoll + (6969*m2Div3)/100 +
(6969*m2Div6)/100 + ...
(100*(Ta - Ts)*(50*Vst +
5*((157*Vst)/500)^(1/2)))/419)/(1000*Vst)))/(20*((m2Div1 + ...
m2Div3 + m2Div6 - 500)/(1000*Vst) + 1)) + 719433/20)

```

Fboiler=(1/(3600*boilereff))* PtinC % kg fuel inlet boiler

```

%%%%%%%%%%%%%%%%%%%%%%%%%%%%%%%%%%%%%%%%%%%%%%%%%%%%%%%%%%%%%%%%%%%%%%%% Fboiler2 calculation
%%%%%%%%%%%%%%%%%%%%%%%%%%%%%%%%%%%%%%%%%%%%%%%%%%%%%%%%%%%%%%%%%%%%%%%%

```

```

Ptin2= (553080*((6969*m2Div6)/100 - (m2Div6*(Ts + (20*m2Div1 -
500*Tcoll + (6969*m2Div3)/100 ...
+ (6969*m2Div6)/100 + (100*(Ta - Ts)*(50*Vst +
5*((157*Vst)/500)^(1/2)))/419)/(1000*Vst)) ...
/((m2Div1 + m2Div3 + m2Div6 - 500)/(1000*Vst) + 1) +
3031))/((996567*m2Div6)/2000 - ...
(143*m2Div6*(Ts + (20*m2Div1 - 500*Tcoll + (6969*m2Div3)/100 +
(6969*m2Div6)/100 + ...
(100*(Ta - Ts)*(50*Vst +
5*((157*Vst)/500)^(1/2)))/419)/(1000*Vst)))/(20*((m2Div1 + ...
m2Div3 + m2Div6 - 500)/(1000*Vst) + 1)) + 719433/20) -
(4609*((6969*m2Div6)/100 - ...
(m2Div6*(Ts + (20*m2Div1 - 500*Tcoll + (6969*m2Div3)/100 +
(6969*m2Div6)/100 + ...
(100*(Ta - Ts)*(50*Vst +
5*((157*Vst)/500)^(1/2)))/419)/(1000*Vst)))/(m2Div1 + ...
m2Div3 + m2Div6 - 500)/(1000*Vst) + 1) + 3031)*((13*m2Div6*(Ts +
(20*m2Div1 - ...
500*Tcoll + (6969*m2Div3)/100 + (6969*m2Div6)/100 + (100*(Ta -
Ts)*(50*Vst + ...
5*((157*Vst)/500)^(1/2)))/419)/(1000*Vst)))/(2000*((m2Div1 + m2Div3
+ m2Div6 - ...
500)/(1000*Vst) + 1)) - (90597*m2Div6)/200000 +
174597/2000))/((996567*m2Div6)/2000 ...
- (143*m2Div6*(Ts + (20*m2Div1 - 500*Tcoll + (6969*m2Div3)/100 +
(6969*m2Div6)/100 + ...
(100*(Ta - Ts)*(50*Vst +
5*((157*Vst)/500)^(1/2)))/419)/(1000*Vst)))/(20*((m2Div1 + ...
m2Div3 + m2Div6 - 500)/(1000*Vst) + 1)) + 719433/20)

```

```

Fboiler2=(1/(3600*boilereff))* Ptin2
%%%%%%%%%%%%%%%%%%%%%%%%%%%%%%%%%%%%%%%%%%%%%%%%%%%%%%%%%%%%%%%%%%%%%%%%

```

```

%fat*Cstortank*Vst is cost which we must pay each year for 40 years
for
%storage tank but our simulation is for 1 hr so we should divide
this to
%365x24 to obtain the cost of storage tank for each hour

```

```

% Ctot= Fboiler * Cfboiler + fat*Cstortank*Vst /(365*24)

```

```

Ctot= Fboiler * Cfboiler + (fas*Csolar*Asp +
fat*Cstortank*Vst)/(365*24)

```

```

else

```

```

A = [0 0 1;0 1 0;1 0 0 ]

```

```

b = [100;100;100]

```

```

lb= [0,0,0]

```

```

ub= [0,0,100]

```

```

x0= [0,0,0]

```

```

fun = @(x) (553080*((6969*x(3))/100 - (x(3)*(Ts + (20*x(1) -
500*Tcoll + (6969*x(2))/100 ...
+ (6969*x(3))/100 + (100*(Ta - Ts)*(50*Vst +
5*((157*Vst)/500)^(1/2)))/419)/(1000*Vst))) ...
/((x(1) + x(2) + x(3) - 500)/(1000*Vst) + 1) +
3031))/((996567*x(3))/2000 - ...
(143*x(3)*(Ts + (20*x(1) - 500*Tcoll + (6969*x(2))/100 +
(6969*x(3))/100 + ...
(100*(Ta - Ts)*(50*Vst +
5*((157*Vst)/500)^(1/2)))/419)/(1000*Vst)))/(20*((x(1) + ...
x(2) + x(3) - 500)/(1000*Vst) + 1)) + 719433/20) -
(4609*((6969*x(3))/100 - ...
(x(3)*(Ts + (20*x(1) - 500*Tcoll + (6969*x(2))/100 + (6969*x(3))/100
+ ...
(100*(Ta - Ts)*(50*Vst +
5*((157*Vst)/500)^(1/2)))/419)/(1000*Vst)))/((x(1) + ...
x(2) + x(3) - 500)/(1000*Vst) + 1) + 3031)*((13*x(3)*(Ts + (20*x(1)
- ...
500*Tcoll + (6969*x(2))/100 + (6969*x(3))/100 + (100*(Ta -
Ts)*(50*Vst + ...
5*((157*Vst)/500)^(1/2)))/419)/(1000*Vst)))/(2000*((x(1) + x(2) +
x(3) - ...
500)/(1000*Vst) + 1)) - (90597*x(3))/200000 +
174597/2000))/((996567*x(3))/2000 ...
- (143*x(3)*(Ts + (20*x(1) - 500*Tcoll + (6969*x(2))/100 +
(6969*x(3))/100 + ...
(100*(Ta - Ts)*(50*Vst +
5*((157*Vst)/500)^(1/2)))/419)/(1000*Vst)))/(20*((x(1) + ...
x(2) + x(3) - 500)/(1000*Vst) + 1)) + 719433/20)

```

```

x = fmincon(fun,x0,A,b,[],[],lb,ub)

```

```

m2Div1=x(1)

```

```

m2Div3=x(2)
m2Div6=x(3)

m2Div5 = m2Div6
m1ST = m2Div1 + m2Div3 + m2Div6

M4 = (m2Div5)/(m1ST)
M5 = 0

% PtinC=Ptin2 because Ptin1 is shut down

PtinC =(553080*((6969*m2Div6)/100 - (m2Div6*(Ts + (20*m2Div1 -
500*Tcoll + (6969*m2Div3)/100 ...
+ (6969*m2Div6)/100 + (100*(Ta - Ts)*(50*Vst +
5*((157*Vst)/500)^(1/2)))/419)/(1000*Vst))) ...
/((m2Div1 + m2Div3 + m2Div6 - 500)/(1000*Vst) + 1) +
3031))/((996567*m2Div6)/2000 - ...
(143*m2Div6*(Ts + (20*m2Div1 - 500*Tcoll + (6969*m2Div3)/100 +
(6969*m2Div6)/100 + ...
(100*(Ta - Ts)*(50*Vst +
5*((157*Vst)/500)^(1/2)))/419)/(1000*Vst)))/(20*((m2Div1 + ...
m2Div3 + m2Div6 - 500)/(1000*Vst) + 1)) + 719433/20) -
(4609*((6969*m2Div6)/100 - ...
(m2Div6*(Ts + (20*m2Div1 - 500*Tcoll + (6969*m2Div3)/100 +
(6969*m2Div6)/100 + ...
(100*(Ta - Ts)*(50*Vst +
5*((157*Vst)/500)^(1/2)))/419)/(1000*Vst)))/((m2Div1 + ...
m2Div3 + m2Div6 - 500)/(1000*Vst) + 1) + 3031))*((13*m2Div6*(Ts +
(20*m2Div1 - ...
500*Tcoll + (6969*m2Div3)/100 + (6969*m2Div6)/100 + (100*(Ta -
Ts)*(50*Vst + ...
5*((157*Vst)/500)^(1/2)))/419)/(1000*Vst)))/(2000*((m2Div1 + m2Div3
+ m2Div6 - ...
500)/(1000*Vst) + 1)) - (90597*m2Div6)/200000 +
174597/2000))/((996567*m2Div6)/2000 ...
- (143*m2Div6*(Ts + (20*m2Div1 - 500*Tcoll + (6969*m2Div3)/100 +
(6969*m2Div6)/100 + ...
(100*(Ta - Ts)*(50*Vst +
5*((157*Vst)/500)^(1/2)))/419)/(1000*Vst)))/(20*((m2Div1 + ...
m2Div3 + m2Div6 - 500)/(1000*Vst) + 1)) + 719433/20)

Fboiler=(1/(3600*boilereff))* PtinC % kg fuel inlet boiler

%%%%%%%%%%%%%%%%%%%%%%%%%%%%%%%%%%%%%%%%%%%%%%%%%%%%%%%%%%%%%%%%%%%%%%%%555 Fboiler2 calculation %%%%%%%%%%

Ptin2=(553080*((6969*m2Div6)/100 - (m2Div6*(Ts + (20*m2Div1 -
500*Tcoll + (6969*m2Div3)/100 ...
+ (6969*m2Div6)/100 + (100*(Ta - Ts)*(50*Vst +
5*((157*Vst)/500)^(1/2)))/419)/(1000*Vst))) ...
/((m2Div1 + m2Div3 + m2Div6 - 500)/(1000*Vst) + 1) +
3031))/((996567*m2Div6)/2000 - ...

```

```

(143*m2Div6*(Ts + (20*m2Div1 - 500*Tcoll + (6969*m2Div3)/100 +
(6969*m2Div6)/100 + ...
(100*(Ta - Ts)*(50*Vst +
5*((157*Vst)/500)^(1/2)))/419)/(1000*Vst)))/(20*((m2Div1 + ...
m2Div3 + m2Div6 - 500)/(1000*Vst) + 1)) + 719433/20) -
(4609*((6969*m2Div6)/100 - ...
(m2Div6*(Ts + (20*m2Div1 - 500*Tcoll + (6969*m2Div3)/100 +
(6969*m2Div6)/100 + ...
(100*(Ta - Ts)*(50*Vst +
5*((157*Vst)/500)^(1/2)))/419)/(1000*Vst)))/((m2Div1 + ...
m2Div3 + m2Div6 - 500)/(1000*Vst) + 1) + 3031)*((13*m2Div6*(Ts +
(20*m2Div1 - ...
500*Tcoll + (6969*m2Div3)/100 + (6969*m2Div6)/100 + (100*(Ta -
Ts)*(50*Vst + ...
5*((157*Vst)/500)^(1/2)))/419)/(1000*Vst)))/(2000*((m2Div1 + m2Div3
+ m2Div6 - ...
500)/(1000*Vst) + 1)) - (90597*m2Div6)/200000 +
174597/2000))/((996567*m2Div6)/2000 ...
- (143*m2Div6*(Ts + (20*m2Div1 - 500*Tcoll + (6969*m2Div3)/100 +
(6969*m2Div6)/100 + ...
(100*(Ta - Ts)*(50*Vst +
5*((157*Vst)/500)^(1/2)))/419)/(1000*Vst)))/(20*((m2Div1 + ...
m2Div3 + m2Div6 - 500)/(1000*Vst) + 1)) + 719433/20)

```

```
Fboiler2=(1/(3600*boilereff))* Ptin2
```

```

%fat*Cstortank*Vst is cost which we must pay each year for 40
years for
%storage tank but our simulation is for 1 hr so we should divide
this to
%365x24 to obtain the cost of storage tank for each hour

% Ctot= Fboiler * Cfboiler + fat*Cstortank*Vst /(365*24)

Ctot= Fboiler * Cfboiler + (fas*Csolar*Asp +
fat*Cstortank*Vst)/(365*24)

```

```
end
```

```
%% mFileErrorCode = 95;
```

```
% --- Set outputs ---
```

```

M1 = m2Div1 / mindiv1
M2 = m2Div3 / mHX2U1
M3 = m2Div6 / mHX2U2

```

```

trnOutputs(1) = M1; % inlet steam production fluid controller
trnOutputs(2) = M2 ;% HX2 source side outlet fluid controller
trnOutputs(3) = M3 ;%
trnOutputs(4) = M4 ;% Div5 control signal
trnOutputs(5) = M5 ;% Div2 control signal
trnOutputs(6) = Ctot ;
trnOutputs(7) = Fboiler ;

```

E. Validation Code

The following file is used MATLAB code for validation part, Section 6.1 .

```

Cex=9.070 % [$/Gj]
Cw=152585.5 % [$/yr.km]

```

```

Hp1= 2.795 % [Gj/ton]
Hp2= 2.779 % [Gj/ton]
Hp3= 2.632 % [Gj/ton]
Hp4= 2.619 % [Gj/ton]
Hp5= 2.605 % [Gj/ton]
Hp6= 2.766 % [Gj/ton]
Hp7= 2.776 % [Gj/ton]
Hp8= 2.760 % [Gj/ton]
Hp9= 2.751 % [Gj/ton]
Hp10= 2.738 % [Gj/ton]
Hp11= 2.710 % [Gj/ton]
Hp12= 2.666 % [Gj/ton]
Hp13= 2.688 % [Gj/ton]

```

```

D16= 2.17 % [km]
D17= 1.70 % [km]
D18= 1.90 % [km]
D19= 1.38 % [km]
D110= 0.2 % [km]
D111= 1.55 % [km]
D112= 1.33 % [km]
D113= 3.95 % [km]

```

```

D26 = 2.25 % [km]
D27 = 1.85 % [km]
D28 = 2 % [km]
D29 = 1.48 % [km]
D210 = 0.2 % [km]
D211 = 1.48 % [km]
D212 = 1.43 % [km]
D213 = 2.98 % [km]

```

```

D36 = 0.85 % [km]
D37 = 0.5 % [km]

```

D38 = 0.67 % [km]
D39 = 0.01 % [km]
D310 = 1.60 % [km]
D311 = 1.53 % [km]
D312 = 1.05 % [km]
D313 = 5.80 % [km]

D46 = 0.20 % [km]
D47 = 0.32 % [km]
D48 = 0.22 % [km]
D49 = 0.75 % [km]
D410 = 2.30 % [km]
D411 = 1.70 % [km]
D412 = 0.80 % [km]
D413 = 3.42 % [km]

D56 = 2.19 % [km]
D57 = 1.85 % [km]
D58 = 2.05 % [km]
D59 = 1.45 % [km]
D510 = 0.23 % [km]
D511 = 1.65 % [km]
D512 = 1.40 % [km]
D513 = 4.53 % [km]

%% mass balance

syms y16 y26 y36 y46 y56 y17 y27 y37 y47 y57 y18 y28 y38 y48 y58
y19 y29 y39 y49 y59 y110 y210 y310 y410 y510 y112 y212 y312 y412
y512 y111 y211 y311 y411 y511 y113 y213 y313 y413 y513 m16 m17 m18
m19 m110 m111 m112 m113 m26 m27 m28 m29 m210 m211 m212 m213 m36 m37
m38 m39 m310 m311 m312 m313 m46 m47 m48 m49 m410 m411 m412 m413 m56
m57 m58 m59 m510 m511 m512 m513

%%Cw

x6 = 219000 - (y16+y26+y36+y46+y56)
x7 = 5840 - (y17+y27+y37+y47+y57)
x8 = 13140 - (y18+y28+y38+y48+y58)
x9 = 35040 - (y19+y29+y39+y49+y59)
x10 = 245280 - (y110+y210+y310+y410+y510)
x11 = 151840 - (y111+y211+y311+y411+y511)
x12 = 86140 - (y112+y212+y312+y412+y512)
x13 = 81395 - (y113+y213+y313+y413+y513)

Cmin=Cex*Hp6*x6 + Cex*Hp7*x7 + Cex*Hp8*x8 + Cex*Hp9*x9+
Cex*Hp10*x10+ Cex*Hp11*x11+ Cex*Hp12*x12+ Cex*Hp13*x13 ...

+ Cw*D16*m16 + Cw*D17*m17 + Cw*D18*m18 + Cw*D19*m19 +
 Cw*D110*m110 + Cw*D111*m111 + Cw*D112*m112 + Cw*D113*m113 ...
 + Cw*D26*m26 + Cw*D27*m27 + Cw*D28*m28 + Cw*D29*m29 +
 Cw*D210*m210 + Cw*D211*m211 + Cw*D212*m212 + Cw*D213*m213 ...
 + Cw*D36*m36 + Cw*D37*m37 + Cw*D38*m38 + Cw*D39*m39 +
 Cw*D310*m310 + Cw*D311*m311 + Cw*D312*m312 + Cw*D313*m313 ...
 + Cw*D46*m46 + Cw*D47*m47 + Cw*D48*m48 + Cw*D49*m49 +
 Cw*D410*m410 + Cw*D411*m411 + Cw*D412*m412 + Cw*D413*m413 ...
 + Cw*D56*m56 + Cw*D57*m57 + Cw*D58*m58 + Cw*D59*m59 +
 Cw*D510*m510 + Cw*D511*m511 + Cw*D512*m512 + Cw*D513*m513

Cmin = (5688435676744253*m16)/17179869184 +
 (8912756359875789*m17)/34359738368 ...
 + (4980657965812941*m18)/17179869184 +
 (904382630634455*m19)/4294967296 + ...
 (2746539*m26)/8 + (4849588019344179*m27)/17179869184 +
 305171*m28 + ...
 (7759340830950687*m29)/34359738368 +
 (8912756359875789*m36)/68719476736 ...
 + (305171*m37)/4 + (3512674565362811*m38)/34359738368 +
 (3355390629600297*m39)...
 /2199023255552 + (8388476574000743*m46)/274877906944 +
 (3355390629600297*m47)...
 /68719476736 + (576707764462551*m48)/17179869184 +
 (915513*m49)/8 + ...
 (2870431827665879*m56)/8589934592 +
 (4849588019344179*m57)/17179869184 ...
 + (5373867805219225*m58)/17179869184 +
 (7602056895188173*m59)/34359738368 ...
 + (8388476574000743*m110)/274877906944 +
 (8126336681063219*m111)/34359738368 ...
 + (6972921152138117*m112)/34359738368 +
 (5177262885516083*m113)/8589934592 ...
 + (8388476574000743*m210)/274877906944 +
 (7759340830950687*m211)/34359738368 ...
 + (7497200938013163*m212)/34359738368 +
 (7811768809538191*m213)/17179869184 ...
 + (8388476574000743*m310)/34359738368 +
 (4010740361944105*m311)/17179869184 ...
 + (5504937751687987*m312)/34359738368 +
 (7602056895188173*m313)/8589934592 ...
 + (6029217537563033*m410)/17179869184 +
 (8912756359875789*m411)/34359738368 ...
 + (8388476574000743*m412)/68719476736 +
 (8965184338463293*m413)/17179869184 ...
 + (4823374030050427*m510)/137438953472 +
 (8650616466938265*m511)/34359738368 ...
 + (7339917002250649*m512)/34359738368 +
 (5937468575034901*m513)/8589934592 ...
 - (1765384313806447*y16)/70368744177664 -
 (1771766758903361*y17)/70368744177664 ...
 - (62583*y18)/2500 - (7023242584644303*y19)/281474976710656 -
 (1765384313806447*y26) ...

```

/70368744177664 - (1771766758903361*y27)/70368744177664 -
(62583*y28)/2500 - ...
(7023242584644303*y29)/281474976710656 -
(1765384313806447*y36)/70368744177664 ...
- (1771766758903361*y37)/70368744177664 - (62583*y38)/2500 -
(7023242584644303*y39)...
/281474976710656 - (1765384313806447*y46)/70368744177664 -
(1771766758903361*y47)...
/70368744177664 - (62583*y48)/2500 -
(7023242584644303*y49)/281474976710656 - ...
(1765384313806447*y56)/70368744177664 -
(1771766758903361*y57)/70368744177664 - ...
(62583*y58)/2500 - (7023242584644303*y59)/281474976710656 -
(3495026935070175*y110)...
/140737488355328 - (6918570485054911*y111)/281474976710656 -
(6806239451349223*y112)...
/281474976710656 - (76188*y113)/3125 -
(3495026935070175*y210)/140737488355328 - ...
(6918570485054911*y211)/281474976710656 -
(6806239451349223*y212)/281474976710656 - ...
(76188*y213)/3125 - (3495026935070175*y310)/140737488355328 -
(6918570485054911*y311)...
/281474976710656 - (6806239451349223*y312)/281474976710656 -
(76188*y313)/3125 - ...
(3495026935070175*y410)/140737488355328 -
(6918570485054911*y411)/281474976710656 ...
- (6806239451349223*y412)/281474976710656 - (76188*y413)/3125 -
(3495026935070175*y510) ...
/140737488355328 - (6918570485054911*y511)/281474976710656 -
(6806239451349223*y512) ...
/281474976710656 - (76188*y513)/3125 +
911943429334101417818673/43980465111040000

```

```

%%%%%%%%%%%%%%%%%%%%%%%%%%%%%%%%%%%%%%%%%%%%%%%%%%%%%%%%%%%%%%%%%%%%%%%%
%%%%%%%%%%%%%%%%%%%%%%%%%%%%%%%%%%%%%%%%%%%%%%%%%%%%%%%%%%%%%%%%%%%%%%%% fmincon function %%%%%%%%%%%%%%%%%%%%%%%%%%%%%%%%%%%%%%%%%%%%%%%%%%%%%%%%%%%%%%%%%%%%%%%%%
%%%%%%%%%%%%%%%%%%%%%%%%%%%%%%%%%%%%%%%%%%%%%%%%%%%%%%%%%%%%%%%%%%%%%%%%

```

```

Hp1= 2.795 % [Gj/ton]
Hp2= 2.779 % [Gj/ton]
Hp3= 2.632 % [Gj/ton]
Hp4= 2.619 % [Gj/ton]
Hp5= 2.605 % [Gj/ton]
Hp6= 2.766 % [Gj/ton]
Hp7= 2.776 % [Gj/ton]
Hp8= 2.760 % [Gj/ton]
Hp9= 2.751 % [Gj/ton]
Hp10= 2.738 % [Gj/ton]
Hp11= 2.710 % [Gj/ton]

```



```

332880
232870
232870
232870
232870
730000
730000
730000
730000
730000
54750
54750
54750
54750
23725
23725
23725
23725
]
%%%%%%%%%%%%%%%%%%%%%%%%%%%%%%%%%%%%%%%%%%%%%%%%%%%%%%%%%%%%%%%%%%%%%%%%
x0= zeros(80x1)

fun = @(x) (5688435676744253*x(1))/17179869184 +
(8912756359875789*x(2))/34359738368 ...
+ (4980657965812941*x(3))/17179869184 +
(904382630634455*x(4))/4294967296 + ...
(2746539*x(5))/8 + (4849588019344179*x(6))/17179869184 +
305171*x(7) + ...
(7759340830950687*x(8))/34359738368 +
(8912756359875789*x(9))/68719476736 ...
+ (305171*x(10))/4 + (3512674565362811*x(11))/34359738368 +
(3355390629600297*x(12))...
/2199023255552 + (8388476574000743*x(13))/274877906944 +
(3355390629600297*x(14))...
/68719476736 + (576707764462551*x(15))/17179869184 +
(915513*x(16))/8 + ...
(2870431827665879*x(17))/8589934592 +
(4849588019344179*x(18))/17179869184 ...
+ (5373867805219225*x(19))/17179869184 +
(7602056895188173*x(20))/34359738368 ...
+ (8388476574000743*x(21))/274877906944 +
(8126336681063219*x(22))/34359738368 ...
+ (6972921152138117*x(23))/34359738368 +
(5177262885516083*x(24))/8589934592 ...
+ (8388476574000743*x(25))/274877906944 +
(7759340830950687*x(26))/34359738368 ...
+ (7497200938013163*x(27))/34359738368 +
(7811768809538191*x(28))/17179869184 ...
+ (8388476574000743*x(29))/34359738368 +
(4010740361944105*x(30))/17179869184 ...
+ (5504937751687987*x(31))/34359738368 +
(7602056895188173*x(32))/8589934592 ...
+ (6029217537563033*x(33))/17179869184 +
(8912756359875789*x(34))/34359738368 ...

```

```

+ (8388476574000743*x(35))/68719476736 +
(8965184338463293*x(36))/17179869184 ...
+ (4823374030050427*x(37))/137438953472 +
(8650616466938265*x(38))/34359738368 ...
+ (7339917002250649*x(39))/34359738368 +
(5937468575034901*x(40))/8589934592 ...
- (1765384313806447*x(41))/70368744177664 -
(1771766758903361*x(42))/70368744177664 ...
- (62583*x(43))/2500 - (7023242584644303*x(44))/281474976710656
- (1765384313806447*x(45)) ...
/70368744177664 - (1771766758903361*x(46))/70368744177664 -
(62583*x(47))/2500 - ...
(7023242584644303*x(48))/281474976710656 -
(1765384313806447*x(49))/70368744177664 ...
- (1771766758903361*x(50))/70368744177664 - (62583*x(51))/2500 -
(7023242584644303*x(52)) ...
/281474976710656 - (1765384313806447*x(53))/70368744177664 -
(1771766758903361*x(54)) ...
/70368744177664 - (62583*x(55))/2500 -
(7023242584644303*x(56))/281474976710656 - ...
(1765384313806447*x(57))/70368744177664 -
(1771766758903361*x(58))/70368744177664 - ...
(62583*x(59))/2500 - (7023242584644303*x(60))/281474976710656 -
(3495026935070175*x(61)) ...
/140737488355328 - (6918570485054911*x(62))/281474976710656 -
(6806239451349223*x(63)) ...
/281474976710656 - (76188*x(64))/3125 -
(3495026935070175*x(65))/140737488355328 - ...
(6918570485054911*x(66))/281474976710656 -
(6806239451349223*x(67))/281474976710656 - ...
(76188*x(68))/3125 - (3495026935070175*x(69))/140737488355328 -
(6918570485054911*x(70)) ...
/281474976710656 - (6806239451349223*x(71))/281474976710656 -
(76188*x(72))/3125 - ...
(3495026935070175*x(73))/140737488355328 -
(6918570485054911*x(74))/281474976710656 ...
- (6806239451349223*x(75))/281474976710656 - (76188*x(76))/3125
- (3495026935070175*x(77)) ...
/140737488355328 - (6918570485054911*x(78))/281474976710656 -
(6806239451349223*x(79)) ...
/281474976710656 - (76188*x(80))/3125 +
911943429334101417818673/43980465111040000

```

```
x = fmincon(fun,x0,A,b,[],[],lb,ub)
```